Dipl.-Ing. Michael Schön

NUMERICAL MODELLING OF ANAEROBIC DIGESTION PROCESSES IN AGRICULTURAL BIOGAS PLANTS

DISSERTATION

EINGEREICHT AN DER LEOPOLD FRANZENS UNIVERSITÄT INNSBRUCK
FAKULTÄT FÜR BAUINGENIEURWISSENSCHAFTEN
zur Erlangung des akademischen Grades

„DOKTOR DER TECHNISCHEN WISSENSCHAFTEN“

Innsbruck, Februar 2009

Dipl.-Ing. Michael Schön

NUMERICAL MODELLING OF ANAEROBIC DIGESTION PROCESSES IN AGRICULTURAL BIOGAS PLANTS

DISSERTATION

EINGEREICHT AN DER LEOPOLD-FRANZENS-UNIVERSITÄT INNSBRUCK

FAKULTÄT FÜR BAUINGENIEURWISSENSCHAFTEN

zur Erlangung des akademischen Grades

“DOKTOR DER TECHNISCHEN WISSENSCHAFTEN“

Innsbruck, Februar 2009

Advisor (1st referee):

Doz. Dipl.-Ing. Dr. techn. **Bernhard Wett**

Arbeitsbereich Umwelttechnik, Institut für Infrastruktur
Fakultät für Bauingenieurwissenschaften
Universität Innsbruck - Austria

Co-advisor (2nd referee):

Prof. Dr. rer. nat. **Harald Horn**

Lehrstuhl für Siedlungswasserwirtschaft
Technische Universität München - Germany

If we knew what it was we were doing,
it would not be called research, would it?
Albert Einstein (1879-1955)

DANKSAGUNG

Ich möchte allen danken, die auf die eine oder andere Weise zum Gelingen dieser Arbeit beigetragen haben. Besonders bedanken möchte ich mich bei

Dr. Bernhard Wett für die Unterstützung meiner Arbeit am Institut in den vergangenen Jahren und für die Betreuung meiner Dissertation.

Prof. Harald Horn, der sich freundlicherweise bereit erklärte, die Zweitbegutachtung dieser Arbeit zu übernehmen.

ACKNOWLEDGEMENT

I would like to express my gratitude to all who have contributed to the completion of this thesis in one way or another. Special thanks go to

Dr. Bernhard Wett for supporting me in my work at the institute in the last years and for his guidance during my dissertation.

Prof. Harald Horn, who kindly accepted to review my dissertation.

ZUSAMMENFASSUNG

Der Schwerpunkt dieser Dissertation ist die numerische Simulation anaerober Faulprozesse in landwirtschaftlichen Biogasanlagen. Zu diesem Zweck wurde das allgemein anerkannte Anaerobic Digestion Model No.1 (ADM1) zusammen mit einer entsprechenden Simulationssoftware verwendet. Durch die Anwendung des ADM1 konnten mit entsprechenden Modifikationen und Anpassungen des Modells verschiedene Aspekte untersucht und simuliert werden. Den Kern dieser Arbeit bilden fünf wissenschaftliche Aufsätze (Papers), in denen die Ergebnisse dieser Untersuchungen zusammengefasst sind.

In drei einleitenden Kapiteln erhält der Leser zunächst Hintergrundinformation zu den in den Papers vorgestellten und angewandten Konzepten. Im **Paper (A)** wird dann in einem allgemeinen Überblick auf die Anwendbarkeit und Potenziale verschiedener erneuerbarer Energien (EE) im alpinen Raum eingegangen. Neben unstrittigen positiven Auswirkungen auf Energiesicherheit, Arbeitsmarkt und Luftqualität müssen allerdings einige Einschränkungen bezüglich der Nutzung und Wirtschaftlichkeit von EE in diesen Regionen berücksichtigt werden. Als ein wichtiger Aspekt in Zusammenhang mit dem Kernthema dieser Dissertation konnte für landwirtschaftliche Kleinbiogasanlagen ein gutes Potenzial festgestellt werden, falls es gelingt, das Kosten-Nutzen-Verhältnis noch weiter zu verbessern.

In **Paper (B)** konnte die biokinetische Modellierung als systematisches Werkzeug zur Unterstützung der Bemessung und Optimierung einer Biogasdemonstrationsanlage, welche den wissenschaftlichen Rahmen dieser Dissertation bildet, genutzt werden. Mit Hilfe von numerischen Simulationen konnten verschiedene Reaktorkonfigurationen bezüglich Beschickungsraten und Gärkammerunterteilung analysiert werden. Zur Kalibrierung der Modellparameter wurden verschiedene Datensätze aus Messkampagnen und Experimenten zur Güllevergärung im Groß- und Labormaßstab herangezogen.

Da Mehrkammersysteme, wie sie in der Demonstrationsanlage verwendet werden, relativ anfällig für Überlastungssituationen sind, wurden in **Paper (C)** die günstigen Auswirkungen der Co-Fermentation von Gülle mit anderen Substraten auf die Prozesstabilität untersucht. Um das Verhalten der Biogasanlage bei einer kombinierten Beschickung mit Gülle und Bioabfall vorhersagen zu können, wurde ein numerisches Modell erstellt und mit Daten aus Laborexperimenten einkalibriert. Die Kalibrierung hatte eine individuelle Zulaufcharakterisierung beider Substrate bei übereinstimmenden kinetischen Koeffizienten zum Ziel. Hierdurch konnte ein einheitlicher Parametersatz, der zur Simulation von Co-Fermentation geeignet ist, erhalten werden. Die Rechenläufe zeigten, dass ein konstanter Basiszulauf von Gülle vorübergehende „Schockladungen“ durch säurehaltige Co-Substrate abschwächen oder sogar kompensieren kann.

Da das Anfahren allgemein als die kritischste Phase beim Betrieb einer Biogasanlage angesehen wird, wurden in **Paper (D)** die Erkenntnisse zu Untersuchungen verschiedener Inbetriebnahmestrategien zusammengefasst. Diese beinhalten Laborexperimente zu zwei unterschiedlichen Szenarios mit stufenweiser Erhöhung der Beschickungsmenge beziehungsweise der Betriebstemperatur. Ein interessanter Aspekt war hierbei, dass trotz einer hydraulischen Verweilzeit von nur drei Tagen bei maximaler Beschickungsrate ein Reaktorversagen ausblieb. Dieser Umstand wurde der aus dem Viehbestand zufließenden Biomasse zugeschrieben. Für weitere Untersuchungen wurde ein numerisches Modell basierend auf ADM1 generiert und mit Daten aus den Laborexperimenten kalibriert. Die Modellerstellung umfasste auch die Implementierung von Temperaturtermen in den mikrobiellen Wachstumsfunktionen, um die angewandten Temperatursteigerungen berücksichtigen zu können. Unter anderem

konnten die Annahmen bezüglich der permanenten Beimpfung durch den Viehbestand durch die Simulationen bestätigt werden.

In **Paper (E)** richtete sich der Schwerpunkt der Untersuchungen auf die Populationsdynamik im Reaktor während potenzieller Überlastungssituationen. Hierzu wurden zwei verschiedene Fallbeispiele analysiert und mittels des ADM1 Prozesstabilitätsindikatoren abgeleitet. Der erste Fall beinhaltet ein Faulturmversagen in der kommunalen Kläranlage Salzburg und im zweiten Fall wurde das Nichteintreten des erwarteten Versagens des Laborreaktors aus Paper (D) untersucht. In den betrachteten Fällen stellten sich Beschickungsindikatoren wie die organische Belastungsrate, welche üblicherweise als Bemessungsparameter verwendet werden, als ungeeignet für die Bemessung unter dynamischen Bedingungen heraus. Als zweckdienlicher für die Erfassung der Anlagenstabilität unter instationären Verhältnissen erwies sich stattdessen die Anwendung von Indikatoren, die den Reaktorstatus abbilden.

Die abschließenden Schlussfolgerungen der Dissertation umfassen allgemeine Anmerkungen zur Modellierung landwirtschaftlicher Biogasanlagen und damit in Zusammenhang stehende Einschränkungen des Anaerobic Digestion Model No.1.

ABSTRACT

The main focus of this dissertation is the numerical simulation of anaerobic digestion processes in agricultural biogas plants. For this purpose, the widely recognised Anaerobic Digestion Model No.1 (ADM1) has been utilised together with corresponding simulation software. By application of the ADM1 different aspects have been investigated and simulated including corresponding modifications and adjustments of the model. The outcomes of these investigations are presented in 5 scientific papers which constitute the core of this work.

Before going into detail, the reader is provided with some background information on the concepts presented and applied in the papers in 3 introductory chapters. After that, a general overview on the applicability and potentials of different renewable energy sources in alpine regions is given in **paper (A)**. Besides undisputed beneficial effects on issues such as energy security, employment and air quality, some distinctions in alpine regions regarding the utilisation and economic efficiency of RES have to be taken into account. As an important outcome related to the core topic of this dissertation, small-scale agricultural biogas plants were found to have a good potential in alpine regions especially if the cost-benefit ratio gets improved further on.

Secondly, bio kinetic modelling was applied as a systematic tool in order to support process design and optimisation of a demonstration biogas plant which constitutes the main scientific framework and background of this thesis. In **paper (B)** different reactor configurations regarding loading rates and volume partitions were investigated by means of numerical simulations. Based on monitoring campaigns and experiments in full- and lab-scale data sets of manure digestion were used for parameter calibration.

Since multi-chamber systems as applied in the demonstration plant are quite vulnerable to overloading situations, beneficial impacts on the process robustness through the co-digestion of manure with other substrates were investigated in **paper (C)**. In order to predict plant performance at combinations of manure and biowaste, a numerical model was set up and calibrated with data from lab experiments. Calibration focused on individual influent characterisation of both substrates but on consistent selection of kinetic coefficients in order to generate a uniform set of parameters applicable for the simulation of co-fermentation. The simulations confirmed that a constant baseflow of manure can mitigate or even compensate temporary “shock loading” with more acidic co-substrates.

Since the start-up phase is generally considered as the most critical step in the operation of anaerobic digesters, **paper (D)** summarises the findings on the investigation of different start-up strategies. This included lab experiments on two scenarios with a stepwise load and temperature increase, respectively. An interesting aspect was the fact that despite a retention time of only 3 days at maximum loading rate no reactor failure occurred which was attributed to incoming cattle-borne archaeal biomass. For further investigations, a numerical model based on ADM1 was established and calibrated by means of experimental data. Model set-up included the incorporation of temperature terms in the bacterial growth functions to account for the applied temperature increase. Among others, assumptions regarding the permanent re-seeding from the livestock could be confirmed by the simulations.

In **paper (E)** a focus was put on the investigation of population dynamics during potential digester overload conditions. Two different case studies were investigated and ADM1 was utilised to derive digester stability indicators. The first scenario included a digester failure at a municipal WWTP and in the second case study the non-occurrence of the expected upset situation in the lab-scale digester introduced in paper (D) was further analysed. Loading indi-

cators such as the organic loading rate as a commonly utilised design parameter for digesters turned out to be unsuitable for the design under dynamic conditions in the investigated case studies. Instead, the utilisation of indicators reflecting the reactor state proved to be more adequate for the assessment of the stability of reactors in transient situations.

The final conclusions are covering some general remarks on the modelling of agricultural biogas plants and associated limitations of the Anaerobic Digestion Model No.1 (ADM1).

INCLUDED PAPERS

A Schoen M. A., De Toffol S., Wett B., Insam H. and Rauch W. (2007).
Comparison of renewable energy sources in alpine regions.
Managing Alpine Future. Borsdorf, A., Stötter, J., Veulliet, E. (Eds.). Austrian Academy of Sciences Press, ISBN 978-3-7001-6571-2.

B Wett B., Schoen M. A., Phothilangka P., Wackerle F. and Insam H. (2007).
Model-based design of an agricultural biogas plant: application of Anaerobic Digestion Model No. 1 for an improved four chamber scheme.
Water Science and Technology, 55 (10), 21-28.

C Schoen M. A., Phothilangka P., Eladawy A., Insam H. and Wett B. (2007).
Farmscale co-fermentation of manure and organic waste.
IWA-workshop on anaerobic digestion in mountain area and isolated rural zones. 5-7/Jun/2007, Chambéry, France

D Schoen M. A., Sperl D., Gadermaier M., Goberna M., Franke-Whittle I., Insam H. and Wett B. (2008).
Comparison of biogas plant start-up procedures based on lab- and full-scale data and on numerical modelling.
Second international symposium on energy from biomass and waste. 17-20/Nov/2008, Venice, Italy

E Schoen M. A., Sperl D., Gadermaier M., Goberna M., Franke-Whittle I., Insam H., Ablinger J. and Wett B. (2009).
Population dynamics at digester overload conditions.
Submitted to Bioresource Technology

TABLE OF CONTENTS

1 INTRODUCTION 1

1.1 Brief review on the long history of anaerobic digestion technologies 1
1.2 Scope and structure of the thesis 2

2 LITERATURE REVIEW 4

2.1 Biogas utilisation and agricultural aspects 4
2.1.1 General issues 4
2.1.2 Configurations of biogas systems 5
2.2 Anaerobic digestion 8
2.2.1 Microbial aspects of the anaerobic process 8
2.2.2 Factors affecting anaerobic digestion 13
2.3 Anaerobic Digestion Model No.1 22

3 MATERIALS AND METHODS 26

3.1 Lab-scale biogas plant 26
3.1.1 Digesters 26
3.1.2 Gas meter 26
3.2 Bio4Gas demonstration plant 27
3.3 Mathematical modelling and simulation 31
3.3.1 Simulation software 31
3.3.2 Model calibration 32

4 COMPARISON OF RENEWABLE ENERGY SOURCES IN ALPINE REGIONS (A) 35

5 APPLICATION OF ADM 1 FOR AN IMPROVED FOUR CHAMBER SCHEME (B) 44

6 FARMSCALE CO-FERMENTATION OF MANURE AND ORGANIC WASTE (C) 54

7 COMPARISON OF BIOGAS PLANT START-UP PROCEDURES (D) 64

8 POPULATION DYNAMICS AT DIGESTER OVERLOAD CONDITIONS (E) 74

9 CONCLUSIONS 88

9.1 Motivation for modelling biogas plants 88
9.2 Limitations of the applicability of ADM1 89
9.2.1 Influent characterisation 89
9.2.2 pH 90
9.2.3 Impact of temperature dynamics 90
9.2.4 Fate of sulphur and phosphorus compounds 90

10 REFERENCES 92

A APPENDIX A 97

A.1 ADM1 model matrix 97
A.2 Extended ADM1 model matrix 99
A.3 ADM1 processes 100
A.4 ADM1 parameters 101
A.5 ADM1 variables 103

B APPENDIX FOR PAPER (B) 104

B.1 Measured results 104
B.2 Model calibration 105
B.3 Simulation results 108

C APPENDIX FOR PAPER (C) 110

C.1 Measured results 110
C.2 Model calibration 111
C.3 Simulation results 115

D APPENDIX FOR PAPER (D) 117

D.1 Measured results 117
D.2 Model calibration 124
D.3 Simulation results 132

E APPENDIX FOR PAPER (E) 134

E.1 Measured results 134
E.2 Model calibration 135
E.3 Simulation results 138

INDEX OF FIGURES

Figure 1-1 Schematic of an Imhoff tank 1

Figure 2-1 Principal options for conversion and utilisation of biogas and digestate in plants using renewables (illustration may not be exhaustive) 4

Figure 2-2 General classification methods of biogas systems 5

Figure 2-3 Main steps and pathways of anaerobic digestion. Inert fraction of organic matter is not displayed (modified from Batstone *et al.*, 2002a). 9

Figure 2-4 Thermodynamic (Gibb's energy $\Delta G'$) dependence on H_2 partial pressure. Calculations based on standard values for free energies at pH 7.0, 25°C (adapted from Batstone *et al.*, 2002a). 11

Figure 2-5 Relative growth rate of psychrophilic, mesophilic and thermophilic methanogens (redrawn from van Lier et al., 1997) 14

Figure 2-6 Effect of pH on the relationship between the bicarbonate alkalinity of the liquid phase and the carbon dioxide content of the gas phase in an anaerobic process at T=35°C (based on calculations given in Grady et al., 1999; Tchobanoglous et al., 2003) 17

Figure 2-7 Rate of degradation of different types of substrate vs. retention time (left) and gas yield/production rate vs. retention time (adapted from Eder and Schulz, 2006) 21

Figure 2-8 Biochemical processes of anaerobic digestion implemented in ADM1 (adapted from Batstone *et al.*, 2002a) 22

Figure 2-9 Conversion processes in anaerobic digestion as used in the ADM1. Biochemical reactions are implemented as irreversible, while physico-chemical reactions are implemented as reversible. (adapted from Batstone *et al.*, 2000; Batstone *et al.*, 2002a). 23

Figure 3-1 Setup and a schematic layout of the lab scale digesters (Eladawy, 2005) 26

Figure 3-2 Gas meters on top of the lab digesters 27

Figure 3-3 Layout and flow scheme of the 4-chamber pilot plant with cylindrical shape and thermo-gas-lift system 28

Figure 3-4 Numerical CFD simulation of oscillations between C1 and C2 (left) and the annular flow of substrate in C3 and C4 (right) (Premstaller and Feurich, 2006) 29

Figure 3-5 *BIO4GAS* demonstration plant after completion 30

Figure 3-6 *BIO4GAS* demonstration plant during construction works 30

Figure 3-7 State-space model 31

Figure 3-8 Scheme of model calibration and validation 32

Figure 3-9 Scheme of ADM1/SIMBA influent characterisation 34

Figure 4-1 Electricity generation from renewables in EU-25 (left,EC, 2005) and total primary energy supply by source in Austria (right,IEA, 2004) 37

Figure 4-2 Number of biogas plants and installed el. power in Germany and Austria. For better comparability the values for Austria were multiplied with a

factor F equalising the different sizes of both countries (Schoen *et al.*, 2007b). 40

Figure 5-1 The anaerobic model as implemented including biochemical processes: (1) acidogenesis from sugars, (2) acidogenesis from amino acids, (3) acetogenesis from LCFA, (4) acetogenesis from propionate, (5) acetogenesis from butyrate and valerate, (6) aceticlastic methanogenesis, and (7) hydrogenotrophic methanogenesis (Batstone *et al.*, 2002b) 46

Figure 5-2 4-chamber biogas plant for co-fermentation of piggery manure and biowaste with a total volume of 190 m³ 47

Figure 5-3 Set-up of 4 lab-scale digesters with a volume of 0.1 m³ each for parallel digestion tests 48

Figure 5-4 Improved flow scheme of the 4-chamber pilot plant with cylindrical shape 48

Figure 5-5 4-chamber system represented by serial ADM1 digesters edited in the SIMBA-environment for the simulation of gas production in individual chambers 49

Figure 5-6 Calibration runs for gas production comparing best fit disintegration rate (*kdis* = 0.5, left) and default parameter (*kdis* = 0.096, right) 50

Figure 5-7 Simulated distribution of gas production and pH within the 4 chamber system at high loading with and without recycling (recycle pumping rates of 0/0 and 50/20 from left to right) 52

Figure 5-8 Calculated COD degradation for high loading with recycle pumping rates of 0/0 (left) and 50/20 (right), the value for 100 % is related to the largest COD stream including the recycle flux in each case 52

Figure 6-1 Number of biogas plants and installed el. power in Germany and Austria (modified from FV Biogas, 2005 (Germany), Eder and Schulz, 2006 (Austria)). For better comparability the values for Austria were multiplied with a factor F equalising the different sizes of both countries. 56

Figure 6-2 Layout and flow scheme of the 4-chamber pilot plant with cylindrical shape and gas-lift-system 57

Figure 6-3 Set-up and schematic layout of 2-lane 2-step reactors with a volume of 0.1 m³ each for digestion tests (A,B) and 2-reactor-model represented by serial ADM1 digesters edited in the SIMBA-environment (C) 59

Figure 6-4 Measured and calibrated gas production rates and pH for biowaste (left) and manure (right) 60

Figure 6-5 Progress of ammonia concentration and ammonia inhibition term for biowaste (left) and manure (right) 62

Figure 7-1 Layout and flow scheme of the 4-chamber pilot plant with cylindrical shape and gas-lift-system 66

Figure 7-2 Loading rates and temperature progression in the lab-scale reactors 67

Figure 7-3 Measured values for gas production rate, NH_4-N, pH, gas quality and organic acids in the lab reactors 70

Figure 7-4 Simulation results and measured values for gas production rate (B1, A2), pH (B1, A2), total and soluble COD. Presentation for B1 includes gas production rate without addition of bacterial mass (*XB* = 0). 71

Figure 7-5 Measured gas quality in chambers 1, 2, 4 and gas production in chamber 4 73

Figure 8-1 Gas production rate, methane content and pH for both digesters (FT1 & FT2). Note that unil day 34 (sludge by-pass to FT2; dotted line) gas production and CH_4 refer to an average value for FT1 and FT2; after day 34 it refers to FT2. 76

Figure 8-2 Loading rates and temperature progression in the lab-scale reactors 77

Figure 8-3 WWTP Salzburg simulation results and measured values for gas production, pH and methane content. Note that on day 34 digester FT1 was shut down and sludge was by-passed to FT2. 82

Figure 8-4 Loading and gas production rates, pH, organic acids, NH_4-N and total COD progression in lab-scale reactor B1 82

Figure 8-5 Simulation results and measured values for gas production, pH, total and soluble COD in the start-up experiment. Simulated gas production curves include different ratios of additional biomass (XB). 83

Figure 8-6 Measured relative portion of methanogens in reactor B1 and in the feed (per g sludge; left) and simulation values for acetate degarders (Xac) (per kg COD; right) in reactor B1 83

Figure 8-7 Simulation results of key indicators for Salzburg WWTP (upper charts) and start-up experiment (lower charts). Note that different y-axis scaling was used for F/M and ACN. 85

Figure B-1 Simulation model of two lab reactors for manure digestion edited in the SIMBA environment 105

Figure B-2 Simulation results vs. measured values of biogas production from manure 108

Figure B-3 Simulation results vs. measured values of pH for manure 109

Figure C-1 Simulation model of two lab reactors for biowaste digestion edited in the SIMBA environment 111

Figure C-2 Simulation results vs. measured values of biogas production from biowaste 115

Figure C-3 Simulation results vs. measured values of biogas production from manure 116

Figure C-4 Simulation results vs. measured values of pH for biowaste 116

Figure C-5 Simulation results vs. measured values of pH for manure 116

Figure D-1 Simulation model of a lab-scale digestion reactor edited in the SIMBA environment 124

Figure D-2 A1 and A2 simulation results vs. measured values for biogas production and pH 132

Figure D-3 B1 and B2 simulation results vs. measured values for biogas production and pH 132

Figure D-4 A1 and A2 simulation results vs. measured values for total and soluble COD 132

Figure D-5 B1 and B2 simulation results vs. measured values for total and soluble COD 133

Figure D-6 B1 simulation results vs. measured values for biogas production at different fluxes of additional active biomass to account for incoming cattle-borne biomass (in % of particulate COD; see also *fXB_Xc* in fraction balances in Table D-4) 133

Figure E-1 Simulation model of WWTP Salzburg digesters edited in the SIMBA environment 135

Figure E-2 WWTP Salzburg simulation results and measured values for gas production, pH and methane content. Note that on day 34 digester FT1 was shut down and sludge was by-passed to FT2. 138

Figure E-3 Measured relative portion of methanogens in reactor B1 and in the feed (per g sludge; left) and simulation values for acetate degarders (Xac) (per kg COD; right) in reactor B1 139

Figure E-4 Simulation results of key indicators for Salzburg WWTP (upper charts) and start-up experiment (lower charts). Note that different y-axis scaling was used for F/M and ACN. 139

INDEX OF TABLES

Table 2-1 Examples of different products from glucose degradation 10

Table 2-2 Energetics of syntrophic degradation 12

Table 2-3 Reactions related to methanogenesis (with standard temperatures) 13

Table 5-1 Input values of manure 50

Table 5-2 Calibrated ADM1 model parameters 51

Table 5-3 Simulated input loadings and resulting gas production rates 51

Table 6-1 Input values of manure and biowaste 58

Table 6-2 Calibrated ADM1 model parameters for manure and biowaste 61

Table 7-1 Characteristics of the feeding substrates 68

Table 7-2 Calibrated ADM1 model parameters including inflow characterization 72

Table 8-1 Characteristics of the feeding substrates 78

Table 8-2 Average values for sludge fed from the pre-thickener to the digesters at WWTP Salzburg as used for ADM1 simulations. Note that only direct feeds from the pre-thickener to the digesters were used (not taking into account feeds of FT1 to FT2 on day 0-34 and 40-54) 79

Table 8-3 Calibrated ADM1 model parameters including influent characterisation 84

Table A-1 ADM1 matrix for soluble components (physico-chemical rate equations not included; Batstone *et al.*, 2002a) 97

Table A-2 ADM1 matrix for particulate components (physico-chemical rate equations not included; Batstone *et al.*, 2002a) 98

Table A-3 ADM1 matrix for acid-base reactions and for liquid-gas reactions as implemented in Matlab/SIMBA 99

Table A-4 ADM1 processes as implemented in Matlab/SIMBA 100

Table A-5 ADM1 stoichiometric parameters as implemented in Matlab/SIMBA 101

Table A-6 ADM1 kinetic parameters as implemented in Matlab/SIMBA 102

Table A-7 ADM1 variables as implemented in Matlab/SIMBA 103

Table B-1 Feeding characteristics of manure 104

Table B-2 Characteristics of digested manure 104

Table B-3 Biogas production of manure in lab experiments 105

Table B-4 Fraction balance for manure 106

Table B-5 Calibrated parameter set for manure digestion 107

Table B-6 Influent file for manure digestion 108

Table C-1 Feeding characteristics of biowaste 110

Table C-2 Characteristics of digested biowaste 110

Table C-3 Biogas production of biowaste in lab experiments 111

Table C-4 Fraction balance for biowaste 112

Table C-5 Calibrated parameter set for biowaste digestion (co-digestion with manure) 113
Table C-6 Calibrated parameter set for manure digestion (co-digestion with biowaste) 114
Table C-7 Influent file for biowaste digestion 115
Table D-1 Feeding characteristics of inoculum and manure 117
Table D-2 Characteristics of digested substrates 117
Table D-3 Biogas production, pH and gas quality of digested substrates in lab experiments 120
Table D-4 Fraction balance 125
Table D-5 Calibrated uniform parameter set for A1, A2, B1 and B2 129
Table D-6 Influent files for start-up simulations 130
Table E-1 TS, biogas production, gas quality and pH at WWTP Salzburg 134
Table E-2 Calibrated uniform parameter set for WWTP Salzburg 136
Table E-3 Influent file for WWTP Salzburg simulations 137

1 INTRODUCTION

1.1 BRIEF REVIEW ON THE LONG HISTORY OF ANAEROBIC DIGESTION TECHNOLOGIES

The formation of different gases (e.g. CH_4, NH_3, H_2S, CO_2) as a result of anaerobic digestion of organic matter as well as energy generation from methane is known a long time ago. These biological process technologies are among the oldest availed by humanity and have been developed over many centuries (Batstone *et al.*, 2002a). The first systematic investigations on biogas were conducted around 1770 by the Italian natural scientist Alessandro Volta. He collected marsh gases from lakes and performed combustion experiments. The English physicist Michael Faraday also experimented with marsh gas and identified it as a hydrocarbon. But it was not until 1821 when the Italian scientist Amedeo Avogadro managed to identify the chemical formula for methane (CH_4). In the 19th century the famous French bacteriologist Louis Pasteur conducted experiments on biogas generation from cow manure and discovered together with the German chemist Felix Hoppe-Seyler the microbiological formation of CH_4/CO_2 from acetate. Pasteur then suggested to utilize the manure from the Parisian horse fleet for gas production to fuel the street lighting (Eder and Schulz, 2006).

By the end of the 19th century the development and utilisation of anaerobic digestion received great impacts when it was discovered that it can be used for wastewater treatment. It is reported that the first digestion plant was built at a leper colony in Bombay, India in 1897. The produced gas was used for lightning and beginning from 1907 it powered an engine for electricity generation (Eladawy, 2005). It was also in 1907 when the German engineer and inventor Karl Imhoff - a pioneer and a driving force for major advancements in wastewater engineering in the early 20th century - developed the so-called Imhoff tank (Figure 1-1) which was the first anaerobic digester in wastewater treatment (Eder and Schulz, 2006).

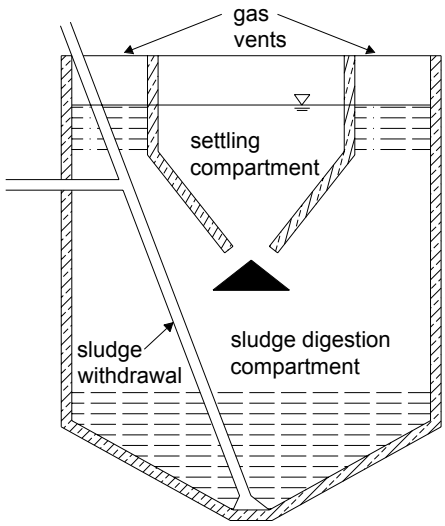

Figure 1-1 Schematic of an Imhoff tank

Throughout the 20th century, many considerable research achievements have been made and anaerobic digestion technology experienced continuous improvement. The

most important advances have been obtained in the last few decades. Driven by the oil crisis in the 1970s together with the introduction of modern 'high rate' reactors with a high cost-effectiveness, anaerobic digestion gained widespread acceptance (van Lier et al., 2001).

In parallel to the application of anaerobic digestion as a process step in wastewater treatment, numerous stand-alone large scale biogas plants for heat and power generation have been put into operation, especially in Europe. These facilities utilize a wide range of suitable input substrates stemming from agricultural, industrial, and municipal sources and provide an alternative to traditional energy sources and a possible contribution to mitigate climate change effects (IPCC, 2007a).

Initially triggered by reduced energy supplies after World War II and during the oil crisis in the 1970s, agriculture was identified to be a potential supplier of waste material (mainly manure) serving as feedstock for biogas plants. In recent years, the number of biogas plants underwent outstanding growth which is mainly prompted by a continued rise in prices for energy from fossil fuels (e.g. coal, oil, natural gas, uranium). Moreover, there is a generally increased ecological awareness in society that is reflected in a paradigm shift in environmental policy (e.g. Kyoto protocol goals for climate protection) coming along with associated amendments in legislation, governmental subsidies and incentives such as "green-pricing" initiatives that allows biogas-generated electricity to be sold at a premium. In turn, this is a major driver for ongoing technical progress and scientific research.

Regarding agriculture, manure-utilising plants can improve the carbon footprint of an agricultural facility compared to the sole storage of manure which would release remarkable emissions of CH_4 to the atmosphere. Through the combustion of methane ($CH_4 + 2O_2 \rightarrow CO_2 + 2H_2O$), methane is converted into carbon dioxide which reduces greenhouse effect contributions since CH_4 has a global warming potential (GWP) of 25 and CO_2 a GWP of only 1 (IPCC, 2007b). However, the aforementioned environmentally-related legislation initiated a shift from anaerobic digesters using mainly animal wastes to a growing number of agro-industrial facilities exploiting specially grown energy crops. Meanwhile, this trend is not without controversy as many farms switched to an exclusive cultivation of energy crops which can cause ecological problems and may compete with other land uses. This and related issues will be discussed later on.

1.2 SCOPE AND STRUCTURE OF THE THESIS

The main focus in this dissertation is the numerical simulation of anaerobic digestion processes in agricultural biogas plants. For this purpose, the widely recognised Anaerobic Digestion Model No.1 (ADM1) has been utilised together with corresponding simulation software. In the context of a research project dealing with the development of novel concepts for agricultural biogas plants, different aspects have been investigated and simulated including corresponding modifications and adjustments of the mathematical model. This was supplemented by laboratory experiments as well as on-site measurement campaigns and the data gained there was used for calibration and validation of the numerical models.

The outcomes of this dissertation are presented in 5 scientific papers which constitute the core of this work together with a concluding summary in chapter 9 (Conclusions). When preparing the different papers it has been tried to follow a conceptual thread by

covering consecutive subjects that comprise issues such as biogas plant design, co-digestion of different substrates and start-up strategies. The articles as listed in the table below are labelled with capital letters which are used in the thesis for connecting the papers with an associated appendix containing supplementary information for each paper (except Appendix A which holds general information on ADM1). The following chapters 1 through 3 present an introduction to, and an explanation of the concepts presented and applied in the papers.

A	Schoen M. A., De Toffol S., Wett B., Insam H. and Rauch W. (2007). Comparison of renewable energy sources in alpine regions. *Managing Alpine Future. Borsdorf, A., Stötter, J., Veulliet, E. (Eds.). Austrian Academy of Sciences Press, ISBN 978-3-7001-6571-2.*
B	Wett B., Schoen M. A., Phothilangka P., Wackerle F. and Insam H. (2007). Model-based design of an agricultural biogas plant: application of Anaerobic Digestion Model No. 1 for an improved four chamber scheme. *Water Science and Technology, 55 (10), 21-28.*
C	Schoen M. A., Phothilangka P., Eladawy A., Insam H. and Wett B. (2007). Farmscale co-fermentation of manure and organic waste. *IWA-workshop on anaerobic digestion in mountain area and isolated rural zones. 5-7/Jun/2007, Chambéry, France*
D	Schoen M. A., Sperl D., Gadermaier M., Goberna M., Franke-Whittle I., Insam H. and Wett B. (2008). Comparison of biogas plant start-up procedures based on lab- and full-scale data and on numerical modelling. *Second international symposium on energy from biomass and waste. 17-20/Nov/2008, Venice, Italy*
E	Schoen M. A., Sperl D., Gadermaier M., Goberna M., Franke-Whittle I., Insam H., Ablinger J. and Wett B. (2009). Population dynamics at digester overload conditions. *Submitted to Bioresource Technology*

2 LITERATURE REVIEW

This chapter provides a general overview of some of the microbial aspects of anaerobic digestion (AD) and their mathematical simulation. The purpose is to give some background information to the interpretation of the results presented in the subsequent chapters. In a prefatory section, some aspects of biogas utilisation will be explained in brief.

2.1 BIOGAS UTILISATION AND AGRICULTURAL ASPECTS

2.1.1 GENERAL ISSUES

With an overall growth of 70% between 1970 and 2004, the largest contribution to global greenhouse gas (GHG) emissions has come from the energy supply sector with an increase of 145% (IPCC, 2007a). Thus, innovations and improvements in this field can have major effects on this issue and contribute to mitigate climate change and its accompanying effects. Among other advantages, energy recovery from renewables can help to reduce GHG emissions since - unlike combustion of natural gas, liquefied gas, oil and coal - energy generation from biogas (Figure 2-1) is an almost carbon-neutral way to produce energy from regional available raw materials. Carbon dioxide emissions emerging from the biogas combustion process are part of the natural carbon cycle and get absorbed and consumed by plants while growth.

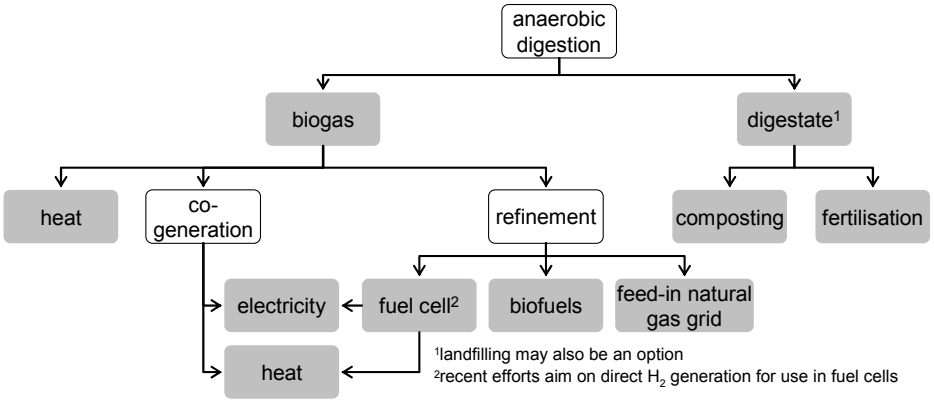

Figure 2-1 Principal options for conversion and utilisation of biogas and digestate in plants using renewables (illustration may not be exhaustive)

Besides hydro power, solar energy, biomass energy and wind energy, biogas plants are important producers of electricity and heat from renewables. However, there are some shortcomings. Below, major benefits and drawbacks of energy production with biogas plants are listed (EPA, 2005; IPCC, 2007a, b, c; Wikipedia, 2008).

Benefits:

- utilization of locally available, renewable resources
- no supply costs in the case of agricultural waste products utilisation
- almost carbon-neutral energy supply

- local energy supply – no overland lines required
- controllable performance – adjustable to demand
- capability to provide base load electricity
- improved fertilisation quality compared to raw agricultural wastes

Drawbacks:

- high initial investment costs and regular staff expenses
- possibility of unpleasant odour
- biogas plants which are not absolutely gastight have detrimental effects on the environment since methane has a global warming potential of 25 (time horizon 100 years) which means a 25 times higher contribution to greenhouse effect than CO_2
- requirement of sufficient land area for storage and spreading of digestate
- exclusive cultivation of energy crops may cause ecological problems (monocultures, intensive farming)
- widespread use of agricultural land for biomass production for energy may compete with other land uses and may have implications for food production costs and food security (not valid in the case of agricultural waste products utilisation)

2.1.2 CONFIGURATIONS OF BIOGAS SYSTEMS

Generally, for the production of biogas by anaerobic digestion processes, residues from livestock farming, food processing industries, waste water treatment sludge, and other organic wastes can be utilised. Anaerobic digesters can be designed and engineered to operate using a number of different variants and process configurations. An overview on classification methods is given in Figure 2-2.

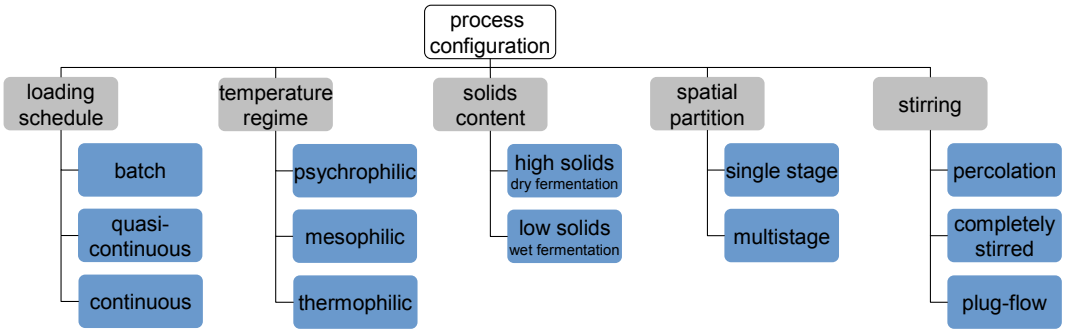

Figure 2-2 General classification methods of biogas systems

Anaerobic digestion processes can be classified according to the total solids (TS) content of the slurry in the digester and categorized further on the basis of number of reactors used, into single stage and multi stage. In single stage reactors, the different stages of anaerobic digestion occur in one reactor while multi stage processes make use of two or more reactors that separate the steps in space.

When looking at the total solids content (TS) of the feedstock to the digesters, biogas reactors can either be designed to operate at a high solids content (TS > ~20%), or at a low solids concentration. Plants treating substrates with high solids content are referred

to as dry fermentation reactors, those with low solids content are called wet fermentation systems. Also, there are combinations of both (semi-dry or wet-dry). Low-solids digesters can transport material through the system using standard pumps with a significantly lower energy input but require more volume and area due to an increased liquid-to-feedstock ratio. The dry fermentation process utilises solid, stackable biomass and organic waste, which cannot be pumped. It is mainly based on a batch wise operation with a high TS content ranging from 20 to 50% at mesophilic temperatures. Dry fermentations systems are operated in a variety of specifications with and without percolation in digesters having a box or container shape accessible for loading machinery as well as in digesters formed by an airtight plastic sheeting filled with substrate without any further conditioning. Digesters which solely work on the dry system with very little or no additional liquid are inoculated with digested substrate and thus, inoculants and fresh material have to be mixed in suitable ratios beforehand. In dry–wet fermentation systems the substrates don't need to be mixed or inoculated as bacteria rich percolation liquid re-circulated from the digester effluent takes over the role of the bacterial inoculation and process starting. The liquid that is heated in a heat exchanger, is either sprayed over the biomass from nozzles on top of the tank or flooded into the reactor (Eder and Schulz, 2006; Koettner, 2002).

Regarding the flow pattern of anaerobic digesters two basic types can be distinguished: batch and continuous. In continuous flow reactors which normally are completely mixed the processes involved in anaerobic digestion proceed spatially as well as temporally in parallel steps whereas batch reactors exhibit temporally staggered sequences. The operation of batch-type digesters consists of loading the digester with organic materials and allowing it to digest. Once the digestion is complete, the effluent is removed and the process is repeated. For example, covered lagoons and anaerobic sequencing batch reactors (SBR) are operated in batch mode.

- A covered lagoon consists of a pond containing the organic wastes which is fitted with an impermeable cover that collects the biogas. The cover can be placed over the entire lagoon or over the part that produces the most methane. The substrate enters at one end of the lagoon and the effluent is removed at the other. Cover lagoons are not heated and operate at ambient temperatures which implies seasonal variations in reaction and conversion rates. The advantage of anaerobic lagoons are relatively low costs which are partly offset by lower energy yields and poor effluent quality.

- Anaerobic sequencing batch reactors (SBR) are discontinuously operated in a fill and draw mode. Filling of the tank is followed by a reaction period yielding biogas. During this stage the substrate is allowed to settle to the bottom of the tank and the solids separate from the effluent liquor. After that the supernatant and the digested substrate are withdrawn except a small portion which is retained in the tank in order to inoculate the incoming feed with active microorganisms.

In a continuous or quasi-continuous digester, organic material is constantly or regularly fed into the digester where it is moved forward either mechanically or by the force of the new feed pushing out digested material. Unlike batch-type digesters, continuous digesters produce biogas without the interruption of loading material and unloading effluent. Continuous digesters include plug-flow systems, continuous stirred tank reactors (CSTR), and high-rate biofilm systems such as upflow anaerobic sludge blanket reactors (UASB).

- In most cases, a plug-flow digester comprises a stirred and heated horizontal tank which is fed at one end and the emptied at the other. By continuous feeding a 'plug' of substrate is slowly moved through the tank towards the effluent. This mode of operation has various advantages including the prevention of premature removal of fresh substrate through hydraulic short-circuiting and a high sanitising potential. Since the plug flow digester is a growth based system where the biomass is not conserved, it is less efficient than a retained biomass system (e.g. UASB) and inoculation may be required.

- Basically, a continuous stirred tank reactor (CSTR) consists of a closed vessel equipped with stirring devices providing mixing of the content. The reactor is continuously fed with substrate and due to the mixing it can be assumed that the concentrations of the compounds inside the vessel equal those at the effluent. Also, there is no liquid-solid separation or stratification and, hence, the solids retention time (SRT) is the same as the hydraulic retention time (HRT). Since the biomass is suspended in the main liquid and will be removed together with the effluent, relatively long HRTs are required to avoid an outwash of the slow-growing methanogens. The CSTR system is also addressed by the Anaerobic Digestion Model No.1 (Batstone *et al.*, 2002a) which represents one of the major issues of the work presented in this thesis as will be discussed in subsequent chapters.

- Upflow anaerobic sludge blanket reactors (UASB) belong to the group of so-called high-rate anaerobic reactors. The term "high-rate" refers to reactor configurations that provide significant retention of active biomass, resulting in large differences between the SRT and the HRT, and operation at relatively short HRTs, often on the order of two days or less (Grady *et al.*, 1999). In an UASB digester the influent is introduced into the bottom of the vessel with a relatively uniform flow across the reactor cross section and distributed such that an upward flow is created. In the upper portion of the tank a cone shape with a widening cross section is introduced reducing the flow as it rises. As a consequence, combined with the flow rising upward from the bottom, gradually descending sludge will be hold in equilibrium forming a blanket which suspends in the tank. Small sludge granules begin to form whose surface area is covered with aggregations of bacteria. Finally the aggregates form into dense compact biofilms referred to as "granules". Substrate flows upwards through the blanket and is degraded and converted to biogas by the anaerobic microorganisms. Treated effluent exits the granular zone and flows upward into the gas-liquids-solids separator. There, the gas is collected in a hood and the supernatant liquid is discharged while separated solids settle back to the reaction zone. The combined effects of influent distribution and gas production result in mixing of the influent with the granules. Some variants of biofilm reactors use upflow reactors provided with an internal packing to improve sludge blanket stability. The media have a high specific surface and allow for the growth of attached biomass.

Generally, choice of reactor type is determined by waste characteristics, especially particulate solid contents. Consequently, the process must be able to convert solids to gas without clogging the anaerobic reactor. Solids and slurry waste are mainly treated in continuous flow stirred tank reactors (CSTR), while soluble organic wastes are treated using high-rate biofilm systems such as UASB reactors (Boe, 2006). However, regarding anaerobic co-digestion based on manure slurry and organic wastes, which is the main focus in this thesis, it should be noted that high-rate biofilm systems are not suit-

able for treating such kinds of substrate since they are not effective in converting particulate solids to gas and tend to clog while digesting slurries. As explained previously, these reactors have very low HRTs and bacteria are retained in these reactors. The bacteria convert the soluble constituents to gas but have little opportunity to hydrolyze and degrade the particulate solids, unless the solids become attached to the biomass (Burke, 2001).

Further design aspects are factors such as the solid retention time, organic and hydraulic loading rates and type of substrate. These issues will be discussed later on in chapter 2.2.2.

2.2 ANAEROBIC DIGESTION

As already mentioned, anaerobic process technologies, initially intended for food and beverage production, have been developed and applied over many centuries (Batstone *et al.*, 2002a). With the employment of AD for treatment of organic waste and biogas production, an environmentally attractive technology has been established. It has several environmental benefits with regard to waste treatment, pollution reduction, production of CO_2-neutral renewable energy and improvement of agricultural practices by recycling of plant nutrients (Boe, 2006).

From a microbiological viewpoint, the anaerobic degradation of complex organic matter into methane and certain by-products is a complex multi-step process of metabolic interactions performed by a well-organised community of microbial populations. Accordingly, a variety of microorganisms coexist in anaerobic digesters even when a single substrate is utilized and their concerted activity is necessary for the complete bioconversion of organic materials to methane, carbon dioxide as well as trace gases such as hydrogen sulphide and hydrogen. Maintaining a healthy bacterial population heavily depends on the microbial status and suitable operating conditions (Björnsson, 2000; Lee et al., 2009).

2.2.1 MICROBIAL ASPECTS OF THE ANAEROBIC PROCESS

Digestion of particulate composites can be roughly subdivided into four phases, termed hydrolysis/liquefaction, acidogenesis, acetogenesis and methanogenesis (Figure 2-3). These phases are a series of interlinked reactions proceeding spatially as well as temporally in consecutive and parallel steps and hence, influence one another.

Hydrolysis is a process where complex macromolecular organic matter comprising carbohydrates, proteins and fats is subject to enzymatic degradation and transformed to monosaccharides, amino acids and long chain fatty acids (LCFA). Further anaerobic digestion finally leads from acidogenesis, acetogenesis and methanogenesis via intermediates and by-products to biogas production (CH_4, CO_2).

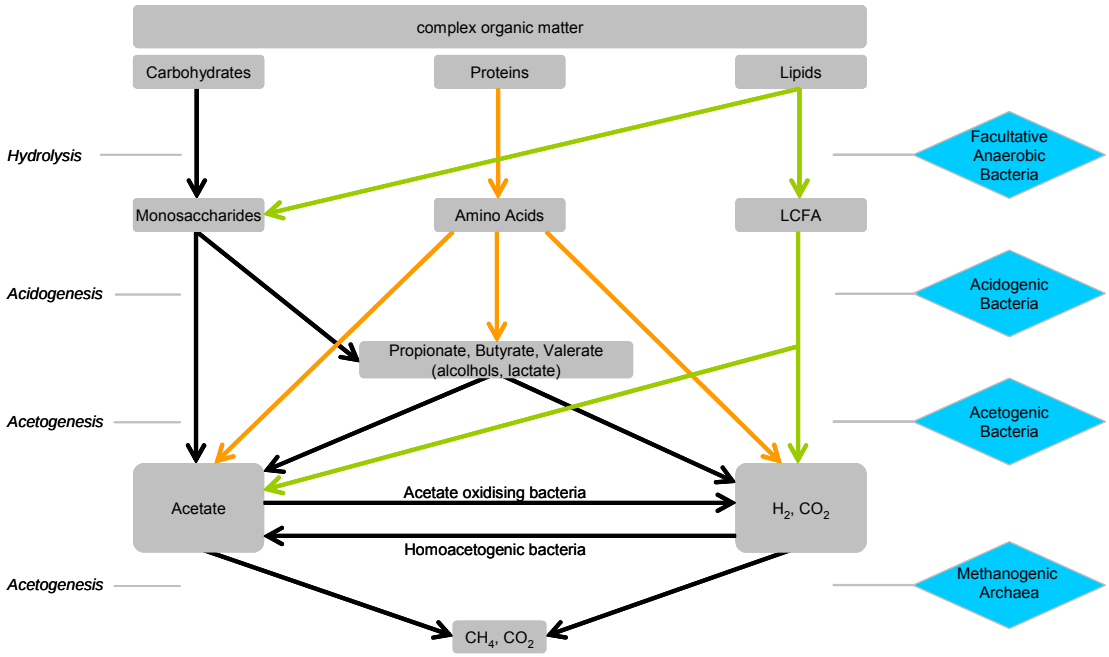

Figure 2-3 Main steps and pathways of anaerobic digestion. Inert fraction of organic matter is not displayed (modified from Batstone *et al.*, 2002a).

2.2.1.1 Hydrolysis

As complex organic polymeric materials cannot be utilized by microorganisms unless they are broken down to soluble compounds, anaerobic degradation starts with the hydrolysis step in which the organic polymers get solubilised into simpler and more soluble intermediates which can then pass the cell membrane (Pavlostathis and Giraldo-Gomez, 1991). Once inside the cell, these simple molecules are used to provide energy and to synthesize cellular components. This phase is also termed liquefaction as the degradation processes involve the dissociation of water.

Hydrolytic reactions which comprise two phases are propelled by extracellular enzymes secreted by bacteria which are obligate or facultative anaerobes. In the first phase a bacterial colonization takes place where the hydrolytic bacteria cover the surface of solids. Bacteria on the particle surface release enzymes and produce the monomers which can be utilized by the hydrolytic bacteria themselves, as well as by the other bacteria. In the second phase the particle surface will be degraded by the bacteria at a constant depth per unit of time (Vavilin et al., 1996).

Released enzymes include cellulase, cellobiase, xylanase and amylase for degrading carbohydrates into simple sugars (monosaccharides), protease for degrading protein into amino acids and lipase for degrading lipids into glycerol and LCFA.

The overall hydrolysis rate depends on organic material size, shape, surface area, biomass concentration, enzyme production and adsorption (Parawira *et al.*, 2005; Grady *et al.*, 1999; Boe, 2006). It is commonly found that hydrolysis is the rate-limiting step for digestion when the substrate is in particulate form (e.g. swine waste, cattle manure and sewage sludge) while methanogenesis is the rate-limiting step for readily degradable substrate (Vavilin et al., 1996; Vavilin et al., 1997).

2.2.1.2 Acidogenesis

The step subsequent to hydrolysis is referred to as acidogenesis (also termed fermentation) which is generally defined as an anaerobic acid-producing microbial process without an additional electron acceptor or donor (Gujer and Zehnder, 1983). The monosaccharides and amino acids resulting from hydrolysis are degraded to a number of simpler products such as volatile fatty acids (VFA) including propionic acid (CH_3CH_2COOH) and butyric acid ($CH_3CH_2CH_2COOH$) as well as acetic acid (CH_3COOH). However, the organisms oxidising LCFA are required to utilise an external electron acceptor such as hydrogen ions or CO_2 to produce H_2 or formate (Batstone *et al.*, 2002a).

The degradation of monosaccharides (e.g. glucose) can manifest in different pathways which leads to the emergence of different products (Table 2-1) such as VFA, lactate, and ethanol with different yields of energy. The dominant pathway depends on several factors such as substrate concentration, pH and dissolved hydrogen concentrations. For example, under very high organic loads, lactic acid production becomes significant. At higher pH (>5) the production of VFA is increased, whereas at low pH (<5) more ethanol is produced. At even lower pH (<4) all processes may cease.

Table 2-1 Examples of different products from glucose degradation

Products	Reaction		
Acetate	$C_6H_{12}O_6 + 2H_2O$	$\rightarrow$	$2CH_3COOH + 2CO_2 + 4H_2$
Propionate + Acetate	$3C_6H_{12}O_6$	$\rightarrow$	$4CH_3CH_2COOH + 2CH_3COOH + 2CO_2 + 2H_2O$
Butyrate	$C_6H_{12}O_6$	$\rightarrow$	$CH_3CH_2CH_2COOH + 2CO_2 + 2H_2$
Lactate	$C_6H_{12}O_6$	$\rightarrow$	$2CH_3CHOHCOOH$
Ethanol	$C_6H_{12}O_6$	$\rightarrow$	$2CH_3CH_2OH + 2CO_2$

(Batstone *et al.*, 2002a)

However, hydrogen partial pressure has been reported to have most influence on the fermentation pathway. At low partial pressures of hydrogen the fermentation pathway to acetate and hydrogen is favoured rather than ethanol or butyrate formation. Thus, in a system where the hydrogen-utilising organisms (such as methanogens) maintain low partial pressure of hydrogen, the fermentation pathway to acetate and hydrogen contributes the main carbon flow from carbohydrates to methane formation. However, higher VFA and alcohols are still produced continuously by the degradation of lipids and amino acids (Schink, 1997; Boe, 2006). These products can not be utilised directly by the methanogens and must be degraded further in a subsequent process that is referred to as acetogenesis (Björnsson, 2000).

Acidogenesis is often the quickest step in the anaerobic conversion of complex organic matter in liquid phase digestions. So, process-failure in the anaerobic digestion of complex organic matter due to the influence of various toxic or inhibitory components leads to a halt of methane production and an accumulation of long- and short-chain fatty acids (Vavilin et al., 1996).

2.2.1.3 Acetogenesis

As already mentioned before, the degradation of higher organic acids formed in acidogenesis is an oxidation step with no internal electron acceptor. Thus, the oxidising organisms (normally bacteria) require an additional electron acceptor such as hydrogen ions or CO_2 for the conversion to acetate, carbon dioxide and hydrogen (Batstone *et al.*, 2002a). This intermediate conversion is crucial for the successful production of biogas, as these compounds can not be utilised directly by methanogens. Since acetogens are obligate hydrogen producers and in the same time depend on a low partial pressure of hydrogen, they maintain a syntrophic (mutually beneficial) relationship with hydrogen-consuming methanogenic archaea. This interspecies hydrogen transfer where the methanogens serve as a hydrogen sink allows the fermentation reactions to proceed. Syntrophy means, literally, “eating together” and is a special case of symbiotic cooperation between two metabolically different types of microbial organisms which depend on each other for degradation of a certain substrate, typically for energetic reasons (Schink, 1997; Björnsson, 2000).

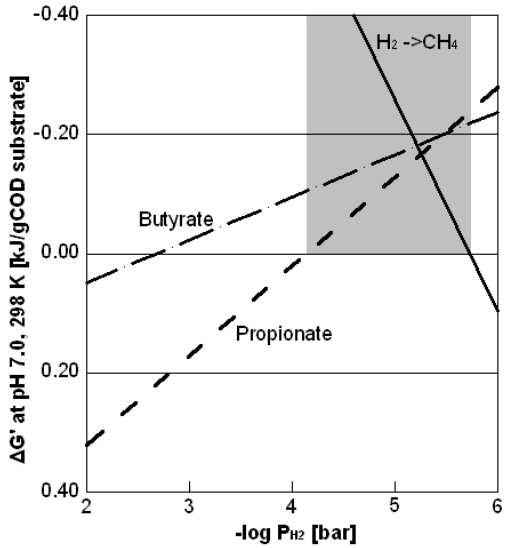

Figure 2-4 Thermodynamic (Gibb’s energy ΔG’) dependence on H_2 partial pressure. Calculations based on standard values for free energies at pH 7.0, 25°C (adapted from Batstone *et al.*, 2002a).

As shown in Figure 2-4, low H_2 partial pressure is essential for acetogenic reactions to be thermodynamically favourable ($\Delta G' < 0$), whereas hydrogen consuming methanogenesis becomes more favourable at higher pressures. Thus, these reactions can only occur simultaneously within a narrow range of very low P_{H2}. The shaded area shows the theoretical operating region for syntrophic acetogenesis from propionate.

An example of the free energy yield for the conversion of butyrate to acetate and methane is shown in Table 2-2. The degradation of butyrate to acetate is not energetically feasible because it carries out a reaction which is endergonic under standard conditions, but is dependent on co-culture with a hydrogen-scavenging partner organism (hydrogenotrophic methanogens). The second reaction in Table 2-2 provides a yield of energy which is partly transferred by the methanogens back to the acetogens. Thus, the overall syntrophic reaction is thermodynamically favourable with a small energy yield ($\Delta G' < 0$). The low energy yield makes the organisms very slow-growing and sen-

sitive to changes in organic load and flow rate. Acetogens are sensitive to environmental changes, and long periods are likely to be required for these bacteria to adjust to new environmental conditions (Björnsson, 2000).

Table 2-2 Energetics of syntrophic degradation

Reaction			ΔG°'
Acetogenesis from butyric acid:			[kJ mol^{-1}]
$2CH_3CH_2CH_2COOH + 4H_2O$	→	$4CH_3COO^- + 4H^+ + 4H_2$	96 (2·48)
Methanogenesis from hydrogen:			
$4H_2 + CO_2$	→	$CH_4 + 2H_2O$	-131
Syntrophic reaction:			
$2CH_3CH_2CH_2COOH + CO2 + 2H_2O$	→	$4CH_3COO^- + 4H^+ + CH_4$	-35

Björnsson, 2000; Schink, 1997

Acetogenic bacteria not only profit from hydrogenotrophic methanogens, but also aceticlastic methanogens, as acetate removal has an influence on the energetics of VFA oxidizing reactions, especially in iso-valerate degradation, where three molecules of acetate and only one molecule of H_2 are formed. Moreover, acetate accumulation may have a biochemical inhibitory effect on acetogenesis (Boe, 2006).

2.2.1.4 Methanogenesis

During methanogenesis, the fermentation products such as acetate and H_2/CO_2 are converted to CH_4 and CO_2 by methanogenic archaea which are strict obligate anaerobes. Other methanogens are able to grow on one-carbon compounds such as formate, methanol and methylamine. Generally, methanogens are specialists in substrate utilisation, as some of them can use only one substrate.

The archaea relevant for anaerobic digestion are commonly divided into two groups: one group, termed aceticlastic methanogens, split acetate into methane and carbon dioxide. The second group, termed hydrogenotrophic methanogens use hydrogen as the electron donor and CO_2 as the electron acceptor to produce methane. Nearly all known methanogenic species are able to produce methane from H_2/CO_2, whereas only a few species of methanogens are believed to be capable of utilising acetate as a substrate. However, it has been estimated from stoichiometric relations that about 70% of the methane formed in anaerobic digesters is derived via the acetate pathway. The hydrogen pathway is more energy yielding than the acetate pathway, and is normally not rate limiting. It is, however, of fundamental importance due to its ability to keep the hydrogen pressure low in the system (Klass, 1984; Pavlostathis and Giraldo-Gomez, 1991;Björnsson, 2000).

Moreover, apart from methanogenic reactions, the inter-conversion between hydrogen and acetate catalysed by so-called homoacetogenic bacteria also plays an important role in the methane formation pathway. Depending on the external hydrogen concentration, homoacetogens can either oxidize or synthesize acetate which allows for contention with several different microbes, including methanogens. As can be seen from Table 2-3, the H_2 consumption by hydrogenotrophic methanogenesis is thermodynamically more favourable than homoacetogenesis ($\Delta G°'<0$). Regarding acetate consump-

tion, aceticlastic methanogenesis is also more favourable than acetate oxidation. As already mentioned, hydrogenotrophic methanogenesis works better at high hydrogen partial pressure (Figure 2-4), while aceticlastic methanogenesis is independent from hydrogen partial pressure. At higher temperatures (> 30°C) the acetate oxidation pathway becomes more favourable (Boe, 2006).

Table 2-3 Reactions related to methanogenesis (with standard temperatures)

	Reaction			$\Delta G°'$ [kJ mol^{-1}]
Hydrogenotrophic methanogenesis	$4H_2 + CO_2$	→	$CH_4 + 2H_2O$	-135.0
Aceticlastic methanogenesis	CH_3COOH	→	$CH_4 + CO_2$	-31.0
Acetate oxidation	$CH_3COOH + 2H_2O$	→	$4H_2 + 2CO_2$	+104.0
Homoacetogenesis	$4H_2 + CO_2$	→	$CH_3COOH + 2H_2O$	-104.0

Boe, 2006; Schink, 1997; Batstone *et al.*, 2002a

Hydrogenotrophic methanogenesis has been found to be a major controlling process in the overall scheme of anaerobic digestion. Its failure will strongly affect the syntrophic acetogenic bacteria and the fermentation process as a whole (Schink, 1997). The accumulation of reduced fermentation products in anaerobic digester is mainly due to inadequate removal of hydrogen and acetate due to several reasons. For example, high organic load increases hydrogen and VFA production beyond the capacity of methanogens resulting in accumulation of VFA, or the decreasing in capacity of methanogens due to inhibition by toxic compounds or pH drop (<6) (Boe, 2006).

The hydrogen-consuming methanogens are among the fastest growing organisms in the anaerobic digestion process as their minimum doubling time has been estimated to be six hours, compared with 2.6 days for the slow-growing acetoclastic methanogens. Also, hydrogenotrophic methanogens have been found to be less sensitive to environmental changes than acetoclastic methanogens. Hence, methanogenesis from acetate tends to be rate limiting in the anaerobic treatment of easily hydrolysable substrates (Björnsson, 2000).

2.2.2 FACTORS AFFECTING ANAEROBIC DIGESTION

The performance of an anaerobic process is affected by many factors. These range from process factors such as the solid retention time, organic and hydraulic loading rates to environmental factors such as temperature, pH, nutrient supply, and the presence of toxics to operational factors such as mixing and the characteristics of the waste being treated. The most important factors will be discussed in the following.

2.2.2.1 Temperature

As in all biological processes, anaerobic processes are affected by temperature. This includes the physical-chemical properties of all components in the digester (e.g. viscosity and surface tension) as well as the thermodynamic and kinetic behaviour of the biological processes. Anaerobic digestion can be operated in a wide range of temperatures and anaerobic bacteria are generally divided into three thermal groups including psychrophiles (<20°C), mesophiles (20-40°C), thermophiles (45-70°C) (van Lier et al., 1997;Batstone *et al.*, 2002a), and even extreme- thermophiles (>60°C) (Boe, 2006).

Most important is the effect of temperature on the growth rate and activity of the methanogenic organisms. Within the temperature range of one species the growth rate increases exponentially with temperature following the Arrhenius equation until an optimum temperature is reached. A further arbitrary increase of the temperature is not possible since this would alter the macromolecules and subsequently impede their metabolism. Thus, the growth rate undergoes an exponential decline if the optimum temperature is exceeded (Figure 2-5). The same is true for the methanogenic activity, being the sum of the most important catabolic reactions of the methanogens (van Lier et al., 1997).

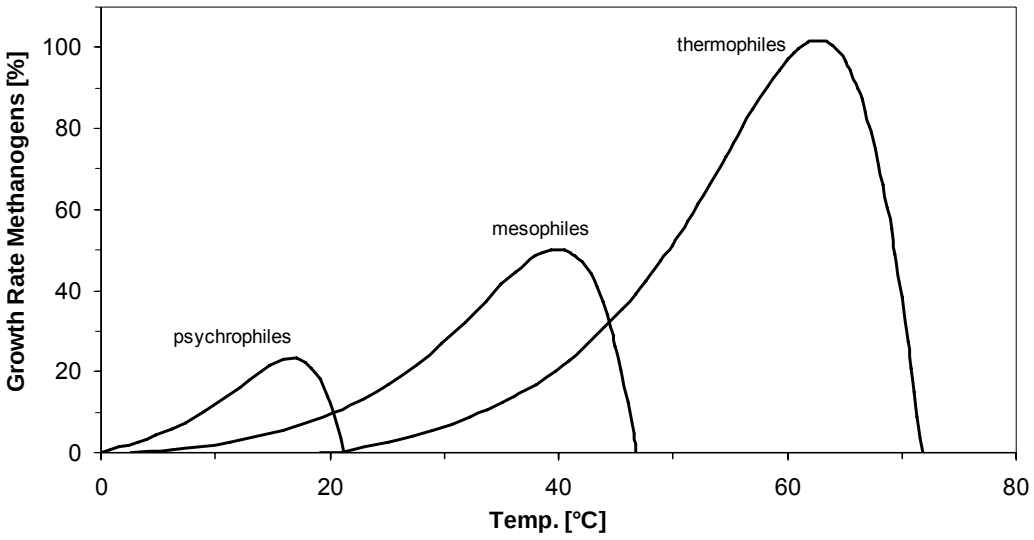

Figure 2-5 Relative growth rate of psychrophilic, mesophilic and thermophilic methanogens (redrawn from van Lier et al., 1997)

Pavlostathis and Giraldo-Gomez, proposed a modified double Arrhenius equation (Eq. 2-1) for the effect of temperature on the net microbial activity (k) recognising that there are two opposing processes (a synthetic and a degradative process):

$$k = k_1 \cdot e^{a_1 \cdot (T - T_0)} - k_2 \cdot e^{a_2 \cdot (T - T_0)} \qquad \text{Eq. 2-1}$$

At low temperatures (i.e. $T<T_0$) the degradative process is insignificant and the net result is an increase in microbial activity. However, when the temperature reaches its optimum value, the effect of the degradative process is much higher than the synthetic process leading to a sharp decrease in the net microbial activity. Further, it was found that the values of bio kinetic coefficients as used in the Monod equation (or variations thereof; Eq. 2-2) like the yield coefficient (Y) and the microorganisms decay coefficient (b) during the conversion of volatile fatty acids (i.e. acetic, propionic, and butyric) were nearly unaffected by temperature. However, both the maximum specific substrate utilization rate (μ_{max}/Y) and the half-velocity coefficient (K_S) varied with temperature (Pavlostathis and Giraldo-Gomez, 1991).

$$\mu = \frac{\mu_{max} \cdot S}{K_S + S} - b \qquad \text{Eq. 2-2}$$

where μ = specific growth rate [T^{-1}], μ_{max}= max. specific growth rate [T^{-1}], S = concentration of the growth limiting substrate [ML^{-3}], K_S = half-velocity coefficient [ML^{-3}], b = spec. microorganisms decay rate [T^{-1}].

Methanogenesis under psycrophilic conditions is characterized by lower rates and hence, a low methane production. In turn, this requires longer solids retention times (SRT) and smaller loading rates. At the same time, problems may occur due to a low mixing intensity and a poor substrate-biomass contact caused by the lower biogas production. It has been found that, if the temperature is shifted from the mesophilic to the psychrophilic range, the microbial population can be very similar in composition and a large number of mesophiles remain active despite the low metabolic rates. This indicates that psychrotolerant rather than psycrophilic microorganisms are involved. In general, the existence of psychrophilic organisms in the anaerobic digestion process is still unclear (van Lier et al., 1997).

Thermophilic anaerobic degradation is characterized by exactly the opposite characteristics as the psychrophilic degradation. The higher temperature allows higher loading rates, shorter SRT, microbes grow in most cases very fast and therefore a higher methane production can be expected. Further advantages are the pathogen inactivation at higher temperatures and smaller reactor sizes due to the shorter SRT. The methane can be used as fuel for heating the reactor which helps to control the operational costs. However, decreased process stability is frequently mentioned as a disadvantage of thermophilic treatment. Due to the higher growth rate and shorter SRT the maintenance of the biomass is more difficult and problems caused by incomplete degradation can occur. The microorganisms either accumulate too fast or are washed out of the reactor.

Moreover, changes in temperature have a fundamental influence on the anaerobic system, mainly because of changes in physico-chemical parameters such as equilibrium coefficients and their overall effects on the system are generally more important than those due to changes in biochemical parameters (Batstone *et al.*, 2002a). For example, increasing temperature decreases pK_A (negative logarithm of the acid ionisation constant) of ammonia, thus, increases the fraction of free-ammonia (NH_3) which is inhibitory to microorganisms. In addition, increasing temperature increases pK_A of VFA, which increase its undissociated fraction, especially at low pH (4-5). This makes the thermophilic process more sensitive to inhibition (Björnsson, 2000; Boe, 2006).

2.2.2.2 pH and buffering systems

In order to determine whether a substance is acidic or basic, the pH method of expression was developed. pH is defined as the negative logarithm of the hydrogen-ion (H^+) concentration and represents a highly important characteristic as it affects equilibria between most chemical species.

Optimal growth of each of the microbial groups involved in anaerobic degradation is closely connected with pH since it impacts on enzyme activity in microorganisms which is a prerequisite for their metabolism. Activity reaches a maximum at its optimal pH only within a specific pH range which is different for each group of microorganisms: for methanogenic archaea the optimal pH comprises a quite narrow interval of 5.5 - 8.5. For the acidogens pH ranges from 8.5 down to pH 4 (Hwang et al., 2004) with an optimum around 6 have been reported. As for the acetogens and methanogens the optimum is around 7 and the growth rate of methanogens falls sharply at pH < 6.6, pH in

an anaerobic one-step treatment process should be maintained close to neutrality (6.5-8.0) since acidogenesis also functions at pH approaching neutrality and methanogenesis is often the rate-limiting step (Bischofsberger et al., 2005; Björnsson, 2000; Boe, 2006; Eder and Schulz, 2006; Grady et al., 1999).

Carbon dioxide produced in the fermentation and methanogenesis phases of the digestion process (roughly 30 to 50% CO_2 content) acts as a weak acid. Due to the partial pressure of gas in a digester, the carbon CO_2 solubilises and reacts reversibly with water to form carbonic acid (Bischofsberger et al., 2005; Tchobanoglous et al., 2003):

$$CO_2 + H_2O \rightleftharpoons H_2CO_3$$

A sufficient level of alkalinity is needed to buffer the pH drop due to the formation of carbonic acid and other acids originally contained or occurring in the substrate during the digestion process (i.e. VFA). Alkalinity is principally due to salts of weak acids and strong bases, and such substances act as buffers to resist a drop in pH resulting from acid addition. Alkalinity is thus a measure of the buffer capacity and is expressed in terms of calcium carbonate with concentrations in the range of 3000 to 5000 mg/L as $CaCO_3$ (Tchobanoglous et al., 2003). The presence and concentration of a buffering compound depends on the composition of the substrate and the total organic load.

For an anaerobic process functioning within the acceptable pH range, the pH is controlled primarily by the bicarbonate buffering system. Bicarbonate alkalinity is produced by the destruction of nitrogen-containing matter and the reaction of the released ammonia nitrogen with the carbon dioxide produced in the reaction (Grady et al., 1999). The following equation is representative for the formation of alkalinity under anaerobic conditions, due to the conversion of organic compounds containing proteins (i.e. nitrogen)(Tchobanoglous et al., 2003):

$$NH_3 + H_2O + CO_2 \rightarrow NH_4^+ + HCO_3^-$$

As illustrated in Figure 2-6, the concentration of bicarbonate alkalinity in solution is related to the CO_2 content of the gas space in the digester and the digester pH. When acids (e.g. VFA) begin to accumulate in an anaerobic process, they are neutralized by the bicarbonate alkalinity present as illustrated for acetic acid (HAc) in the following equation:

$$HCO_3^- + HAc \rightleftharpoons H_2O + CO_2 + Ac^-$$

Under unstable operating conditions, VFAs will react with bicarbonate alkalinity, both reducing its concentration and producing carbon dioxide, which increases the CO_2 content of the gas space. According to Figure 2-6 both of these changes act to decrease the pH in the digester. Thus, stable operation is generally achieved by the maintenance of a relatively high concentration of bicarbonate alkalinity so that increased VFA production can be tolerated with a minimal decrease in digester pH (Grady et al., 1999). However, it should be noted that the principal consumer of alkalinity in a digester is carbon dioxide, and not VFA as is commonly believed (Tchobanoglous et al., 2003).

Manure digesters normally have high feed bicarbonate buffering capacity and a high ammonia content, which makes the pH stable around 7.5-8.0, and the system can tolerate rather high concentration of VFA before pH drop (Boe, 2006).

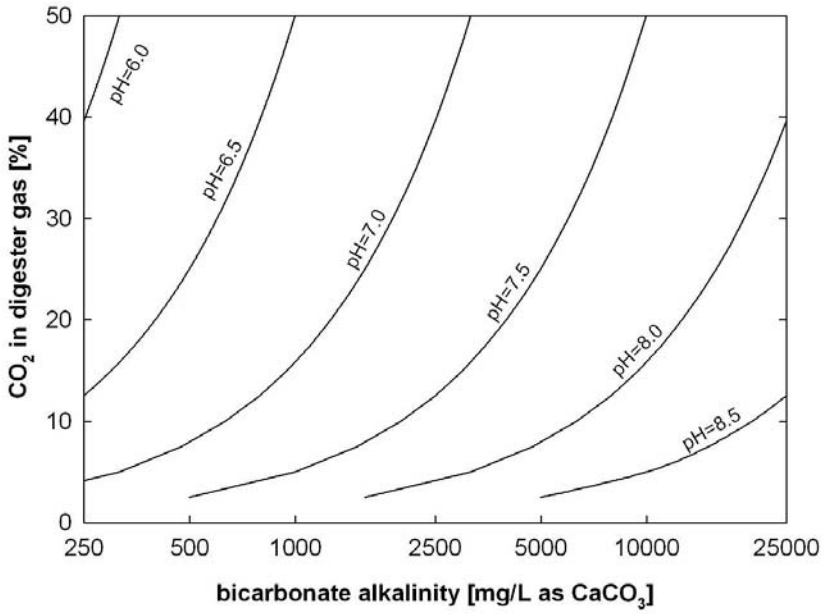

Figure 2-6 Effect of pH on the relationship between the bicarbonate alkalinity of the liquid phase and the carbon dioxide content of the gas phase in an anaerobic process at T=35°C (based on calculations given in Grady et al., 1999; Tchobanoglous et al., 2003)

2.2.2.3 Substrate, nutrients and trace elements

Substrate type and compositions directly determines the biogas yield since the organisms involved in anaerobic digestion must have sources of energy, carbon for the synthesis of new cellular material, inorganic elements (i.e. nutrients) such as nitrogen, phosphorus, sulfur, potassium, calcium, and magnesium, and organic nutrients (also termed growth factors) to continue to reproduce and function properly (Tchobanoglous et al., 2003). Substrate composition also determines the chemical conditions in the reactor, for example the resultant pH and whether certain degradation products and intermediates reach inhibitory concentrations.

Anaerobic substrate input is often measured in terms of total chemical oxygen demand (COD) or total volatile solids (VS). It is important to distinguish between the available degradable fraction (substrate) and the total input, as a considerable fraction of the input may be anaerobically not biodegradable. In general, the term “substrate” refers to the degradable fraction of the input (Batstone *et al.*, 2002b; Møller *et al.*, 2004).

Biomass yields are much lower in anaerobic processes than in aerobic ones as only 4 to 10% of the COD removed is converted into biomass resulting in reduced nutrient requirements (Grady et al., 1999; Gray, 2004). However, at times, proceeding degradation can cause depletion of some of the nutrients turning them into limiting factors and slowing down or inhibit further synthesis (Bischofsberger et al., 2005). On the other hand, most nutrients can be inhibitory if present in high concentrations.

Efficient biodegradation requires that carbon sources and nutrients are available in sufficient amounts in the substrate. The most important nutrients are nitrogen and phosphorous and ratios of C:N = 10:1 to 30:1, N:P = 5:1 to 7:1 as well as COD:N:P = 420:7:1 to 1500:7:1 had been suggested (Bischofsberger et al., 2005; Eder and Schulz, 2006; Gray, 2004). Trace elements are nutrients which are essential but required only

in minor concentrations such as fluorine, iodine, chromium, manganese, zinc, nickel, cobalt and copper. A deficiency of trace elements can have growth limiting effects on the microorganisms whereas too high concentrations of mainly heavy metals can have inhibitory or toxic effects (Bischofsberger et al., 2005; Tchobanoglous et al., 2003). All in all, it can be assumed that all required substances are present in sufficient quantities, especially in swine and cow manure which is subject matter of this thesis.

2.2.2.4 Inhibition and Toxicity

Unfortunately, the literature has not always made a clear distinction between inhibition and toxicity. Within the area of general restriction of biological processes, (Batstone *et al.*, 2002a) suggests the following two definitions according to (Speece, 1996):

- toxicity: an adverse effect (not necessarily lethal) on biological metabolism
- inhibition: an impairment of biological function

Toxicity normally has irreversible effects whereas inhibition is reversible. It should be recognised that, in general, inhibition precedes toxicity as the concentration of a compound is increased. Inhibitory substances either affect the cell structure or the enzymes involved in metabolism (Eder and Schulz, 2006). Further definitions can be made regarding different forms of enzymatic inhibition:

a) Competitive inhibition is a form of enzyme inhibition where binding of the inhibitor to the enzyme prevents binding of the substrate and vice versa. The inhibitor binds to the same active site as the normal enzyme substrate, without undergoing a reaction and preventing the substrate molecule to enter the active site while the inhibitor is there. In this case, the maximum speed of the reaction is unchanged and any given competitive inhibitor concentration can be overcome by increasing the substrate concentration in which case the substrate will outcompete the inhibitor in binding to the enzyme. b) Non-competitive inhibition differs from competitive inhibition in that the inhibitor always binds to the enzyme at a site other than the enzyme's active site. The inhibitor causes a change in the structure and shape of the enzyme which impedes the enzyme's ability to bind with a substrate correctly. This reduces the concentration of 'active' enzyme resulting in a decrease in the maximum rate of reaction. In this mode of inhibition, there is no competition between the inhibitor and the substrate, so increasing the concentration of the substrate still does not allow the maximum enzyme activity rate to be reached. c) Uncompetitive inhibition takes place when an enzyme inhibitor binds only to the complex formed between the enzyme and the substrate (E-S complex). This reduction in the effective concentration of ES reduces both the maximum enzyme activity and the effective K_m (half saturation constant) and cannot be overcome.

Inhibitory compounds are either present already in the substrate or generated during the degradation. The most common inhibitors are formed during degradation of the substrate, such as VFA, LCFA, and ammonia. Some inhibitors are present already in the substrate, such as sulfur compounds, heavy metals and antibiotics (Boe, 2006). Inhibitory effects of these compounds are not inherent but solely depend on concentration and emerge when a certain threshold is exceeded. As mentioned previously, this can be a reversible effect and activity will recover when concentrations fall below thresholds.

The toxicity of NH_3 and VFAs is pH dependent since only the nonionised forms exhibit microbial toxicity. The pK_A for the dissociation of ammonia is approximately 9.3 (at

25°C), so NH_3 is present primarily as the ionised species (i.e. NH_4^+) at the pH values typically occurring in anaerobic processes. VFAs as the main methanogenic precursors (pK_A 4.7-4.9 at 25°C) cause inhibition at pH values below 7. The organisms most affected are aceticlastic and hydrogenotrophic methanogens as well as acetogenic organisms. The last two are in a syntrophic relationship and a decrease in activity of hydrogenotrophic methanogens will cause an apparent decrease in activity of organic oxidising organisms, due to the accumulation of hydrogen and formate (Batstone *et al.*, 2002a). VFAs in their nonionised form (i.e. at low pH) can penetrate and cross the cell membrane. Inside the cell, where a higher pH is maintained, they are ionised, and the released hydrogen ion will cause a decrease in the intercellular pH and a disruption of homeostasis (Björnsson, 2000; Boe, 2006). Moreover, pK_A values change with temperature, hence, the proportion of nonionised forms which are present depends on both pH and temperature Grady et al., 1999.

LCFA are intermediates of the anaerobic digestion of lipids and their associated forms have been found to be inhibitory to various microorganisms even at low concentrations. They can affect the acetogenic bacteria, which are responsible for the oxidation as well as aceticlastic and H_2-oxidizing methanogens by adsorbing onto the cell wall membrane leading to an inhibition of the transport of essential nutrients. Therefore, factors such as cell surface area to LCFA concentration ratio, and pH may have an influence. In general, heavy inhibition is irreversible (i.e. toxic), as recovery cannot be affected by a decrease in influent LCFA concentrations. While the most heavily inhibited organisms are probably aceticlastic methanogens, all organisms are inhibited to a varying degree (Batstone *et al.*, 2002a; Hwu *et al.*, 1996).

Sulfide (S^{2-}) is produced in an anaerobic process through the reduction of sulfate (SO_4^{2-}) present in the influent and by the degradation of sulfur-containing organic matter (e.g. proteins). Only soluble sulfides are inhibitory and concentrations >200 mg/L cause strong inhibition. Sulfide reacts with heavy metal cations forming highly insoluble precipitates and thus, the addition of smaller amounts of sulfide can reduce the toxicity of heavy metals. At pH <7 (pK_A 7.05), sulfide converts to H_2S (via HS^-) which increases the corrosivity of the gas and results in the formation of sulfur oxides when the gas is burned which can be corruptive to engine parts. Hydrogen sulfide is sparingly soluble in water, so it will partition between the liquid and gas phases exhibiting inhibitory effects at concentrations > 20,000 ppm in the gas and >5 mg/L in the liquid phase, respectively (Eder and Schulz, 2006; Grady et al., 1999).

Sulfate (SO_4^{2-}) itself shows no inhibitory or toxic effects, but it can serve as an electron acceptor to sulfate reducing bacteria. Different from methanogens, sulfate-reducing bacteria are metabolically versatile, and a broad community of sulfate reducers can use all products of primary fermentations and oxidize them to carbon dioxide, simultaneously reducing sulfate to sulfide, which is inhibitory, as discussed previously (Schink, 1997). At low concentrations of sulfate, sulfate-reducing bacteria compete with methanogenic archaea for hydrogen and acetate, and at high concentration the sulfate-reducing bacteria also compete with acetogenic bacteria for propionate and butyrate. Sulfate-reducing bacteria can easily outcompete hydrogenotrophic methanogens for hydrogen Stams et al., 2005 This effect is proportional to influent sulfate and it has been reported that hydrogenotrophic methanogens were completely washed-out due to competition with hydrogen-utilising sulfate reducers in an anaerobic reactor treating sulfate-rich wastewater (Boe, 2006).

As already mentioned previously, heavy metals such as chromium, copper, nickel, cadmium, and zinc can have inhibitory or toxic effects on anaerobic digestion. The metal ions bind to the ion-exchange site on the cell membrane and form a matrix with extracellular enzymes. However, particularly high concentrations are required to have a significant effect. Apart from that, other factors such as solubility, pH, and the concentration of sulfide present will affect their concentration in the digester. Consequently, heavy metal inhibition is often prevented by the sulfide produced in the anaerobic process (Grady et al., 1999; Gray, 2004).

Methanogenic bacteria are very sensitive to oxygen which is possibly introduced to the reactor by insufficient substrate pre-conditioning (e.g. crushing). However, any oxygen present in the digester will be rapidly consumed by facultative anaerobic bacteria present in the group of hydrolysing and acidogenic bacteria within the mixed culture in an anaerobic digester (Björnsson, 2000; Eder and Schulz, 2006).

Antibiotics from livestock feed additives and disinfectants can also be inhibitory or even toxic to anaerobic digestion when present in high concentrations. In the field of manure digestion, these substances normally do not cause inhibition if used at recommended levels except when it is applied to the complete livestock or stables get sanitised (Boe, 2006; Eder and Schulz, 2006).

2.2.2.5 Internal mixing and retention time

An effective mixing system is critical to the successful operation of an anaerobic process. It provides

- close contact between the raw and digesting sludges and between the microorganisms and their substrates
- maintenance of a uniform temperature and solids mixture throughout the tank, and prevention of localised accumulation of inhibitory dense substances
- prevention of scum formation and settlement of dense solids
- encouragement of the release of gas from the sludge in the lower regions of the digester

Poor mixing will lead to stratification within the digester and will result in partially digested sludge being withdrawn Eder and Schulz, 2006; Gray, 2004.

The solids retention time (SRT) equals the period that solids are retained in the digester and is a crucial factor affecting reactor performance. SRT requirements depend on the characteristics of the utilised substrate: the easier a substrate can be degraded the shorter the required SRT (Figure 2-7 left). An estimation for the minimum SRT can be gained from the generation times of the microorganisms involved in anaerobic digestion. If SRT is shorter than the generation time of the slowest group of organisms (normally acetogens) a net washout of these will occur. The determination of the maximum SRT is governed by technical and economical aspects since at a certain point, the ratio of additional gas yield to reactor volume deteriorates. Short retention times provide high gas production rates (related to the reactor volume) since mainly the easily degradable substrates are degraded. Regarding the total organic load, short SRTs have poor gas yields (related to the mass of volatile solids applied). In turn, long retention times the gas yield increases and the gas production rate deteriorates (Figure 2-7 right). Moreover, it should be noted that different types of substrate have different

specific gas yields. Generally, SRT controls the types of microorganisms that can grow in the process and influences the degree of degradation as well as the gas yield to a great extent (Eder and Schulz, 2006; Grady et al., 1999).

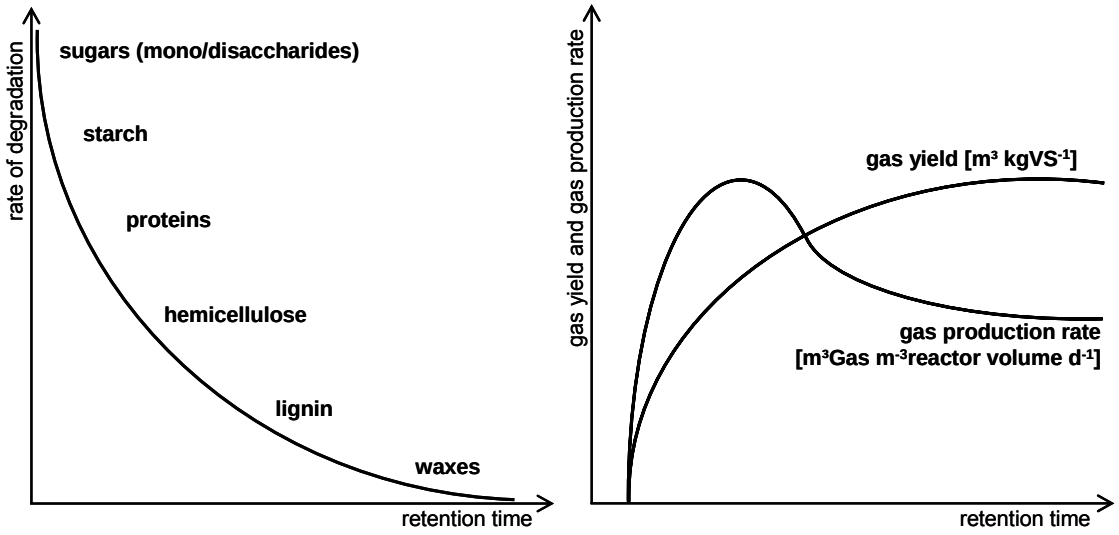

Figure 2-7 Rate of degradation of different types of substrate vs. retention time (left) and gas yield/production rate vs. retention time (adapted from Eder and Schulz, 2006)

2.2.2.6 Organic loading rate

The volumetric organic loading rate (OLR) is related to the retention time through the active biomass concentration in the bioreactor and is used to characterise the loading on anaerobic treatment systems. The OLR provides useful information for the design and operation of anaerobic processes as its knowledge is to quantify how effectively the reactor volume is being utilised. It can be expressed in terms of the mass of volatile solids applied and is calculated as follows:

$$OLR = \frac{Q \cdot C}{V} = \frac{C}{HRT} \qquad \text{Eq. 2-3}$$

where OLR is the volumetric organic loading rate [kgVS $m^{-3}d^{-1}$], Q the influent flow rate [m^3d^{-1}], C the concentration of volatile solids in the substrate [kgVS m^{-3}] and V the bio-reactor volume [m^3]. For completely mixed anaerobic reactors operated without solids recycling the hydraulic retention time (HRT) and the SRT are identical. For digestion systems, which incorporate solids recycle, the SRT will be greater than the HRT and the OLR indicates both the anaerobic digester volume utilisation efficiency and the overall process loading (Grady *et al.*, 1999).

Retention time and OLR are inversly proportional to each other and thus, have to be aligned when designing the reactor layout. The maximum possible OLR depends on both the process temperature and the retention time: the lower the temperature and the longer the retention time the higher the OLRs that can be processed. This maximum value depends also on the specific plant type. The higher the OLR the higher the risk to exceed the performance limit of the degrading biomass. Feeding the system above its sustainable OLR results in low biogas yield due to accumulation of inhibiting sub-

stances such as fatty acids in the digester slurry. Typically, OLR ranges from 2 to 6 kgVS $m^{-3}d^{-1}$ (Eder and Schulz, 2006; Grady et al., 1999).

2.3 ANAEROBIC DIGESTION MODEL NO.1

A major part of the results presented in the papers included in this dissertation is derived from numerical modelling based on the application of the Anaerobic Digestion Model No. 1 (ADM1). In the following, fundamentals and principles of the ADM1 will be explained in brief. Numerical modelling is a tool that allows to investigate the static and dynamic behaviour of a system without doing – or at least reducing – the number of practical experiments. An experimental approach would be very time-consuming if all varieties of combinations and mixtures, temperature and pressure in a complex chemical process would be investigated to identify the optimum combination (Eladawy, 2005). With the results of a few experiments, the rest of the experimental domain can be simulated by a model after proper calibration and validation.

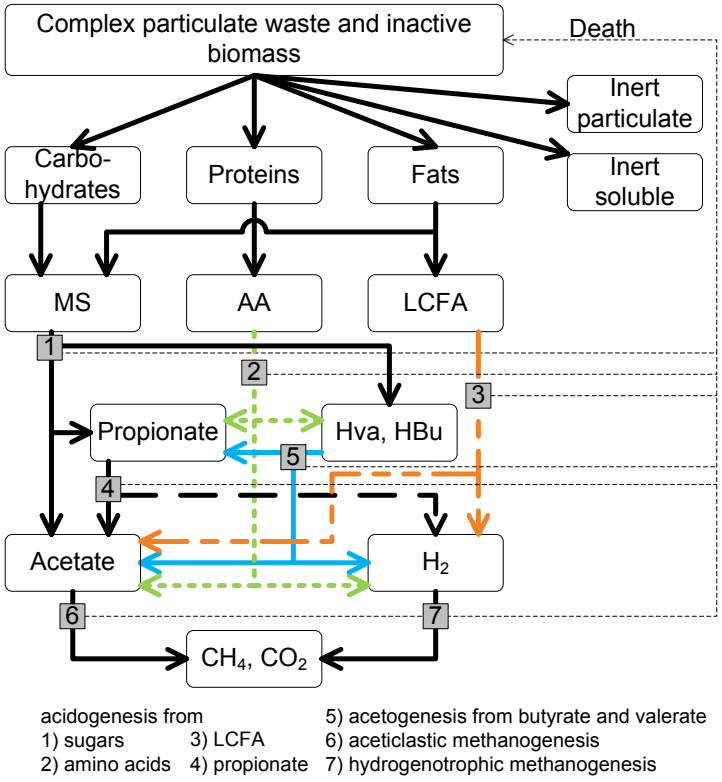

Figure 2-8 Biochemical processes of anaerobic digestion implemented in ADM1 (adapted from Batstone *et al.*, 2002a)

The ADM1 as proposed by the IWA Task Group for Mathematical Modelling of Anaerobic Digestion Processes (Batstone *et al.*, 2002a) is a structured but highly complex model which describes 7 groups of bacteria and archaea (included in a total of 32 dynamic state concentration variables) catalyzing 19 biochemical kinetic processes coupled to 105 kinetic and stoichiometric parameters (Kleerebezem and van Loosdrecht, 2006a). The set of differential equations (DE) of the ADM1 for the calculation of the variables include 10 DE to model the evolution of soluble matter concentrations in the liquid phase and two DE to model inorganic carbon and inorganic nitrogen levels in the liquid phase. Particulate matter and biomass concentrations in liquid phase are de-

scribed by another 12 DE. Additional 8 DE are used to calculate cations and anions levels in the liquid phase and acid–base reactions in order to determine the pH of effluent, ionised forms of organic acids, as well as free ammonia nitrogen and bicarbonate concentrations. Moreover, there are 3 gas–liquid mass transfer equations describing the stripping of methane, carbon dioxide and hydrogen. An overview of the structure is shown in Figure 2-8, while the biochemical kinetic matrix, processes and variables can be found in Appendix A.

The processes in an anaerobic digester comprise a series of interlinked reactions proceeding spatially as well as temporally in sequential and parallel steps. Generally, conversion processes in anaerobic digestion can be divided into two main types referred to as biochemical and physico-chemical reactions (Figure 2-9).

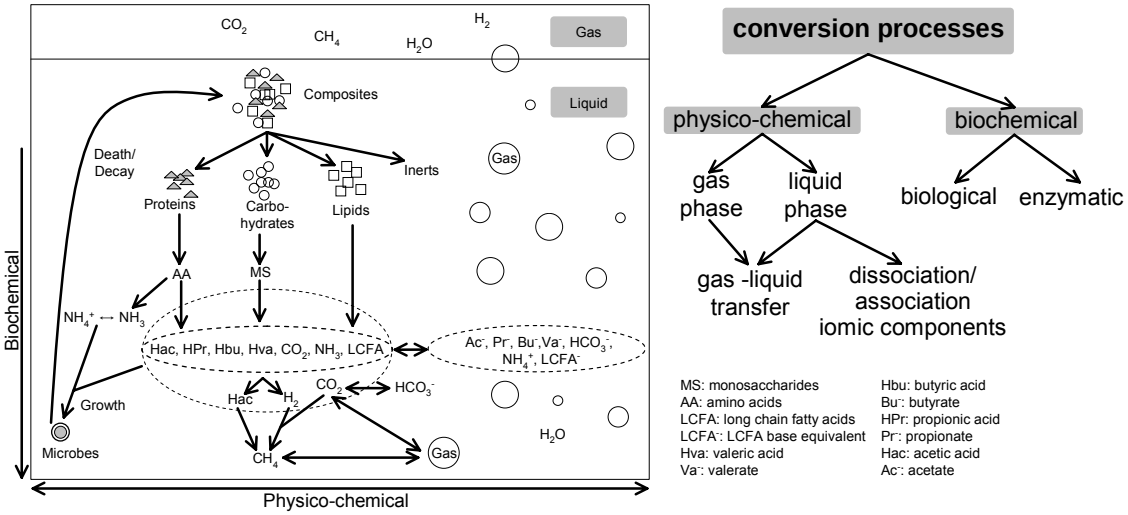

Figure 2-9 Conversion processes in anaerobic digestion as used in the ADM1. Biochemical reactions are implemented as irreversible, while physico-chemical reactions are implemented as reversible. (adapted from Batstone *et al.*, 2000; Batstone *et al.*, 2002a).

- Biochemical reactions:

The biochemical conversion processes are catalysed by intra- or extracellular enzymes produced by microorganisms which subsequently generate bioavailable substrates for digestion. Generally, in ADM1 the anaerobic digestion process is divided into two extracellular steps (disintegration and hydrolysis) as well as three intracellular steps (acidogenesis, acetogenesis and methanogenesis)(Figure 2-8). In the disintegration and hydrolysis steps large complex particulate compounds are disintegrated to shorter chain polymers like carbohydrate, protein, and lipid particulate substrate, as well as particulate and soluble inert material. Two separate groups of acidogens degrade monosaccharide and amino acids to mixed organic acids (C2-C5), hydrogen and carbon dioxide. The organic acids are subsequently converted to acetate, hydrogen and carbon dioxide by acetogenic groups that utilise LCFA, butyrate and valerate, and propionate. The hydrogen produced by these organisms is consumed by a hydrogen-utilising methanogenic group, and the acetate by an aceticlastic methanogenic group (Batstone *et al.*, 2002a).

- Physico-chemical reactions:

These processes are not biologically mediated and encompass within ADM1 liquid-liquid reactions (i.e. ion association/dissociation) and gas-liquid transfer. However, solid precipitation is not included in ADM1. Dissociation/association processes are often referred to as equilibrium processes, and can be described by algebraic equations to calculate the concentration of hydrogen ions, free ammonia, VFA and carbon dioxide. The three main process gas components are: CO_2, CH_4 and H_2, as well as water vapour (Batstone *et al.*, 2002a).

For substrate uptake Monod-type kinetics are used as the basis for all intracellular biochemical reactions. Biomass growth is implicit in substrate uptake:

$$\rho = k_m \cdot \frac{S}{K_S + S} \cdot X \cdot I_1 \cdot I_2 \cdot ... I_n \qquad \text{Eq. 2-4}$$

where ρ is the substrate uptake rate [kgCOD_S $m^{-3}d^{-1}$], k_m is the maximum specific uptake rate [kgCOD_S kgCOD_$X^{-1}d^{-1}$], S is the substrate concentration [kgCOD_S m^{-3}], K_S is the half-saturation coefficient [kgCOD m^{-3}], and X is the substrate-specific biomass concentration [kgCOD_X m^{-3}], and $I_1...I_n$ are modifiers included to describe inhibition by a number of factors including hydrogen (acetogenic groups), free ammonia (aceticlastic methanogens) and pH (all groups). pH inhibition is implemented as one of two empirical equations, while hydrogen and free ammonia inhibition are represented by non-competitive functions. The other uptake-regulating functions are secondary Monod kinetics for inorganic nitrogen (ammonia and ammonium), to prevent growth when nitrogen is limited, and competitive uptake of butyrate and valerate by the single group that utilises these two organic acids. Death of biomass is represented by first order kinetics, and dead biomass is maintained in the system as composite particulate material (Batstone *et al.*, 2002b).

In the following, the principals in modelling of biochemical processes within ADM1 will be shown. The modelling concept is based on a Peterson matrix format wherein the model components, the processes and the associated process rates are organized in a structured way. Processes are organized in rows and model components in columns. Additionally, process rates ρ are formulated for each process used. The quantitative interrelation between substances as they change with time is defined via stoichiometric coefficients with a positive or a negative sign indicating production or consumption, respectively. The reaction rate for a substance *i* is obtained as the sum of productions and consumptions per time step.

For each component and its corresponding biological kinetic rate expressions and coefficients as included in the ADM1 matrix (Appendix A), the mass balance within a system boundary can be expressed via liquid phase equations as follows (assuming a constant reactor volume):

$$\frac{dS_{liq,i}}{dt} = \frac{q_{in} \cdot S_{in,i}}{V_{liq}} - \frac{q_{out} \cdot S_{liq,i}}{V_{liq}} + \sum_{j=1-19} \rho_j \cdot \nu_{i,j} \qquad \text{Eq. 2-5}$$

$$\text{Accumulation} = \text{Input} - \text{Output} + \text{Reaction}$$

where the reaction term is the sum of the kinetic rates ρ_J for process *j* [kgCOD$m^{-3}d^{-1}$] multiplied by the stoichiometric coefficients $\nu_{i,J}$ [-]. S_i is the component concentration [kgCODm^{-3}], q is the flow [m^3d^{-1}], and V_{liq} is the volume of the reactor [m]. Within the

reaction term, there are a number of specific processes (such as growth, hydrolysis, decay etc.) that also influence other components.

The overall specific reaction term (r_i) for each component *i* is obtained by the sum of the product of the stoichiometric coefficients ν_i in column *i* with their associated process rates ρ_i. For example, the overall rate of reaction for monosaccharides (r_1) is:

$$r_1 = \sum_j \rho_j \cdot \nu_{i,j} = k_{hyd,ch} \cdot X_{ch} + (1 - f_{fa,li}) \cdot k_{hyd,li} \cdot X_{li} - k_{m,su} \cdot \frac{S_{su}}{K_s + S} \cdot X_{su} \cdot I_1 \quad \text{Eq. 2-6}$$
$$= \text{hydrolysis of carbohydr.} + \text{hydrolysis of lipids} - \text{uptake of sugars}$$

with the coefficients and abbreviations as given in Batstone *et al.*, 2002a and Appendix A.

The gas phase rate equations are very similar to the liquid phase equations (Eq. 2-5), except there is no advective influent flow, and can be written as follows (assuming a constant gas volume):

$$\frac{dS_{gas,i}}{dt} = - \frac{q_{gas} \cdot S_{gas,i}}{V_{gas}} + \rho_{T,i} \cdot \frac{V_{liq}}{V_{gas}} \quad \text{Eq. 2-7}$$

where $S_{gas,i}$ is the gas concentration of gas *i* [kmole m^{-3}], q_{gas} is the gas flow [$m^3 d^{-1}$], and V_{liq} and V_{gas} are the volumes of the reactor and the headspace [m^3], respectively. $\rho_{T,i}$ is the kinetic transfer rate of gas i [kmole $m^{-3} d^{-1}$] to the gas headspace which can be calculated for example for CO_2 as follows:

$$\rho_{T,CO2} = k_L a_{CO2} \cdot (S_{liq,CO2} - K_{H,CO2} \cdot p_{gas,CO2}) \quad \text{Eq. 2-8}$$

where k_La is the dynamic gas–liquid transfer coefficient [d^{-1}], $K_{H,CO2}$ is the Henry's law equilibrium constant [kmole $m^{-3} bar^{-1}$], $p_{gas,CO2}$ is the CO_2 gas phase partial pressure [bar] and $S_{liq,CO2}$ is the liquid CO_2 concentration [kmole m^{-3}].

Within ADM1, COD [kgCOD m^{-3}] was chosen as the chemical component base unit, with inorganic carbon (HCO_3^- and CO_2) and nitrogen (NH_4^+ and NH_3) in [kmoleC m^{-3}] and [kmoleN m^{-3}], respectively. The advantage of the Peterson matrix presentation method (ADM1 matrix in Appendix A) is that the conservation of COD, nitrogen and carbon can be easily checked and balancing is implicit in the equations. The stoichiometric coefficients (after adjustment to consistent units) for each matrix row should add up to Zero, as COD, carbon or nitrogen lost from reactants must flow to products (Batstone *et al.*, 2002a). For comprehensive particulars regarding the utilised parameters, variables, coefficients and abbreviations the reader is referred to Appendix A.

3 MATERIALS AND METHODS

In this chapter, materials and methods which form the basis of the work presented in the enclosed scientific papers are described in detail. This includes information on the setup of the utilised lab-scale and pilot-scale biogas plants as well as on mathematical simulation software and model calibration procedures.

3.1 LAB-SCALE BIOGAS PLANT

In order to conduct anaerobic digestion tests and analyses under defined boundary conditions, a lab-scale biogas plant with four continuous stirred tank reactors (CSTR) was utilised (Figure 3-1).

3.1.1 DIGESTERS

Each of the four cylindrical shaped CSTR with a diameter of 300 mm and a volume of 100 L is equipped with a mechanical stirrer, heating jackets and insulation. The four stirrers were connected via a transmission belt with one drive in order to maintain the same stirring velocity in each reactor. The heating jackets were connected with a computerized temperature control unit which allows for easy changing of the temperature values required in the experiment with an accuracy of ± 0.5° C.

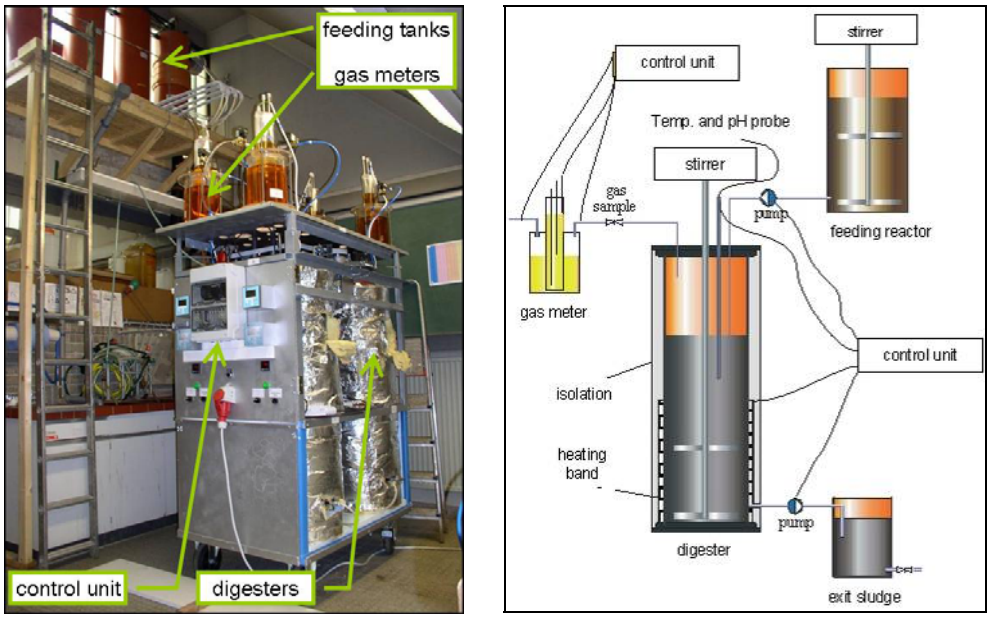

Figure 3-1 Setup and a schematic layout of the lab scale digesters (Eladawy, 2005)

3.1.2 GAS METER

Four gas meters on the top of the lab digesters were used to measure gas production (Figure 3-2). Each of them consists of two concentrical, hydraulically connected cylinders with 100 mm in diameter and 520 mm in height (inner) and 200 mm in diameter and 295 mm in height (outer), respectively.

Colored water (methyl orange) inside the gas meter was used to indicate the gas volume. The gasflow into and out of the gas meters was controlled by electrical valves which were operated according to signals induced by three level rods. The rods were situated inside the inner cylinder, with the first one attached to the cylinder base indicating the zero water level and the second and third one indicating water levels X_1 and X_2. When biogas from the digester flows into the gas meter, the water inside the outer cylinder is displaced to the inner one. There, when the rising water level increases from X_1 to X_2, the gas inlet valve is switched off and the gas outlet valve opens. Subsequently, the water level falls back to X_1 and the gas inlet opens again. Each increase of the water level from X_1 to X_2 was monitored by a counter in the control unit. From that number the total gas amount can be calculated using the following equation:

$$G_T = n \cdot a \cdot h \qquad \text{Eq. 3-1}$$

where:
G_T .... total amount of gas production [m^3]
n ..... number of times the water level increased from X_1 to X_2 [-]
a ..... cross section area of the inner cylinder [m^2]
h ..... the difference in water level between X_1 and X_2 [m]

Figure 3-2 Gas meters on top of the lab digesters

3.2 BIO4GAS DEMONSTRATION PLANT

In regions with a small structured agriculture, as it is the case in the alpine parts of Austria, the construction of biogas plants is often considered to be uneconomical. Due to costly individual planning, small facilities generate higher specific costs than larger plants which keeps many potential operators from such an investment. Therefore, commercially available biogas plants covering the size range < 100 kW_{el} are lacking.

To meet this obstruction, in the framework of the research project *BIO4GAS* the development of an innovative 4-chamber (Figure 3-3) system with a standardised design and construction elements was initiated in order to provide an affordable, cost-effective, small-scale (< 100 kW_{el}) biogas plant (Schoen et al., 2008).

After preliminary studies and lab tests which are widely covered in the papers included in this dissertation, the plant (approx. 20 kW_{el}) was constructed and taken into operation at the Tyrolean farming school in Rotholz, Austria (Landwirtschaftliche Lehranstalt

Rotholz) which is hosting a livestock mainly consisting of cattle (around 100 livestock units).

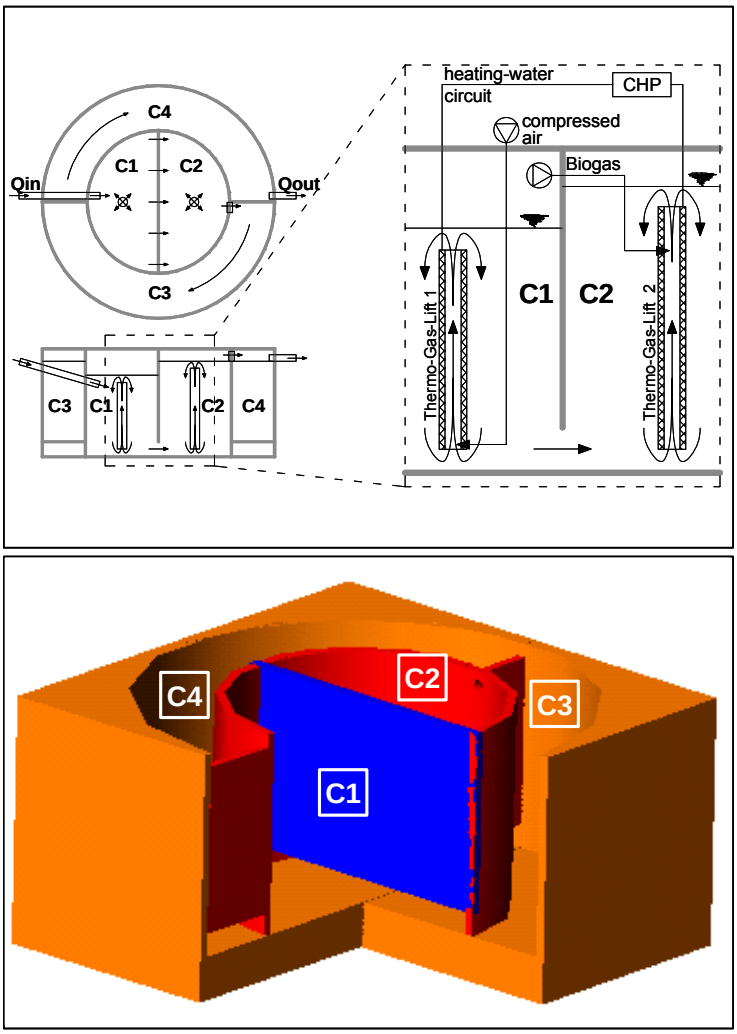

Figure 3-3 Layout and flow scheme of the 4-chamber pilot plant with cylindrical shape and thermo-gas-lift system

The projected pilot plant has a circular-shaped 4-chamber layout which is formed by two concentric cylinders. The inner cylinder and the outer ring contain two chambers, respectively, each separated by scum baffles. The mode of operation is as follows: substrate is pumped to chamber 1 (C1) and biogas production starts. Since the construction is gas-tight, gas pressure in the head space of C1 displaces liquid below the baffle to C2. The outflow from C2 to C3 is accomplished by a weir outlet situated right under the top sealing of the reactor. Within C3 and C4 an annular flow is induced intermittently by a stirrer which mobilises settled solids. Deposits in C1 and C2 are avoided by periodical opening of a pressure relief valve between the headspaces of those chambers. When the valve is opened, the different gas pressures in C1 and C2 get balanced which is accompanied by oscillations and a subsequent recycle flow between C1 and C2 (Figure 3-4).

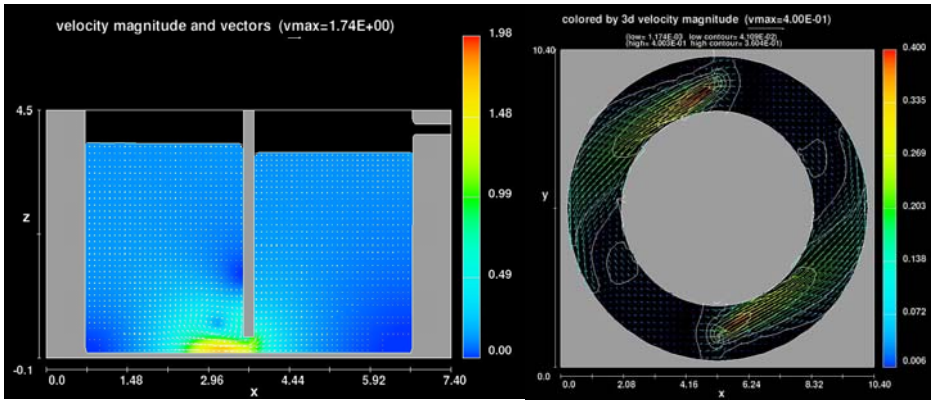

Figure 3-4 Numerical CFD simulation of oscillations between C1 and C2 (left) and the annular flow of substrate in C3 and C4 (right) (Premstaller and Feurich, 2006)

One of the innovative features of the plant is the thermo-gas-lift system (Figure 3-3) which is installed in C1 and C2. This patented device serves for both mixing and heating of the substrate. The latter is accomplished through the double-walled layout of the thermo-gas-lift pipe acting as a heat exchanger which is filled with a heating medium. Agitation of the material results from three effects:

- following the principle of an airlift pump, compressed air is introduced at the lower end of the thermo-gas-lift in C1 resulting in upward moving air bubbles. Since the air-substrate mixture inside the pipe is less dense than the surrounding material, it rises upwards towards the upper end of the pipe inducing a continuous mixing current. The same applies for the thermo-gas-lift in C2 where the gas pressure in the headspace of C1 is used to inject the produced biogas into the lift in C2 instead of compressed air.
- additionally, substrate is mechanically carried upwards by the rising air bubbles
- as there is hot water in the double wall of the pipe, substrate is conveyed upwards by a convective flow of heat

The compressed air which is blown into C1 serves yet another purpose: the oxygen is used by microorganisms along the extended flow-path of the head-spaces of all 4 chambers for biogas desulphurisation which extends the service limit of the gas engine in the combined heat and power unit (CHP) of the plant.

One of the major advantages of the *BIO4GAS* plant is a partial supersession of mechanical stirrers as agitation and mixing in C1 and C2 is accomplished by the thermo-gas-lifts and the oscillations induced by the gas pressure relief valve. This saves energy and investment costs. Despite the standardised construction elements actually causing invariant dimensions of the reactor, the plant is able to adapt to a wide range of livestock at different agricultural sites since the chambers are hydraulically decoupled. In times of low loading rates (i.e. high retention times) C3 and C4 can serve as post-fermentation reactors or even as gastight storage tanks.

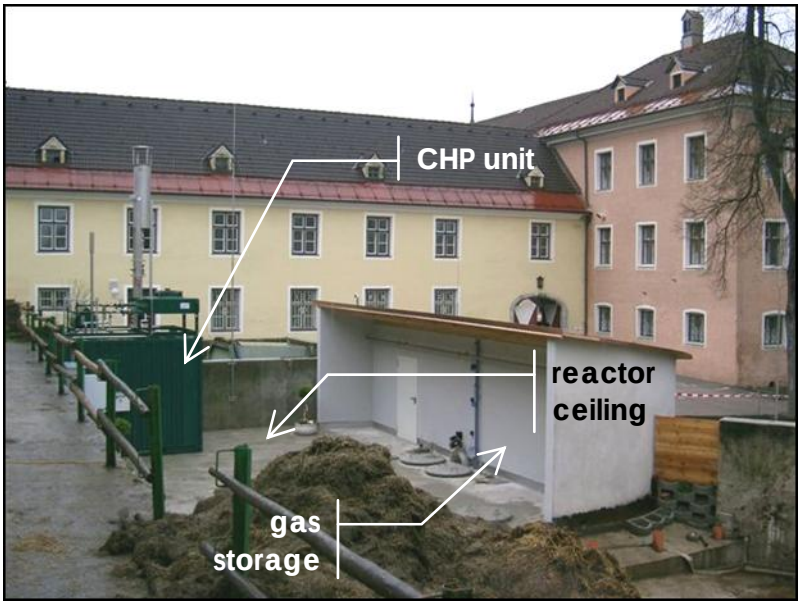

Figure 3-5 *BIO4GAS* demonstration plant after completion

Different from a completely mixed reactor, a serial reactor system like the circular-shaped 4-chamber layout of the plant causes a plug-flow of the substrate and the produced biogas. Among other advantages, this entails less odour generation, improved sanitising and desulphurisation as well as higher gas production rates through the prevention of hydraulic short-circuiting of the substrate.

Figure 3-6 *BIO4GAS* demonstration plant during construction works

In the framework of the research project BIO4GAS gas and sludge sample ports for each chamber have been installed. By means of the drawn samples different physical and chemical parameters are determined (e.g. temperature, pH, organic acids, total solids, volatile solids, COD, NH4-N). Gas quality was quantified in terms of the portions of methane, carbon dioxide, oxygen and hydrogen sulfide which allows for the assessment of the development of the gas quality along the different chambers.

3.3 MATHEMATICAL MODELLING AND SIMULATION

3.3.1 SIMULATION SOFTWARE

Mathematical models and simulations can serve as an invaluable basis in design, analysis and process optimisation of, for example, biogas plant systems. Based on a model, dynamic simulation allows the evaluation of the time characteristics of the parameters of a biogas plant for different load scenarios and configurations without having to interfere with the real plant. This may save time and money since, for example, the need for real-world test series with expensive measurement equipment is minimised.

SIMBA for the use with Matlab®/Simulink™ is a software package for modelling and dynamic simulation of biological wastewater treatment processes. SIMBA is conceived as an open system, so that the user can add self-defined models and functions (ifak, 2005). The Matlab/Simulink environment is using principles of state-space modelling in a graphical representation consisting of blocks and lines (signals). Collectively the blocks and lines in a block diagram describe an overall dynamic system defined by time-based relationships between signals and state variables. The solution of a block diagram is obtained by evaluating these relationships over time. Typically the current values of outputs are functions of the previous values of temporal variables (states) where the change of the states is defined via mathematical equations. In principle input (u) is fed to a state-space model that is variable in time. A dynamic output is generated, based on both, the dynamic input (u) and the model's state (x). The state (x) of the system is defined as the values of state variables at any instant point of time (MathWorks, 2008).

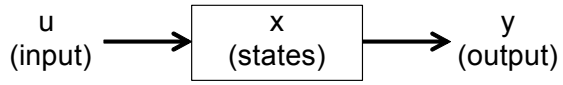

Figure 3-7 State-space model

For the purpose of simulating the processes in biogas plants as described in the papers included in this dissertation, the ADM1 implementations in SIMBA were utilised. Originally, within SIMBA the ADM1 simulation tools were intended to simulate dynamic processes which can be found in the anaerobic digesters of wastewater treatment plants. Thus, for simulations concerning stand-alone biogas plants, corresponding adaptations were necessary. Especially in the parameter set which includes the kinetic and stoichiometric factors for the anaerobic digestion processes adjustments had to be applied. These customisations were accomplished in the course of the model calibration process which was applied for each case study (see following section).

For comprehensive details concerning the model setup, parameters and variables used with SIMBA the reader is referred to Appendix A and the individual appendices associated with the papers included in this dissertation.

3.3.2 MODEL CALIBRATION

3.3.2.1 General issues

Model calibration and validation are necessary requirements and preliminary steps prior to model application. The purpose of calibration is to optimise a parametric model by changing the values of input parameters in an attempt to match field conditions in reality within some acceptable criteria. Then, it allows the user to describe the system under study (e.g. the anaerobic digestion process) and calculate different scenarios with reasonable predictions and results. Besides that, the calibration procedure can be a very useful exercise to understand the model's sensitivity to different influences.

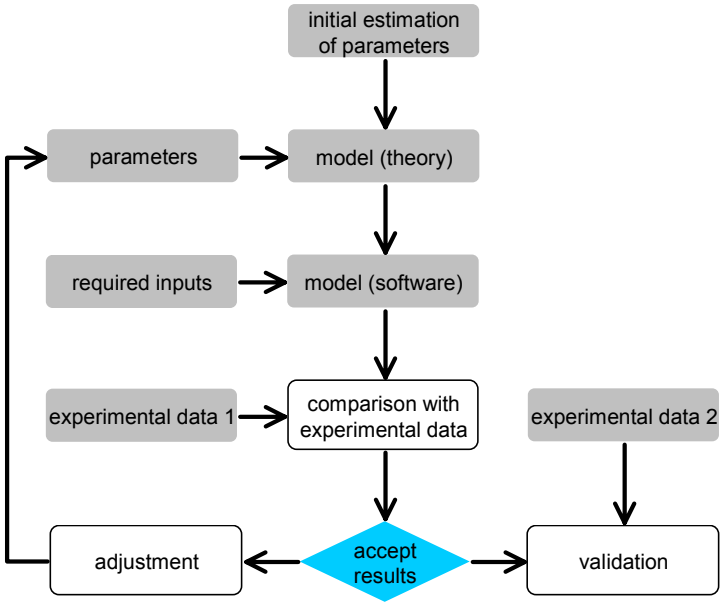

Figure 3-8 Scheme of model calibration and validation

Generally, the calibration procedure for a numerical model follows a basic scheme as depicted in Figure 3-8. After a first model run with an initial guess of the model parameters, results are compared with those gained from experimental work or on-site measurements at a full-scale plant. If the simulated data does not match the real-world results within an acceptable range (to be judged by the user via specified simulation assessment criteria) parameters have to be adjusted – preferably in a systematic way – iteratively until a satisfying parameter set for the data has been developed.

After calibration the model has to be validated by comparison with of one or more different and independent sets of experimental data in order to determine whether the model represents and correctly reproduces the behaviours of the real-world system. Note that there is still the possibility that measured data is corrupt by some reason (e.g. systematic errors; undetected defects in the measurement equipment).

3.3.2.2 ADM1 calibration in SIMBA

The first step in calibration and one of the key-points for the successful application of a mathematical model is to achieve a good influent characterisation, especially for complex influent substrates as used in biogas plants (Huete et al., 2006). ADM1 requires a detailed characterization identifying the concentrations of soluble and particulate carbohydrates, protein, lipids, as well as inert components fed to the anaerobic digestion system. However, full identification of the concentrations of all these compounds is generally not possible, at least not on a regular basis as measurement facilities are not available. Instead, in most cases only a limited number of component concentrations are known even though the quality of the output of ADM1 in terms of treatment performance, biomass composition, and chemical characteristics depends strongly on the influent characteristics (Kleerebezem and van Loosdrecht, 2006b; Page *et al.*, 2008).

Besides kinetic and stoichiometric coefficients the parameter set as used in ADM1 also comprises factors determining influent characterisation. A default parameter set is given in (Batstone *et al.*, 2002a) for municipal wastewater, and slight modifications in parameter values have recently been suggested (Batstone et al., 2006). However, it is unlikely that this parameter set is appropriate for the description of anaerobic digestion of dairy manure or other substrates used in biogas plants (Page et al., 2008). One of the main goals of the research work conducted was to develop parameter sets for the simulation of biogas plants and to verify ADM1 results with experimental data from the different case studies presented in the papers included in this dissertation.

In SIMBA primary influent characterisation is realised by means of values for the volumetric flow rate (*Q*), the concentrations of particulate COD (COD_x), soluble COD (COD_s), total Kjeldahl nitrogen (*TKN*) or, in some cases, ammonium-nitrogen (NH_4-*N*). Within the program, COD_s concentration values are further divided via split-factors (*fCODs_yy*) into soluble components such as monosaccharides (*Ssu*), amino acids (*Saa*), long chain fatty acids (*Sfa*) and soluble inerts (*Ssi*). Particulate biodegradable substrates in terms of COD_x are represented in the composite fraction *Xc*. In the disintegration step which is accomplished by fractionating factors (*fyy_Xc*), the composites (*Xc*) are disintegrated to short chain molecules of particulate substrates such as carbohydrates (*Xch*), proteins (*Xpr*) and lipids (*Xli*), soluble and particulate inerts (*Xsi* and *Xxi*, respectively), and decay products (*Xp*) (Figure 3-9). All the mentioned factors are subject to iterative adjustment within the calibration procedure and should preferably be cross-checked with experienced data from the literature.

Additionally, influent characterisation is further carried out by modification of the variable carbon and nitrogen contents of some of the ADM1 components as given in table 2.6 of the ADM1 description in (Batstone *et al.*, 2002a). This applies for composites (*Xc*), proteins (*Xpr*), particulate and soluble inerts (*Xi* and *Si*), and amino acids (*Saa*) where C and N contents can be adjusted within a reasonable range.

The estimation of the split-factors (*fCODs_yy*), the fractionating factors (*fyy_Xc*) and the adjustable C and N contents was performed with the help of mass balances for COD, C_{total} and N_{total} as illustrated in Figure 3-9. COD, C and N contents of all components were totalled with regard to different steps such as ‘influent’, ‘after disintegration’ and ‘after digestion’ and compared to corresponding measured data. According to the principles of mass conservation, proper calibration was tied to the following conditions: throughout all three steps the sums of COD, C and N contents of all components must remain constant and preferably have a good match with measured values.

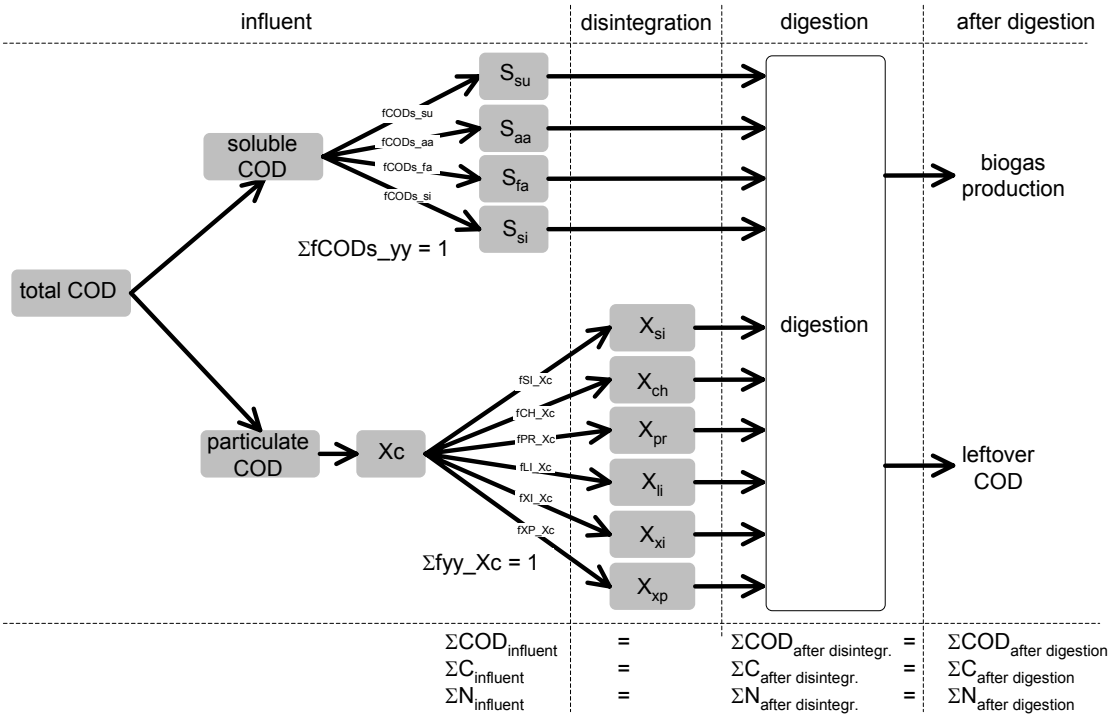

Figure 3-9 Scheme of ADM1/SIMBA influent characterisation

From that, the lumped carbon and nitrogen contents of the composites *Xc* (*C_Xc* and *N_Xc*) can be calculated back from the mass balance as illustrated in the following equations:

$$C\_Xc \cdot \sum fyy\_Xc = (fsi\_Xc \cdot C\_si)+(fch\_Xc \cdot C\_ch)+(fpr\_Xc \cdot C\_pr)+ \\ +(fli\_XC \cdot C\_li)+(fxi\_Xc \cdot C\_xi)+(fxp\_Xc \cdot C\_xp) \qquad \text{Eq. 3-2}$$

$$N\_Xc \cdot \sum fyy\_Xc = (fsi\_Xc \cdot N\_si)+(fpr\_Xc \cdot N\_pr)+ \\ +(fxi\_Xc \cdot N\_xi)+(fxp\_Xc \cdot N\_xp) \qquad \text{Eq. 3-3}$$

where $\Sigma fyy\_Xc = 1$ per definition.

After successful completion of the influent characterisation, other sensitive parameters such as the kinetic coefficients (e.g. disintegration rate *kdis*) are considered within the calibration procedure. Of course, adjustment of kinetic parameters must be done within a reasonable range known from literature or experience. Reported modifications to kinetic parameters have been on the order of 20–50%. Also, interdependencies must be considered: for example, decay and uptake (and hence growth) rates are heavily correlated, and it is possible to increase the decay rate while simultaneously increasing the uptake rate to have zero net impact on outputs (Batstone et al., 2006).

4 COMPARISON OF RENEWABLE ENERGY SOURCES IN ALPINE REGIONS (A)

Schoen M. A., De Toffol S., Wett B., Insam H. and Rauch W. (2007)

Comparison of renewable energy sources in alpine regions

Reformatted version of paper originally published in:

Managing Alpine Future. Austrian Academy of Sciences Press, ISBN 978-3-7001-6571-2.

COMPARISON OF RENEWABLE ENERGY RESOURCES IN ALPINE REGIONS

Schoen M.A.[1], De Toffol S.[1], Wett B.[1], Insam H.[2] and Rauch W.[1]

[1]University of Innsbruck, Unit of Environmental Engineering, (Austria)
[2]University of Innsbruck, Institute of Microbiology, (Austria)

Abstract: In recent years, renewable energy sources (RES) received great attention as an alternative to traditional energy sources and as a possible contribution to mitigate climate change effects. Austria aims on increasing the share of renewables in the energy mix and thus took a wide variety of measures. For alpine regions there are some distinctions regarding applicability and potentials of RES which have been investigated in this paper. It has been found that hydropower, bioenergy and geothermal energy have good potentials whereas photovoltaics and wind energy face some restrictions.

Keywords: Alpine environment, energy potentials, greenhouse gas, renewables

INTRODUCTION

Background

In recent years, renewable energy sources (RES) received great attention as an alternative to traditional energy sources and as a possible contribution to mitigate climate change effects (IPCC, 2007a). The number of facilities utilizing renewables for power generation underwent outstanding growth (Figure 4-1) which may be attributed to a generally increased ecological awareness, permanently rising prices for fossil fuels and a paradigm shift in European environmental policy (e.g. Kyoto protocol, UNFCCC, 1997) with accompanying subsidies and an according legislation.

According to the “EU Directive for Electricity produced from Renewable Energy Sources” (2001/77/EC), a 21% share of renewables in the energy mix for electricity consumption is targeted within the EU with its 25 member states by 2010. For 2003, RES provided 14% (corresponding to 394 TWh) in electricity generation (EC, 2005).

RES play a prominent role in Austria’s energy supply. Consisting primarily of large hydropower schemes and biomass use (which comprised more than 98% of renewable energy supply in Austria in 2001), the overall share of RES amounts to 21.5 % of primary energy supply. Mainly due to policy support and high fossil fuel prices in the 1970s, total renewable energy supply has increased steadily over the past few decades (Figure 4-1). Electricity generation from RES (RES-E) raised from 37 TWh in 1997 (without pumping electricity) to 40.3 TWh (with 87% from hydropower) in 2006 (e-control, 2007). Having hence the largest ratio of RES-E among the EU-25 states with 70 % (1997), Austria aims on increasing this share to 78.1 % in 2010 (as an indicative target) in fulfilment of the mentioned EU Directive.

However, from a today’s viewpoint, it is very unlikely that Austria will succeed in accomplishing this ambitious goal as well as its efforts to meet the Kyoto-obligations. For example, total 2004 greenhouse gas (GHG) emissions were 15.7 % above 1990 levels although a target of minus 13 % is to be met according to the 2008–2012 Kyoto proto-

col commitment period (UNFCCC, 2006, e-control, 2007 and ADTL, 2007). Facing these discrepancies and a continued increase in energy demand (annual increase >2 %), the government agreed in 2007 to take intensified measures to extend the share of renewables in the energy mix, being aware that effective emissions reduction is only possible in combination with measures for improved energy efficiency and energy savings (BMLFUW, 2007; e-control, 2007; ADTL, 2007).

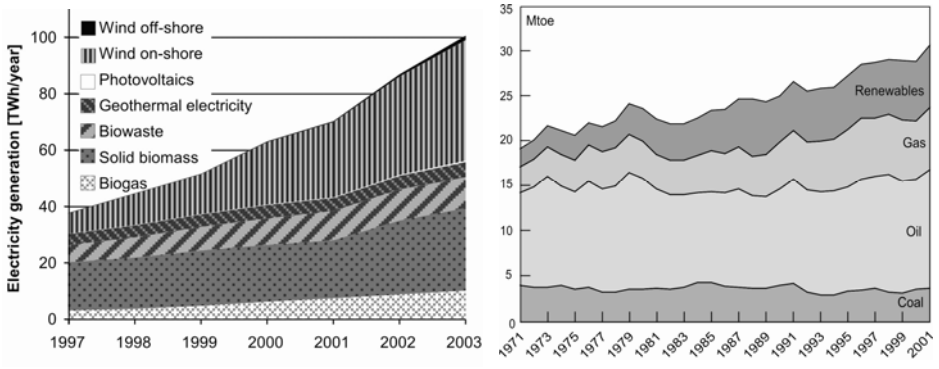

Figure 4-1 Electricity generation from renewables in EU-25 (left,EC, 2005) and total primary energy supply by source in Austria (right,IEA, 2004)

As an outcome of countless research work conducted against the background of climate change and affiliated topics, it is very likely that temperature extremes and heavy precipitation events will continue to become more frequent also in alpine regions (IPCC, 2007c), having major consequences for the utilization of different kinds of RES. However, intensity and frequency of projected extreme events vary depending on the emissions scenario.

As there are partly considerable differences between alpine environments and lowland regions regarding the technical and economic applicability as well as the ecological sustainability of RES, a differentiating approach appears to be reasonable and essential in order to develop planning and decision criteria at regional level. Within this study, numerous sources have been reviewed with a special focus on potentials and restrictions of exploitation of RES in the alpine environment. Referring to Austria in wide parts of this study is mainly due to the country's appropriateness to serve as a predestined example for an alpine region.

Each RES has unique characteristics in terms of level of maturity, ecological and socio-economic appropriateness as well as technological, financial, legal and resource-related requirements for applicability. Employment and future development of different RES technologies of course depend to a large extent on the set-up of national and supranational legislation including governmental and administrative incentives and barriers. This approach has a controversial aspect as differing grants can lead to market distortion. Also, considering GHG savings, a life-cycle approach should be applied including all emissions during manufacturing, operation and decommissioning.

Hydropower, solid biomass for heat and geothermal energy are the most mature RES, and they are largely cost-competitive without special policy support. Concerning Austria's energy supply, the focus historically concentrated primarily in large hydropower plants and biomass use. Less mature, emerging renewables (i.e. wind power, solar technologies and newer forms of bioenergy) which have been entering the markets in

recent years, have received governmental support for both technological development and market deployment (IEA, 2004).

Definitions

Primary energies embodied in RES are transformed by energy conversion processes to more convenient energy carriers which form the three sectors of renewable energy: electricity production (RES-E), biofuels as well as heating and cooling. For the present text, according to the definitions made in EC, 2005, renewable energy resources comprise the following, non-fossil technologies: hydropower, biomass, biogas, geothermal energy, solar energy (photovoltaic and thermal), wind energy, and wave and tidal power. The latter is not considered in this study due to a poor relevance for Austria and neighbouring alpine regions.

INDIVIDUAL RES TECHNOLOGIES AND THEIR RELEVANCE FOR ALPINE REGIONS

Hydropower (HP)

General

Hydroelectric power is derived from the potential energy of falling or flowing water driving a water turbine that spins a generator. The energy extracted is proportional to the rate of flow and the difference in elevation between the source and the water's outflow (head). HP generation is either done by: run-of-river plants, impoundment hydropower plants (including damming water in a reservoir), pumped-storage plants or combinations of the above. While run-of-river and small HP plants provide base load electricity due to a poor storage capacity, impoundment and pumped storage hydroelectricity produces electricity to supply high peak demands and is utilized to compensate for grid oscillations.

Energy potential

Traditionally, HP has the lion's share in the Austrian energy mix. In 2005, 58 % of the country's electricity production originated from HP plants (compared to 11 % in EU-25). With an energy efficiency of around 90 %, HP is the most efficient conversion of energy (Verbund, 2006). Due to a beneficial topographical position, with ample water resources and large hydraulic heads, renewable energy from water was utilized long before climate protection and global warming became topics of public awareness.

According to (Verbund, 2006), Austria has a theoretical HP potential of 150,000 GWh. 56,200 GWh are quantified as economically feasible of which 40,000 GWh (71 %) are already exploited until present day. For Tyrol the economically feasible potential amounts to 6000 GWh (ADTL, 2007). For the EU-15 states an increase in HP electricity between 1 to 4 % and 15 to 25 % is projected from the 2001 level until 2020 for large and small-scale HP respectively (Ragwitz *et al.*, 2005).

Aspects in alpine regions

Generally, it can be stated that HP is more economically attractive than other options (UNDP, 2000). However, together with wind energy, HP in alpine regions represents an energy source characterised by a natural volatility. Other than in lowland regions, most of the energy is produced by impoundment HP producing valuable peak load electricity. Plants access large heads but rather widely branched catchment areas which imply storage facilities. Subsequently, its potential in terms of available water resources is

very sensitive to impacts of climate change like precipitation and snow and glacier melt (De Toffol *et al.*, 2007).

Moreover, dams and reservoirs serve for flood control purposes as they increase minimum discharge levels in winter and compensate flood peaks in summer. Drawbacks involve changes in the downstream river environment (e.g. scouring of river beds and loss of riverbanks, fluctuations in river flow) and disruption of surrounding aquatic ecosystems (e.g. hindering fish migration).

Bioenergy (BE)

General

Biomass which is utilized for heat production, electricity generation and biofuel refinement includes various forms. It comprises solid, liquid and gaseous organic feedstock like solid biomass (e.g. wood chips, purpose-grown energy crops), biogas (e.g. sewage sludge gas, gas from biogas plants fed with substrates of agricultural origin) and liquid biofuels, usually either bioalcohols or bio-oils produced from biomass (e.g. bioethanol, biodiesel, biodimethylether). Biomass also includes the organic component of industrial and municipal waste, but not inorganic waste.

Energy potential

Together with large-scale hydropower, the use of biomass in Austria is among the highest in Europe comprising more than 98% (54.5 + 43.9) of renewable energy supply (primary energy) in Austria in 2001 (IEA, 2004). When converted to electricity via digestion and gasification the efficiency (electrical) averages out at 10 to 40 % whereas in CHP units for the combustion of biomass efficiencies (overall) of > 80% are reported (UNDP, 2000). This can be attributed to a very high appropriateness of solid biomass for thermal energy generation (e-control, 2007).

In Austria, 43,646 GWh have been converted from solid biomass to energy in 2004 including 1112 GWh for electricity production from biomass and biogas (e-control, 2007). Based on studies in Ragwitz *et al.*, 2005 and e-control, 2007, an annual bioenergy potential of additional 23,352 GWh (comprising 14,456 GWh from energy crops, 6,116 GWh from solid biomass and 2,780 GWh from residual materials) has been determined. Biogas which has been used primarily for electricity production so far is thought to have the potential to substitute 15% of the current natural gas consumption (FGW, 2007). According to studies by (Ragwitz *et al.*, 2005) biomass electricity generation are expect to increase by more than a factor of three by 2020. A factor of more than four has been calculated for biogas electricity.

Aspects in alpine regions

Among other factors, the potential capacity of an (agricultural) biogas plant depends on the available feedstock which in turn depends on the available acreage and livestock. As in alpine regions farm structures are rather small-sized, most plants have to be designed for small-scale operation (Figure 4-2) which has often been considered economically unfavourable due to costly individual planning and dimensioning. These shortcomings are for example challenged by development of an innovative plant (BIO4GAS) with standardised design and construction elements applicable to a wide range of livestock (Wett *et al.*, 2006b).

For both, biomass and biogas saturation effects have been observed due to shortened feedstock availability and subsequent increase of prices. For example, for solid bio-

mass the situation tightens in mountainous regions compared to plain woodland: the higher the demand the higher the costs as more and more difficult accessible mountain forests have to be harvested.

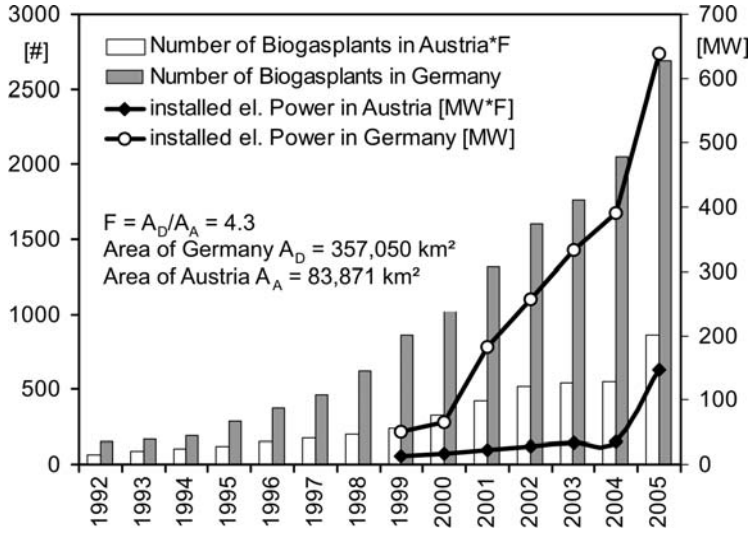

Figure 4-2 Number of biogas plants and installed el. power in Germany and Austria. For better comparability the values for Austria were multiplied with a factor F equalising the different sizes of both countries (Schoen *et al.*, 2007b).

Geothermal energy (GE)

General

Geothermal use is commonly divided into two categories: electricity production and direct application. Direct application of GE can involve a wide variety of end uses, e.g. district heating and air condition systems. Four types of power plants are commonly used to generate electrical power from GE depending on temperature, depth, and quality of the water and steam in the area. Dry steam, flash steam, and binary-cycle systems use either steam or hot water from underground to drive a turbine that spins a generator. Enhanced Geothermal Systems (Hot-dry-rock systems) utilize water that is pumped into hot rocks in the earth, rather than harvesting hot water already stored in the earth.

Geothermal exchange heat pumps are used for direct application of GE and can be used basically everywhere because they are suitable for low-temperature resources (UNDP, 2000). These pumps utilize the Earth's ability to store heat in the ground and water masses as heating and/or cooling sources with the help of heat exchangers and loop systems containing refrigerant. Applications range from large plants for district heating to on-site exploitation for single houses.

Energy potential

GE is sparsely exploited in Austria. By 2003, only twelve district heating plants were in operation providing 41.5 MW thermal power. Two of the plants are operated in hybrid mode, producing electricity via ORC-turbines (3 GWh in 2006). 160,000 heat pump plants (approx capacity. 834 MW, annual heat output of 1,767 GWh) used for service water treatment (approx. 77%), heating purposes, heat recovery, and air dehumidifica-

tion were in operation by 2001 (AEA, 2003; e-control, 2007). Regarding energy efficiency, direct use of GE has a much higher degree of efficiency (50-70 %) than electricity production with 5-20 % (UNDP, 2000).

On the basis of the current economic and geological frame conditions, Austria's total geothermal potential is in the range of 2,000 MW of thermal energy and about 7 MW electricity (AEA, 2003). With regard to direct geothermal exploitation of ground and surface water a study for the Alpenrhein region (comprises parts of Austria, Switzerland and Liechtenstein) was conducted (Rauch *et al.*, 2003). In this region an energy quantity of 150 GWh per year is extracted from the groundwater for heating and cooling purposes today. Assuming an induced temperature change of 1°C, an additional, theoretically utilisable potential of 1900 GWh can be determined. However, the limiting factors of hydraulic and thermal short circuits as well as feasible water abstraction restrict this potential to 300 GWh.

Aspects in alpine regions
Generally, geothermal power plants are unaffected by changing weather conditions and diurnal variations. Thus, they are able to provide baseload power. However, upper reach regions of alpine rivers can be favourable for geothermal applications using groundwater as aquifers consist of material with a rather high permeability.

Solar energy (SE)

General
SE comprises the following forms of energy:

- Photovoltaic SE is the direct conversion of sunlight into electricity utilizing the photovoltaic effect: of generating free electrons from the energy of light particles (UNDP, 2000).
- Solar thermal electric power plants generate electricity by converting SE to heat in order to drive a steam turbine in a thermal power plant.
- Low-temperature SE is the direct conversion of sunlight into low-temperature heat (up to 100°C). Such systems can be sized for single houses or for collective buildings and district heating.

Because solar electricity and heating offer an intermittent source of energy, most standalone systems are equipped with a storage unit to provide energy during the night or during days with insufficient sunshine.

Energy potential
According to (e-control, 2007), at the end of 2006, photovoltaic systems with a total capacity of about 36 MW were in operation in Austria, feeding an annual output of about 13 GWh to the public grid. This equals a share of less than 1% of the country's electricity production. With 774 GWh (2,785 TJ) in 2001, solar thermal power also made minor contributions to renewable energy supply. There were 2500 million m² of solar collectors in operation: 24% for swimming pool heating; 75% for water and space heating and 1% for drying biomass products (IEA, 2004). Reported energy efficiencies for photovoltaic cells range between 5-30% (UNDP, 2000; Verbund, 2006).

Aspects in alpine regions
Highest energy outputs could be gained for PV sites at higher altitudes due to clearer sky and snow reflection, better cooling of the panels through lower temperatures and

higher wind speeds. This especially applies in fall and winter when haze and fog cause less energy output in the valley (Bergauer-Culver and Jaeger, 1998). On the other hand, there are only few non-valley sites which could be quantified as feasible because of factors like site development costs, available space and impairment of nature or landscape.

Wind energy (WE)

General

Electricity from wind power (offshore and onshore) is generated by converting the rotation of turbine blades into electrical current by means of an electrical generator. The power output of a turbine is proportional to the cube of the current wind speed. The annual energy output of a wind turbine is determined by such parameters as average wind speed, statistical wind speed distribution, turbulence intensities, and roughness of the surrounding terrain (UNDP, 2000).

Negative environmental aspects connected to the use of wind turbines can include acoustic noise emission, visual impact on the landscape, impact on bird life, moving shadows caused by the rotor, and electromagnetic interferences.

Energy potential

By end of 2006, 127 windparks (> 600 turbines) with a capacity of 953 MW and an annual output of 1,737 GWh were in operation in Austria (e-control, 2007). Thus, Austria ranks sixth in the EU with installed wind power per capita and first among the landlocked states. This entails relatively high production costs and subsidy requirements compared to states with a shoreline.

The main problem with WE is the fluctuation in generation due to weak winds or storm shut down. This also applies when the plants are distributed over large areas and has significant repercussions on the European electricity system (UCTE, 2005). Consequently, conventional power plants have to backup electricity demand which raises further costs.

Aspects in alpine regions

Besides offshore sites, mountainous regions are preferred locations for wind farms due to reduced air viscosity and the phenomenon of topographic acceleration which can make large differences to the amount of energy that is produced. Investigations revealed some potential sites for WE in Tyrol, all located above 1500 m of altitude. Development of this sites would involve difficulties like accessibility, grid incorporation, competing land uses and landscape aspects (ADTL, 2003).

CONCLUSIONS AND DISCUSSION

Renewable energy generally has a positive effect on energy security, employment and on air quality. But in the long term RES must achieve cost-competitiveness with conventional fuels to reach a permanently high share in the energy mix. For alpine regions there are some distinctions regarding applicability and potentials of RES. A further expansion of HP as for example agreed by the Tyrolean government is intended to ensure a higher independence from energy imports and emission-free energy production but of course holds the risk of ecological impairments. There are potentials for BE for instance in small-scale agricultural biogas plants. In general, it should be noted that further expansion of BE can lead to contentions between acreage for food and energy

crops and a subsequent increase of food prices. Regarding GE in alpine valley settlements, it can be stated that there is plenty potential especially for decentralized heat pump systems in business and industry facilities. The same applies for solar thermal applications. The economic efficiency of photovoltaic electricity currently depends to a high degree on governmental incentives. Generally there are adverse effects on solar energy facilities in valley sites as insolation time is reduced by the mountains. As mentioned before, only hilltops are preferred locations for WE in alpine regions. But in most cases disadvantages like development costs and impairments of the landscape outweigh possible benefits.

REFERENCES

ADTL 2003 *Energieleitbild Tirol 2000 – 2020 [in German]* Untergruppe Energie des Tiroler Raumordnungsbeirates, Tiroler Landesregierung Innsbruck, Austria.

ADTL 2007 *Wirtschafts- und Arbeitsmarktbericht Tirol 2007 [in German]* Abteilung Wirtschaft und Arbeit, Amt der Tiroler Landesregierung Innsbruck, Austria.

AEA 2003 *Renewable Energy in Austria* Austrian Energy Agency (E.V.A.) Vienna, Austria.

BERGAUER-CULVER B and JAEGER C 1998 Estimation of the energy output of a photovoltaic power plant in the Austrian alps. *Solar Energy, 62,5, 319–324.*

BMLFUW 2007 *Anpassung der Klimastrategie Österreichs zur Erreichung des Kyoto-Ziels 2008-2013 [in German]* BM für Land- und Forstwirtschaft, Umwelt und Wasserwirtschaft Vienna, Austria.

DE TOFFOL S, ENGELHARD C and RAUCH W 2007 Influence of climate change on the water resources in an alpine region *Submitted for publication.*

E-CONTROL (2007) Ökostrom sowie Energieverbrauchsentwicklung und Vorschläge zur Effizienzsteigerung [in German]. Energie-Control GmbH, August 2007, Vienna, Austria.

EC (2005) European Commission.Communication from the Commission. The support of electricity from renewable energy sources 2005, COM(2005) 627 final. 7/ Dec/2005, Brussels, Belgium.

FGW 2007 *Biogas: Potenzial in Österreich [in German]* Pressegespräch Fachverband Gas Wärme Presentation, accessed Sep. 2007, www.klimaaktiv.at.

IEA (2004) *International Energy Agency: Renewable Energy: Market & Policy Trends in IEA Countries,* ISBN 92-64-107916-2004, IEA Publications, Paris, France.

IPCC 2007a *Summary for Policymakers. Climate Change 2007: Mitigation. Fourth Assessment Report of the Intergovernmental Panel on Climate Change* Cambridge University Press, Cambridge, UK and New York, USA.

IPCC 2007b *Summary for Policymakers. Climate Change 2007: The Physical Science Basis. Fourth Assessment Report of the Intergovernmental Panel on Climate Change* Cambridge University Press, Cambridge, UK and New York, USA.

RAGWITZ M, SCHLEICH J, HUBER C, RESCH G, FABER T, VOOGT M, COENRAADS R, CLEIJNE H and BODO P 2005 *FORRES 2020: Analysis of the renewable energy sources' evolution up to 2020. Final Report* Karlsruhe, Germany.

RAUCH W, STEGNER U, F.OSTERKORN, T.BLANK, M.GASSER, A.PFEFFERKORN, M.OBERMAYR, O.WOHLWEND, G.RIEDI and E.HILBE 2003 *Thermische Nutzung der Gewässer d. Alpenrheintales [in German]* Internationale Regierungskommission Alpenrhein Bregenz, Austria.

SCHOEN M A, PHOTHILANGKA P, ELADAWY A, INSAM H and WETT B (2007) Farmscale Co-fermentation of manure and organic waste. *IWA-workshop on anaerobic digestion in mountain area and isolated rural zones.* 5-7/Jun/2007, Chambéry, France (Proceedings).

UCTE 2005 *Statistical Yearbook 2005* Union for the co-ordination of transmission of electricity Brussels, Belgium.

UNDP 2000 *World Energy Assessment* United Nations Development Programme New York, USA.

UNFCCC (1997) Kyoto Protocol to the United Nations Framework Convention on Climate Change. *Conference of the Parties on Its Third Session.* 10/Dec/1997, Kyoto, Japan.

UNFCCC 2006 *GHG DATA 2006-Highlights from Greenhouse Gas Emissions Data for 1990–2004 for Annex I Parties. United Nations Framework Convention on Climate Change*

VERBUND 2006 *Verbund-Nachhaltigkeitsbericht 2006 [in German]* Österreichische Elektrizitätswirtschafts-Aktiengesellschaft (Verbundgesellschaft) Vienna, Austria.

WETT B, SCHOEN M, PHOTHILANGKA P, WACKERLE F and INSAM H 2006 Model-based design of an agricultural biogas plant: application of Anaerobic Digestion Model No.1 for an improved 4 chamber scheme. *Water Science and Technology, 55,10, 21-28.*

5 APPLICATION OF ADM 1 FOR AN IMPROVED FOUR CHAMBER SCHEME (B)

Wett B., **Schoen M. A.**, Phothilangka P., Wackerle F. and Insam H. (2007)

Model-based design of an agricultural biogas plant: application of Anaerobic Digestion Model No. 1 for an improved four chamber scheme

Reformatted version of paper originally published in:

Water Science and Technology, 55 (10), 21-28

MODEL-BASED DESIGN OF AN AGRICULTURAL BIOGAS PLANT: APPLICATION OF ANAEROBIC DIGESTION MODEL NO.1 FOR AN IMPROVED FOUR CHAMBER SCHEME

Wett B.[1], Schoen M.[1], Phothilangka P.[1], Wackerle F.[2] and Insam H.[3]

[1]University of Innsbruck, Unit of Environmental Engineering, (Austria)
[2]Management Center Innsbruck MCI, Universita¨ tsstr. 15, 6020 Innsbruck, Austria
[3]ARC Seibersdorf Research GmbH, Studio BioTreaT, Technikerstr. 25d, 6020 Innsbruck, Austria

Abstract: Different digestion technologies for various substrates are addressed by the generic process description of Anaerobic Digestion Model No. 1. In the case of manure or agricultural wastes a priori knowledge about the substrate in terms of ADM1 compounds is lacking and influent characterisation becomes a major issue. The actual project has been initiated for promotion of biogas technology in agriculture and for expansion of profitability also to rather small capacity systems. In order to avoid costly individual planning and installation of each facility a standardised design approach needs to be elaborated. This intention pleads for bio kinetic modelling as a systematic tool for process design and optimisation. Cofermentation under field conditions was observed, quality data and flow data were recorded and mass flow balances were calculated. In the laboratory different substrates have been digested separately in parallel under specified conditions. A configuration of four ADM1 model reactors was set up. Model calibration identified disintegration rate, decay rates for sugar degraders and half saturation constant for sugar as the three most sensitive parameters showing values (except the latter) about one order of magnitude higher than default parameters. Finally, the model is applied to the comparison of different reactor configurations and volume partitions. Another optimisation objective is robustness and load flexibility, i.e. the same configuration should be adaptive to different load situations only by a simple recycle control in order to establish a standardised design.

Keywords: ADM1; agricultural wastes; anaerobic digestion; biogas; manure; modelling

INTRODUCTION

IWA's Anaerobic Digestion Model No.1 (ADM1) represents a universally applicable bio kinetic model for the mathematical description of anaerobic digestion of different types of organic substrates (Batstone *et al.*, 2002a). In the vast majority of investigations on applications of ADM1 done so far sewage sludge was the object of research. Sets of validated parameters for sewage sludge digestion have been suggested (e.g. Blumensaat and Keller, 2005) and transfer across the model interface of information about the feed sludge has been reported (Wett *et al.*, 2006a). In case of manure or other agricultural wastes a priori knowledge about the substrate in terms of ADM1 compounds is lacking and influent characterisation becomes a major issue. Only few studies concerning ADM1 parameter estimation for agricultural wastes are available till present day (e.g. Kalfas *et al.*, 2005).

ADM1 describes digestion of particulate composites as a 5-stage process involving disintegration, hydrolysis, acidogenesis, acetogenesis and methanogenesis, of which the last 3 process steps are represented by growth kinetics of the specific degrading biomass (Figure 5-1). In the first step composite solids and cells of microorganisms are decomposed to their principal constituents including carbohydrates, proteins and fats. Additionally, inert particulate and soluble matter emerge which are not affected by the subsequent reactions. This process step is named disintegration and represents a characterisation of the input substrate. Subsequently, the macromolecular products are subject to enzymatic degradation and transformed to monosaccharides (MS), amino acids (AA) and long chain fatty acids (LCFA). Further anaerobic digestion leads from an acetogenic and a methanogenic phase to biogas production (CH_4, CO_2).

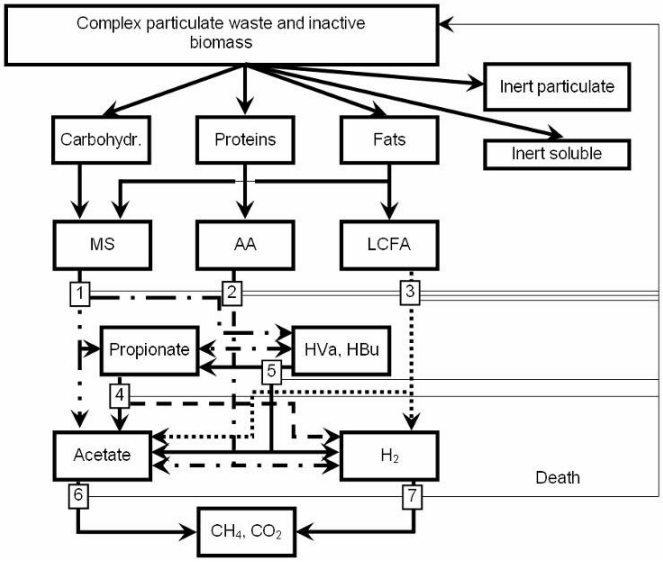

Figure 5-1 The anaerobic model as implemented including biochemical processes: (1) acidogenesis from sugars, (2) acidogenesis from amino acids, (3) acetogenesis from LCFA, (4) acetogenesis from propionate, (5) acetogenesis from butyrate and valerate, (6) aceticlastic methanogenesis, and (7) hydrogenotrophic methanogenesis (Batstone *et al.*, 2002b)

Additionally, inert particulate and soluble matter emerge which are not affected by the subsequent reactions. This process step is named disintegration and represents a characterisation of the input substrate. Subsequently, the macromolecular products are subject to enzymatic degradation and transformed to monosaccharides (MS), amino acids (AA) and long chain fatty acids (LCFA). Further anaerobic digestion leads from an acetogenic and a methanogenic phase to biogas production (CH_4, CO_2). Owing to the model complexity and number of states only a limited number of variables can be covered by quality measurements. Model calibration procedures allow systematic analysis of the collected data of detected concentrations and provide the possibility to check the results for plausibility. Accurately defined cause-and-effect relationships lead to an increased process comprehension and make the biogas plant more transparent.

Here, the model is applied to develop an optimised four chamber scheme for an agricultural biogas plant. Compared to a completely mixed reactor the four-chamber scheme approaches plug-flow characteristics and obviously attains a “better” end-product in terms of odour generation and hygienic aspects and, additionally, yields

higher gas production rates. These advantages are paid off by less process stability, especially when

overloading the first compartment. Required recycle rates and appropriate combination of co-substrates need to be investigated.

METHODS

To cover both tasks – proper influent characterisation of agricultural wastes and close model–design interaction – long-term monitoring campaigns were conducted both on the full-scale and laboratory-scale (Figure 5-2 and Figure 5-3). In a biogas plant sited on a pig farm (Figure 5-2), co-fermentation under field conditions was observed, quality data (TSS, VSS, COD_x, COD_s, N_{total}, NH_4^+-N, C, S, CH_4, CO_2, pH) and flow data were recorded and mass flow balances were calculated. Gas samples were analysed by chromatography (methane and carbon dioxide) and carbon was detected by an IR-based C-S-analyser. In the lab different substrates (biowaste and manure) taken from the farm have been digested separately in parallel under specified conditions in a 2-reactor-system each (continuously stirred anaerobic reactors, Figure 5-3). One week prior to feeding with the substrates sewage sludge from WWTP Innsbruck, Austria was put into the reactors and served as inoculum. Moreover variations in the feed-flow have been induced in order to improve parameterization for model calibration.

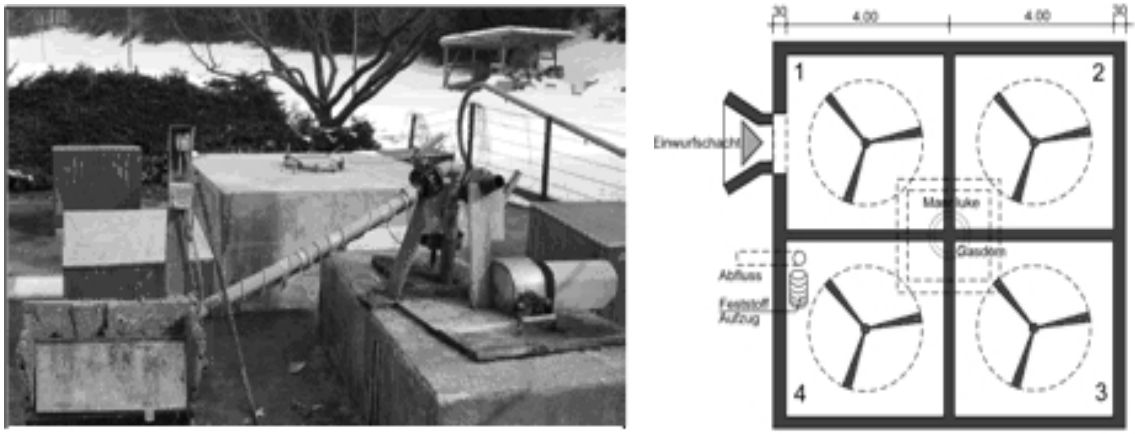

Figure 5-2 4-chamber biogas plant for co-fermentation of piggery manure and biowaste with a total volume of 190 m³

The subsequent calibration procedure was based on the principle of mass conservation of nitrogen (ammonia release characterising influent proteins) and carbon (gas yield, -composition and corresponding degradation performance). A configuration of 2 ADM1 model reactors was set up by using the Matlab-Simulink® based commercial simulator SIMBA©. Data sets from lab-scale experiments of manure digestion were used for parameter calibration.

The projected 4-chamber pilot plant (Figure 5-4) has a layout formed by two concentric cylinders. The inner cylinder and the outer ring contain two chambers each separated by baffles. The mode of operation is as follows: substrate is pumped to chamber 1 (K1) and biogas production starts. Since the construction is gas-tight, gas pressure of the head space of chamber 1 displaces liquid below the baffle to K2. The outflow from K2

to K3 is accomplished by a weir outlet situated right under the top sealing of the reactor. Within K3 and K4 an annular flow is induced intermittently by a stirrer which mobilises settled solids. Deposits in K1 and K2 are avoided by periodical opening of a relief valve causing an oscillation and a subsequent recycle flow between K1 and K2.

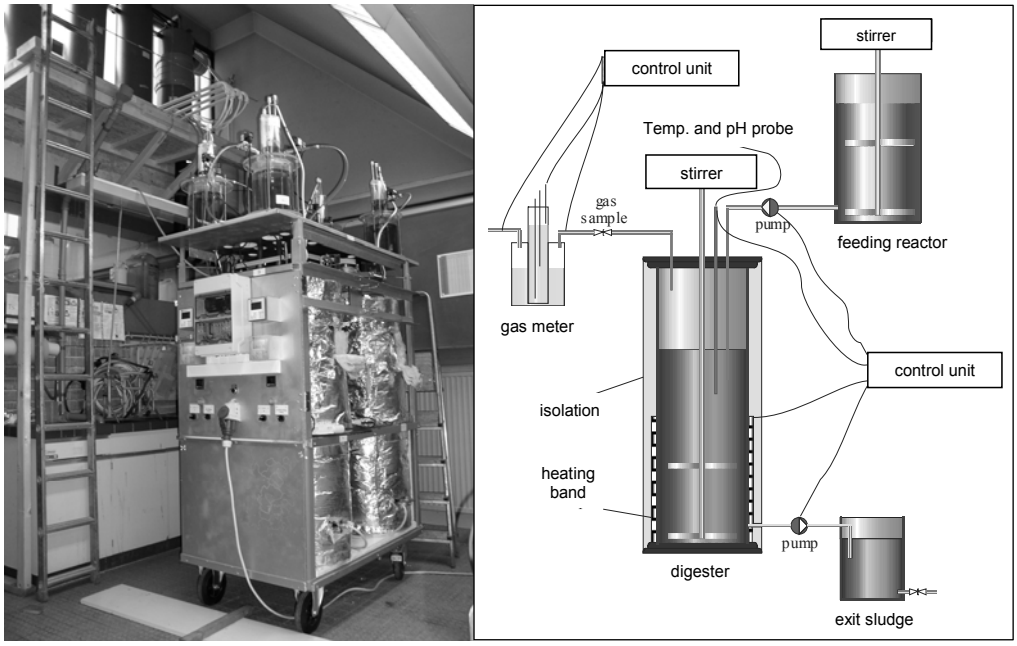

Figure 5-3 Set-up of 4 lab-scale digesters with a volume of 0.1 m³ each for parallel digestion tests

For the comparison of different reactor configurations and volume partitions the calibrated parameters were applied to a 4-reactor-model in SIMBA© representing the pilot plant (Figure 5-5). Recycle flows from chamber 2 to 1 and chamber 4 to 1 were simulated separately. Another optimisation objective was robustness and load flexibility, i.e. the same configuration should be adaptive to different load situations only by recycle control in order to establish a standardised design. Therefore the optimised scheme was tested for different load scenarios and pH and gas-flow distribution were studied.

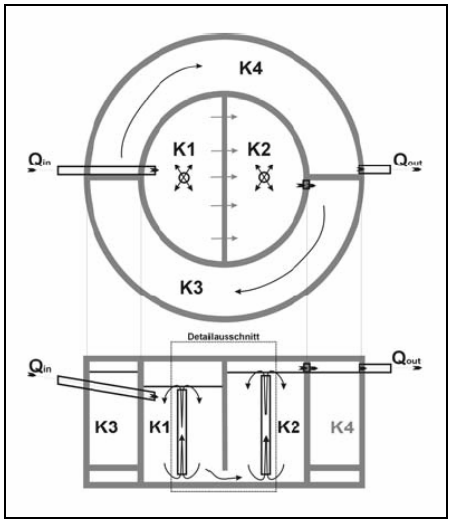

Figure 5-4 Improved flow scheme of the 4-chamber pilot plant with cylindrical shape

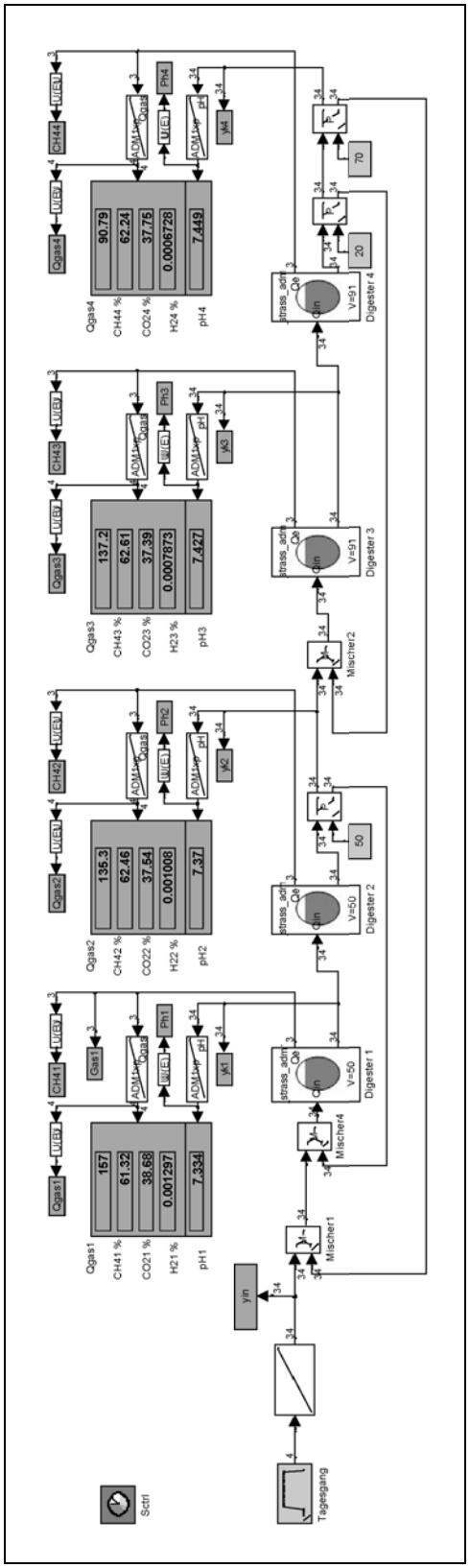

Figure 5-5 4-chamber system represented by serial ADM1 digesters edited in the SIMBA-environment for the simulation of gas production in individual chambers

RESULTS

Measured values of the input substrate can be seen from Table 5-1. Gas production and pH was measured daily while feed tanks were refilled and sampled weekly.

Table 5-1 Input values of manure

Week	CSBs	CSBx	Ntot	NH4-N	Norg	TSS	VSS	TC	TIC	S
	[mg/l]	[mg/l]	[mg/l]	[mg/l]	[mg/l]	[g/l]	[g/l]	[g/l]	[g/l]	[g/l]
1	-	-	-	-	-	-	-	-	-	-
2	8086	36020	1936	187	1749	36.0	25.3	13.8	0.26	0.11
3	9058	44248	2135	301	1833	44.8	31.2	17.2	0.31	0.14
4	9146	43217	1880	157	1722	41.1	29.7	14.8	0.26	0.13
average	8763	41162	1984	215	1768	40.6	28.7	15.3	0.28	0.13

Figure 5-6 below shows the results of calibration with the 2-reactor-model. Lab experiments comprised two phases: an initial stabilization phase when the digesters where fed with 75 liters of inoculum each on day 0 and no further feeding for 8 days. After that period the reactors were fed with manure from the pig farm under mesophilic conditions. The feeding was done semicontinously, i.e. a batch of 7.5 liters was put to the reactors once a day.

As can be seen from Figure 5-6 simulated and measured values matched well with exception of the period from day 25 to 30. Since there was a continuous feeding up to the end of the 30 day period the decrease in the measured gas production is not explicable and is attributed to errors in the measurement device.

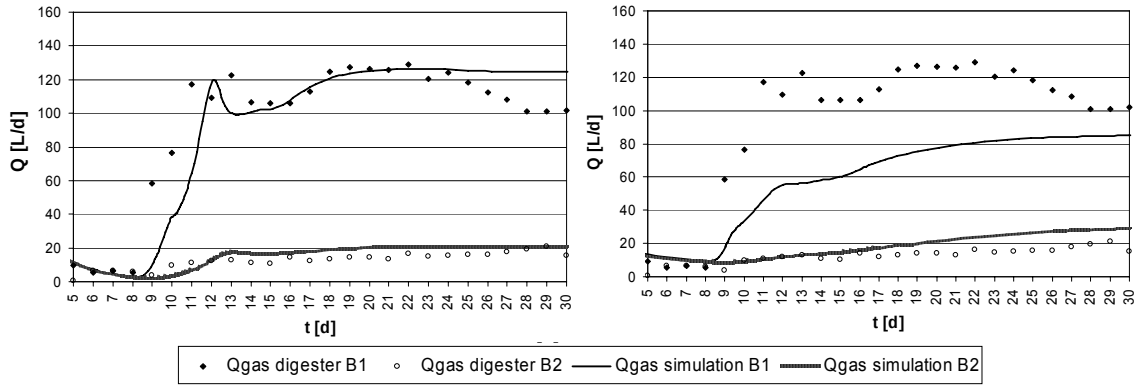

Figure 5-6 Calibration runs for gas production comparing best fit disintegration rate (*kdis* = 0.5, left) and default parameter (*kdis* = 0.096, right)

While calibrating, the coefficients for disintegration (*kdis* in ADM1 terminology), saturation of sugar (*KS_su*) and decay of sugar degraders (*kdec_Xsu*) as well as the carbon and nitrogen contents of the composite fraction (*Xc*) turned out to be the parameters most sensitive to model behaviour. Especially *kdis* revealed a remarkable influence on the distribution of gas production between both digestion steps (compare Figure 5-6). Applying the default disintegration rate for piggery manure (*kdis* = 0.096) leads to an accumulation of particulate substrate and a shift of digestion activity to the second step.

Table 5-2 Calibrated ADM1 model parameters

Parameter	Description	Unit	chosen value	Parameter	Description	Unit	chosen value	ADM 1 default
fSI_XC	fraction SI from composites Xc	[-]	0.015	C_Xc	Carbon content composites Xc	[k mole C/ kg COD]	0.028	
fCH_XC	fraction Xch from composites Xc	[-]	0.34	N_Xc	Nitrogen content composites Xc	[k mole N/ kg COD]	0.00215	
fPR_XC	fraction Xpr from composites Xc	[-]	0.18	kdis	disintegration rate	[1/d]	0.5	0.096
fLI_XC	fraction Xli from composites Xc	[-]	0.14	KS_su	half saturation constant sugar	[kg COD/m³]	0.5	0.533
fXP_XC	fraction Xp from composites Xc	[-]	0.2	kdec_Xsu	decay rate Xsu	[1/d]	0.7	0.01

Of course, the fractionizing factors for the composites also play an important role in model performance as they determine a characterisation of the input substrate. Reported compositions of piggery manure from literature (Møller *et al.*, 2004) indicate a relatively high portion of carbo-hydrates compared to proteins and lipids. Namely, proportions average out to ch / pr = 1.9 and ch / li = 2.4. Given substrate ratios have been used in current calibration study in good agreement with measured total nitrogen and carbon content of the influent flow.

Table 5-2 gives an overview on the applied parameters and their deviation from the default values suggested in the original model description of ADM1 (Batstone *et al.*, 2002a). It should be noted that *kdec_Xsu* (0.7) is of the same order of magnitude as *kdec_Xaa* (0.8, decay rate of amino acid degraders).

After calibration, the parameter set was applied to the 4-reactor-model (Figure 5-5) and 3 different scenarios in terms of varying input loadings were calculated. These were model runs with high, medium and low COD loadings and flow rates of the input substrate to cover the projected range of daily biogas production between 150 and 600 m³/d (Table 5-3). The modelled reactors have volumes of 50 m³ (each of the reactors 1 and 2) and 91 m³ (each of the reactors 3 and 4), respectively.

Table 5-3 Simulated input loadings and resulting gas production rates

	Input Data					Results				
	CODx	CODs	TKN	Q	Pumping rate reactor 2,1 and 4,3	Qgas reactor 1	Qgas reactor 2	Qgas reactor 3	Qgas reactor 4	totQgas
	[g/m³]	[g/m³]	[g/m³]	[m³/d]	[m³/d]	[m³/d]	[m³/d]	[m³/d]	[m³/d]	[m³/d]
low	80,000	20,000	5,000	5	0/0	157	36	6	1	200
					25/10	112	72	13	3	200
medium	80,000	20,000	5,000	10	0/0	259	94	38	5	396
					50/20	185	139	56	16	396
high	120,000	30,000	5,000	10	0/0	431	118	37	8	594
					50/20	311	206	52	22	591

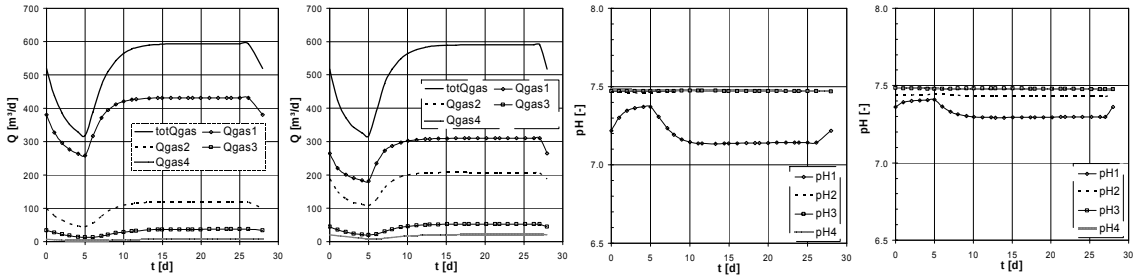

Figure 5-7 Simulated distribution of gas production and pH within the 4 chamber system at high loading with and without recycling (recycle pumping rates of 0/0 and 50/20 from left to right)

Calculations revealed that the average methane contents of the produced biogas were 60, 66, 64 and 63 % for chambers 1-4 respectively and pH levelled off to around 7.5, with the exception of chamber 1. High nitrogen content of the manure released during digestion leads to high corresponding alkalinity. Due to this buffer capacity excessive acidification of reactor 1 is prevented even at high daily organic loading rates up to 30 kg COD/m³. Slight decrease of pH in reactor 1 can be compensated by recycling the subsequent compartment (Figure 5-7).

The simulation results shown in Table 5-3 and Figure 5-7 exhibit a more uniform distribution of biogas production to the 4 reactors when recycle flows between reactor 1/2 and 3/4 are applied. Figure 5-8 depicts the calculated COD degradation within the system. Again, this process turned out to be independent from the input loading and amounts to 65 % respectively.

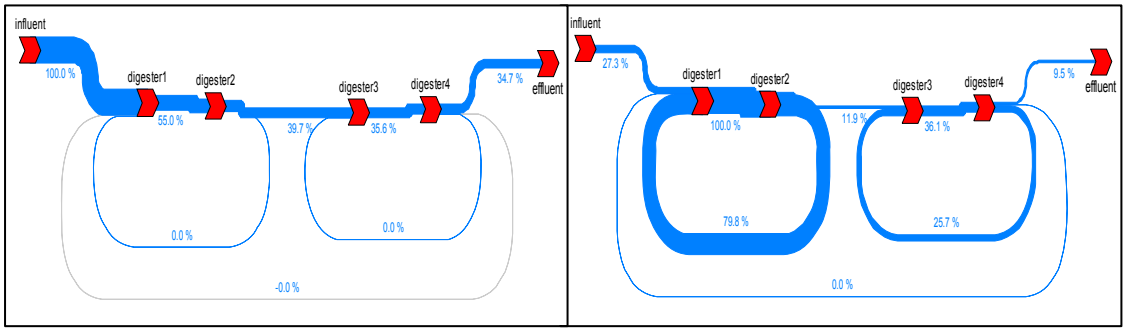

Figure 5-8 Calculated COD degradation for high loading with recycle pumping rates of 0/0 (left) and 50/20 (right), the value for 100 % is related to the largest COD stream including the recycle flux in each case

CONCLUSIONS

ADM1 applied in a 4-reactor-configuration proofed to be an appropriate tool for process design, optimisation and predictions for biogas plants. Simulated digestion of piggery manure showed high pH-stability which is attributed to the high ammonia content in manure. Therefore a baseflow of manure can serve as an optimum substrate for combination with other more acidic co-substrates like dairy wastes or municipal bio-waste.

Sufficient recycling from chamber 2 to 1 (driven by gas pressure yielding from the high-rate activity in the first reactor) can compensate volume limitations. Recycle flow em-

ploys two mechanisms against the threat of overloading – dilution of acidic substrate and mixing of syntrophic biomass, specifically back-feeding of acetogens and of hydrogen consuming methanogens. Depending on the overall retention time SRT chambers 3 and 4 can meet different process requirements: In case of high SRT they serve as hydraulically decoupled low-rate postfermentation reactors or even as gas-tight storage tanks. High load scenarios (Table 5-3) yield to COD loading rates of 30 kg COD per m³ volume and day and SRT or HRT of 5 days in the first tank at zero recycling rate (5.3 kg COD per m^3 of total volume and day). A recycle flow from chamber 4 could prevent pH-dropping in chamber 1 and transfers degradation activity to subsequent compartments. The plant appears very flexible concerning substrate flow and thus, applicable to a wide range of livestock on different agricultural sites.

REFERENCES

Batstone D. J., Keller J., Angelidaki I., Kalyuzhnyi S. V., Pavlostathis S. G., Rozzi A., Sanders W. T. M., Siegrist H. and Vavilin V. A. (2002a). *Anaerobic Digestion Model No.1* Scientific and Technical Report, **13**, IWA, London.

Batstone D. J., Keller J., Angelidaki I., Kalyuzhnyi S. V., Pavlostathis S. G., Rozzi A., Sanders W. T. M., Siegrist H. and Vavilin V. A. (2002b). The IWA Anaerobic Digestion Model No 1 (ADM1) *Water Science and Technology*, **45** (10), 65–73.

Blumensaat F. and Keller J. (2005). Modelling of two-stage anaerobic digestion using the IWA Anaerobic Digestion Model No. 1 ADM1 *Water Research*, **39** 171-183.

Kalfas H., Skiadas I. V., Gavala H. N., Stamatelatou K. and Lyberatos G. (2005). Application of ADM1 for the simulation of anaerobic digestion of olive pulp under mesophilic and thermophilic conditions. *The First International Workshop on the IWA Anaerobic Digestion Model No.1 (ADM1), proceedings*, Lyngby-Denmark.

Møller H. B., Sommer S. G. and Ahring B. K. (2004). Methane productivity of manure, straw and solid fractions of manure *Biomass and Bioenergy*, **26** 485 – 495.

Wett B., Eladawy A. and Ogurek M. (2006a). Description of nitrogen incorporation and release in ADM1. *International Workshop on the IWA Anaerobic Digestion Model No.1*, Copenhagen, in press.

6 FARMSCALE CO-FERMENTATION OF MANURE AND ORGANIC WASTE (C)

Schoen M. A., Phothilangka P., Eladawy A., Insam H. and Wett B. (2007)

Farmscale co-fermentation of manure and organic waste

Reformatted version of paper originally published in:

Proceedings of the IWA-workshop on anaerobic digestion in mountain area and isolated rural zones. 5-7/Jun/2007, Chambéry, France

FARMSCALE CO-FERMENTATION OF MANURE AND ORGANIC WASTE

Schoen M.A.[1] , Phothilangka P.[1], Eladawy A.[1], Insam H.[2] and Wett B.[1]

[1]University of Innsbruck, Unit of Environmental Engineering, (Austria)
[2]Studio BioTreaT, Technikerstr.25d, 6020 Innsbruck, Austria

Abstract: Biogas production reduces demand for fossil fuels and helps to achieve the Kyoto Protocol goals. So far, biogas plants at small-scale (< 100 kW) have often been considered uneconomical, however, this is now challenged by development of an innovative 4-chamber plant with standardised design and construction. This helps to avoid costly individual planning and installation of each facility. For process design and optimisation of a farm-scale pilot-plant biokinetic modelling based on the Anaerobic Digestion Model No.1 (ADM1) was utilized. In the lab different substrates (biowaste and manure) have been digested separately in parallel under specified conditions in a 2-lane 2-step CSTR-system. Subsequently, a configuration of 2 ADM1 model reactors was set up for analysing experimental digestion performance. Calibration of the numerical model focused on individual influent characterisation of both substrates but on consistent selection of kinetic coefficients in order to generate a uniform set of parameters applicable for simulation of co-fermentation. High loading of the biowaste reactor lead to pH-drop and system failure mainly due to lower ammonia concentration and corresponding buffer capacity, while manure digestion remained stable.

Keywords: Anaerobic digestion, ADM1, agricultural wastes, biogas, co-fermentation, manure, modelling

INTRODUCTION

Since the late seventies, anaerobic digestion (AD) has experienced an outstanding growth in research and full-scale application. Numerous large scale biogas plants have been established especially in Northern Europe which combine waste from agriculture, industry and households and produce both biogas and a liquid fertiliser which is recirculated back on farmland. Several types of digesters are successfully operated at large scale (10,000 to 100,000 tons per year) treating different types of solid wastes (van Lier *et al.*, 2001). In Europe, there are more than 4500 biogas plants (including landfill sites) in operation today. The average biogas production growth rate in the biogas sector was more than 6% per year in 2002. The total European biogas production was estimated to 92 PJ/year in 2002 and the total European potential is estimated to 770 PJ/year in 2020 (Jönsson, 2004). As an example, Figure 6-1 depicts the fast growing number of plants in Germany and Austria over the last decades. Due to amendments in legislation, government subsidies and up rating of legally guaranteed electricity tariffs in Austria as well as in Germany there was a notable leap of the number of plants and in installed electrical power in 2005.

As a consequence of technical progress and permanently rising prices for non-renewable energy sources (e.g. coal, oil, natural gas, uranium), biogas systems undergo growing importance. As the biogas production cycle is an integrated system of resources utilization, organic waste treatment, nutrient recycling and redistribution, and renewable energy production, numerous energetic, environmental and agricultural benefits are created (Lens *et al.*, 2004 in Wiese and Haeck, 2006). These advantages

combined with the present energy conservation policies as well as the strong demand for the reduction of atmospheric CO2 emissions are in favour of the further development of advanced AD techniques (van Lier *et al.*, 2001).

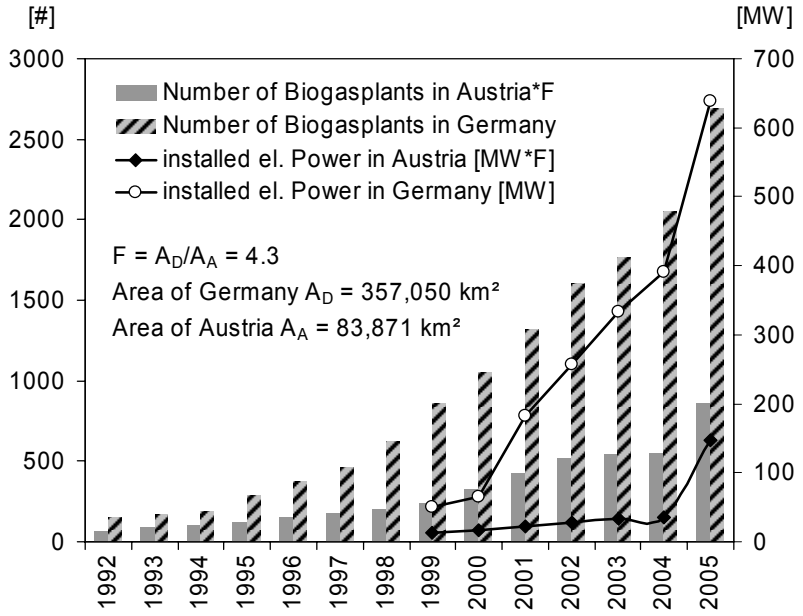

Figure 6-1 Number of biogas plants and installed el. power in Germany and Austria (modified from FV Biogas, 2005 (Germany), Eder and Schulz, 2006 (Austria)). For better comparability the values for Austria were multiplied with a factor F equalising the different sizes of both countries.

The steady increase of biogas plants mentioned before was additionally benefited by the parallel processing of manure as basic substrate together with organic wastes which had been deposited or treated elsewhere so far. This procedure is known as co-digestion and the utilized input substrates can range from the organic fraction of municipal solid wastes, to animal wastes, to municipal sludges, to organic wastes primarily from food industries. Whereas initially only organic wastes and agricultural by-products were used for co-digestion, today more and more energy crops are grown for increased energy yields (Bischofsberger *et al.*, 2005).

The major goal of the project presented in this paper is the improvement of cost-efficiency of small agricultural biogas systems which is not at hand so far because of costly individual planning and installation of each facility. Thus, the development of an innovative 4-chamber system (Figure 6-2) with standardised design and construction was initiated which is on the other hand applicable to a wide range of livestock. Different from a completely mixed reactor, the circular-shaped 4-chamber scheme features plug-flow characteristics. Among other advantages, this entails less odour generation and improved sanitising as well as higher gas production rates by preventing hydraulic short-circuiting. Moreover, the construction features a patented lifter system (Thermo-Gas-Lift) acting as both a heat exchanger and a mixing device which partly supersedes the application of mechanical stirrers.

Currently, a farm-scale co-fermentation pilot-plant applying the 4-chamber system mentioned above is under construction. Given the inherent complexity of the processes associated with AD, the system is quite vulnerable to abrupt operating changes espe-

cially when overloading the first compartment. It is known that manure is a rather inertial and pH-stable substrate due to a high buffering capacity (Angelidaki *et al.*, 1993 and Angelidaki *et al.*, 1999) whereas the system reacts very sensitive to overloading with pure biowaste or whey for example. Because whey does not have any buffering capacity, the rapid formation of volatile acids reduces the pH, thus resulting in complete digester failure. Ghaly *et al.*, (2000) reported a total breakdown of gas production and a pH drop from 5.6 to 3.3 when feeding a two-stage mesophilic anaerobic digester with raw cheese whey (pH = 4.9). Thus, an appropriate combination of co-substrates could be a remedy. A combination of different input substrates requires the ability to predict plant performance (Angelidaki *et al.*, 1999). Biokinetic modelling based on the Anaerobic Digestion Model No.1 (ADM1) was applied for process design and optimisation.

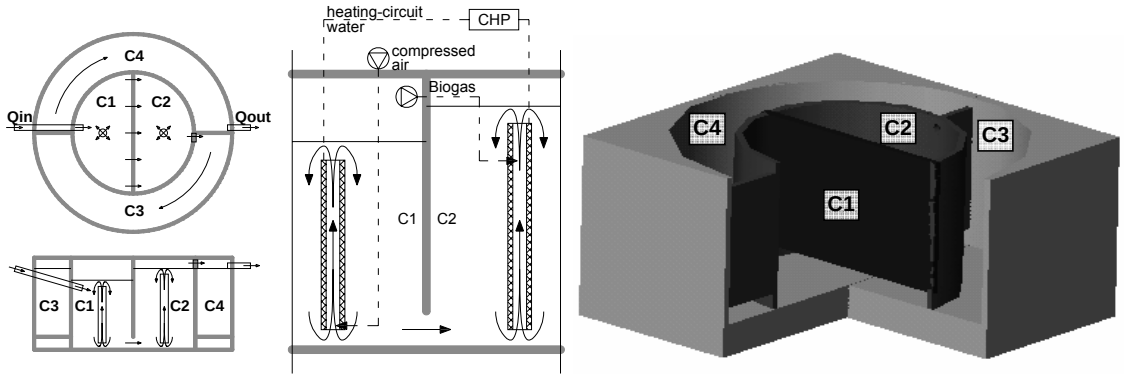

Figure 6-2 Layout and flow scheme of the 4-chamber pilot plant with cylindrical shape and gas-lift-system

METHODS

Recently the AD specialist group of IWA proposed ADM1 (Batstone *et al.*, 2002a) as a universally applicable bio kinetic model which allows the mathematical description of anaerobic digestion of different types of organic substrates (Steyer *et al.*, 2006). ADM1 describes digestion of particulate composites as a 5-stage process involving disintegration, hydrolysis, acidogenesis, acetogenesis and methanogenesis. In the first step named disintegration composite solids and cells of microorganisms are degraded to their principal constituents including carbohydrates, proteins and fats. Additionally, inert particulate and soluble matter emerge which are not affected by the subsequent reactions. Thereafter, the macromolecular products are subject to enzymatic decomposition and transformed to monosaccharides, amino acids and long chain fatty acids. Further anaerobic digestion finally leads via acetogenesis and methanogenesis to biogas production (CH_4, CO_2).

Till now most model applications focus on anaerobic digestion of sewage sludge and sets of validated parameters have been suggested (e.g. Blumensaat and Keller, 2005). In case of manure or other agricultural wastes a priori knowledge about the substrate in terms ADM1 compounds is lacking and influent characterisation becomes a major issue (Wett *et al.*, 2006b). To cover both tasks – proper influent characterisation of the substrates and close model-design interaction – different substrates (biowaste and manure) normally serving as input for a biogas plant sited on a pig farm have been di-

gested separately in parallel under specified conditions in the lab. For this purpose, a 2-lane 2-step digester system (Figure 6-3 A and B) was setup consisting of four anaerobic continuously stirred tank reactors (CSTR) with a volume of 0.1 m³ each. Measured characteristics of the investigated materials are listed in Table 6-1. Gas production and pH were measured daily while feed tanks were refilled and sampled weekly.

Table 6-1 Input values of manure and biowaste

Week	**COD_s** [mg/L]		**COD_x** [mg/L]		**N_{tot}** [mg/L]		**NH_4-N** [mg/L]		**N_{org}** [mg/L]	
	*M	B	M	B	M	B	M	B	M	B
1	0	0	0	0	0	0	0	0	0	0
2	8086	7207	36020	95938	1936	1930	187	64	1749	1865
3	9058	3278	44248	40409	2135	857	301	137	1833	711
4	9146	10645	43217	42799	1880	913	157	53	1722	860
avg.	8763	7043	41162	59715	1984	1233	215	85	1768	1145
Week	**TSS** [g/L]		**VSS** [g/L]		**TC** [g/L]		**TIC** [g/L]		**S** [g/L]	
	M	B	M	B	M	B	M	B	M	B
1	0	0	0	0	0	0	0	0	0	0
2	36.0	66.8	25.3	59.6	13.8	43.0	0.26	1.34	0.11	0.21
3	44.8	26.2	31.2	22.3	17.2	11.4	0.31	0.50	0.14	0.06
4	41.1	33.0	29.7	28.8	14.8	13.6	0.26	0.64	0.13	0.09
avg.	40.6	42.0	28.7	36.9	15.3	22.7	0.28	0.83	0.13	0.12

* M = manure, B = biowaste

For calibration of the numerical model, measured data from the lab experiments served as a basis. A configuration of 2 ADM1 model reactors representing one lane of the parallel reactors was set up by using the Matlab-Simulink® based commercial simulator SIMBA© (v.5.12) focusing on the appropriate choice of parameters and coefficients. Model calibration was supported by a carbon and nitrogen mass balance applying the principle of mass conservation. With the help of a spread sheet the composition of ADM1-compounds was compared for 3 states of the investigated substrates, namely before disintegration, after disintegration and after digestion. In detail, influent values for the numerical model included COD_x, COD_s and TKN which were split into the ADM1-fractions containing C and N according to the ratios given in the ADM1 model description (Batstone *et al.*, 2002a). Some of these fractions have variable N and C-contents and it is possible to adjust those values within a certain range. After that, an estimation of disintegration factors (e.g. fraction Xch from Xc) was applied in order to calculate feed composition in terms of C and N after disintegration. Finally all simulated ADM1 compounds of digested sludge were listed and their C and N contents were totalled. Proper calibration was tied to the following conditions: the sums of C and N contents of all compounds must remain constant and equal the measured values throughout all 3 states.

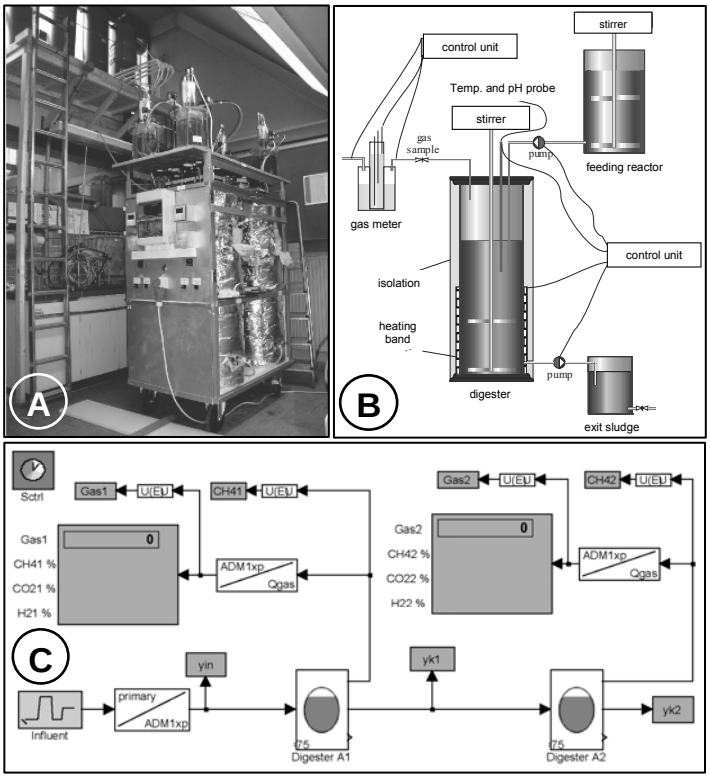

Figure 6-3 Set-up and schematic layout of 2-lane 2-step reactors with a volume of 0.1 m³ each for digestion tests (A,B) and 2-reactor-model represented by serial ADM1 digesters edited in the SIMBA-environment (C)

RESULTS AND DISCUSSION

Figure 6-4 below shows the results of the calibration with the 2-reactor-model. One week prior to feeding with the substrates sewage sludge from WWTP Innsbruck, Austria was put into the reactors and served as inoculum. Lab experiments comprised two phases: an initial stabilization phase when the digesters where fed with 75 litres of inoculum each on day 0 and no further feeding for 8 days. After that period, the 2-lane 2-step reactor systems was fed with biowaste (reactors A1 and A2) and manure (reactors B1 and B2) with characteristics according to Table 6-1 and then digested under mesophilic conditions (37°C). For the manure fraction feeding was done semi-continuously, i.e. beginning from day 9 a batch of 7.5 liters was put to the reactors once a day. Biowaste was also fed with 7.5 L/d but as a rapid acidification due to a high share of whey was detected in digester A1 feeding was stopped between day 17 and 22 in order to enable recovery of the reactor. But these measures were ineffective and system failure was inevitable. The benefit of this situation was a data set providing the chance for calibrating and simulating overloading and system failure due to digester acidification.

Table 6-2 gives an overview on the applied model parameters and their deviation from the default values suggested in the original model description of ADM1 (Batstone *et al.*, 2002a). Disintegration distributes COD and nitrogen to the ADM1 compounds and thus, the fractionizing factors for the composites Xc play an important role in model performance as they determine a characterisation of the input substrate.

The fraction XP of decay products (fXP_XC) considers inactive biomass in the particulate composites XC of the feed. XP was introduced in Wett *et al.*, 2006a and was implemented in the simulation software.

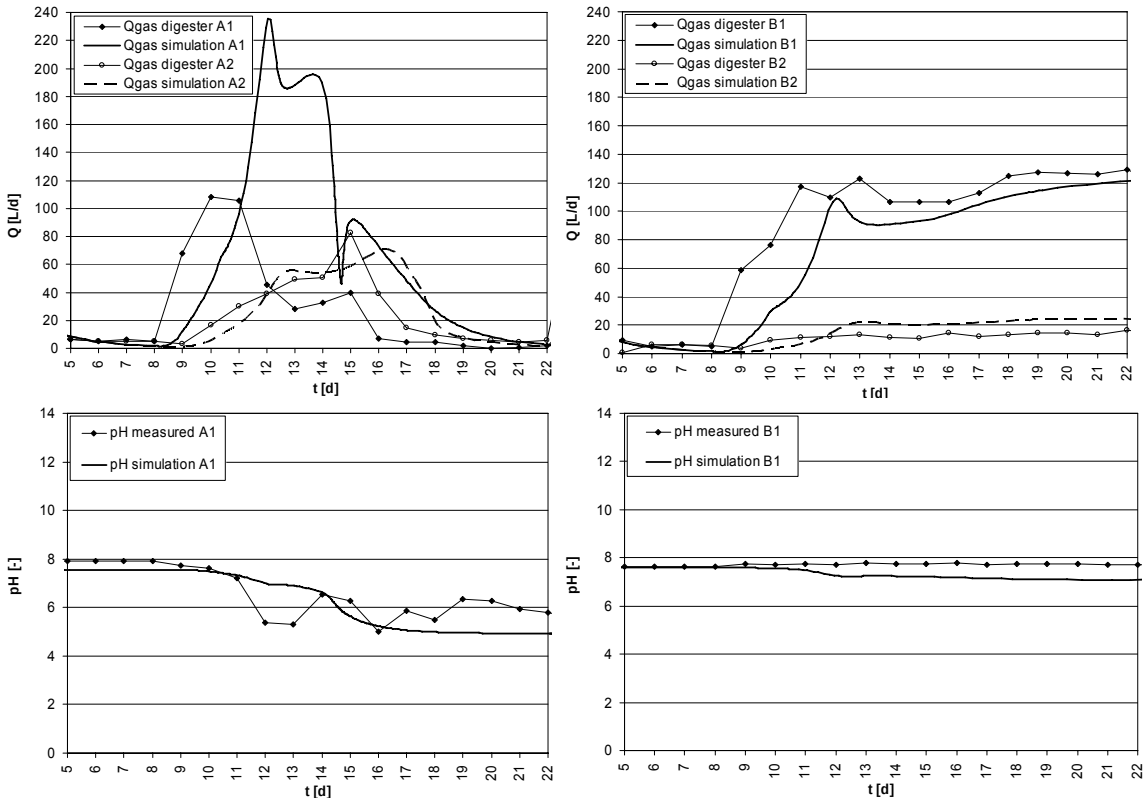

Figure 6-4 Measured and calibrated gas production rates and pH for biowaste (left) and manure (right)

As already stated in the ADM1-model description, the coefficients for disintegration (*kdis* in ADM1 terminology), saturation of sugar (*KS_su*), uptake rate of sugars (*km_su*), decay rate of sugar degraders (*kdec_Xsu*), uptake rate acetate (*km_ac*), decay rate of acetate degraders (*kdec_Xac*) and free ammonia inhibition coefficient (*KI_NH3*) as well as the carbon and nitrogen contents of the composite fraction (*Xc*) turned out to be very sensitive to model behaviour.

As can be seen from Figure 6-4, a satisfactory agreement between simulated and measured values could be obtained for manure. For biowaste the model prediction fitted quite well with the experimental data, although the first-step increase of gas production in digester A1 was overestimated by the simulation. It is obvious that a lower acetate uptake rate (e.g. *km_ac* = 4) in the model would improve agreement with measured biowaste digestion and a higher acetate uptake rate (e.g. *km_ac* = 30) could match manure digestion data. The chosen acetate up-take rate (*km_ac* = 12) as the most sensitive parameter for this application represents a trade-off for the sake of a uniform co-fermentation parameter set.

Among others, the pH of the digestion process is determined by the volatile fatty acids (VFA) introduced by the feed or produced by the process. Overloading leads to a rapid accumulation of VFA and population of methanogenous organisms (*Xac*) is not yet established to cope with such an F/M ratio. Resulting acidification and pH-drop slows

down all relevant process rates and becomes manifest in a total breakdown of gas-production. The bicarbonate buffer of manure corresponding to the ammonia concentration (Table 6-1) is 2.5 times higher for manure compared to biowaste. Both higher VFA content and lower buffer capacity of biowaste leads to a significant pH-drop and system failure while manure digestion remains stable.

Table 6-2 Calibrated ADM1 model parameters for manure and biowaste

Parameter	Description	chosen value		Parameter	Description	chosen value	ADM 1 suggestion**
		B*	M			B and M	
fSI_XC [-]	fraction SI from Xc	0.015	0.0150	kdis [d^{-1}]	disintegration rate	0.65	0.41/0.096 for B/M
fXI_XC [-]	fraction XI from Xc	0.300	0.1250	KS_su [kg COD/m³]	half saturation constant sugar	0.5	0.533 for M
fCH_XC [-]	fraction Xch from Xc	0.275	0.3400	kdec_Xsu [d^{-1}]	decay rate Xsu	0.7	0.01 for M
fPR_XC [-]	fraction Xpr from Xc	0.110	0.1800	km_su [d^{-1}]	Uptake rate sugars	30.0	49.3 for M
fLI_XC [-]	fraction Xli from Xc	0.300	0.1400	km_ac [d^{-1}]	max. uptake rate acetate	12.0	10.9 for M
fXP_XC [-]	fraction Xp from Xc	0.000	0.2000	kdec_Xac [d^{-1}]	decay rate Xac	0.02	0.01 for M
C_Xc [kmole C/ kg COD]	Carbon content Xc	0.028	0.028	KI_NH3 [kmole N/m3]	inhib. coeff. NH3 in p11***	0.0018	0.018 for M
N_Xc [kmole N/ kg COD]	Nitrogen content Xc	0.0011	0.0026				

* B = biowaste, M = manure **Suggestions according to appendix A of ADM1 model description (Angelidaki *et al.*, 1993) *** p11= uptake of acetate

Ammonia inhibition is a separate issue showing opposite dynamics. The pH and temperature determine the ionization degree of ammonia, and free ammonia in turn controls the rate of the methanogenic step. When the methanogenic step gets inhibited acetate accumulates and subsequently gas production breaks down. Within the model, free ammonia inhibition is implemented via the following inhibition term which is applied to the process rate determining the uptake of acetate:

$$I\_NH3 = \frac{1}{1 + S_{NH3}/KI\_NH3}$$

with
I_NH3…Inhibition term for free ammonia
KI_NH3 … free ammonia inhibition coefficient (according to Table 6-2)
S_{NH3}…free ammonia concentration

As can be seen from Figure 6-5, there is a clear correlation between the level of inhibition and the concentration of free ammonia which slows down methanogenesis to about 30% for both substrates in the initial period. The inhibition term for biowaste ap-

proaches a value of 1 (i.e. no inhibition) as the free ammonia concentration decreases. This mechanism of inhibition relief tends to stabilize the process and total failure is prevented, unless a disturbance of a magnitude exceeding the buffer capacity of the medium, i.e., pH breakdown, before stabilization occurs.

During digestion of piggery manure, significant pH changes or sudden process failure has not been observed despite the fact that ammonia inhibition remains relatively high (Figure 6-5) for the given load scenario. By contrast, for biowaste the system collapsed due to a fast generation of VFA notwithstanding a relief of ammonia inhibition.

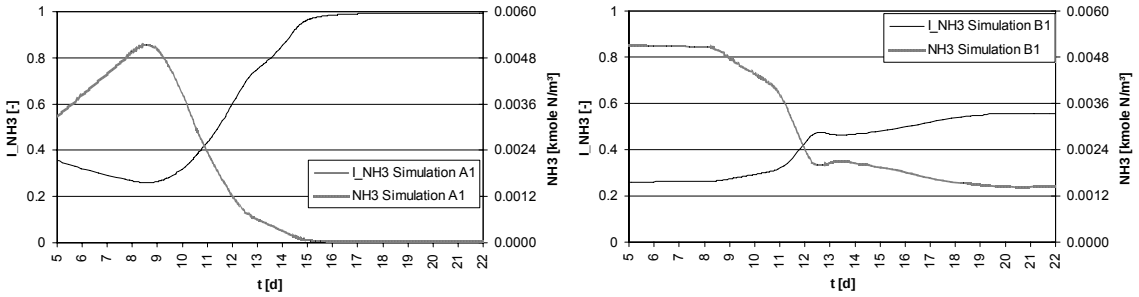

Figure 6-5 Progress of ammonia concentration and ammonia inhibition term for biowaste (left) and manure (right)

CONCLUSIONS

In general, multi-chamber systems are more sensitive to overload situations due to steeper concentration gradients. Co-fermentation of “slow food” like manure together with more acidic “fast food” like biowaste shows additional beneficial impacts on the process robustness. Simulated digestion of piggery manure showed high pH-stability which is attributed to the high ammonia and corresponding bicarbonate content in manure. Therefore, a constant baseflow of manure can serve as an optimum substrate for compensating temporary “shock loading” with more acidic co-substrates which have to be processed quickly (occurring for example in harvest time). The presented simulation examples clearly demonstrated the feasibility of numerical modelling of co-digestion applying one uniform set of parameters for substrates with differing characteristics.

REFERENCES

Angelidaki I., Ellegaard L. and Ahring B. K. (1993). A Mathematical Model for Dynamic Simulation of Anaerobic Digestion of Complex Substrates: Focusing on Ammonia Inhibition. Biotechnology and Bioengineering, 42 159-166.

Angelidaki I., Ellegaard L. and Ahring B. K. (1999). A Comprehensive Model of Anaerobic Bioconversion of Complex Substrates to Biogas. Biotechnology and Bioengineering, 63 (3), 363–372.

Batstone D. J., Keller J., Angelidaki I., Kalyuzhnyi S. V., Pavlostathis S. G., Rozzi A., Sanders W. T. M., Siegrist H. and Vavilin V. A. (2002). Anaerobic Digestion Model No.1 Scientific and Technical Report, 13, IWA, London.

Bischofsberger W., Dichtl N., Rosenwinkel K.-H., Seyfried C. F. and Böhnke B. (2005). Anaerobtechnik [in German], 2nd Edition, ISBN 3-540-06850-3, Springer-Verlag, Heidelberg, Germany.

Blumensaat F. and Keller J. (2005). Modelling of two-stage anaerobic digestion using the IWA Anaerobic Digestion Model No. 1 ADM1 Water Research, 39 171-183.

Eder B. and Schulz H. (2006). Biogas Praxis [in German], 3rd Edition, ISBN 3-936896-13-5, ökobuch Verlag, Staufen, Germany.

FV Biogas (2005). Hintergrunddaten [in German]. Download from www.biogas.org/datenbank/file/notmember/presse/Pressegespr_Hintergrunddaten1.pdf, Access Date 26.01.2007.

Ghaly A. E., Ramkumar D. R., Sadaka S. S. and Rochon J. D. (2000). Effect of reseeding and pH control on the performance of a two-stage mesophilic anaerobic digester operating on acid cheese whey. Canadian Agricultural Engineering, 42 (4), 173-183.

Jönsson O. (2004). Upgrading and Use of Biogas as Fuel of Motor Vehicles. IEA Bioenergy - Seminar on the production and use of biogas, Jyväskylä, Finland.

Lens P., Hamelers B., Hoitink H. and Bidlingmaier W., (eds) (2004). Resource Recovery and Reuse in Organic Solid Waste Management. Intergrated Environmental Technology Series, ISBN 1 84339 054 X, IWA Publishing.

Steyer J. P., Bernard O., Batstone D. J. and Angelidaki I. (2006). Lessons learnt from 15 years of ICA in anaerobic digesters Water Science and Technology, 53 (4-5), 25-33.

van Lier J. B., Tilche A., Ahring B. K., Macarie H., Moletta R., Dohanyos M., Hulshoff Pol L. W., Lens P. and Verstraete W. (2001). New perspectives in anaerobic digestion. Water Science and Technology, 43 (1), 1-18.

Wett B., Eladawy A. and Ogurek M. (2006a). Description of nitrogen incorporation and release in ADM1. Water Science and Technology, 54 (4), 67–76.

Wett B., Schoen M., Phothilangka P., Wackerle F. and Insam H. (2006b). Model-based design of an agricultural biogas plant – application of Anaerobic Digestion Model No.1 for an improved four chamber scheme. Water Science and Technology, 55 (10), 21-28.

Wiese J. and Haeck M. (2006). Instrumentation, control and automation for full-scale manure-based biogas systems. Water Science and Technology, 54 (9), 1-8.

7 COMPARISON OF BIOGAS PLANT START-UP PROCEDURES (D)

Schoen M. A., Sperl D., Gadermaier M., Goberna M., Franke-Whittle I., Insam H. and Wett B. (2008)

Comparison of biogas plant start-up procedures based on lab- and full-scale data and on numerical modelling

Reformatted version of paper originally published in:

Proceedings of Second International Symposium on Energy from Biomass and Waste. International Waste Working Group, 17-20/Nov/2008, Venice, Italy.

COMPARISON OF BIOGAS PLANT START-UP PROCEDURES BASED ON LAB- AND FULL-SCALE DATA AND ON NUMERICAL MODELLING

Schoen M.A.[1], Sperl D.[2], Gadermaier M.[2], Goberna M.[2], Franke-Whittle I.[2], Insam H.[2] and Wett B.[1]

[1]University of Innsbruck, Institute of Infratructure, Technikerstr.13, 6020 Innsbruck, Austria
[2]University of Innsbruck, Institute of Microbiology, Technikerstr.25d, 6020 Innsbruck, Austria

Abstract: Two different start-up scenarios have been investigated at a lab-scale to test their adequacy to be applied at a farm-scale manure biogas plant: 1) starting with an inoculum from a stably operating biogas plant and increasing the load stepwise, and 2) filling up the fermenter completely with raw manure and increasing the operation temperature from 20 to 37°C stepwise. A numerical model based on the Anaerobic Digestion Model ADM1 was established and calibrated by means of experimental data. Incorporation of temperature terms in bacterial growth functions allowed a realistic description of the syntropic degradation of the huge initial substrate pool within a start-up time of one month. Two phenomena have been observed: non-occurrence of reactor failure despite high loading rates targeting minimum retention times of 3 days and a poor adaptation of the degradation of sugars within the start-up process. Both effects could be analysed by the mechanistic model.

INTRODUCTION

The production of energy from renewable energy sources (RES) as an alternative to conventional energy generation has received increasing attention and faced an outstanding market growth in recent years. This may be attributed to the permanently rising prices of fossil fuels (e.g. coal, oil) and an increased ecological awareness in the society (Schoen *et al.*, 2007a). Among different RES, biogas plants are particularly efficient in terms of resource management. The biogas production cycle is an integrated system of resource utilization, organic waste treatment, nutrient recycling and redistribution, as well as renewable energy production. Thus, it provides numerous energetic, environmental and agricultural benefits (Wiese and Haeck, 2006).

In this paper a special focus is put on small full-scale biogas plants. In regions with a small structured agriculture, as it is the case in Austria, the construction of biogas plants is often considered to be uneconomical. Due to costly individual planning, small facilities generate higher specific costs than larger plants. Thus, many potential operators refrain from such an investment. To meet this obstruction, the development of an innovative 4-chamber system (Figure 7-1) with a standardised design and construction elements was initiated in order to provide an affordable, cost-effective, small-scale (<100 kW_{el}) biogas plant (Wett *et al.*, 2006b). Despite the standardised construction elements, the plant is able to adapt to a wide range of livestock since the chambers are hydraulically decoupled and through application of internal recycling systems.

In a first step, a pilot plant (approx. 20 kW_{el}) with some novel features was designed and constructed as well as scientifically overseen. The plant features a circular-shaped 4-chamber system which allows for a plug-flow of the substrate, which is mainly cattle manure, and the gas produced. Among other advantages, this entails less odour generation, improved sanitising and desulphurisation as well as higher gas production

rates through the prevention of hydraulic short-circuiting. Moreover, the construction includes a patented lifter system (Thermo-Gas-Lift) acting both as a heat exchanger providing the system with the required process temperature and a mixing device which partly supersedes the application of mechanical stirrers.

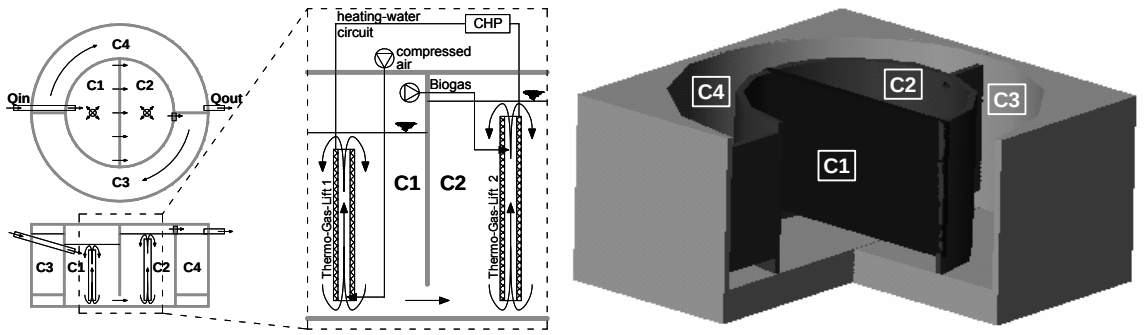

Figure 7-1 Layout and flow scheme of the 4-chamber pilot plant with cylindrical shape and gas-lift-system

Prior to putting into operation, it was necessary to concern about the start-up strategy of the plant. The start-up phase is generally considered the most critical step in the operation of anaerobic digesters and it is very important to pay special attention to an adequate start-up strategy which is related to a number of different factors (e.g. initial loading rate, hydraulic retention time). After the successful establishment of a proper microbial community, anaerobic digesters are expected to run without much attention as long as operating conditions are not significantly altered (Griffin *et al.*, 1998). As a poor start-up can lead to prolonged periods of acclimation and ineffective removal of organic matter, parameters such as the amount of inoculum and the initiation of the feeding should be controlled to reach the design load quickly and to avoid accumulation of unwanted intermediate products such as organic acids (Angelidaki *et al.*, 2006).

Over the last decades, mathematical modelling has become very popular as a supporting tool for the design, operation and control of activated sludge systems in waste water treatment technology. In the anaerobic field (including sludge digestion and biogas plants) this development is observable only since a few years but with a rapidly growing number of users (researchers and practioners) and related publications. It is obvious that the possibility of simulating the processes in a biogas plant by application of a calibrated numerical model allows for notable cost and time savings compared to extensive lab or pilot scale tests. Thus, numerical modelling was used in the present project in the design and optimization stage of the pilot plant.

The work presented in this paper deals with the start-up phase of the pilot plant, including preliminary lab experiments and on-site measurements as well as numerical modelling with application of the anaerobic digestion model No. 1 (ADM1) introduced by Batstone *et al.*, 2002a.

METHODS

In the present study, two different start-up approaches were investigated at a lab-scale for their adequacy to be applied at the pilot full-scale plant including the use of seed material from a biogas plant treating similar substrate as well as process acclimatiza-

tion by gradual temperature and load increase, respectively. The results would determine the selection of a start-up strategy for the pilot plant and its control system would be modified in order to provide best operation conditions.

Lab experiments

In order to investigate the two start-up strategies for the pilot plant at a lab-scale, four continuous stirred tank reactors (CSTR) referred to as A1, A2, B1 and B2 were used. The 100 L reactors feature mechanical mixers, insulation, heating jackets as well as analysis and measurement equipment. The reactors were operated as follows:

Prior to substrate addition, A1 and B1 were inoculated with 15 L seeding sludge from an operating biogas reactor treating similar substrate as the pilot-plant (i.e. mainly cattle manure) plus 60 L of tap water each. Both reactors were operated at a constant temperature of 37°C and fed once a day with cattle manure originating from the location of the pilot plant with increasing loading rates from 0.75 up to 6 L d^{-1} (A1) and from 0.75 up to 24 L d^{-1} (B1) (Figure 7-2).

A2 and B2 were initially loaded with 75 L of cattle manure originating from the location of the pilot plant and subsequently subjected to a temperature increase from 20°C up to 37°C either at 1°C d^{-1} (A2) or at 0.5°C d^{-1} (B2) (Figure 7-2). When both reactors reached 37°C they were also fed with manure corresponding to the loading rates of A1 and B1 (6 L d^{-1} and 24 L d^{-1}). The experiment was run for 42 days and the progression of important parameters (including gas production rate, gas quality, pH, COD, NH_4-N, organic acid content) was monitored and analyzed.

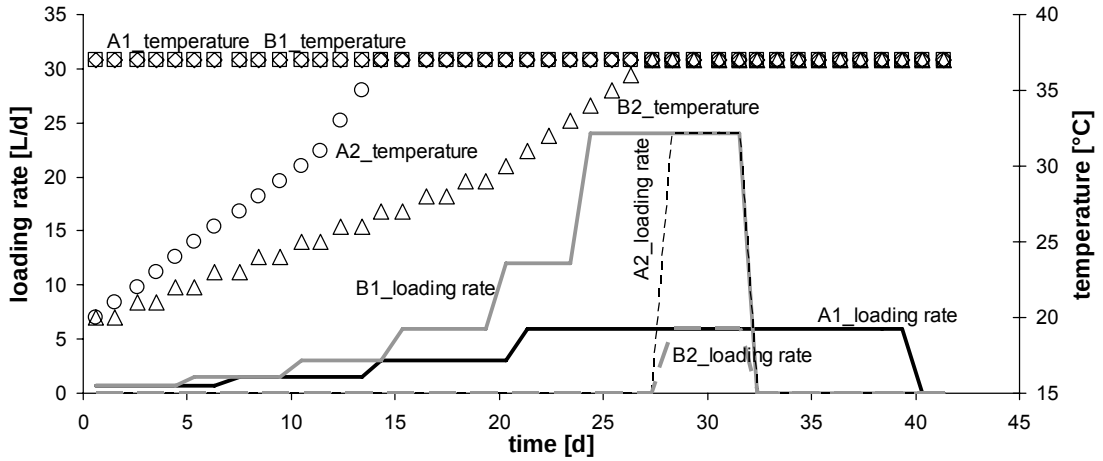

Figure 7-2 Loading rates and temperature progression in the lab-scale reactors

The inoculum used in A1 and B1 was obtained from an operating biogas plant. Cattle manure was obtained from the agricultural school in Rotholz (Austria), where the pilot full-scale plant is located. Prior to utilization both materials were sieved (5mm mesh size) and homogenized to prevent clogging. The prepared feeding solution was stored in plastic containers at 4°C until use. Effluent sludge was sampled and analysed twice a week, and gas production and pH were measured daily. Characteristics of the substrates used are presented in Table 7-1.

Table 7-1 Characteristics of the feeding substrates

	TS	VS	pH	COD_{tot}	COD_{sol}	NH_4-N	org. acids
	[%]	[% TS]	[-]	[mg/L]	[mg/L]	[mg/L]	[mg/L]
inoculum*	4.9	66.9	8.7	49589	11789	2232	1702
manure**	4.1	68.6	8.4	36672	12403	1035	3312

*before dilution with tap water **average values of 4 batches

According to Table 7-1 the manure feeding rates of reactors A1 and B1 which were increased from 0.75 up to 6 L d^{-1} (A1) and 24 L d^{-1} (B1) can be expressed as an average organic loading rate (OLR) of 0.3 up to 2.3 kg VS m^{-3} d^{-1} (A1) and 9.1 kg VS m^{-3} d^{-1} (B1), resulting in a hydraulic retention time (HRT) of 100 d down to 13 d (A1) and 3 d (B1).

The volume of biogas produced was quantitated using a gas meter located on top of each reactor. Gas samples were collected daily in gas-tight bags and gas composition (CH_4, CO_2 and H_2) measured using a Biogas Monitor BM 2000 (Geotechnical Instruments, Leamintong, UK). Sludge pH was measured with a WTW MLP4 pH meter immediately after each sampling. Total and soluble COD (COD_{tot}, COD_{sol}) as well as ammonium nitrogen concentrations (NH_4-N) were measured with HachLange cuvette tests for spectrophotometric analysis. Total solids and volatile solids (TS, VS) were determined by drying the samples at 105°C and subsequently at 550°C. Organic acids were determined by titration in a Mettler-Toledo DL53 titrator.

Numerical modelling

In this section, a special focus is put on the numerical simulation of the start-up experiments. By means of the Matlab/Simulink based simulator SIMBA a numerical model of the lab reactors was set up and data sets from the lab-scale experiments were used for model calibration. SIMBA applies IWA's Anaerobic Digestion Model No.1 (ADM1; Batstone *et al.*, 2002a) for its calculations of the biokinetic processes involved in anaerobic digestion. ADM1 is a universally applicable bio kinetic model which allows for the mathematical description of the anaerobic digestion of different types of organic substrates. ADM1 describes digestion of particulate composites as a 5-stage process involving disintegration, hydrolysis, acidogenesis, acetogenesis and methanogenesis. In the disintegration step composite solids (*Xc*) and cells of microorganisms are degraded to their principal constituents including carbohydrates, proteins and fats. Additionally, inert particulate and soluble matter emerge which are not affected by the subsequent reactions. Thereafter, the macromolecular products are subject to enzymatic decomposition and transformed to monosaccharides, amino acids and long chain fatty acids. Further anaerobic digestion finally leads via acetogenesis and methanogenesis to biogas production (Schoen *et al.*, 2007b).

Model calibration was mainly based on fitting the simulated values to the data gained from the lab experiments by an appropriate choice of the model parameters and coefficients. The major goal was the determination of a uniform parameter set for the four lab experiments. In this regard, the major difficulty is to find a reasonable and detailed inflow characterization when ADM1 is used for inhomogeneous substrates like liquid manure. This was done by determination of the proportional distribution of carbohydrates, lipids, proteins and inert constituents within the substrate. In a first step, values from

the literature reviewed served as a starting basis followed by the utilization of a carbon and nitrogen mass balance. The composition of the different ADM1-compounds was listed and their C and N contents compared to the measured values for three different states: before disintegration, after disintegration and after digestion. Proper calibration was tied to the following conditions: throughout all three states the sums of C and N contents of all compounds must remain constant and preferably have a good match with the measured values.

In anaerobic digestion there are three major operating temperature ranges: psychrophilic, mesophilic and thermophilic (approx. 4-15°C; 20-40°C; 45-70°C). Within those ranges, the activity of the different groups of organisms increases with increasing temperature until an optimum is reached. A further increase of temperature beyond this optimum is followed by a rapid activity drop to zero (Batstone *et al.*, 2002a; Pavlostathis and Giraldo-Gomez, 1991).

Normally, ADM1 does not feature continuous functions to take into account kinetic effects due to temperature progressions since common modelling concerns stable process temperatures. Instead, separate parameter values for either thermophilic or mesophilic conditions are given. As the lab experiments in reactors A2 and B2 included a temperature increase from 20 up to 37°C, it was necessary to implement the mentioned dependencies on biochemical reactions within ADM1. According to the suggestions in Batstone *et al.*, 2002a and Pavlostathis and Giraldo-Gomez, 1991 this was modelled via a double Arrhenius equation of the following form:

$$k = b_1 \cdot e^{[a_1 \cdot (T-30)]} - b_2 \cdot e^{[a_2 \cdot (T-30)]}$$

where k denotes the relative activity, T the actual temperature and a and b are coefficients. The equation takes values between 0 for poor and 1 for optimum temperature conditions (i.e. 37°C) within the mesophilic range. Within ADM1 it was added to the growth rates of the enzymatical and bacterial groups involved in the form of an inhibition term.

On-site investigations

Based on the most favourable start-up strategy found in the lab experiments, the pilot plant was set into operation in April 2008. During the start-up phase and the initial operation period, the plant was constantly monitored. All data from the digesters as well as from the combined heat and power unit (CHP) were logged for evaluation and samples were taken in regular intervals for lab analysis.

RESULTS

Lab experiments

All lab-scale reactors showed quite similar characteristics regarding gas production and pH values up to day 26 (Figure 7-3). After an initial lag phase, biogas production increased up to a peak value followed by a sharp decrease after the feeding was stopped. It should be noted that there was no pH drop or other reactor failure in B1 despite a HRT of only 3 days at maximum feeding rate. An expected washout of methanogens did not occur which is attributed to incoming methanogenic archaea stemming from the alimentary system of the cattle.

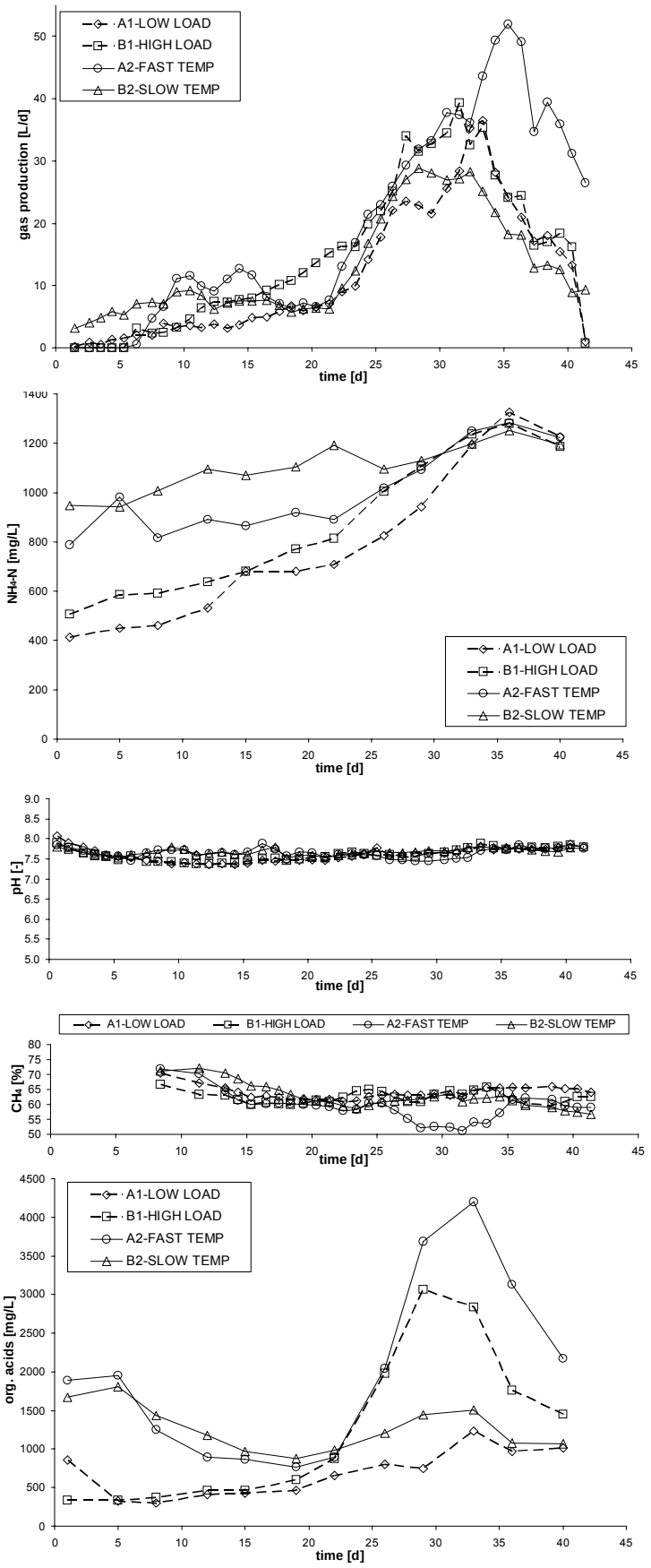

Figure 7-3 Measured values for gas production rate, NH_4-N, pH, gas quality and organic acids in the lab reactors

Numerical modelling

Figure 7-4 depicts the comparison between simulated and measured results of the numerical models for A1, B1, A2 and B2. For the sake of comparability between the two high rate/temperature cases additional values are shown for B1 and A2. As can be seen, model prediction fitted quite well with experimental data, especially for COD and pH. However, for A2 there was an underestimation of the gas production which is a trade off to a uniform parameter set for all four lab experiments.

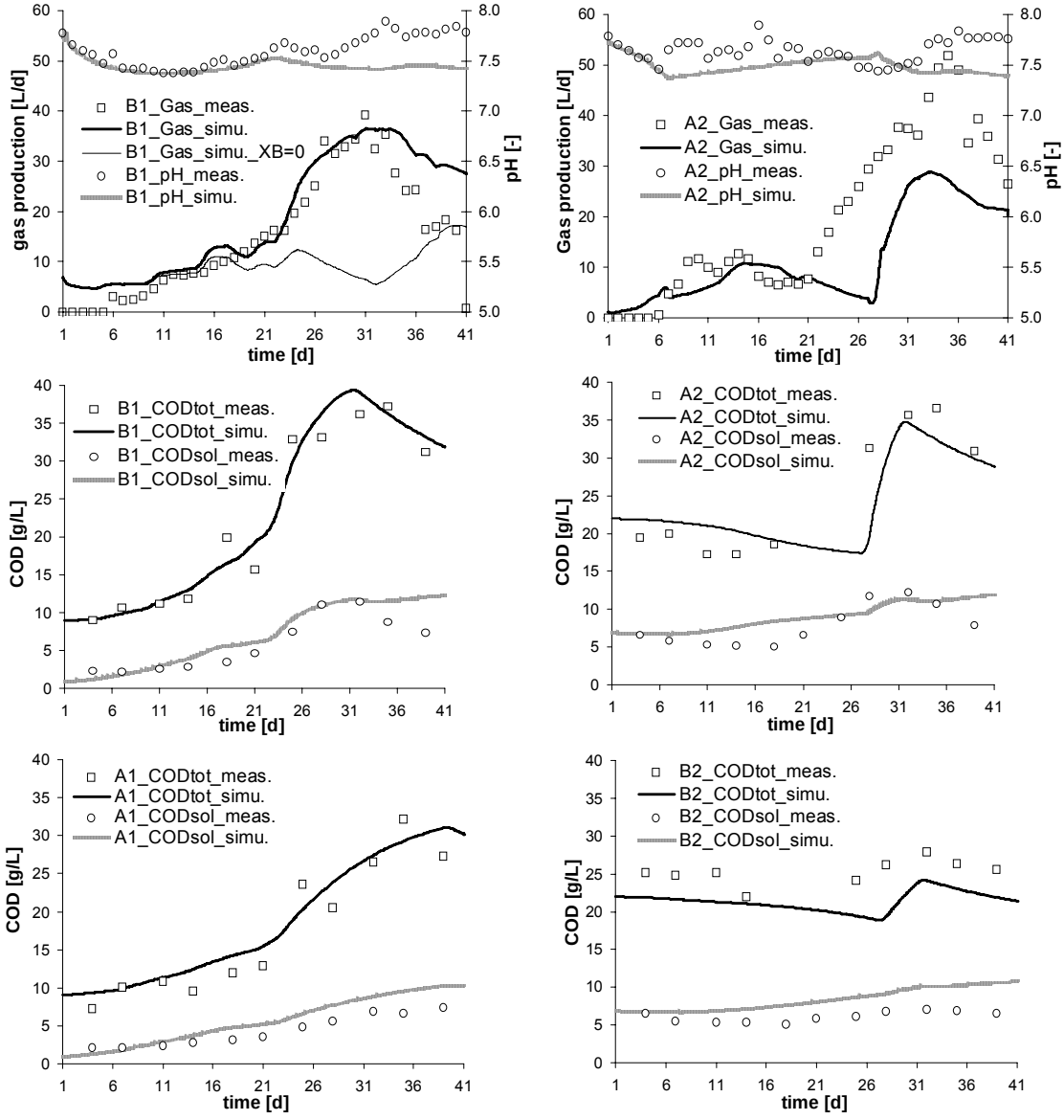

Figure 7-4 Simulation results and measured values for gas production rate (B1, A2), pH (B1, A2), total and soluble COD. Presentation for B1 includes gas production rate without addition of bacterial mass (*XB* = 0).

Following the above made assumption that the non-occurrence of a methanogen washout was due to incoming archaea, an additional influent of biomass (*fXB_Xc*) was introduced within the model. *fXB_Xc* represents an adjustable portion of the composite fraction *Xc* which is fed to the model reactors. It was calibrated to an optimized value of

1%, whereas values of 0% (Figure 7-4) and 2% led to underestimated and overestimated gas productions, respectively.

In the model, disintegration distributes COD and NH_4-N to the ADM1 compounds and thus, the fractionizing factors (*fxx_Xc*) for the particulate composites (*Xc*) play an important role in model performance as they determine a characterisation of the input substrate. Table 7-2 shows these factors as well as the parameters which turned out to be very sensitive for model behaviour. The given substrate ratios indicate a relatively high portion of carbohydrates (*CH*) compared to proteins (*PR*) and lipids (*LI*) with proportions of *CH/PR* = 1.9 and *CH/LI* = 5.0 which is in good accordance with reported compositions of cattle manure in the literature (e.g. Møller *et al.*, 2004). For the kinetic parameters, the maximum uptake rate of sugars (*km_su*) revealed a remarkable influence on the simulation results. It had to be reduced from an initial value of 30 to 8 d^{-1} to avoid an overestimation of gas production. Obviously, there is a poor adaptation of the degradation of sugars within the start-up process. In the subsequent section it will be revealed that this phenomenon was not observable in the long term which could be seen from applying the parameters to a model of the real plant.

Table 7-2 Calibrated ADM1 model parameters including inflow characterization

parameter	description	unit	initial value	optim. value
fSI_XC	fraction sol. inerts of Xc	[-]	-	0.05
fCH_XC	fraction carbohydr. of Xc	[-]	-	0.35
fPR_Xc	fraction proteins of Xc	[-]	-	0.18
fLI_Xc	fraction lipids of Xc	[-]	-	0.07
fXP_Xc	fraction decay prod. from inact. biomass of Xc	[-]	-	0.1
C_Xc	carbon content Xc	[kmoleC/kgCOD]	-	0.0299
N_Xc	nitrogen content Xc	[kmoleN/kgCOD]	-	0.0022
kdis	disintegration rate	[d^{-1}]	0.5	0.1
khyd	hydrolysis rate CH, LI, PR	[d^{-1}]	10	0.31
km_su	max. uptake rate sugars	[d^{-1}]	30	8
KS_xx	half saturation coefficients va, bu, pro	[kgCOD/m³]	0.1	0.5
KS_ac	half satururation coefficient acetate	[kgCOD/m³]	0.15	0.75

Xc...composite fraction, va...valerate, bu...butyrate, pro... propionate

On-site investigations

Although gas quality was lower, it was decided to opt for a start-up strategy in the pilot plant as applied in the lab experiments in A2 and B2 since other parameters like gas production did not differ notably. By utilizing cattle manure originating from the plant site with a subsequent gradual heating-up there are cost savings as transportation costs for the inoculum do not apply and heating power requirements are reduced. So far, measurements revealed that total gas production of the 90 livestock units ranges around 150-200 m³/d (Figure 7-5) where 63% and 37% of the CH4 produced is generated in chambers 1+2 and 3+4, respectively. It should be noted that the start-up phase is not totally completed yet and values may slightly change.

As mentioned above, the calibrated parameter set was applied to a numerical model of the pilot plant and run until steady-state conditions. A maximum uptake rate of sugar (*km_su*) of 8 d^{-1} as used for the lab experiments could not reproduce the measured values whereas a value of 20 d^{-1} yielded a gas production of 160 m^3 d^{-1} and a CH_4 distribution of 69% (chambers 1+2) and 31% (chambers 3+4). This is in good agreement with the on-site data (representing nearly steady-state) and proves the statement that sugar degradation was not fully established within the start-up process.

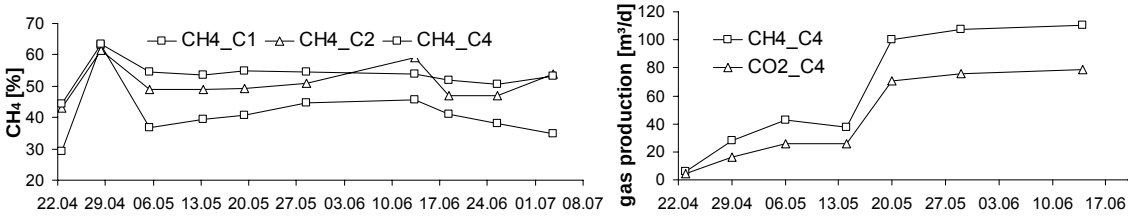

Figure 7-5 Measured gas quality in chambers 1, 2, 4 and gas production in chamber 4

CONCLUSIONS

In order to investigate two different start-up approaches for biogas plants, lab-scale experiments, on-site measurements as well as numerical modelling were accomplished. Despite maximum loading (HRT 3d) no reactor failure occurred which is attributed to incoming cattle-borne archaeal biomass. In the numerical model this was met by incorporation of a flux of active biomass equivalent to 1% of the particulate COD in the feed flow. Further, a poor adaptation of the degradation of sugars within the start-up process was observed which is released when the plant reaches steady-state.

REFERENCES

Angelidaki I., Chen X., Cui J., Kaparaju P. and Ellegaard L. (2006). Thermophilic anaerobic digestion of source-sorted organic fraction of household municipal solid waste: Start-up procedure for continuously stirred tank reactor. Water Research 40, 2621 – 2628.

Batstone D. J., Keller J., Angelidaki I., Kalyuzhnyi S. V., Pavlostathis S. G., Rozzi A., Sanders W. T. M., Siegrist H. and Vavilin V. A. (2002). Anaerobic Digestion Model No.1 Scientific and Technical Report, 13, IWA, London.

Griffin M. E., McMahon K. D., Mackie R. I. and Raskin L. (1998). Methanogenic population dynamics during start-up of anaerobic digesters treating municipal solid waste and biosolids. Biotechnology and Bioengineering, 57 (3), 342-355.

Møller H. B., Sommer S. G. and Ahring B. K. (2004). Methane productivity of manure, straw and solid fractions of manure Biomass and Bioenergy 26 485 – 495.

Pavlostathis S. G. and Giraldo-Gomez E. (1991). Kinetics of anaerobic treatment: a critical review. Critical Reviews in Environmental Control, 21 (5,6), 411-490.

Schoen M., De Toffol S., Wett B., Insam H. and Rauch W. (2007a). Comparison of Renewable Energy Resources in Alpine Regions, in: Borsdorf, A., Stötter, J., Veulliet, E. (Eds.),. *Managing Alpine Future*, Austrian Academy of Sciences Press, ISBN 978-3-7001-6571-2.

Schoen M. A., Phothilangka P., Eladawy A., Insam H. and Wett B. (2007b). Farmscale Co-fermentation of manure and organic waste. IWA-workshop on anaerobic digestion in mountain area and isolated rural zones 5-7/Jun/2007, Chambéry, France (Proceedings).

Wett B., Schoen M., Phothilangka P., Wackerle F. and Insam H. (2006b). Model-based design of an agricultural biogas plant: application of Anaerobic Digestion Model No.1 for an improved 4 chamber scheme. Water Science and Technology, 55 (10), 21-28.

Wiese J. and Haeck M. (2006). Instrumentation, control and automation for full-scale manure-based biogas systems. Water Science and Technology, 54 (9), 1-8.

8 POPULATION DYNAMICS AT DIGESTER OVERLOAD CONDITIONS (E)

Schoen M. A., Sperl D., Gadermaier M., Goberna M., Franke-Whittle I., Insam H., Ablinger J. and Wett B. (2009)

Population dynamics at digester overload conditions

submitted to:

Bioresource Technology

POPULATION DYNAMICS AT DIGESTER OVERLOAD CONDITIONS

Schoen M.A.[1], Sperl D.[2], Gadermaier M.[2], Goberna M.[2], Franke-Whittle I.[2], Insam H.[2], Ablinger J.[3] and Wett B.[1]

[1]University of Innsbruck, Institute of Infratructure, Technikerstr.13, 6020 Innsbruck, Austria
[2]University of Innsbruck, Institute of Microbiology, Technikerstr.25d, 6020 Innsbruck, Austria
[3]Salzburger Abfallbeseitigung GmbH, Aupoint 15, 5101 Bergheim/Salzburg, Austria

Abstract: Two different case studies concerning potential overload situations of anaerobic digesters were investigated and mathematically modelled by means of the Anaerobic Digestion Model No.1 (ADM1). The first scenario included a digester failure at a municipal WWTP which occurred during revision works of the upstream digester within a two-step digestion system when the sludge was directly by-passed to the 2nd-step reactor. Secondly, the non-occurrence of a highly expected upset situation in a lab-scale digester fed with cattle manure was investigated. ADM1 was utilised to derive indicators which were used to investigate the relationship between digester stability and biomass population dynamics. Conventional design parameters such as the organic loading rate appeared unsuitable for process description under dynamic conditions. Indicators reflecting the biokinetic state (e.g. F_{net}/M_{net} or the VFA/alkalinity ratio) are more adequate for the assessment of the stability of reactors in transient situations.

Keywords: ADM1; anaerobic digestion; cattle manure; digester overload

INTRODUCTION

The degradation of organic matter in anaerobic digesters occurs through four basic phases, termed hydrolysis, acidogenesis, acetogenesis and methanogenesis. These phases are a series of interlinked reactions proceeding spatially as well as temporally in consecutive and parallel steps and hence, influence one another (Schink, 1997). Due to the highly sensitive interdependence of the different microbial groups involved, there is always a potential risk of process instability.

Previous research has found that around 70% of the methane produced in the digestion process comes from the transformation of acetate to methane (methanogenesis), usually by the aceticlastic methanogens (e.g. Tchobanoglous *et al.*, 2003). When methanogenesis is not rapid enough due to some upset, volatile fatty acids (VFA) accumulate, which may lead to a decrease in the pH and a cessation of the methane production. Returning to normal operating conditions can be costly and time-consuming. Remedy actions can include reducing the organic loading rate (OLR) to the point where the VFA production rate is less than their maximum consumption rate. This will allow for the consumption of the excess VFA and a return of neutral pH until stable conditions occur again. If this measure is not sufficient, decrease in loading must be coupled with the addition of appropriate chemicals for pH correction (Grady *et al.*, 1999). In the worst case, it could be necessary to empty the complete reactor and start again, including a period with reduced gas production, and thus an associated loss of income.

In the present paper two different case studies concerning overload situations of anaerobic digesters were investigated and mathematically modelled by means of IWA's Anaerobic Digestion Model No.1 (ADM1;Batstone *et al.*, 2002a). The first scenario in-

cluded a digester failure at WWTP Salzburg (Austria) which occurred during revision works of the upstream digester within a two-step digestion system when the sludge was directly by-passed to the 2nd-step reactor. In the second scenario, the non-occurrence of an expected upset situation in a lab-scale digester fed with cattle manure was investigated. This experiment was part of a project dealing with different start-up options for agricultural biogas plants and is described in Schoen *et al.*, 2008. Although a washout of methanogens was expected due to deliberately high loading rates and a hydraulic retention time of only 3 days, a reactor breakdown failed to appear. This was attributed to a continuous reseeding with methanogenic biomass stemming from the alimentary system of the livestock.

For deeper examination, mathematical modelling by application of ADM1 for both cases was utilised to derive indicators which were used to investigate the relationship between digester stability and biomass population dynamics.

METHODS

Case study 1: digester upset at WWTP Salzburg

The municipal WWTP Salzburg (Austria) is operated as a 2-stage system (high-rate/low-rate) for a design-load of 680,000 PE. Excess sludge from both stages is mixed together in one pipe and passes a pre-thickening unit before it is fed into two digesters connected in series. Both reactors have an operating volume of 8160 m³ (effectively only 6860 m³ due to sand deposits detected during revision) and a gas space of 920 m³.

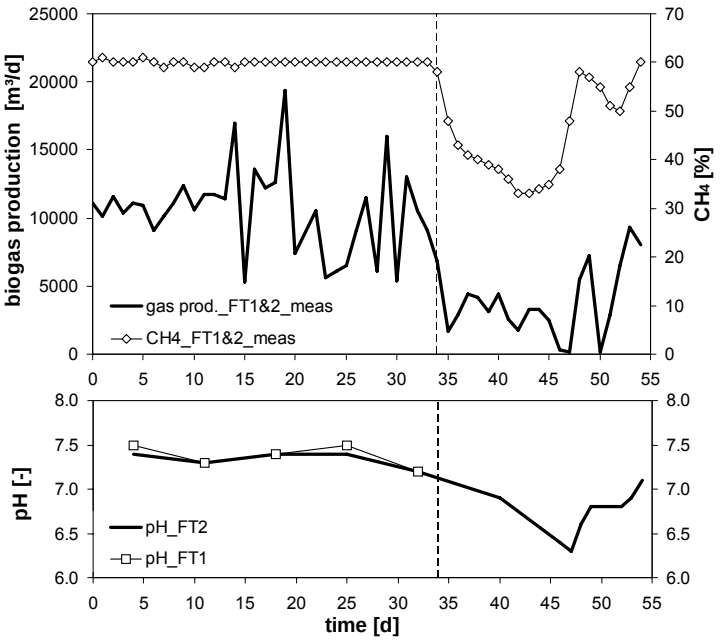

Figure 8-1 Gas production rate, methane content and pH for both digesters (FT1 & FT2). Note that unil day 34 (sludge by-pass to FT2; dotted line) gas production and CH_4 refer to an average value for FT1 and FT2; after day 34 it refers to FT2.

In the course of revision works, the upstream digester (FT1) was shutdown and the sludge was directly by-passed to the 2nd-step reactor (FT2) (day 34 in Figure 8-1). Due

to a poor adaptation of FT2 to direct feeding from the pre-thickener, an average HRT of only 14 days and a yet unexplained slight pH decrease in the feeding sludge from the pre-thickener beginning about 10 days before, there was remarkable breakdown of pH, gas production, and methane content in FT2. On day 40 it was decided to recover FT2 by inoculating the feed with sludge from FT1 that was withdrawn from there to a storage tank after the shut-down of FT1. However, the recovery was not the subject-matter of the present investigation.

Case study 2: Non-occurrence of expected reactor failure during start-up experiment

In the context of a research project dealing with the development of novel concepts for agricultural biogas plants, a pilot plant was constructed and commissioned at a cattle farm (Wett *et al.*, 2006b). In order to investigate a proper start-up strategy for the plant, two different start-up approaches were investigated at a lab-scale for their adequacy to be applied at the pilot full-scale plant. This included the use of seed material from a biogas plant treating similar substrate as well as process acclimatization by gradual temperature and load increase, respectively. As reported in Schoen *et al.*, 2008, the results determined the selection of the optimum start-up strategy for the pilot plant with modifications of its control system in order to provide the best operation conditions. Furthermore, the data gained from the lab analyses served as a basis for the calibration of a numerical kinetic model (applying ADM1) which was setup in order to mathematically simulate the anaerobic processes during the start-up.

In the experiments, four continuous stirred tank reactors (CSTR) referred to as A1, A2, B1 and B2 were used. The 100 L (75 L operating volume + 25 L gas space) digesters feature mechanical mixers, insulation, heating jackets as well as analysis and measurement equipment. The focus in this paper is placed on “B1” which was inoculated with 15 L seeding sludge from an operating biogas reactor treating similar substrate as the pilot-plant (i.e. mainly cattle manure) plus 60 L of tap water prior to substrate addition. The reactor was operated at a constant temperature of 37 °C and fed once a day with cattle manure originating from the location of the pilot plant with increasing loading rates from 0.75 up to 24 L d^{-1} (Figure 8-2).

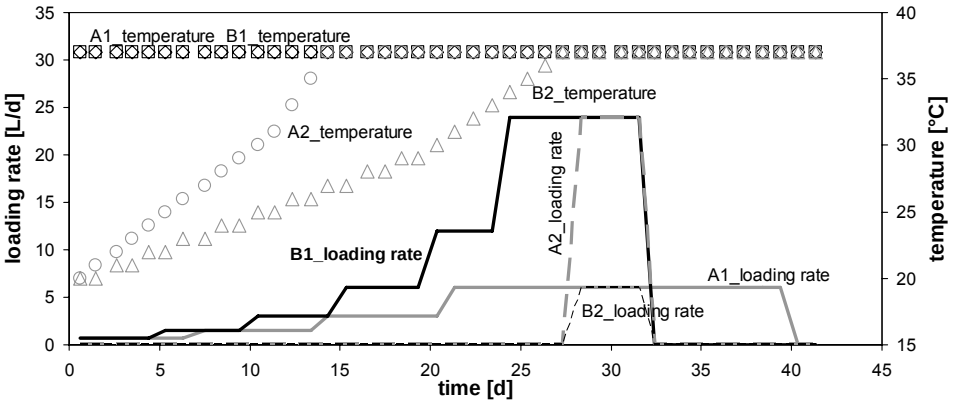

Figure 8-2 Loading rates and temperature progression in the lab-scale reactors

The experiment was run for 42 days and the progression of important parameters (including gas production rate, gas quality, pH, COD, NH_4-N, organic acid content) was

monitored and analyzed. The characteristics of the inoculum and the cattle manure used in B1 are presented in Table 8-1. The manure feeding rates of B1 can be expressed as an average organic loading rate (OLR) of 0.3 up to 9.1 kg VS m-3d-1, resulting in a hydraulic retention time (HRT) of 100 days down to 3 days.

Besides finding a proper start-up strategy, the purpose of steadily increasing the load was to investigate the lowest possible limit of HRT in order to avoid a reactor failure due to the washout of methanogens. However, despite a minimum HRT of 3 days, the expected failure did not occur (Figure 8-4) due to reasons discussed below.

Table 8-1 Characteristics of the feeding substrates

	TS	VS	pH	COD_{tot}	COD_{sol}	NH_4-N	org. acids
	[%]	[% TS]	[-]	[mg/L]	[mg/L]	[mg/L]	[mg/L]
inoculum*	4.9	66.9	8.7	49589	11789	2232	1702
manure**	4.1	68.6	8.4	36672	12403	1035	3312

*before dilution with tap water **average values of 4 batches

Methanogenic population

In order to quantify the methanogenic community composition in reactor B1, the ANAEROBECHIP microarray (Goberna *et al.*, 2009) was hybridised with sludge DNA from B1 which was extracted using the PowerSoil™ DNA isolation kit (MO BIO Laboratories Inc., California). Six genera of methanogens were detected, which were then targeted using real time quantitative PCR as described by Franke-Whittle *et al.*, 2009. After quantification of the number of 16S rRNA gene copies per μl^{-1} DNA in the samples, the results were converted to grams of methanogenic cells per gram sludge. These calculations were based on several broad assumptions: 1) DNA extraction efficiency is equivalent among samples, 2) methanogens have an average of 2.5 copies of the 16S rRNA gene per cell (Klappenbach *et al.*, 2001) 3) most methanogens in the reactor (mesophilic *Methanosarcina* sp.) have an average 1.9 µm diameter, (Kendall and Boone, 2006), a spherical shape and a cytosolic density of 1 g cm^{-3}.

Biokinetic modelling tools

By means of the Matlab/Simulink based simulator SIMBA, numerical models of both case studies were set up and data sets from the lab-scale experiments and from the WWTP were used for model calibration. SIMBA applies IWA's Anaerobic Digestion Model No.1 (ADM1; Batstone *et al.*, 2002a) for its calculations of the biokinetic processes involved in anaerobic digestion. ADM1 is a universally applicable bio kinetic model which allows for the mathematical description of the anaerobic digestion of different types of organic substrates. ADM1 describes digestion of particulate composites as a 5-stage process involving disintegration, hydrolysis, acidogenesis, acetogenesis and methanogenesis. In the disintegration step, composite solids (Xc) and cells of microorganisms are degraded to their principal constituents including carbohydrates, proteins and fats. Additionally, inert particulate and soluble matter emerge which are not affected by the subsequent reactions. Thereafter, the macromolecular products are subject to enzymatic decomposition and transformed to monosaccharides, amino acids and long chain fatty acids. Further anaerobic digestion finally leads to biogas production via acetogenesis and methanogenesis.

Model calibration was based mainly on fitting the simulated values to the measurement data by an appropriate choice of the model parameters and coefficients. For both investigated cases, an almost uniform parameter set regarding kinetic and stoichiometric coefficients could be determined and applied. For both models an appropriate, reasonable and detailed inflow characterisation had to be found especially when ADM1 is used for inhomogeneous substrates like liquid manure. This was done by determination of the proportional distribution of carbohydrates, lipids, proteins and inert constituents within the substrate. In a first step, values from the literature reviewed served as a starting basis followed by a detailed calibration protocol based on COD-, carbon- and nitrogen mass balances.

Table 8-2 Average values for sludge fed from the pre-thickener to the digesters at WWTP Salzburg as used for ADM1 simulations. Note that only direct feeds from the pre-thickener to the digesters were used (not taking into account feeds of FT1 to FT2 on day 0-34 and 40-54).

day	TS	COD	NH_4-N	Q
	[g/L]	[mg/L]	[mg/L]	[m³/d]
0-9	43.9	52315	1949	606
10-19	42.3	55044	2043	567
20-29	44.7	54034	2008	562
30-34	41.0	40709	1548	591
35-39	45.4	44577	1681	472
40-49	41.3	44914	1693	567
50-54	48.8	53769	1999	374

In case study 1, average concentration values as given in Table 8-2 were extracted from routine WWTP operating data for the use with ADM1 simulations. Based on the relative sludge contributions from the high-rate and the low-rate stage, influent COD was estimated by a typical relationship between total solids content and COD of 1.2 kg COD kg TS^{-1} and 1.0 kg COD kg TS^{-1} for the high-rate and the low-rate stage, respectively.

Determination of key indicators for digester stability

The stability and efficiency of the overall digestion process depends on the stability of the individual biochemical processes involved. Process upsets can result from temporarily high loadings, deviations in the environment provided, or the presence of toxic or inhibitory materials in the bioreactor influent (Grady *et al.*, 1999). Also, any significant increase in the concentration of intermediate substrates (e.g. VFAs) may inhibit directly, through toxicity and energetics, the kinetics of other biochemical processes and lead to digester instability (Batstone *et al.*, 2002a). Since the ADM1 provides a particularly suitable generic model structure and is sufficiently complex to characterize digester dynamics under various reactor configurations and feeding protocols (Batstone *et al.*, 2002a; Straub *et al.*, 2006), it was utilised to investigate the relationship between digester stability and biomass population dynamics. For this purpose, the calculation of different key indices for digester stability were implemented into the models in order to gain a comparable basis for both cases.

According to Switzenbaum *et al.*, 1990, an ideal indicator would have intrinsic meaning as it must reflect the current metabolic status of the system. However, this indicator is

difficult to obtain due to the fact that microbial ecosystems developed in a particular anaerobic reactor are unique to that particular system (reactor hydraulics, feeding pattern, waste composition, etc.). There is considerable debate in the literature on finding the best way to monitor digester stability and includes the following widely recognised parameters: (1) pH, (2) gas production rates and gas composition (methane and carbon dioxide), (3) gas phase hydrogen concentration, (4) volatile acids to alkalinity ratio, and (5) the acetate capacity number (ACN). In general, the first three mentioned indicators together with individual measurements of VFAs and alkalinity are good for detecting gradual changes but, however, none of them can determine how close a digester is to failure (Conklin *et al.*, 2008; Switzenbaum *et al.*, 1990). Both experience and theoretical analysis indicate that pH is not a good indicator of process upsets. Because of the buffering capacity inherent in the system, the pH changes very slowly and by the time noticeable decline in pH occurs, the upset may be well under way (Grady *et al.*, 1999; Zickefoose and Hayes, 1976). The gas production rate, and more specifically the methane yield, can potentially be a good indicator of the metabolic status of the digester. Lowering of methane yield, when compared to the influent organic loading rate, can be a warning sign for the accumulation of soluble acid products in the liquid phase. Unfortunately, this is again the result of an imbalance rather than a warning of it. Regarding the applicability of hydrogen concentrations as reactor stability indicators, ambivalent results can be found in literature. In a review, Switzenbaum et al., 1990 state that although a change in hydrogen concentration may be rapid for an upset situation, it is not always apparent why this change has occurred and thus limits the application of hydrogen as a stand-alone indicator.

For the early detection of upcoming process deterioration and reactor failure due to organic or hydraulic overloads as well as toxic events, more sensitive indicators are required. In this study, the VFA/alkalinity ratio and the acetate capacity number (ACN) were utilised for this purpose and implemented into the simulation models. The ratio of volatile fatty acids to alkalinity indicates the relative proportion of compounds acting to lower the pH and of buffering capacity to maintain it. The alkalinity represents the ability of a digester to neutralize the acids formed during digestion or present in the incoming waste. The accumulation of VFAs reflects a kinetic uncoupling between acid producers and consumers and is typical of stress situations. Accumulation of VFA can also be a cause of subsequent problems if the system lacks enough buffering capacity to avoid a drop in the pH (Grady *et al.*, 1999; Switzenbaum *et al.*, 1990). The VFA/alkalinity ratio is expressed in equivalents of acetic acid/equivalents of calcium carbonate and generally, values between 0.1 and 0.4 are considered to indicate favourably operating conditions without the risk of acidification (de Haas and Adam, 1995; Sánchez *et al.*, 2005; Switzenbaum *et al.*, 1990; Zickefoose and Hayes, 1976). Increases above 0.3–0.4 indicate upset and the need for corrective action. If the ratio exceeds 0.8, pH depression as well as inhibition of methane production can occur and the process can fail (Zhao and Viraraghavan, 2004). However, each plant has its own characteristic ratio for efficient digestion.

For the implementation into ADM1, VFAs were calculated as the sum of total valerate, butyrate, propionate, and acetate including both the dissociated (HVa^-, HBu^-, $HPro^-$, HAc^-) and non-ionised forms (valeric, butyric, propionic and acetic acid). The numbers were converted to mol L^{-1} and multiplied by 60 to gain g HAc-equivalents L^{-1}. Alkalinity was assumed to be mainly due to bicarbonate and VFA. The alkalinity simulation results were calculated by a charge balance summing the bicarbonate, all ionised forms of VFA as well as ions from the influent (Scat and San) scaled to eq L^{-1}. Finally it was

multiplied by 50 which equals the equivalent weight of calcium carbonate in order to gain g $CaCO_3$-equivalents L^{-1} of alkalinity. However, under certain circumstances these numbers may need further conversion to represent total VFAs and total alkalinity taking into account that other influences may contribute to alkalinity and total organic acids. Koch *et al.*, 2009 conducted digestion experiments with pure maize silage and found corresponding correction factors for maize digestion through statistical evaluation of gas chromatography and titration measurement data. For the purposes of this paper, however, corrections not applied.

As mentioned above, the acetate capacity number (ACN), defined as the ratio between the maximum acetate utilization rate and the acetate production rate, was used to index digester instability. Critical to stability under varying loading and environmental conditions, however, is not the acetate concentration but rather the acetate utilization capacity of the acetoclastic community beyond the steady-state production rate. The ACN is a measure for this excess acetate capacity and the lower the number, the less excess substrate utilization capacity exists in the digester and thus the greater the instability. Values of less than 1.0 under steady-state conditions indicate impending digester failure (Conklin *et al.*, 2008; Straub *et al.*, 2006).

In the simulation models, the maximum acetate utilization rate of the microbial community was calculated as

$$\rho_{11,max} = km\_ac \cdot Xac \cdot I_{pH\_ac} \cdot I_{NH3,Xac} \cdot I_{IN}$$

where km_ac is the maximum specific substrate utilization constant [kgCOD_S kgCOD_X^{-1} d^{-1}], Xac the biomass concentration of acetate degraders [kgCOD m^{-3}], I_{pH_ac} and $I_{NH3,Xac}$ [-] are inhibition terms accounting for pH and free ammonia inhibition and I_{IN} [-] is an uptake-regulating function to prevent growth when inorganic nitrogen (ammonium and ammonia) is limited. For the Monod term, it was assumed that Sac/(KS_ac + Sac) = 1 when the rate is at maximum. The acetate production rate was determined from the sum of biochemical processes producing acetate:

$$\sum_{j=5}^{10} \rho_{j=5\text{-}10} \cdot \nu_{i=7,j=5\text{-}10} = \rho_5 \cdot (1 - Y_{su}) \cdot f_{AC\_SU} + \rho_6 \cdot (1 - Y_{aa}) \cdot f_{AC\_AA} + \rho_7 \cdot (1 - Y_{fa}) \cdot f_{AC\_FA} +$$
$$+\rho_8 \cdot (1 - Y_{c4}) \cdot f_{AC\_VA} + \rho_9 \cdot (1 - Y_{c4}) \cdot f_{AC\_BU} + \rho_{10} \cdot (1 - Y_{pro}) \cdot f_{AC\_PRO}$$

with denotations according to ADM1 terms given in (Batstone *et al.*, 2002a): ρ_j are the kinetic process rates [kgCOD $m^{-3}d^{-1}$], Y_i the biomass yields [kgCOD_X kgCOD_S^{-1}] and f_{AC_S} the fractions of acetate yield from substrate S [kg COD kg COD^{-1}].

RESULTS AND DISCUSSION

Case study 1

Figure 8-3 shows measured values and simulation results of the numerical model for gas production, pH and methane content for WWTP Salzburg. The model outputs for gas production and analytical data corresponded well. However, there were deviations for pH and methane content.

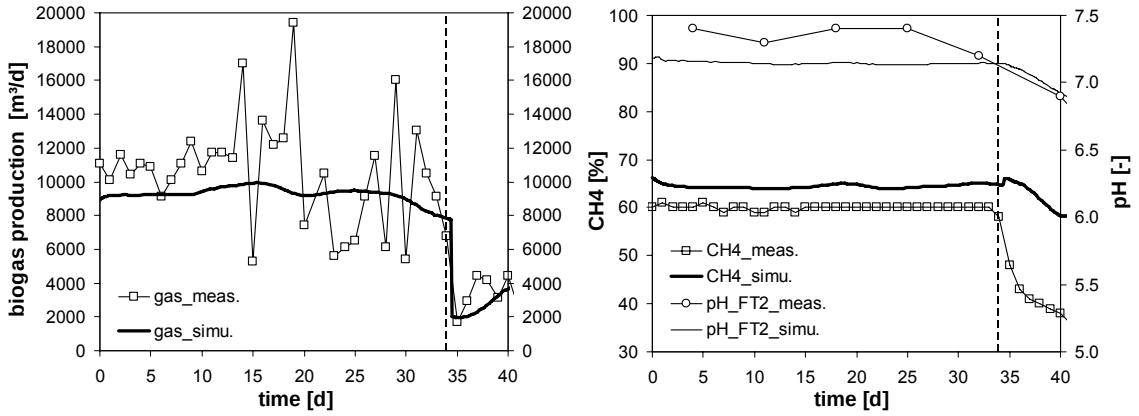

Figure 8-3 WWTP Salzburg simulation results and measured values for gas production, pH and methane content. Note that on day 34 digester FT1 was shut down and sludge was by-passed to FT2.

Case study 2

In the lab-scale start-up experiments, biogas production increased up to a peak value after an initial lag phase, and then sharply decreased after the feeding was stopped (Figure 8-4). As mentioned previously, there was no pH drop or other reactor failure in digester B1 although a washout of methanogens was expected due to a HRT of only 3 days at maximum feeding rate. This was attributed to incoming methanogenic archaea stemming from the alimentary system of the cattle. Since many of the methanogenic organisms identified in anaerobic digesters are similar to those found in the stomach of ruminant animals, the reactor was continuously inoculated from the feedstock. This outweighed the loss of biomass due to short retention times (Boe, 2006; Tchobanoglous *et al.*, 2003).

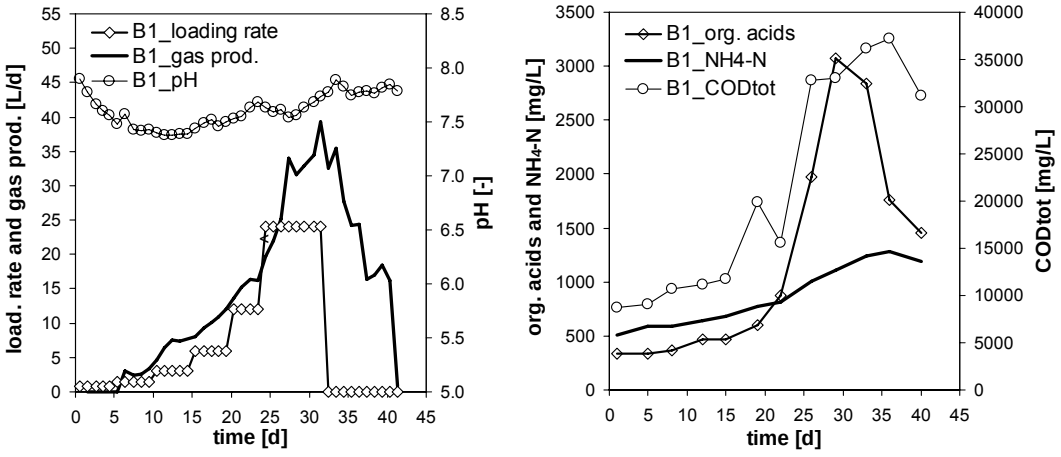

Figure 8-4 Loading and gas production rates, pH, organic acids, NH_4-N and total COD progression in lab-scale reactor B1

Figure 8-5 depicts the comparison between measured and simulated results of the numerical model for digester B1. It can be seen that the model predicted reasonably well the dynamic behaviour of the start-up process in lab-scale, especially COD was predicted accurately. Following the assumption made above that the non-occurrence of a

methanogen washout was due to incoming archaea, an additional influent of biomass was introduced within the model. It was implemented as an adjustable portion of the particulate COD which is fed to the model reactor and was calibrated to an optimized value of 1 %. Within that flux of additional biomass, the portion of acetate degraders (Xac) was set to a value of 33.5 % (hence, Xac=0.34 %). Biomass portions of 2 % and 0 % in feed COD (corresponding to 0.67 % and 0 % of acetate degraders) led to overestimated and underestimated gas productions, respectively (Figure 8-5).

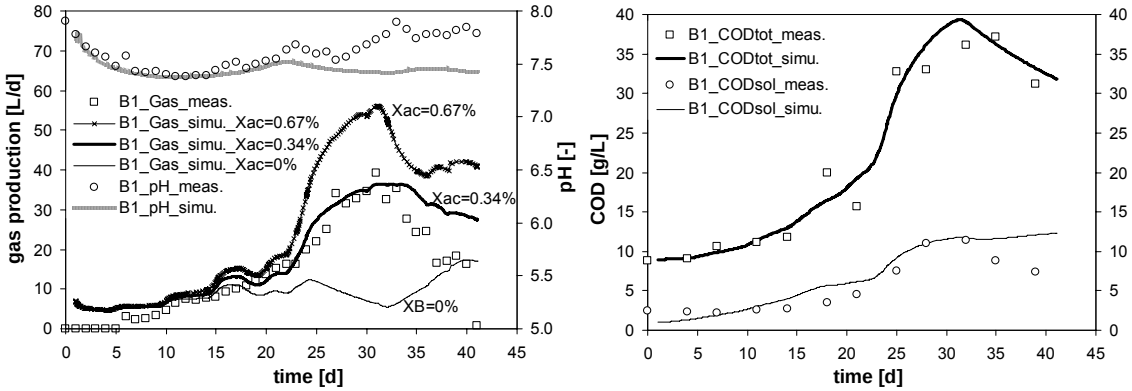

Figure 8-5 Simulation results and measured values for gas production, pH, total and soluble COD in the start-up experiment. Simulated gas production curves include different ratios of additional biomass (XB).

Methanogenic population

The methanogenic community found in B1 was mainly composed of *Methanosarcina* (>95%). Figure 8-6 displays the measured relative portion of methanogens in the sludge in reactor B1 as well as the corresponding simulation results for the start-up experiment. It should be noted that the model produces continuous results whereas there are only four points of measured data between day 12 and 33 as well as one value for the feeding materials manure and inoculum, respectively. Both graphs have similar trends indicating a gradual washout due to decreasing HRT, although there are differences in the order of magnitude since the cell water content is unknown and thus, the measured values are not directly convertible.

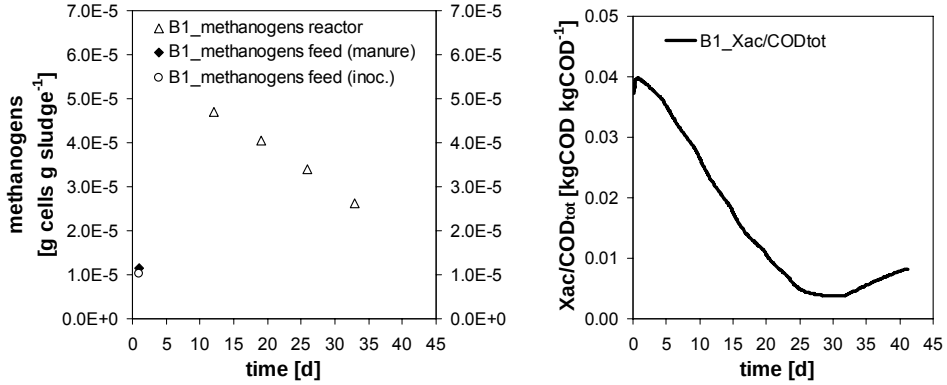

Figure 8-6 Measured relative portion of methanogens in reactor B1 and in the feed (per g sludge; left) and simulation values for acetate degarders (Xac) (per kg COD; right) in reactor B1

However, when comparing the quantitative proportion of methanogens in the feeding substrate and in the reactor sludge (P_{rf}), both measured and simulated results show values in the same order of magnitude. Given approximately 1.0E-5 g cell g sludge^{-1} in the feeding (Figure 8-6), P_{rf} amounts to a mean percentage of 31% for the measurement data points. In the simulation the value averages out at 22 %. This reveals that there is already a relevant quantity of biomass in the feed to prevent a digester upset.

Biokinetic modelling

In the models, particulate COD is distributed to the ADM1 compounds in the disintegration step and thus, the fractionizing factors (fxx_Xc) for the particulate composites (Xc) as well as the carbon and nitrogen contents of Xc play an important role in model performance, determining a characterisation of the input substrate. Table 8-3 shows these factors as well as the parameters which turned out to be sensitive for the behaviour of both models. Many parameters, principally those with low or no sensitivity on model outputs, have been applied without any optimisation as compared to the standard values given in ADM1.

For the WWTP Salzburg model, the biodegradable fractions of Xc (fCH_XC, fPR_XC and fLI_XC) are similar to values reported in literature (e.g. Huete *et al.*, 2006). Also, the kinetic parameters (km_su, km_ac) were within the range of literature values (e.g. Batstone *et al.*, 2002a; Blumensaat and Keller, 2005), whereas the decay rate of aceate degraders (kdec_Xac) had to be increased by an order of magnitude to meet satisfying simulation results.

For the start-up experiment, the given substrate ratios indicate a relatively high portion of carbohydrates (CH) compared to proteins (PR) and lipids (LI) with proportions of CH/PR = 1.9 and CH/LI = 5.0. This is in good accordance with reported compositions of cattle manure in the literature (e.g. Møller *et al.*, 2004). Within the kinetic parameters, the maximum uptake rate of sugars (km_su) revealed a remarkable influence on the simulation results. It had to be reduced from an initial value of 30 to 8 d^{-1} to avoid an overestimation of gas production. Obviously, there is a poor adaptation of the degradation of sugars within the start-up process. In Schoen *et al.*, 2008 it was revealed that this phenomenon was not observable in the long term which could be seen from applying the parameters to a model of the farm-scale pilot plant. This is in accordance with findings of Page *et al.*, 2008 where biogas production in bench-scale digesters was overpredicted by ADM1 but with correct results for full-scale systems.

Table 8-3 Calibrated ADM1 model parameters including influent characterisation

Parameter	Description	Value		Parameter	Description	Value	
		SBG[1]	SU			SBG[1]	SU
fSI_XC [-]	fraction SI	0.01	0.05	C_Xc	Carbon	0.02	0.02
fXI_XC [-]	fraction XI	0.10	0.24	N_Xc	Nitrogen	0.00	0.00
fCH_XC [-]	fraction Xch	0.16	0.35	kdis	disintegration	1.0	0.1
fPR_XC [-]	fraction Xpr	0.14	0.18	km_su	Uptake rate	30	8
fLI_XC [-]	fraction Xli	0.27	0.07	km_ac	max. uptake	20	30
fXP_XC[2] [-]	fraction Xp	0.29	0.10	kdec_Xac	decay rate	0.13	0.02

[1]SBG:Salzburg WWTP, SU:start-up experiment

[2]fXP_XC considers inert products from biomass decay in Xc as introduced in Wett *et al.*, 2006a

Discussion of results for digester stability indicators

For both models, the VFA/alkalinity ratio and the ACN were calculated as described above. Additionally, the organic loading rate (OLR), the food to microorganism ratio (F/M), the food to net microorganism ratio (F/M_{net}), and the net food to net microorganism ratio (F_{net}/M_{net}) were assessed according to the formulas given below:

$$OLR = COD_{input} \cdot Q/V$$

$$F/M = COD_{input} \cdot Q/(COD_{reactor} \cdot V)$$

$$F/M_{net} = COD_{input} \cdot Q/(Xac \cdot V)$$

$$F_{net}/M_{net} = COD_{degr} \cdot Q/(Xac \cdot V)$$

where COD_{input} is the COD concentration in the influent of the digester [kg COD m^{-3}], Q is the volumetric flow rate [$m^3 d^{-1}$], V is the digester volume [m^3], $COD_{reactor}$ is the COD concentration in the digester [kg COD m^{-3}], COD_{degr} is the concentration of degradable COD in the digester [kg COD m^{-3}] and Xac is the concentration of acetate degraders in the digester [kg COD m^{-3}]. For the sake of uniformity with the other indicators, the OLR is expressed on a COD basis. For conversion to commonly used units for the OLR such as kgVSS $m^{-3}d^{-1}$, values must be divided by 1.4, which represents a rough approximation of the COD/VSS ratio of biomass (Tchobanoglous *et al.*, 2003).

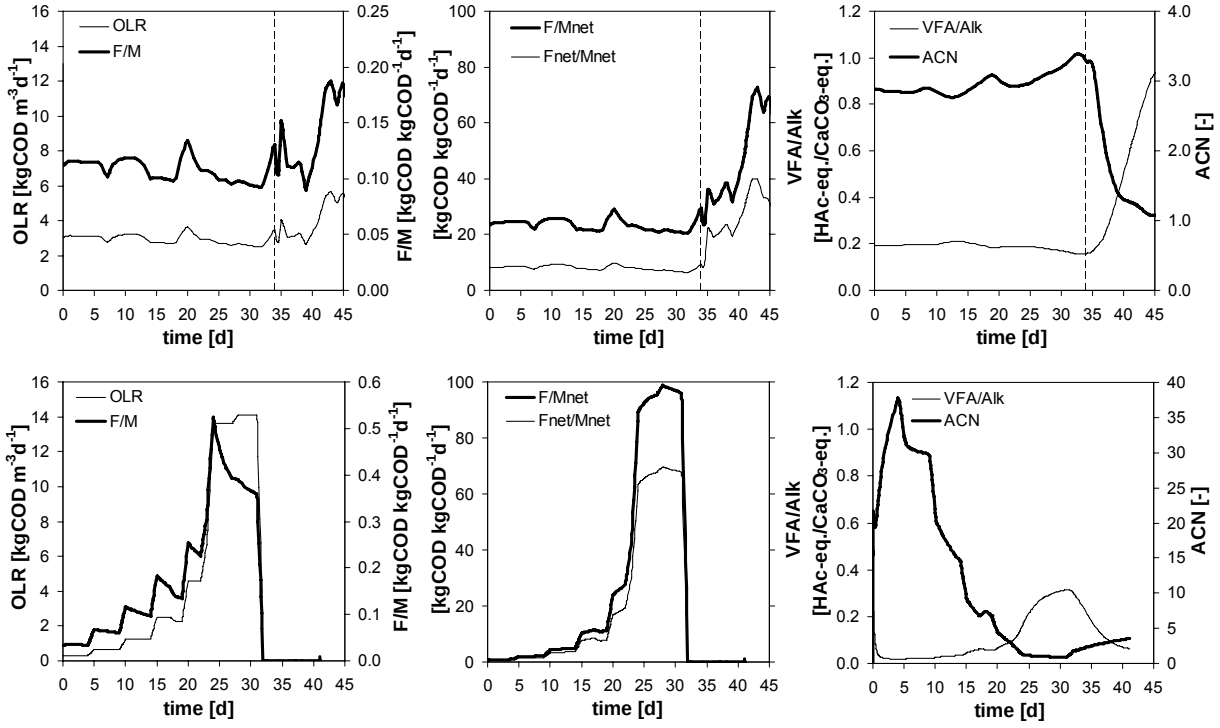

Figure 8-7 Simulation results of key indicators for Salzburg WWTP (upper charts) and start-up experiment (lower charts). Note that different y-axis scaling was used for F/M and ACN.

When examining the results for the digester failure at WWTP Salzburg in Figure 8-7, it can be seen that there is a remarkable upward shift in F/M_{net} and F_{net}/M_{net}. The values of both loading indicators nearly doubled, reflecting the overload situation as soon as

the sludge was directly by-passed to digester FT2 (day 34). This occurred parallel to the reactor breakdown, which is clearly indicated by the VFA/alk and ACN results. Both reactor state indicators indicated impending failure as they exceed the range of a normal reactor status and approach values of >0.9 and <1.0, respectively. In contrast, failure was not indicated by the OLR as it increased insignificantly within its normal range of variation. The same is true for the F/M ratio. Thus, although the OLR is commonly used as a steady-state design parameter, it appears not to be suitable for the design under dynamic conditions.

Given the experiences from case study 1, a digester breakdown would appear likely for the start-up experiment due to F/M and OLR values that are more than double and F/M_{net} and F_{net}/M_{net} values that are 1.5 times higher compared to the Salzburg case (Figure 8-7). The actual non-occurrence of a reactor failure supports the assumption of continuous re-inoculation from the feedstock as described above and is confirmed by the values for VFA/alk and ACN. However, by the end of the experiment ACN values approached ≈1.0 and it is possible the digester would have failed if feeding had been continued.

CONCLUSIONS

ADM1 was used to simulate digester behaviour under potential overload conditions for two different scenarios. The application of the ADM1 to estimate reactor stability highlighted the importance of considering methanogen population dynamics in modelling.

For the digester failure at the municipal WWTP Salzburg, the feasibility of predicting reactor upsets via stability indicators by means of simulation was shown. Parameters such as the net food to net microorganism ratio (F_{net}/M_{net}) as well as the VFA/alklinity ratio and the acetate capacity number (ACN) clearly indicated impending failure. However, loading indicators such as the organic loading rate (OLR) as a commonly utilised design parameter for digesters, turned out to be unsuitable for the design under dynamic conditions in the investigated case studies. Instead of loading parameters, the utilisation of indicators reflecting the biokinetic process state is more adequate for the assessment of the stability of reactors in transient situations.

Regarding the non-occurrence of a highly expected manure digester breakdown due to very short HRT, the assumption of a continuous re-seeding of methanogens from the livestock was proved correct. Modelling showed that the additional flow of biomass to the reactor prevented failure.

REFERENCES

Batstone, D.J., Keller, J., Angelidaki, I., Kalyuzhnyi, S.V., Pavlostathis, S.G., Rozzi, A., Sanders, W.T.M., Siegrist, H., Vavilin, V.A., 2002a. Anaerobic Digestion Model No.1 (ADM1). IWA Publishing, London, UK.

Batstone, D.J., Keller, J., Steyer, J.P., 2006. A review of ADM1 extensions, applications, and analysis: 2002–2005. Water Science and Technology, 54, 1–10.

Blumensaat, F., Keller, J., 2005. Modelling of two-stage anaerobic digestion using the IWA Anaerobic Digestion Model No. 1 ADM1. Water Research, 39, 171-183.

Boe, K., 2006. Online monitoring and control of the biogas process. Institute of Environment & Resources. Technical University of Denmark, Lyngby, Denmark.

Conklin, A.S., Chapman, T., Zahller, J.D., Stensel, H.D., Ferguson, J.F., 2008. Monitoring the role of aceticlasts in anaerobic digestion: Activity and capacity. Water Research, 42, 4895-4904.

de Haas, D.W., Adam, N., 1995. Use of a simple titration procedure to determine H_2CO_3* alkalinity and volatile fatty acids for process control in waste-water treatment. Water SA, 21, 307-317.

Franke-Whittle, I.H., Goberna, M., Insam, H., 2009. Design and testing of real-time PCR primers for the quantification of Methanoculleus, Methanosarcina, Methanothermobacter and a group of uncultured methanogens. Canadian Journal of Microbiology (in press).

Goberna, M., Gadermaier, M., Schoen, M.A., Franke-Whittle, I.H., Wett, B., Insam, H., 2009. Fingerprinting the microbial communities in organic wastes using oligonucleotide microarrays and real-time PCR. Proceedings of the II International Meeting of Soil Enzimology. Recycling of Organic Wastes in Environmental Restoration and Global Change, Burgos, Spain.

Grady, C.P.L., Daigger, G.T., Lim, H.C., 1999. Biological Wastewater Treatment. Marcel Dekker Inc., New York.

Huete, E., de Gracia, M., Ayesa, E., Garcia-Heras, J.L., 2006. ADM1-based methodology for the characterisation of the influent sludge in anaerobic reactors. Water Science and Technology, 54, 157–166.

Kendall, M.M., Boone, D.R., 2006. The Order Methanosarcinales, in: Dworkin, M., Falkow, S., Rosenberg, E., Schleifer, K-H., Stackebrandt, E. (Eds.), The Prokaryotes. A Handbook on the Biology of Bacteria, Vol. 3. Springer-Verlag, New York, pp. 244-256.

Klappenbach, J.A., Saxman, P.R., Cole, J.R., Schmidt, T.M., 2001. rrndb: the Ribosomal RNA Operon Copy Number Database. Nucleic Acids Research, 29, 181-184.

Koch, K., Wichern, M., Lübken, M., Horn, H., 2009. Reproducing the stability criterion TVFA/Alkalinity in mathematical models., Submitted to Biomass and Bioenergy.

Møller, H.B., Sommer, S.G., Ahring, B.K., 2004. Methane productivity of manure, straw and solid fractions of manure. Biomass and Bioenergy 26, 485 – 495.

Page, D.I., Hickey, K.L., Narula, R., Main, A.L., Grimberg, S.J., 2008. Modeling anaerobic digestion of dairy manure using the IWA Anaerobic Digestion Model no. 1 (ADM1). Water Science and Technology, 58, 689-695.

Sánchez, E., Borja, R., Travieso, L., Martin, A., Colmenarejo, M.F., 2005. Effect of organic loading rate on the stability, operational parameters and performance of a secondary upflow anaerobic sludge bed reactor treating piggery waste. Bioresource Technology, 96,, 335-344.

Schink, B., 1997. Energetics of syntrophic cooperation in methanogenic degradation. Microbiology and Molecular Biology Reviews, 61, 262-280.

Schoen, M.A., Sperl, D., Gadermaier, M., Goberna, M., Franke-Whittle, I., Insam, H., Wett, B., 2008. Comparison of biogas plant start-up procedures based on lab- and full-scale data and on numerical modelling Second international symposium on energy from biomass and waste, International Waste Working Group, 17-20/Nov/2008, Venice, Italy.

Straub, A.J., Conklin, A.S.Q., Ferguson8, J.F., Stensel, H.D., 2006. Use of the ADM1 to investigate the effects of acetoclastic methanogen population dynamics on mesophilic digester stability. Water Science and Technology, 54, 59-66.

Switzenbaum, M.S., Giraldo-Gomez, E., Hickey, R.F., 1990. Monitoring of the anaerobic methane fermentation process. Enzyme and Microbial Technology, 12,, 722-730.

Tchobanoglous, G., Burton, F.L., Stensel, H.D., 2003. Wastewater Engineering: Treatment and Reuse. Metcalf & Eddy, Inc., Tata McGraw-Hill Publishing Company Ltd., 4th Edition.

Wett, B., Eladawy, A., Ogurek, M., 2006a. Description of nitrogen incorporation and release in ADM1. Water Science and Technology, 54, 67–76.

Wett, B., Schoen, M., Phothilangka, P., Wackerle, F., Insam, H., 2006b. Model-based design of an agricultural biogas plant: application of Anaerobic Digestion Model No.1 for an improved 4 chamber scheme. . Water Science and Technology, 55, 21-28.

Zhao, H.W., Viraraghavan, T., 2004. Analysis of the performance of an anaerobic digestion system at the Regina wastewater treatment plant. Bioresource Technology, 95, 301-307.

Zickefoose, C., Hayes, R.B.J., 1976. Anaerobic sludge digestion: operations manual. EPA 430/9-76-001, U.S. Environmental Protection Agency, Washington D.C., USA.

9 CONCLUSIONS

The main focus in this work is the numerical simulation of anaerobic digestion processes in agricultural biogas plants with respect to different fields of interest (e.g. plant design, co-digestion of different substrates and start-up strategies). The final conclusions presented below are covering some general remarks on the modelling of agricultural biogas plants and associated limitations of the Anaerobic Digestion Model No.1 (ADM1).

9.1 MOTIVATION FOR MODELLING BIOGAS PLANTS

In recent years, the number of agricultural biogas plants underwent outstanding growth which is mainly prompted by a continued rise in prices for energy from fossil fuels and by environmentally-related governmental action in order to encourage the use of renewables for energy generation. With the growing number of plants, a broad variety of different anaerobic systems has been developed. Especially in the agricultural sector where the operation of a biogas plant is often only a sideline job for the farmer, there are efforts to construct plants which work with maximum efficiency and a minimum of maintenance requirements at the same time.

Along with the development and propagation of mathematical models such as the ADM1, the interest and activity in anaerobic digestion simulation for full-scale design, operation and optimisation of agricultural biogas plants is rapidly developing. Given the complexity of the processes involved in anaerobic digestion, it is difficult to evaluate the impact of all process variables on the digesters performance and pilot testing is challenging due to the extended time periods that are required to operate these processes. Thus, the use of simulation models for predicting plant behaviour sufficiently accurate over a range of design and operating conditions becomes attractive.

Within the papers included in this dissertation it could be shown that the modelling of agricultural biogas plants regarding different issues is possible with ADM1. Important aspects and outcomes of the papers are:

- validated parameter sets for manure digestion and co-fermentation of manure together with biowaste for application in ADM1/SIMBA were created
- design aspects such as different reactor configurations (loading rates and volume partitions) were investigated by means of numerical simulations
- temperature terms in the bacterial growth functions to assess the impact of temperature dynamics were incorporated in the models
- the feasibility of predicting reactor upsets via stability indicators by means of simulation could be shown

9.2 LIMITATIONS OF THE APPLICABILITY OF ADM1

All models presented in the papers comprise attempts to simulate dynamic and transient digester conditions generated in the underlying real-word experiments (lab-scale and on-site). This was done in order to obtain result data with a dynamic and consequently more detailed performance which holds a higher informative value compared to the simulation of steady-state situations. Major difficulties to overcome in this regard were finding proper initial reactor conditions, a reasonable parameter calibration and influent characterisation. The advantage of ADM1 of being designed as a common platform for the simulation of a wide variety of anaerobic degradation processes represents a generally accepted compromise and thus, includes also some limitations. Shortcomings of ADM1/SIMBA associated with the problems mentioned above were identified in the scope of the investigated case studies and will be addressed shortly in the following.

9.2.1 INFLUENT CHARACTERISATION

One of the key-points for the successful application of ADM1 is to achieve a good influent characterisation, especially for complex substrates since the inflow fractioning is of highest importance for the model calibration and is strongly affecting the output quality in terms of treatment performance, biomass and biogas composition as well as chemical characteristics. The particulate COD entering the digester is assigned to the composite fraction Xc where it is subject to a disintegration process before its hydrolysis. Xc is a lumped compound and a detailed characterisation identifying its portions of carbohydrates, proteins, lipids, as well as inert components is required in order to allocate them respectively to the subsequent hydrolysis. Estimation of the concentrations of all these compounds is often challenging as in many cases the sludge composition is unknown and its identification has to be found during the calibration procedure. Given that, Xc appears to be dispensable and suggests an omission of Xc with a direct distribution of the influent to hydrolysis. However, Xc includes both the influent particulate substrate subject to digestion and the products of the biomass decay, so the elemental composition and the fractionation of Xc in the disintegration step cannot be changed without affecting the products of the decay. This could be overcome with an uncoupling of decay and disintegration, so that the decay proceeds directly to hydrolysis instead of producing Xc.

Moreover, most of the model components are well-known simple compounds (e.g. volatile fatty acids, methane) with undeniable C and N-contents associated. However, there are groups with a different grade of definition (e.g. composites, inerts) and finding reasonable values are left to the user's discretion so that the model can be adapted to each particular case. It should be noted that the ADM1 does not maintain an inherently closed mass balance on carbon and nitrogen. Hence, care must be taken when determining the C and N-contents of the particulate composites in the feed (Xc) since decaying biomass (fixed C and N-contents) is assigned to Xc which is then partially disintegrated into particulates and subsequently hydrolysed into soluble substrate so that the C- and N-cycles must close. Additionally, the ADM1 specifies particulate inerts (XI) as a single compound which comprises both inert products of the disintegration process and inert decay products although these processes are not coupled and produce particles with different nitrogen contents. That means that the nitrogen content of XI cannot be a fixed parameter per definition and needs to be calibrated to the final ammonia concentration in the digester (released nitrogen). This problem was solved by the implementation of an additional fraction XP representing inert products from biomass de-

cay in Xc with a specified, rather invariable nitrogen content. Hence, no impact of decay products on the nitrogen content of XC needs to be considered or calibrated, respectively.

9.2.2 pH

Limited and rather cumbersome possibilities of presetting and regulation of known influent pH values is another shortcoming concerning influent characterisation. pH is calculated via a charge balance and the model solves for the hydrogen ion concentration, and thereby the pH, by ensuring chemical neutrality in solution. Although in that balance separate cations and anions can be defined (preferably in reasonable ranges) in order to represent strong bases or acids, experience showed that those have minor impact on the overall pH in many cases since they are outweighed by other terms in the charge balance. Thus, additional of organic acids have to be assigned to the model influent. Besides that it should be noted that the model does not correct any of the disintegration or hydrolysis rates for pH. An improvement of the model would be the inclusion of corresponding rate correction terms.

9.2.3 Impact of temperature dynamics

Various anaerobic bioconversions proceed very close to thermodynamic equilibrium and hence, thermodynamics provide a basis for prediction whether or not these conversions may occur as a function of the environmental conditions. ADM1 contains no continuous functions to take into account kinetic effects due to temperature progressions since common modelling concerns stable process temperatures. Instead, separate parameter values for either thermophilic or mesophilic conditions are given in the model description. As there was the necessity to have such continuous temperature functions in one of the investigated cases due to a steady operating temperature increase, the problem was overcome by the implementation of a double Arrhenius equation. It was added in the form of an inhibition term to the growth rates of the enzymatic and bacterial groups involved and takes values between 0 for poor and 1 for optimum temperature conditions. Anyway, this issue may be of minor importance for practical use as in most cases steady-state operating temperature conditions will be of interest.

9.2.4 Fate of sulphur and phosphorus compounds

The ADM1 was designed to be readily extendible and as can be seen from the literature, the most commonly requested extensions concerning the fate of sulphur and phosphorus compounds in the model. In anaerobic digestion sulphur is partly released and transformed to H_2S in the gas phase where it is responsible for a large portion of maintenance difficulties associated with engines using digester gas. Additionally, organic sulphur compounds from the transformation of sulphur are the primary agents responsible for significant odour issues with the digested sludge.

Likewise, phosphorus is released as part of the digestion process and is precipitated in a number of different forms. This can be particularly critical to the performance of nutrient removal when regarding wastewater facilities. Another important aspect is the effect of phosphorus on the pH of the digestion system. In its pH calculation, ADM1 considers all major ions except phosphorus. When adding phosphorus to the model, ionic activity effects might be taken into account due to the high valency of the phosphate ion (PO_4^{-3}), which was not necessary so far because of the monovalency of the other ions.

As a final remark, it can be stated that one of the key limitations for anaerobic modelling with a model intended to cover a wide field of applications like ADM1 is the uncertainty in parameter values and variability.

10 REFERENCES

ADTL (2003). *Energieleitbild Tirol 2000 – 2020 [in German]*. Untergruppe Energie des Tiroler Raumordnungsbeirates, Tiroler Landesregierung, Innsbruck, Austria.

ADTL (2007). *Wirtschafts- und Arbeitsmarktbericht Tirol 2007 [in German]*. Abteilung Wirtschaft und Arbeit, Amt der Tiroler Landesregierung, Innsbruck, Austria.

AEA (2003). *Renewable Energy in Austria*. Austrian Energy Agency (E.V.A.), Vienna, Austria.

Angelidaki I., Ellegaard L. and Ahring B. K. (1993). A Mathematical Model for Dynamic Simulation of Anaerobic Digestion of Complex Substrates: Focusing on Ammonia Inhibition. *Biotechnology and Bioengineering*, 42 159-166.

Angelidaki I., Ellegaard L. and Ahring B. K. (1999). A Comprehensive Model of Anaerobic Bioconversion of Complex Substrates to Biogas. *Biotechnology and Bioengineering*, 63 (3), 363–372.

Angelidaki I., Chen X., Cui J., Kaparaju P. and Ellegaard L. (2006). Thermophilic anaerobic digestion of source-sorted organic fraction of household municipal solid waste: Start-up procedure for continuously stirred tank reactor. *Water Research* 40 2621 – 2628.

Batstone D. J., Keller J. and Steyer J. P. (2006). A review of ADM1 extensions, applications, and analysis: 2002–2005. *Water Science and Technology*, 54 (4), 1–10.

Batstone D. J., Keller J., Newell R. B. and Newland M. (2000). Modelling anaerobic degradation of complex wastewater. I: model development. *Bioresource Technology*, 75 67-74.

Batstone D. J., Keller J., Angelidaki I., Kalyuzhnyi S. V., Pavlostathis S. G., Rozzi A., Sanders W. T. M., Siegrist H. and Vavilin V. A. (2002a). *Anaerobic Digestion Model No.1 (ADM1).* IWA Task Group for Mathematical Modelling of Anaerobic Digestion Processes, IWA Publishing, London, UK.

Batstone D. J., Keller J., Angelidaki I., Kalyuzhnyi S. V., Pavlostathis S. G., Rozzi A., Sanders W. T. M., Siegrist H. and Vavilin V. A. (2002b). The IWA Anaerobic Digestion Model No 1 (ADM1) *Water Science and Technology*, 45 (10), 65–73.

Bergauer-Culver B. and Jaeger C. (1998). Estimation of the energy output of a photovoltaic power plant in the Austrian alps. *Solar Energy*, 62 (5), 319–324.

Bischofsberger W., Dichtl N., Rosenwinkel K.-H., Seyfried C. F. and Böhnke B. (2005). *Anaerobtechnik*, 2nd Edition, ISBN 3-540-06850-3, Springer-Verlag, Heidelberg, Germany.

Björnsson L. (2000). *Intensification of the biogas process by improved process monitoring and biomass retention.* PhD Thesis, Department of Biotechnology, Lund University, Sweden.

Blumensaat F. and Keller J. (2005). Modelling of two-stage anaerobic digestion using the IWA Anaerobic Digestion Model No. 1 ADM1 *Water Research*, 39 171-183.

BMLFUW (2007). *Anpassung der Klimastrategie Österreichs zur Erreichung des Kyoto-Ziels 2008-2013 [in German]*. BM für Land- und Forstwirtschaft, Umwelt und Wasserwirtschaft, Vienna, Austria.

Boe K. (2006). *Online monitoring and control of the biogas process.* PhD Thesis, Institute of Environment & Resources, Technical University of Denmark, Lyngby, Denmark.

Burke D. A. (2001). *Dairy waste anaerobic digestion handbook. Options for recovering beneficial products from dairy manure.* Environmental Energy Company, Olympia, WA, USA.

Conklin A. S., Chapman T., Zahller J. D., Stensel H. D. and Ferguson J. F. (2008). Monitoring the role of aceticlasts in anaerobic digestion: Activity and capacity. *Water Research*, 42 (20), 4895-4904.

de Haas D. W. and Adam N. (1995). Use of a simple titration procedure to determine H_2CO_3* alkalinity and volatile fatty acids for process control in waste-water treatment. *Water SA*, 21 (4), 307-317.

De Toffol S., Engelhard C. and Rauch W. (2007). Influence of climate change on the water resources in an alpine region. Submitted for publication.

e-control (2007). Ökostrom sowie Energieverbrauchsentwicklung und Vorschläge zur Effizienzsteigerung [in German]. Energie-Control GmbH, August 2007, Vienna, Austria.

EC (2005). European Commission.Communication from the Commission. The support of electricity from renewable energy sources 2005, COM(2005) 627 final. 7/ Dec/2005, Brussels, Belgium.

Eder B. and Schulz H. (2006). *Biogas Praxis [in German]*, 3rd Edition, ISBN 3-936896-13-5 ökobuch Verlag, Staufen, Germany.

Eladawy A. (2005). *Modelling of Anaerobic Sewage Sludge Digestion – Sludge Characterisation and Process Analysis.* PhD Thesis, Institute of Environmental Engineering, University of Innsbruck, Austria.

EPA (2005). *Anaerobic Digestion: Benefits for Waste Management, Agriculture, Energy, and the Environment. Discussion Paper*. Environmental Protection Agency of Ireland, Wexford, Ireland.

FGW (2007). *Biogas: Potenzial in Österreich [in German]*. Pressegespräch Fachverband Gas Wärme, Presentation, accessed Sep. 2007, www.klimaaktiv.at.

Franke-Whittle I. H., Goberna M. and Insam H. (2009). Design and testing of real-time PCR primers for the quantification of Methanoculleus, Methanosarcina, Methanothermobacter and a group of uncultured methanogens *Canadian Journal of Microbiology (in press).*

FV Biogas (2005). *Hintergrunddaten [in German]*. Download from www.biogas.org/datenbank/file/notmember/presse/Pressegespr_Hintergrunddaten1.pdf, Access Date 26.01.2007.

Ghaly A. E., Ramkumar D. R., Sadaka S. S. and Rochon J. D. (2000). Effect of reseeding and pH control on the performance of a two-stage mesophilic anaerobic digester operating on acid cheese whey. *Canadian Agricultural Engineering*, 42 (4), 173-183.

Goberna M., Gadermaier M., Schoen M. A., Franke-Whittle I. H., Wett B. and Insam H. (2009). Fingerprinting the microbial communities in organic wastes using oligonucleotide microarrays and real-time PCR. *Proceedings of the II International Meeting of Soil Enzimology. Recycling of Organic Wastes in Environmental Restoration and Global Change, Burgos, Spain.*,

Grady C. P. L., Daigger G. T. and Lim H. C. (1999). *Biological Wastewater Treatment.* 2nd Edition, Marcel Dekker Inc., New York.

Gray N. F. (2004). *Biology of wastewater treatment.* 2nd edition, Imperial College Press, London.

Griffin M. E., McMahon K. D., Mackie R. I. and Raskin L. (1998). Methanogenic population dynamics during start-up of anaerobic digesters treating municipal solid waste and biosolids. *Biotechnology and Bioengineering*, 57 (3), 342-355.

Gujer W. and Zehnder A. J. B. (1983). Conversion processes in anaerobic digestion. *Water Science and Technology*, 15 (127-167),

Huete E., de Gracia M., Ayesa E. and Garcia-Heras J. L. (2006). ADM1-based methodology for the characterisation of the influent sludge in anaerobic reactors. *Water Science and Technology*, 54 (4), 157–166.

Hwang M. H., Jang N. J., Hyun S. H. and Kim I. S. (2004). Anaerobic bio-hydrogen production from ethanol fermentation: the role of pH. *Journal of Biotechnology*, 111 (3), 297–309.

Hwu C.-S., Donlon B. and Lettinga G. (1996). Comparative toxicity of long-chain fatty acid to anaerobic sludges from various origins. *Water Science and Technology*, 34 (5-6), 351-358.

IEA (2004). *International Energy Agency: Renewable Energy: Market & Policy Trends in IEA Countries* IEA Publications, Paris, France, ISBN 92-64-107916-2004.

ifak (2005). *SIMBA 5.1 User's guide.* ifak system GmbH, Magdeburg, Germany.

IPCC (2007a). *Summary for Policymakers. Climate Change 2007: Mitigation. Fourth Assessment Report of the Intergovernmental Panel on Climate Change* Cambridge University Press, Cambridge, UK and New York, USA.

IPCC (2007b). *Changes in Atmospheric Constituents and in Radiative Forcing. In: Climate Change 2007: The Physical Science Basis. Contribution of Working Group I to the Fourth Assessment Report of the Intergovernmental Panel on Climate Change*. Solomon, S., D. Qin, M. Manning, Z. Chen, M. Marquis, K.B. Averyt, M.Tignor and H.L. Miller (eds.), Cambridge University Press, Cambridge, UK and New York, USA.

IPCC (2007c). *Summary for Policymakers. Climate Change 2007: The Physical Science Basis. Fourth Assessment Report of the Intergovernmental Panel on Climate Change*. Cambridge University Press, Cambridge, UK and New York, USA.

Jönsson O. (2004). Upgrading and Use of Biogas as Fuel of Motor Vehicles. *IEA Bioenergy - Seminar on the production and use of biogas*, Jyväskylä, Finland.

Kalfas H., Skiadas I. V., Gavala H. N., Stamatelatou K. and Lyberatos G. (2005). Application of ADM1 for the simulation of anaerobic digestion of olive pulp under mesophilic and thermophilic conditions. *The First International Workshop on the IWA Anaerobic Digestion Model No.1 (ADM1), proceedings*, Lyngby-Denmark.

Kendall M. M. and Boone D. R. (2006). *The Order Methanosarcinales, in: Dworkin, M., Falkow, S., Rosenberg, E., Schleifer, K-H., Stackebrandt, E. (Eds.),* .

Klappenbach J. A., Saxman P. R., Cole J. R. and Schmidt T. M. (2001). rrndb: the Ribosomal RNA Operon Copy Number Database. *Nucleic Acids Research*, 29 181-184.

Klass D. L. (1984). Methane from Anaerobic Fermentation. *Science*, 223 (4640), 1021-1028.

Kleerebezem R. and van Loosdrecht M. C. M. (2006a). Critical analysis of some concepts proposed in ADM1. *Water Science and Technology*, 54 (4), 51-57.

Kleerebezem R. and van Loosdrecht M. C. M. (2006b). Waste characterization for implementation in ADM1. *Water Science and Technology*, 54 (4), 167–174.

Koch K., Wichern M., Lübken M. and Horn H. (2009). Reproducing the stability criterion TVFA/Alkalinity in mathematical models. Submitted to Biomass and Bioenergy.

Koettner M. (2002). Biogas and fertilizer production from solid waste and biomass through dry fermentation in batch method. *3rd International Symposium on Anaerobic Digestion of Solid Wastes*, Technical University of Munich18-20/Sep/2002, Munich, Germany.

Lee C., Kim J., Hwang K., O'Flaherty V. and Hwang S. (2009). Quantitative analysis of methanogenic community dynamics in three anaerobic batch digesters treating different wastewaters *Water Research*, 43 (1), 157-165.

Lens P., Hamelers B., Hoitink H. and Bidlingmaier W., (eds) (2004). *Resource Recovery and Reuse in Organic Solid Waste Management.* Intergrated Environmental Technology Series, ISBN 1 84339 054 X, IWA Publishing, .

Mathworks (2008). The MathWorks, Inc. Documentation on modeling dynamic systems with Simulink. Source: www.mathworks.com/access/helpdesk/help/toolbox/simulink/.

Møller H. B., Sommer S. G. and Ahring B. K. (2004). Methane productivity of manure, straw and solid fractions of manure *Biomass and Bioenergy* 26 485 – 495.

Page D. I., Hickey K. L., Narula R., Main A. L. and Grimberg S. J. (2008). Modeling anaerobic digestion of dairy manure using the IWA Anaerobic Digestion Model no. 1 (ADM1). *Water Science and Technology*, 58 (3), 689-695.

Parawira W., Murto M., Read J. S. and Mattiasson B. (2005). Profile of hydrolases and biogas production during two-stage mesophilic anaerobic digestion of solid potato waste *Process Biochemistry*, 40 (9), 2945-2952.

Pavlostathis S. G. and Giraldo-Gomez E. (1991). Kinetics of anaerobic treatment: a critical review. *Critical Reviews in Environmental Control*, 21 (5,6), 411-490.

Premstaller G. and Feurich R. (2006). *Dreidimensionale Strömungssimulation Kleinbiogasanlage*. Scientific report, Unit of Hydraulic Engineering, University of Innsbruck, Austria.

Ragwitz M., Schleich J., Huber C., Resch G., Faber T., Voogt M., Coenraads R., Cleijne H. and Bodo P. (2005). *FORRES 2020: Analysis of the renewable energy sources' evolution up to 2020. Final Report*. Karlsruhe, Germany.

Rauch W., Stegner U., Osterkorn F., Blank T., Gasser M., Pfefferkorn A., Obermayr M., Wohlwend O., Riedi G. and Hilbe E. (2003). *Thermische Nutzung der Gewässer d. Alpenrheintales [in German]*. Internationale Regierungskommission Alpenrhein, Bregenz, Austria.

Sánchez E., Borja R., Travieso L., Martin A. and Colmenarejo M. F. (2005). Effect of organic loading rate on the stability, operational parameters and performance of a secondary upflow anaerobic sludge bed reactor treating piggery waste. *Bioresource Technology*, 96, 335-344.

Schink B. (1997). Energetics of syntrophic cooperation in methanogenic degradation. *Microbiology and Molecular Biology Reviews*, 61 (2), 262-280.

Schoen M., De Toffol S., Wett B., Insam H. and Rauch W. (2007a). Comparison of Renewable Energy Resources in Alpine Regions, in: Borsdorf, A., Stötter, J., Veulliet, E. (Eds.),. *Managing Alpine Future*, Austrian Academy of Sciences Press, ISBN 978-3-7001-6571-2.

Schoen M. A., Phothilangka P., Eladawy A., Insam H. and Wett B. (2007b). Farmscale Co-fermentation of manure and organic waste. *IWA-workshop on anaerobic digestion in mountain area and isolated rural zones* 5-7/Jun/2007, Chambéry, France.

Schoen M. A., Sperl D., Gadermaier M., Goberna M., Franke-Whittle I., Insam H. and Wett B. (2008). Comparison of biogas plant start-up procedures based on lab- and full-scale data and on numerical modelling. *Second international symposium on energy from biomass and waste*, International Waste Working Group, 17-20/Nov/2008, Venice, Italy.

Speece R. E. (1996). *Anaerobic Biotechnology for Industrial Wastewaters.* ISBN 0-965-02260-9, Archae Press, Nashville (TN), USA

Stams A. J. M., Plugge C. M., de Bok F. A. M., van Houten B. H. G. W., Lens P., Dijkman H. and Weijma J. (2005). Metabolic interactions in methanogenic and sulfate-reducing bioreactors. *Water Science and Technology* 52 (1-2), 13-20.

Steyer J. P., Bernard O., Batstone D. J. and Angelidaki I. (2006). Lessons learnt from 15 years of ICA in anaerobic digesters *Water Science and Technology*, 53 (4-5), 25-33.

Straub A. J., Conklin A. S. Q., Ferguson8 J. F. and Stensel H. D. (2006). Use of the ADM1 to investigate the effects of acetoclastic methanogen population dynamics on mesophilic digester stability. *Water Science and Technology*, 54 (4), 59-66.

Switzenbaum M. S., Giraldo-Gomez E. and Hickey R. F. (1990). Monitoring of the anaerobic methane fermentation process. *Enzyme and Microbial Technology*, 12, 722-730.

Tchobanoglous G., Burton F. L. and Stensel H. D. (2003). *Wastewater Engineering: Treatment and Reuse.* Metcalf & Eddy, Inc., Tata McGraw-Hill Publishing Company Ltd., 4th Edition.

UCTE (2005). *Statistical Yearbook 2005*. Union for the co-ordination of transmission of electricity, Brussels, Belgium.

UNDP (2000). *World Energy Assessment*. United Nations Development Programme, New York, USA.

UNFCCC (1997). Kyoto Protocol to the United Nations Framework Convention on Climate Change *Conference of the Parties on Its Third Session*, 10/Dec/1997, Kyoto, Japan.

UNFCCC (2006). *GHG DATA 2006-Highlights from Greenhouse Gas Emissions Data for 1990–2004 for Annex I Parties. United Nations Framework Convention on Climate Change*.

van Lier J. B., Rebac S. and Lettinga G. (1997). High-rate anaerobic wastewater treatment under psychrophilic and thermophilic conditions. *Water Science and Technology*, 35 (10), 199-206.

van Lier J. B., Tilche A., Ahring B. K., Macarie H., Moletta R., Dohanyos M., Hulshoff Pol L. W., Lens P. and Verstraete W. (2001). New perspectives in anaerobic digestion. *Water Science and Technology*, 43 (1), 1-18.

Vavilin V. A., Rytov S. V. and Lokshina L. Y. (1996). A description of hydrolysis kinetics in anaerobic degradation of particulate organic matter. *Bioresource Technology*, 56 (2-3), 229-237.

Vavilin V. A., Lokshina L. Y., Rytov S. V., Kotsyurbenko O. R., Nozhevnikova A. N. and N. P. S. (1997). Modelling methanogenisis during anaerobic conversion of complex organic matter at low temperatures. *Water Science and Technology*, 36 (6-7), 531-538.

Verbund (2006). *Verbund-Nachhaltigkeitsbericht 2006 [in German]*. Österreichische Elektrizitätswirtschafts-Aktiengesellschaft (Verbundgesellschaft), Vienna, Austria.

Wett B., Eladawy A. and Ogurek M. (2006a). Description of nitrogen incorporation and release in ADM1. *Water Science and Technology*, 54 (4), 67–76.

Wett B., Schoen M., Phothilangka P., Wackerle F. and Insam H. (2006b). Model-based design of an agricultural biogas plant: application of Anaerobic Digestion Model No.1 for an improved 4 chamber scheme. *Water Science and Technology*, 55 (10), 21-28.

Wiese J. and Haeck M. (2006). Instrumentation, control and automation for full-scale manure-based biogas systems. *Water Science and Technology*, 54 (9), 1-8.

Wikipedia (2008). Access date: 2008-Nov-04. Source: http://de.wikipedia.org/wiki/Biogasanlage.

Zhao H. W. and Viraraghavan T. (2004). Analysis of the performance of an anaerobic digestion system at the Regina wastewater treatment plant. *Bioresource Technology*, 95 (3), 301-307.

Zickefoose C. and Hayes R. B. J. (1976). Anaerobic sludge digestion: operations manual. *EPA 430/9-76-001*, U.S. Environmental Protection Agency, Washington D.C., USA.

A APPENDIX A

A.1 ADM1 MODEL MATRIX

Table A-1 ADM1 matrix for soluble components (physico-chemical rate equations not included; Batstone *et al.*, 2002a)

Component i	1	2	3	4	5	6	7	8	9	10	11	12	Rate (ρ_j, kg COD·m^{-3}·d^{-1})
j Process	S_{su}	S_{aa}	S_{fa}	S_{va}	S_{bu}	S_{pro}	S_{ac}	S_{h2}	S_{ch4}	S_{IC}	S_{IN}	S_{I}	
1 Disintegration												fsI,xc	$k_{dis}\cdot X_c$
2 Hydrolysis carbohydrates	1												$k_{hyd,ch}\cdot X_{ch}$
3 Hydrolysis of proteins		1											$k_{hyd,pr}\cdot X_{pr}$
4 Hydrolysis of lipids	$1-f_{fa,li}$		$f_{fa,li}$										$k_{hyd,li}\cdot X_{li}$
5 Uptake of sugars	-1				$(1-Y_{su})\cdot f_{bu,su}$	$(1-Y_{su})\cdot f_{pro,su}$	$(1-Y_{su})\cdot f_{ac,su}$	$(1-Y_{su})\cdot f_{h2,su}$		$-\sum_{i=1-9,11-24} C_i\cdot\nu_{i,5}$	$-(Y_{su})\cdot N_{bac}$		$k_{m,su}\cdot\frac{S_{su}}{K_s+S}\cdot X_{su}\cdot I_1$
6 Uptake of amino acids		-1		$(1-Y_{aa})\cdot f_{va,aa}$	$(1-Y_{aa})\cdot f_{bu,aa}$	$(1-Y_{aa})\cdot f_{pro,aa}$	$(1-Y_{aa})\cdot f_{ac,aa}$	$(1-Y_{aa})\cdot f_{h2,aa}$		$-\sum_{i=1-9,11-24} C_i\cdot\nu_{i,6}$	$N_{aa}-(Y_{aa})\cdot N_{bac}$		$k_{m,aa}\cdot\frac{S_{aa}}{K_s+S_{aa}}\cdot X_{aa}\cdot I_1$
7 Uptake of LCFA			-1				$(1-Y_{fa})\cdot 0.7$	$(1-Y_{fa})\cdot 0.3$			$-(Y_{fa})\cdot N_{bac}$		$k_{m,fa}\cdot\frac{S_{fa}}{K_s+S_{fa}}\cdot X_{fa}\cdot I_2$
8 Uptake of valerate				-1		$(1-Y_{c4})\cdot 0.54$	$(1-Y_{c4})\cdot 0.31$	$(1-Y_{c4})\cdot 0.15$			$-(Y_{c4})\cdot N_{bac}$		$k_{m,c4}\cdot\frac{S_{va}}{K_s+S_{va}}\cdot X_{c4}\cdot\frac{1}{1+S_{bu}/S_{va}}\cdot I_2$
9 Uptake of butyrate					-1		$(1-Y_{c4})\cdot 0.8$	$(1-Y_{c4})\cdot 0.2$			$-(Y_{c4})\cdot N_{bac}$		$k_{m,c4}\cdot\frac{S_{bu}}{K_s+S_{bu}}\cdot X_{c4}\cdot\frac{1}{1+S_{va}/S_{bu}}\cdot I_2$
10 Uptake of propionate						-1	$(1-Y_{pro})\cdot 0.57$	$(1-Y_{pro})\cdot 0.43$		$-\sum_{i=1-9,11-24} C_i\cdot\nu_{i,10}$	$-(Y_{pro})\cdot N_{bac}$		$k_{m,pr}\cdot\frac{S_{pro}}{K_s+S_{pro}}\cdot X_{pro}\cdot I_2$
11 Uptake of acetate							-1		$(1-Y_{ac})$	$-\sum_{i=1-9,11-24} C_i\cdot\nu_{i,11}$	$-(Y_{ac})\cdot N_{bac}$		$k_{m,ac}\cdot\frac{S_{ac}}{K_s+S_{ac}}\cdot X_{ac}\cdot I_3$
12 Uptake of hydrogen								-1	$(1-Y_{h2})$	$-\sum_{i=1-9,11-24} C_i\cdot\nu_{i,12}$	$-(Y_{h2})\cdot N_{bac}$		$k_{m,h2}\cdot\frac{S_{h2}}{K_s+S_{h2}}\cdot X_{h2}\cdot I_1$
13 Decay of Xsu													$k_{dec,Xsu}\cdot X_{su}$
14 Decay of Xaa													$k_{dec,Xaa}\cdot X_{aa}$
15 Decay of Xfa													$k_{dec,Xfa}\cdot X_{fa}$
16 Decay of Xc4													$k_{dec,Xc4}\cdot X_{c4}$
17 Decay of Xpro													$k_{dec,Xpro}\cdot X_{pro}$
18 Decay of Xac													$k_{dec,Xac}\cdot X_{ac}$
19 Decay of Xh2													$k_{dec,Xh2}\cdot X_{h2}$
	[kgCOD·m^{-3}]	[kgCOD·m^{-3}]	[kgCOD·m^{-3}]	[kgCOD·m^{-3}]	[kgCOD·m^{-3}]	[kgCOD·m^{-3}]	[kgCOD·m^{-3}]	[kgCOD·m^{-3}]	[kgCOD·m^{-3}]	[kmoleC·m^{-3}]	[kmoleN·m^{-3}]	[kgCOD·m^{-3}]	
	Monosaccharides	Amino acids	Long chain fatty acids	Total valerate	Total butyrate	Total propionate	Total acetate	Hydrogen gas	Methane gas	Inorganic carbon	Inorganic nitrogen	Soluble inerts	Inhibition factors: $I_1 = I_{pH}I_{IN,lim}$ $I_2 = I_{pH}I_{IN,lim}\cdot I_{h2}$ $I_3 = I_{pH}I_{IN,lim}\cdot I_{NH3,Xac}$

Table A-2 ADM1 matrix for particulate components (physico-chemical rate equations not included; Batstone *et al.*, 2002a)

Component i	13	14	15	16	17	18	19	20	21	22	23	24	Rate (ρ_j, kg COD·m^{-3}·d^{-1})
j Process	X_c	X_{ch}	X_{pr}	X_{li}	X_{su}	X_{aa}	X_{fa}	X_{c4}	X_{pro}	X_{ac}	X_{h2}	X_I	
1 Disintegration	-1	$f_{ch,xc}$	$f_{pr,xc}$	$f_{li,xc}$								$f_{xI,xc}$	$k_{dis}\cdot X_c$
2 Hydrolysis carbohydrates		-1											$k_{hyd,ch}\cdot X_{ch}$
3 Hydrolysis of proteins			-1										$k_{hyd,pr}\cdot X_{pr}$
4 Hydrolysis of lipids				-1									$k_{hyd,li}\cdot X_{li}$
5 Uptake of sugars					Y_{su}								$k_{m,su}\cdot\frac{S_{su}}{K_s+S}\cdot X_{su}\cdot I_1$
6 Uptake of amino acids						Y_{aa}							$k_{m,aa}\cdot\frac{S_{aa}}{K_s+S_{aa}}\cdot X_{aa}\cdot I_1$
7 Uptake of LCFA							Y_{fa}						$k_{m,fa}\cdot\frac{S_{fa}}{K_s+S_{fa}}\cdot X_{fa}\cdot I_2$
8 Uptake of valerate								Y_{c4}					$k_{m,c4}\cdot\frac{S_{va}}{K_s+S_{va}}\cdot X_{c4}\cdot\frac{1}{1+S_{bu}/S_{va}}\cdot I_2$
9 Uptake of butyrate								Y_{c4}					$k_{m,c4}\cdot\frac{S_{bu}}{K_s+S_{bu}}\cdot X_{c4}\cdot\frac{1}{1+S_{va}/S_{bu}}\cdot I_2$
10 Uptake of propionate									Y_{pro}				$k_{m,pr}\cdot\frac{S_{pro}}{K_s+S_{pro}}\cdot X_{pro}\cdot I_2$
11 Uptake of acetate										Y_{ac}			$k_{m,ac}\cdot\frac{S_{ac}}{K_s+S_{ac}}\cdot X_{ac}\cdot I_3$
12 Uptake of hydrogen											Y_{h2}		$k_{m,h2}\cdot\frac{S_{h2}}{K_s+S_{h2}}\cdot X_{h2}\cdot I_1$
13 Decay of Xsu	1				-1								$k_{dec,Xsu}\cdot X_{su}$
14 Decay of Xaa	1					-1							$k_{dec,Xaa}\cdot X_{aa}$
15 Decay of Xfa	1						-1						$k_{dec,Xfa}\cdot X_{fa}$
16 Decay of Xc4	1							-1					$k_{dec,Xc4}\cdot X_{c4}$
17 Decay of Xpro	1								-1				$k_{dec,Xpro}\cdot X_{pro}$
18 Decay of Xac	1									-1			$k_{dec,Xac}\cdot X_{ac}$
19 Decay of Xh2	1										-1		$k_{dec,Xh2}\cdot X_{h2}$
						[kgCOD·m–3]							
	Composites	Carbohydrates	Proteins	Lipids	Sugar degraders	Amino acid degraders	LCFA degraders	Valerate and butyrate degraders	Propionate degraders	Acetate degraders	Hydrogen degraders	Particulate inerts	Inhibition factors: $I_1 = I_{pH}\cdot I_{IN,lim}$ $I_2 = I_{pH}\cdot I_{IN,lim}\cdot I_{h2}$ $I_3 = I_{pH}\cdot I_{IN,lim}\cdot I_{NH3,Xac}$

A.2 EXTENDED ADM1 MODEL MATRIX

Table A-3 ADM1 matrix for acid-base reactions and for liquid-gas reactions as implemented in Matlab/SIMBA

	Component i	8	9	10	25	26	27	28	29	30	31	32	33	34	35	36	Rate (ρ_j, kg COD·m^{-3}·d^{-1})
j	Process	S_{h2}	S_{ch4}	S_{IC}	S_{cat}	S_{an}	$S_{va\_}$	$S_{bu\_}$	$S_{pro\_}$	$S_{ac\_}$	S_{hco3}	S_{nh4}	pi_{Sh2}	pi_{Sch4}	pi_{Sco2}	p_{Total}	
A4	valerate acid-base						-1										$k_{A\_Bva}\cdot(S_{va\_}\cdot S_H - K_{ava}\cdot(S_{va}-S_{va\_}))$
A5	butyrate acid-base							-1									$k_{A\_Bbu}\cdot(S_{bu\_}\cdot S_H - K_{abu}\cdot(S_{bu}-S_{bu\_}))$
A6	propionate acid-base								-1								$k_{A\_Bpro}\cdot(S_{pro\_}\cdot S_H - K_{apro}\cdot(S_{pro}-S_{pro\_}))$
A7	acetate acid-base									-1							$k_{A\_Bac}\cdot(S_{ac\_}\cdot S_H - K_{aac}\cdot(S_{ac}-S_{ac\_}))$
A10	inorg. carbon acid-base										-1						$k_{A\_Bco2}\cdot(S_{hco3}\cdot S_H - K_{aco2}\cdot S_{co2})$
A11	inorg. nitrogen acid-base											-1					$k_{A\_Bin}\cdot(S_{nh3}\cdot S_H - K_{ain}\cdot S_{nh4})$
ppSh2		$-V_{gas}/V$											RT/(16/1000)			RT/(16/1000)	$k_La_{H2}\cdot(S_{h2}-pi_{Sh2}\cdot(16/1000)/RT/(K_{H\_h2}))\cdot V/V_{gas}$
ppSch4			$-V_{gas}/V$											RT/(64/1000)		RT/(64/1000)	$k_La_{ch4}\cdot(S_{ch4}-pi_{Sch4}\cdot(64/1000)/RT/(K_{H\_ch4}))\cdot V/V_{gas}$
ppSco2				$-V_{gas}/V$											RT/(1/1000)	RT/(1/1000)	$k_La_{co2}\cdot(S_{co2}-pi_{Sco2}\cdot(1/1000)/RT/(K_{H\_co2}))\cdot V/V_{gas}$
ppTotal													piSh2/pTotal	piSch4/pTotal	piSco2/pTotal	-1	$k_p\cdot(p_{Total}-p_{ext})\cdot V/V_{gas}$

A.3 ADM1 PROCESSES

Table A-4 ADM1 processes as implemented in Matlab/SIMBA

Biochemical processes		Physico-chemical processes	
P1	disintegration	A4	valerate acid-base
P2	hydrolysisofcarbohydrates	A5	butyrate acid-base
P3	hydrolysisofproteins	A6	propionate acid-base
P4	hydrolysis of lipids	A7	acetate acid-base
P5	uptake of sugars	A10	inorganic carbon acid-base
P6	uptake of amino acids	A11	inorganic nitrogen acid-base
P7	uptake of long chain fatty acids (LCFA)		
P8	uptake of valerate	ppSh2	hydrogen stripping
P9	uptake of butyrate	ppSch4	methane stripping
P10	uptake of propionate	ppSco2	carbon dioxid stripping
P11	uptake of acetate	ppTotal	total gas stripping
P12	uptake of hydrogen		
P13	decay of biomass Sugar degraders		
P14	decay of biomass amino acids degraders		
P15	decay of biomass LCFA degraders		
P16	decay of biomass valerate, butyrate degraders		
P17	decay of biomass propionate degraders		
P18	decay of biomass acetate degraders		
P19	decay of biomass hydrogen degraders		

A.4 ADM1 PARAMETERS

Table A-5 ADM1 stoichiometric parameters as implemented in Matlab/SIMBA

Name	Description	Unit
fSI_XC	Soluble inerts from composites	-
fXI_XC	Particulate inerts from composites	-
fCH_XC	Carbonhydrates from composites	-
fPR_XC	Proteins from composites	-
fLI_XC	Lipids from composites	-
N_Xc	Nitrogen content composites	k mole N kg COD^{-1}
N_I	Nitrogen content inerts	k mole N kg COD^{-1}
N_aa	Nitrogen content in amino acids and proteins	k mole N kg COD^{-1}
N_XB	Nitrogen content in biomass	k mole N kg COD^{-1}
C_Xc	Carbon content composites	k mole C kg COD^{-1}
C_SI	Carbon content soluble inerts	k mole C kg COD^{-1}
C_Xch	Carbon content carbohydrates	k mole C kg COD^{-1}
C_Xpr	Carbon content proteins	k mole C kg COD^{-1}
C_Xli	Carbon content lipids	k mole C kg COD^{-1}
C_XI	Carbon content particulate inerts	k mole C kg COD^{-1}
C_su	Carbon content sugars	k mole C kg COD^{-1}
C_aa	Carbon content amino acids	k mole C kg COD^{-1}
C_Sfa	Carbonarbon content fatty acids	k mole C kg COD^{-1}
C_Sbu	Carbon content butyrate	k mole C kg COD^{-1}
C_Spro	Carbon content propionate	k mole C kg COD^{-1}
C_Sac	Carbon content acetate	k mole C kg COD^{-1}
C_XB	Carbon content biomass	k mole C kg COD^{-1}
C_Sva	Carbon content valerate	k mole C kg COD^{-1}
C_Sch4	Carbon content methane	k mole C kg COD^{-1}
fFA_Xli	fraction fatty acids from lipids	kg COD kg COD^{-1}
fBU_SU	fraction butyrate from sugars	kg COD kg COD^{-1}
fBU_AA	fraction butyrate from amino acids	kg COD kg COD^{-1}
fPRO_SU	fraction propionate from sugars	kg COD kg COD^{-1}
fPRO_AA	fraction propionate amino acids	kg COD kg COD^{-1}
fPRO_VA	fraction propionate valerate	kg COD kg COD^{-1}
fAC_SU	fraction acetate from sugars	kg COD kg COD^{-1}
fAC_AA	fraction acetate amino acids	kg COD kg COD^{-1}
fVA_AA	fraction valerate from amino acids	kg COD kg COD^{-1}
fH2_SU	fraction hydrogen from sugars	kg COD kg COD^{-1}
fH2_AA	fraction hydrogen from amino acids	kg COD kg COD^{-1}
fH2_FA	fraction hydrogen from fatty acids	kg COD kg COD^{-1}
fH2_VA	fraction hydrogen from valerate	kg COD kg COD^{-1}
fH2_BU	fraction hydrogen from butyrate	kg COD kg COD^{-1}
fH2_PRO	fraction hydrogen from propionate	kg COD kg COD^{-1}

Table A-6 ADM1 kinetic parameters as implemented in Matlab/SIMBA

Name	Description	Unit	Name	Description	Unit
kdis	disintegration rate	d^{-1}	kdec_Xaa	decay rate amino acids	d^{-1}
khyd_ch	Hydrolysis rate carbohydrates	d^{-1}	kdec_Xfa	decay rate fatty acids	d^{-1}
khyd_pr	hydrolysis rate propionate	d^{-1}	kdec_Xc4	decay rate butyrate and valerate	d^{-1}
khyd_li	hydrolysis rate lipids	d^{-1}	kdec_Xpro	decay rate propionate	d^{-1}
Ysu	Yield uptake sugars	kgCOD_X $kgCOD\_S^{-1}$	kdec_Xac	decay rate acetate	d^{-1}
Yaa	Yield uptake amino acids	kgCOD_X $kgCOD\_S^{-1}$	kdec_Xh2	decay rate hydrogen	d^{-1}
Yfa	Yield uptake LCFA	kgCOD_X $kgCOD\_S^{-1}$	kA_Bva	valerate rate coefficient for acid-base	k mole d^{-1}
Yc4	Yield uptake of buterate and valerate	kgCOD_X $kgCOD\_S^{-1}$	kA_Bbu	butyrate rate coefficient for acid-base	k mole d^{-1}
Ypro	Yield uptake propionate	kgCOD_X $kgCOD\_S^{-1}$	kA_Bpro	propionate rate coefficient for acid-base	k mole d^{-1}
Yac	Yield uptake acetate	kgCOD_X $kgCOD\_S^{-1}$	kA_Bac	acetate rate coefficient for acid-base	k mole d^{-1}
Yh2	Yield uptake hydrogen	kgCOD_X $kgCOD\_S^{-1}$	kA_Bco2	CO2 rate coefficient for acid-base	k mole d^{-1}
KS_su	half saturation coefficient sugars	kg COD m^{-3}	kA_Bin	inorganic nitrogen rate coefficient for acid-base	k mole d^{-1}
KS_aa	half saturation coefficient amino acids	kg COD m^{-3}	Kw	water acid-base equilibrium constant	k mole m^{-1}
KS_fa	half saturation coefficient fatty acids	kg COD m^{-3}	Kava	valerate acid-base equilibrium constant	k mole m^{-1}
KS_c4	half. sat. coeff. valerate and butyrate	kg COD m^{-3}	Kabu	butyrate acid-base equilibrium constant	k mole m^{-1}
KS_pro	half sat. coeff. propionate	kg COD m^{-3}	Kapro	propionate acid-base equilibrium constant	k mole m^{-1}
KS_ac	half sat. coeff. acetate	kg COD m^{-3}	Kaac	acetate acid-base equilibrium constant	k mole m^{-1}
KI_NH3	half. sat. coeeff. NH3 in p11	k mole N m^{-3}	Kaco2	CO2 acid-base equilibrium constant	k mole m^{-1}
KS_IN	half saturation coefficient inorganic N	k mole N m^{-3}	Kain	inorganic nitrogen acid-base equilibrium constant	k mole m^{-1}
KI_H2_fa	half sat. coeff. H2 for p7	kg COD m^{-3}	klaH2	dynamic gas–liquid transfer coefficient	d^{-1}
KI_H2_c4	half. sat. coeff. H2 for p8,9	kg COD m^{-3}	klaCH4	dynamic gas–liquid transfer coefficient	d^{-1}
KS_h2	half sat. coeff. H2 for p12	kg COD m^{-3}	klaCO2	dynamic gas–liquid transfer coefficient	d^{-1}
KI_H2_pro	half sat. coeff. H2 in p10	kg COD m^{-3}	KH_CO2	Henry constant	mol $bar^{-1}m^{-3}$
km_su	max uptake rate sugars	kgCOD_S $kgCOD\_X^{-1}$ d^{-1}	KH_CH4	Henry constant	mol $bar^{-1}m^{-3}$
km_aa	max. uptake rate amino acids	kgCOD_S $kgCOD\_X^{-1}$ d^{-1}	KH_H2	Henry constant	mol $bar^{-1}m^{-3}$
km_fa	max. uptake rate fatty acids	kgCOD_S $kgCOD\_X^{-1}$ d^{-1}	pHUL_a	upper pH limit for p5..10	-
km_c4	max. uptake rate valerate and butyrate	kgCOD_S $kgCOD\_X^{-1}$ d^{-1}	pHLL_a	lower pH limit for p5..10	-
km_pro	max. uptake rate propionate	kgCOD_S $kgCOD\_X^{-1}$ d^{-1}	pHUL_ac	upper pH limit p11	-
km_ac	max. uptake rate acetate	kgCOD_S $kgCOD\_X^{-1}$ d^{-1}	pHLL_ac	lower pH limit for p11	-
km_h2	max. uptake rate hydrogen	kgCOD_S $kgCOD\_X^{-1}$ d^{-1}	pHUL_h2	upper pH limit p12	-
kdec_Xsu	decay rate sugars	d^{-1}	pHLL_h2	lower pH limit p12	-

A.5 ADM1 VARIABLES

Table A-7 ADM1 variables as implemented in Matlab/SIMBA

Name	Formula
fXI_XC	1-fSI_XC-fCH_XC-fPR_XC-fLI_XC-fXP_XC
fCO2_XC	C_Xc - fSI_XC*C_SI - fCH_XC*C_Xch - fPR_XC*C_Xpr -fLI_XC*C_Xli - fXI_XC*C_XI-fXP_XC*C_Xp
fSIN_XC	N_Xc-fSI_XC*N_I-fPR_XC*N_aa-fXI_XC*N_I-fXP_XC*N_Xp
fCO2_Xli	C_Xli - fFA_Xli*C_Sfa - (1-fFA_Xli)*C_Xch
fAC_SU	1-fH2_SU-fBU_SU-fPRO_SU
fCO2_SU	C_Xch-(fBU_SU*C_Sbu+fPRO_SU*C_Spro+fAC_SU*C_Sac)*(1-Ysu) - Ysu*C_XB
fAC_AA	1-fH2_AA-fVA_AA-fBU_AA-fPRO_AA
fCO2_AA	C_Xpr-(fVA_AA*C_Sva+fBU_AA*C_Sbu+fPRO_AA*C_Spro+fAC_AA*C_Sac)*(1-Yaa) - Yaa*C_XB
fAC_FA	1.0-fH2_FA
fCO2_FA	C_Sfa-fAC_FA*C_Sac*(1-Yfa)-Yfa*C_XB
fAC_VA	1-fPRO_VA-fH2_VA
fCO2_VA	C_Sva-(fPRO_VA*C_Spro + fAC_VA*C_Sac)*(1-Yc4) - Yc4*C_XB
fAC_BU	1-fH2_BU
fCO2_BU	C_Sbu-fAC_BU*C_Sac*(1-Yc4)-Yc4*C_XB
fAC_PRO	1-fH2_PRO
fCO2_PRO	C_Spro-fAC_PRO*C_Sac*(1-Ypro)-Ypro*C_XB
fCO2_AC	C_Sac-(1-Yac)*C_Sch4-Yac*C_XB
fCO2_H2	-1*(1-Yh2)*C_Sch4-Yh2*C_XB
pfac_h	Scat+Snh4-Shco3-Sac_/64-Spro_/112-Sbu_/160-Sva_/208-San
SH	-1*pfac_h/2 +0.5*(pfac_h*pfac_h + 4*Kw)^0.5
Iin	(Snh4+Snh3)/(Snh4+Snh3+KS_IN)
I_NH3	KI_NH3/(KI_NH3+Snh3)
I_H2_c4	KI_H2_c4/(KI_H2_c4 + Sh2)
KI_H_a	10^(-1* (pHUL_a+pHLL_a)/2)
IpH_a	KI_H_a^2/(SH^2+KI_H_a^2)
KI_H_h2	10^(-1*(pHUL_h2+pHLL_h2)/2)
IpH_h2	KI_H_h2^3/(SH^3+KI_H_h2^3)
KI_H_AC	10^(-1*(pHUL_ac+pHLL_ac)/2)
IpH_ac	KI_H_AC^3/(SH^3+KI_H_AC^3)
fCH_XB	fCH_XC/(fCH_XC+fPR_XC+fLI_XC)*(1-fP)
fPR_XB	fPR_XC/(fCH_XC+fPR_XC+fLI_XC)*(1-fP)
fLI_XB	fLI_XC/(fCH_XC+fPR_XC+fLI_XC)*(1-fP)
fSIN_XB	N_XB-fP*N_Xp-fPR_XB*N_aa
fCO2_XB	C_XB-fP*C_Xp-fCH_XB*C_Xch-fPR_XB*C_Xpr-fLI_XB*C_Xli
pH	-1*log(SH)
Qgas	kp*(pTOTAL-pext)/(RT*NQ)*V

B APPENDIX FOR PAPER (B)

APPLICATION OF ADM 1 FOR AN IMPROVED FOUR CHAMBER SCHEME

In the following, supplementary information and data for paper (B) is given. These values were primarily used for the setup and calibration of the numerical models as described in the paper.

B.1 MEASURED RESULTS

Table B-1 Feeding characteristics of manure

Week	CSB_{tot}	CSB_s	CSB_x	N_{tot}	NH_4-N	N_{org}	TS	VS	TC	TIC	S
	[mg/l]	[mg/l]	[mg/l]	[mg/l]	[mg/l]	[mg/l]	[g/l]	[g/l]	[g/l]	[g/l]	[g/l]
1	-	-	-	-	-	-	-	-	-	-	-
2	44106	8086	36020	1937	187	1750	36.0	25.3	13.8	0.26	0.11
3	53307	9058	44249	2136	302	1834	44.8	31.2	17.2	0.31	0.14
4	52364	9146	43218	1880	158	1723	41.1	29.7	14.8	0.26	0.13

Table B-2 Characteristics of digested manure

Week	CSB_{tot}		CSB_s		CSB_x		N_{tot}		NH_4-N		N_{org}	
	[mg/L]		[mg/L]		[mg/L]		[mg/L]		[mg/L]		[mg/L]	
	B1	B2	B1	B2	B1	B2	B1	B2	B1	B2	B1	B2
1	27364	27397	561	-	26803	-	1939	1986	714	714	1225	1272
2	21197	23178	798	819	20399	1499	2391	2444	1132	1086	1259	1357
3	27721	22163	1112	976	26609	21187	2888	2419	1005	1137	1883	1281
4	28069	22937	1820	1109	26249	21828	2118	2220	898	1081	1220	1139
5	-	-	-	-	-	-	2097	2237	811	964	1286	1273

Table B-2 (continued)

Week	TS		VS		TC		TIC		S	
	[g/l]		[g/l]		[%]		[%]		[%]	
	B1	B2	B1	B2	B1	B2	B1	B2	B1	B2
1	20.4	20.0	13.4	13.3	33.2	33.3	1.1	1.2	0.9	0.9
2	22.1	24.5	14.1	15.5	32.1	31.3	1.2	1.1	0.9	0.9
3	29.1	24.0	17.9	15.2	31.7	30.6	0.3	0.6	0.7	0.9
4	29.9	24.5	17.6	14.6	31.4	30.2	0.9	0.2	0.5	0.8
5	24.6	26.4	15.8	15.4	27.4	26.4	0.4	0.2	0.6	0.4

Table B-3 Biogas production of manure in lab experiments

Day	reactor B1	reactor B2	Day	reactor B1	reactor B2
0	34.9	0.5	16	106.1	14.2
1	16.6	2.1	17	112.9	12.1
2	16.0	0.0	18	124.8	13.2
3	13.6	0.0	19	127.1	14.2
4	11.8	0.5	20	126.5	14.2
5	9.5	0.5	21	126.0	13.2
6	5.3	6.3	22	128.9	16.4
7	6.5	6.3	23	120.6	14.8
8	5.3	5.8	24	124.2	15.3
9	58.5	3.7	25	118.3	15.8
10	76.3	9.5	26	112.3	16.0
11	117.1	11.1	27	108.3	17.8
12	109.4	12.1	28	101.1	19.5
13	122.7	13.0	29	101.1	21.1
14	106.4	11.1	30	101.7	15.3
15	106.1	10.6			

B.2 MODEL CALIBRATION

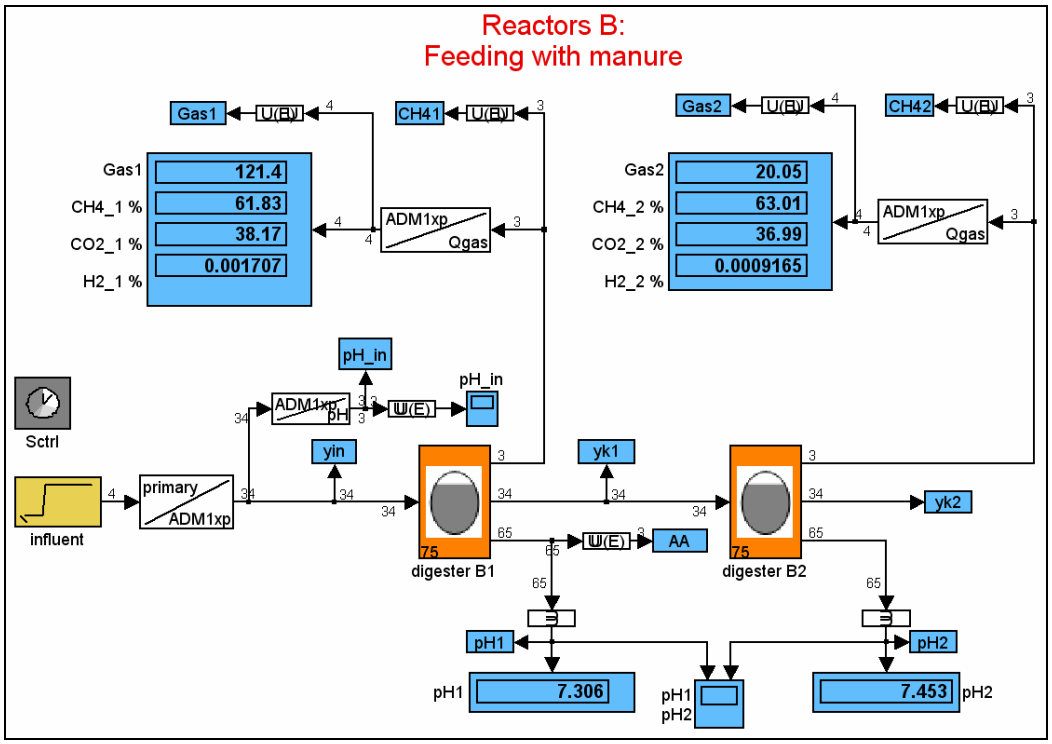

Figure B-1 Simulation model of two lab reactors for manure digestion edited in the SIMBA environment

Table B-4 Fraction balance for manure

Feed							**After disintegration**				**After digestion**		
fraction	COD	TKN		TC	TKN	TC	f_dis	COD	TKN	TC	COD	TKN	TC
	kg COD/m³	k mole N/ kg COD	%	k mole C/kg COD	g/m³	g/m³		kg COD/m³	g/m³	g/m³	kg COD/m³	g/m³	g/m³
SSU	2.717			0.0313		1020.4		2.717		1020.4	0.081		30.6
SAA	2.717	0.00715	10%	0.03	271.9	978.0		2.717	271.9	978.0	0.006	0.6	2.3
SFA	2.717			0.0217		707.4		2.717		707.4	0.063		16.4
SVA				0.024		0				0	0.005		1.3
SBU				0.025		0				0	0.007		2.0
SPRO				0.0268		0				0	0.004		1.4
SAC				0.0313		0				0	0.044		16.4
SH2						0				0	0.000		0.0
SCH4				0.0156		0				0	0.048		8.9
SIC				1		280.0				280.0	0.008		93.1
SIN			100%		215.6				215.6		0.082	1153.8	0.0
Si	0.613	0.0014	2%	0.03	12.0	220.8	0.015	1.2	24.1	443.1	1.077	21.1	387.8
Xc	41.162	0.0026	4%	0.028	1498.3	13830.6					0.769	28.0	258.3
Xch				0.0313		0	0.34	14.0		5256.6	0.021		8.1
Xpr			10%	0.03	0	0	0.18	7.4	740.9	2667.3	0.011	1.1	4.1
Xli				0.022		0	0.14	5.8		1521.4	0.009		2.3
XSU		0.0057	8%	0.0313	0	0					0.055	4.4	20.5
XAA		0.0057	8%	0.0313	0	0					0.038	3.0	14.2
XFA		0.0057	8%	0.0313	0	0					0.159	12.7	59.6
XC4		0.0057	8%	0.0313	0	0					0.099	7.9	37.2
XPRO		0.0057	8%	0.0313	0	0					0.088	7.1	33.2
XAC		0.0057	8%	0.0313	0	0					0.411	32.9	154.3
XH2		0.0057	8%	0.0313	0	0					0.045	3.6	16.8
XI		0.0014	2%	0.03	0	0	0.125	5.1	100.8	1852.3	6.361	124.7	2289.9
XP		0.0043	6%	0.03	0	0	0.2	8.2	495.6	2963.7	9.838	592.2	3541.7
sum	49.926				1998	17037	1.00	49.926	1849	17690	19.238	1993	7000
measured	49.926				1984	15300		49.926	1984	15300	23.918	2261	7200

Table B-5 Calibrated parameter set for manure digestion

Name	Value	Name	Value
fSI_XC	0.015	KS_su	0.5
dummy_fXI_XC	0.125	pHUL_a	5.5
fCH_XC	0.34	pHLL_a	4.5
fPR_XC	0.18	km_aa	26.66
fLI_XC	0.14	KS_aa	0.05
fXP_XC	0.2	km_fa	13.2
N_Xc	0.00215	KS_fa	1
N_I	0.0014	KI_H2_fa	3.00E-06
N_aa	0.0071	km_c4	10
C_Xc	0.028	KS_c4	0.1
C_SI	0.03	KI_H2_c4	1.00E-05
C_Xch	0.0313	km_pro	13
C_Xpr	0.03	KS_pro	0.1
C_Xli	0.022	KI_H2_pro	3.50E-06
C_XI	0.03	km_ac	30
dummy_C_su	0.0313	KS_ac	0.15
dummy_C_aa	0.03	KI_NH3	0.0013
fFA_Xli	0.95	pHUL_ac	7
C_Sfa	0.0217	pHLL_ac	6
fH2_SU	0.19	km_h2	33.3
fBU_SU	0.0772	KS_h2	1.00E-06
fPRO_SU	0.1522	pHUL_h2	8
dummy_fAC_SU	0.5806	pHLL_h2	4.5
N_XB	0.08/14	kdec_Xsu	0.7
C_Sbu	0.025	kdec_Xaa	0.8
C_Spro	0.0268	kdec_Xfa	0.06
C_Sac	0.0313	kdec_Xc4	0.06
C_XB	0.0313	kdec_Xpro	0.02
Ysu	0.1	kdec_Xac	0.02
fH2_AA	0.06	kdec_Xh2	0.3
fVA_AA	0.1531	Kw	2.08E-14
fBU_AA	0.173	Kava	1.35E-05
fPRO_AA	0.0333	Kabu	1.51E-05
dummy_fAC_AA	0.5806	Kapro	1.32E-05
C_Sva	0.024	Kaac	1.74E-05
Yaa	0.15	Kaco2	5.10E-07
fH2_FA	0.3	Kain	1.50E-09
Yfa	0.0454	kA_Bva	1.00E+08
fH2_VA	0.15	kA_Bbu	1.00E+08
fPRO_VA	0.54	kA_Bpro	1.00E+08
fH2_BU	0.2	kA_Bac	1.00E+08
Yc4	0.06	kA_Bco2	1.00E+08
fH2_PRO	0.43	kA_Bin	1.00E+08
Ypro	0.04	klaH2	200
C_Sch4	0.0156	klaCH4	200
Yac	0.025	klaCO2	200
Yh2	0.06	KH_CO2	1/(0.0271*0.08314*(T+273.15))
kdis	0.5	KH_CH4	1/(0.00116*0.08314*(35+273.15))
khyd_ch	10	KH_H2	1/(7.38e-4*0.08314*(35+273.15))
khyd_pr	10	C_Xp	0.03
khyd_li	10	N_Xp	0.06/14
KS_IN	1.00E-04	fP	0.4
km_su	30		

Table B-6 Influent file for manure digestion

Day	CODx	CODs	Ntot/TKN	Q
	g/m³	g/m³	g/m³	m³/d
0	0.0	0.0	0.0	0.0
1	0.0	0.0	0.0	0.0
2	0.0	0.0	0.0	0.0
3	0.0	0.0	0.0	0.0
4	0.0	0.0	0.0	0.0
5	0.0	0.0	0.0	0.0
6	0.0	0.0	0.0	0.0
7	0.0	0.0	0.0	0.0
8	0.0	0.0	0.0	0.0
9	36020.4	8086.0	1936.9	7.5
10	36020.4	8086.0	1936.9	7.5
11	36020.4	8086.0	1936.9	7.5
12	36020.4	8086.0	1936.9	7.5
13	36020.4	8086.0	1936.9	7.5
14	36020.4	8086.0	1936.9	7.5
15	36020.4	8086.0	1936.9	7.5
16	44248.9	9058.0	2135.7	7.5
17	44248.9	9058.0	2135.7	7.5
18	44248.9	9058.0	2135.7	7.5
19	44248.9	9058.0	2135.7	7.5
20	44248.9	9058.0	2135.7	7.5
21	44248.9	9058.0	2135.7	7.5
22	44248.9	9058.0	2135.7	7.5
23	43217.7	9146.0	1880.1	7.5
24	43217.7	9146.0	1880.1	7.5
25	43217.7	9146.0	1880.1	7.5
26	43217.7	9146.0	1880.1	7.5
27	43217.7	9146.0	1880.1	7.5
28	43217.7	9146.0	1880.1	7.5
29	43217.7	9146.0	1880.1	7.5
30	43217.7	9146.0	1880.1	7.5

B.3 SIMULATION RESULTS

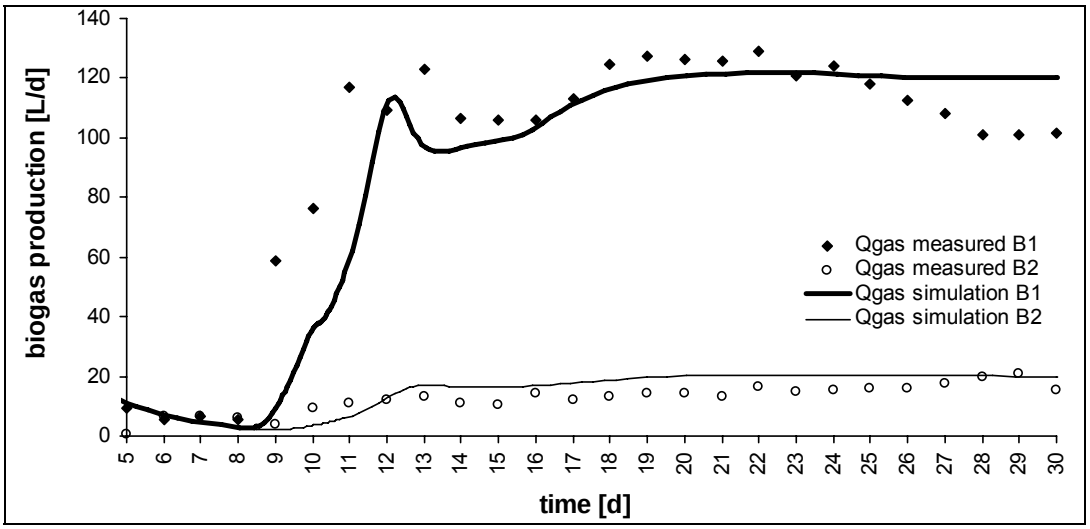

Figure B-2 Simulation results vs. measured values of biogas production from manure

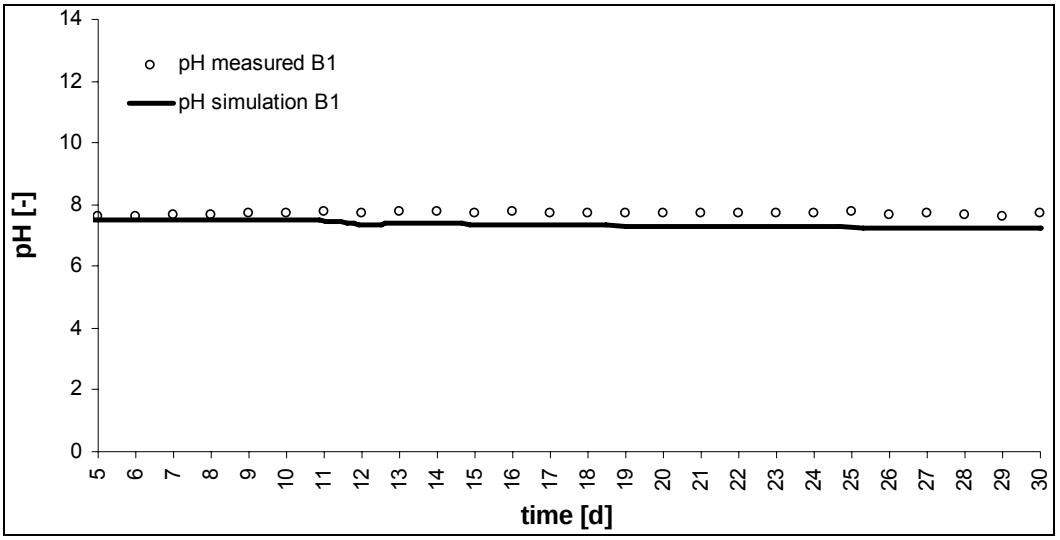

Figure B-3 Simulation results vs. measured values of pH for manure

C APPENDIX FOR PAPER (C)

FARMSCALE CO-FERMENTATION OF MANURE AND ORGANIC WASTE

In the following, supplementary information and data for paper (C) is given. These values were primarily used for the setup and calibration of the numerical models as described in the paper. For information related to manure please refer to Appendix B.

C.1 MEASURED RESULTS

Table C-1 Feeding characteristics of biowaste

Week	CSB_{tot}	CSB_s	CSB_x	N_{tot}	NH_4-N	N_{org}	TS	VS	TC	TIC	S
	[mg/l]	[mg/l]	[mg/l]	[mg/l]	[mg/l]	[mg/l]	[g/l]	[g/l]	[g/l]	[g/l]	[g/l]
1	-	-	-	-	-	-	-	-	-	-	-
2	103145	7207	95938	1930	64	1865	66.8	59.6	43.0	1.3	0.2
3	43687	3278	40409	857	137	711	26.2	22.3	11.4	0.5	0.1
4	53444	10645	42799	913	53	860	33.0	28.8	13.6	0.6	0.1

Table C-2 Characteristics of digested biowaste

Week	CSB_{tot}		CSB_s		CSB_x		N_{tot}		NH_4-N		N_{org}	
	[mg/L]		[mg/L]		[mg/L]		[mg/L]		[mg/L]		[mg/L]	
	A1	A2	A1	A2	A1	A2	A1	A2	A1	A2	A1	A2
1	26419	29564	566	-	25853	-	1805	1888	714	714	1091	1174
2	20970	20500	746	798	20224	19702	2381	2264	1122	1071	1259	1193
3	41724	19931	1179	809	40545	19122	1855	1809	857	1071	998	738
4	-	18661	-	779	-	17882		1582		1239		342
5	-	-	-	-	-	-	1725	1754	1071	898	654	856

Table C-2 (continued)

Week	TS		VS		TC		TIC		S	
	[g/l]		[g/l]		[%]		[%]		[%]	
	A1	A2	A1	A2	A1	A2	A1	A2	A1	A2
1	20.0	22.0	12.9	14.2	32.5	32.4	1.4	1.6	0.8	0.9
2	22.9	22.3	14.1	14.0	31.4	30.8	1.2	0.9	0.8	1.0
3	27.7	21.7	17.9	13.5	37.3	31.1	2.0	0.5	0.2	0.8
4	-	20.2	-	10.1	-	29.7	-	0.3	-	0.8
5	32.4	18.9	18.6	11.5	30.0	25.8	4.7	0.3	1.3	1.0

Table C-3 Biogas production of biowaste in lab experiments

Day	reactor A1	reactor A2	Day	reactor A1	reactor A2
0	15.5	16.1	16	6.9	38.9
1	11.0	10.3	17	4.5	14.5
2	10.6	9.5	18	4.5	9.5
3	8.5	8.7	19	1.6	7.0
4	7.7	7.0	20	0.0	5.8
5	6.5	6.2	21	0.8	4.5
6	5.3	5.4	22	1.6	5.8
7	6.1	5.4	23	1.2	100.4
8	5.3	5.0	24	1.6	51.2
9	68.0	3.3	25	1.2	75.2
10	108.2	16.9	26	0.8	0.4
11	105.8	30.2	27	0.0	3.7
12	45.2	38.9	28	0.4	0.0
13	28.3	49.1	29	0.8	2.9
14	32.6	50.8	30	0.8	0.0
15	39.9	82.7			

C.2 MODEL CALIBRATION

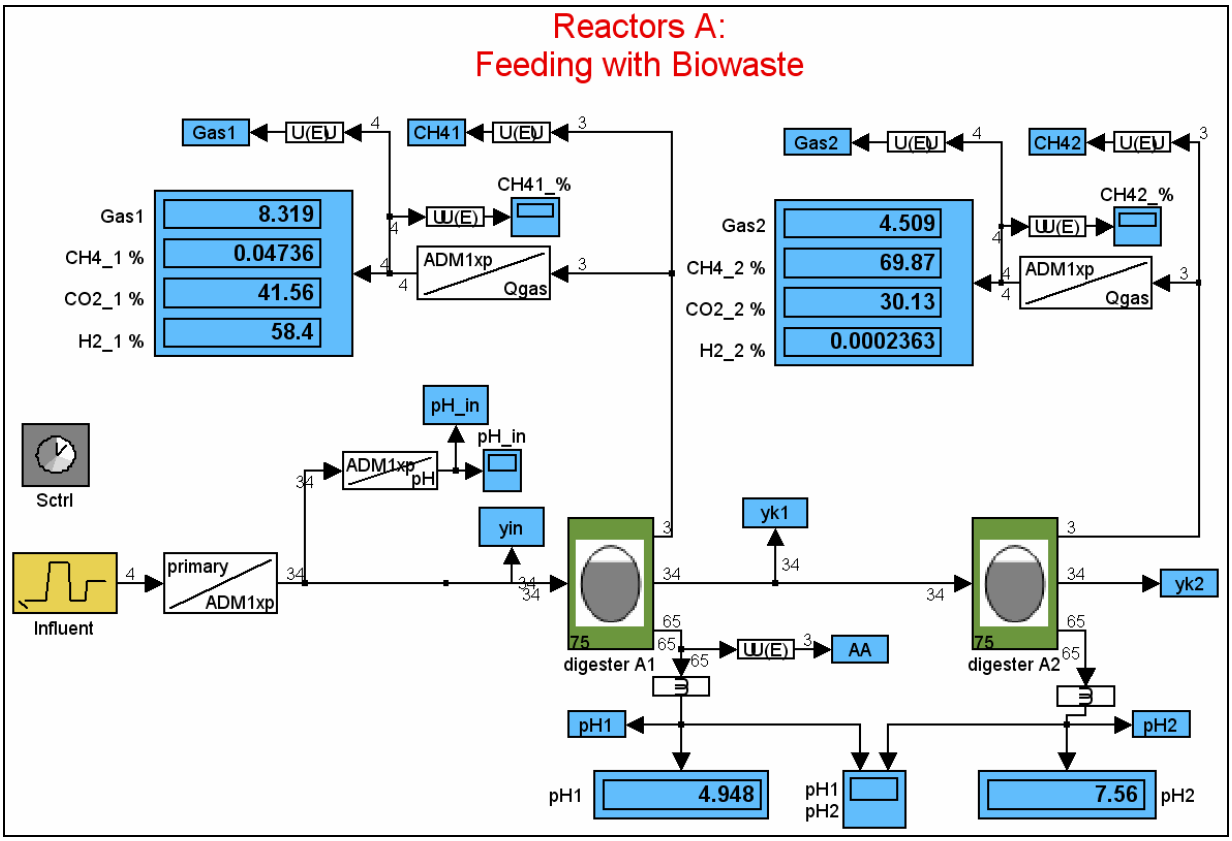

Figure C-1 Simulation model of two lab reactors for biowaste digestion edited in the SIMBA environment

Table C-4 Fraction balance for biowaste

Feed							**After disintegration**				**After digestion**		
fraction	COD	TKN		TC	TKN	TC	f_dis	COD	TKN	TC	COD	TKN	TC
	kg COD/m³	k mole N/ kg COD	%	k mole C/kg COD	g/m³	g/m³		kg COD/m³	g/m³	g/m³	kg COD/m³	g/m³	g/m³
SSU	1.244			0.0313		467.4		1.244		467.4	0.297		111.6
SAA	1.244	0.0072	10.0%	0.0350	124.6	522.6		1.244	124.6	522.6	0.006	0.6	2.7
SFA	1.244			0.0217		324.0		1.244		324.0	0.224		58.3
SVA	0.704			0.0240		202.8		0.704		202.8	0.019		5.4
SBU	0.704			0.0250		211.3		0.704		211.3	0.026		7.9
SPRO	0.704			0.0268		226.5		0.704		226.5	0.014		4.4
SAC	0.704			0.0313		264.5		0.704		264.5	0.214		80.4
SH2				0							0.000		
SCH4				0.0156		0.0				0.0	0.051		9.5
SIC				1.00		830.0				830.0	0.008		96.5
SIN		1.00	100.0	0.0	84.7				84.7		0.076	1068.0	
Si	0.493	0.0011	1.5%	0.0300	7.2	177.5	0.015	1.389	20.4	500.0	1.134	16.7	408.3
Xc	59.715	0.0011	1.6%	0.0280	933.1	20033.9					0.211	3.3	70.9
Xch				0.0313			0.275	16.422		6168.0	0.006		2.1
Xpr		0.00714	10.0%	0.0300			0.110	6.569	656.6	2364.7	0.002	0.2	0.8
Xli				0.0220			0.300	17.915		4729.5	0.006		1.6
XSU		0.0057	8.0%	0.0313							0.022	1.8	8.3
XAA		0.0057	8.0%	0.0313							0.008	0.6	3.0
XFA		0.0057	8.0%	0.0313							0.238	19.0	89.5
XC4		0.0057	8.0%	0.0313							0.073	5.9	27.6
XPRO		0.0057	8.0%	0.0313							0.086	6.8	32.2
XAC		0.0057	8.0%	0.0313							0.441	35.2	165.8
XH2		0.0057	8.0%	0.0313							0.037	3.0	14.0
XI		0.0011	1.5%	0.0300			0.300	17.915	263.3	6449.3	14.645	215.3	5272.2
XP		0.0043	6.0%	0.0300			0.000	0.000	0.0	0.00	6.625	398.8	2384.9
sum	66.759				1150	23261	1	66.759	1150	23261	24.386	1775	8858
measured	66.758				1233	22700	1	66.758	1233	22700	18.661	1754	4900

Table C-5 Calibrated parameter set for biowaste digestion (co-digestion with manure)

Name	Value	Name	Value
fSI_XC	0.015	KS_su	0.5
dummy_fXI_XC	0.3	pHUL_a	5.5
fCH_XC	0.275	pHLL_a	4.5
fPR_XC	0.11	km_aa	26.66
fLI_XC	0.3	KS_aa	0.05
fXP_XC	0	km_fa	13.2
N_Xc	0.0011	KS_fa	1
N_I	0.0011	KI_H2_fa	3.00E-06
N_aa	0.0072	km_c4	10
C_Xc	0.028	KS_c4	0.1
C_SI	0.03	KI_H2_c4	1.00E-05
C_Xch	0.0313	km_pro	13
C_Xpr	0.03	KS_pro	0.1
C_Xli	0.022	KI_H2_pro	3.50E-06
C_XI	0.03	km_ac	12
dummy_C_su	0.0313	KS_ac	0.15
dummy_C_aa	0.03	KI_NH3	0.0018
fFA_Xli	0.95	pHUL_ac	7
C_Sfa	0.0217	pHLL_ac	6
fH2_SU	0.19	km_h2	33.3
fBU_SU	0.0772	KS_h2	1.00E-06
fPRO_SU	0.1522	pHUL_h2	8
dummy_fAC_SU	0.5806	pHLL_h2	4.5
N_XB	0.08/14	kdec_Xsu	0.7
C_Sbu	0.025	kdec_Xaa	0.8
C_Spro	0.0268	kdec_Xfa	0.06
C_Sac	0.0313	kdec_Xc4	0.06
C_XB	0.0313	kdec_Xpro	0.02
Ysu	0.1	kdec_Xac	0.02
fH2_AA	0.06	kdec_Xh2	0.3
fVA_AA	0.1531	Kw	2.08E-14
fBU_AA	0.173	Kava	1.35E-05
fPRO_AA	0.0333	Kabu	1.51E-05
dummy_fAC_AA	0.5806	Kapro	1.32E-05
C_Sva	0.024	Kaac	1.74E-05
Yaa	0.15	Kaco2	5.10E-07
fH2_FA	0.3	Kain	1.50E-09
Yfa	0.0454	kA_Bva	1.00E+08
fH2_VA	0.15	kA_Bbu	1.00E+08
fPRO_VA	0.54	kA_Bpro	1.00E+08
fH2_BU	0.2	kA_Bac	1.00E+08
Yc4	0.06	kA_Bco2	1.00E+08
fH2_PRO	0.43	kA_Bin	1.00E+08
Ypro	0.04	klaH2	200
C_Sch4	0.0156	klaCH4	200
Yac	0.025	klaCO2	200
Yh2	0.06	KH_CO2	1/(0.0271*0.08314*(T+273.15))
kdis	0.65	KH_CH4	1/(0.00116*0.08314*(35+273.15))
khyd_ch	10	KH_H2	1/(7.38e-4*0.08314*(35+273.15))
khyd_pr	10	C_Xp	0.03
khyd_li	10	N_Xp	0.06/14
KS_IN	1.00E-04	fP	0.4
km_su	30		

Table C-6 Calibrated parameter set for manure digestion (co-digestion with biowaste)

Name	Value	Name	Value
fSI_XC	0.015	KS_su	0.5
dummy_fXI_XC	0.125	pHUL_a	5.5
fCH_XC	0.34	pHLL_a	4.5
fPR_XC	0.18	km_aa	26.66
fLI_XC	0.14	KS_aa	0.05
fXP_XC	0.2	km_fa	13.2
N_Xc	0.0026	KS_fa	1
N_I	0.0014	KI_H2_fa	3.00E-06
N_aa	0.0071	km_c4	10
C_Xc	0.028	KS_c4	0.1
C_SI	0.03	KI_H2_c4	1.00E-05
C_Xch	0.0313	km_pro	13
C_Xpr	0.03	KS_pro	0.1
C_Xli	0.022	KI_H2_pro	3.50E-06
C_XI	0.03	km_ac	12
dummy_C_su	0.0313	KS_ac	0.15
dummy_C_aa	0.03	KI_NH3	0.0018
fFA_Xli	0.95	pHUL_ac	7
C_Sfa	0.0217	pHLL_ac	6
fH2_SU	0.19	km_h2	33.3
fBU_SU	0.0772	KS_h2	1.00E-06
fPRO_SU	0.1522	pHUL_h2	8
dummy_fAC_SU	0.5806	pHLL_h2	4.5
N_XB	0.08/14	kdec_Xsu	0.7
C_Sbu	0.025	kdec_Xaa	0.8
C_Spro	0.0268	kdec_Xfa	0.06
C_Sac	0.0313	kdec_Xc4	0.06
C_XB	0.0313	kdec_Xpro	0.02
Ysu	0.1	kdec_Xac	0.02
fH2_AA	0.06	kdec_Xh2	0.3
fVA_AA	0.1531	Kw	2.08E-14
fBU_AA	0.173	Kava	1.35E-05
fPRO_AA	0.0333	Kabu	1.51E-05
dummy_fAC_AA	0.5806	Kapro	1.32E-05
C_Sva	0.024	Kaac	1.74E-05
Yaa	0.15	Kaco2	5.10E-07
fH2_FA	0.3	Kain	1.50E-09
Yfa	0.0454	kA_Bva	1.00E+08
fH2_VA	0.15	kA_Bbu	1.00E+08
fPRO_VA	0.54	kA_Bpro	1.00E+08
fH2_BU	0.2	kA_Bac	1.00E+08
Yc4	0.06	kA_Bco2	1.00E+08
fH2_PRO	0.43	kA_Bin	1.00E+08
Ypro	0.04	klaH2	200
C_Sch4	0.0156	klaCH4	200
Yac	0.025	klaCO2	200
Yh2	0.06	KH_CO2	1/(0.0271*0.08314*(T+273.15))
kdis	0.65	KH_CH4	1/(0.00116*0.08314*(35+273.15))
khyd_ch	10	KH_H2	1/(7.38e-4*0.08314*(35+273.15))
khyd_pr	10	C_Xp	0.03
khyd_li	10	N_Xp	0.06/14
KS_IN	1.00E-04	fP	0.4
km_su	30		

Table C-7 Influent file for biowaste digestion

Day	CODx	CODs	Ntot/TKN	Q
	g/m³	g/m³	g/m³	m³/d
0	0.0	0.0	0.0	0.0
1	0.0	0.0	0.0	0.0
2	0.0	0.0	0.0	0.0
3	0.0	0.0	0.0	0.0
4	0.0	0.0	0.0	0.0
5	0.0	0.0	0.0	0.0
6	0.0	0.0	0.0	0.0
7	0.0	0.0	0.0	0.0
8	0.0	0.0	0.0	0.0
9	95937.9	7207.0	1929.5	7.5
10	95937.9	7207.0	1929.5	7.5
11	95937.9	7207.0	1929.5	7.5
12	95937.9	7207.0	1929.5	7.5
13	95937.9	7207.0	1929.5	7.5
14	95937.9	7207.0	1929.5	7.5
15	95937.9	7207.0	1929.5	7.5
16	40408.8	3278.0	857.3	7.5
17	40408.8	3278.0	857.3	0.0
18	40408.8	3278.0	857.3	0.0
19	40408.8	3278.0	857.3	0.0
20	40408.8	3278.0	857.3	0.0
21	40408.8	3278.0	857.3	0.0
22	40408.8	3278.0	857.3	0.0
23	42799.1	10645.0	912.7	3.75
24	42799.1	10645.0	912.7	3.75
25	42799.1	10645.0	912.7	3.75
26	42799.1	10645.0	912.7	3.75
27	42799.1	10645.0	912.7	3.75
28	42799.1	10645.0	912.7	3.75
29	42799.1	10645.0	912.7	3.75
30	42799.1	10645.0	912.7	3.75

C.3 SIMULATION RESULTS

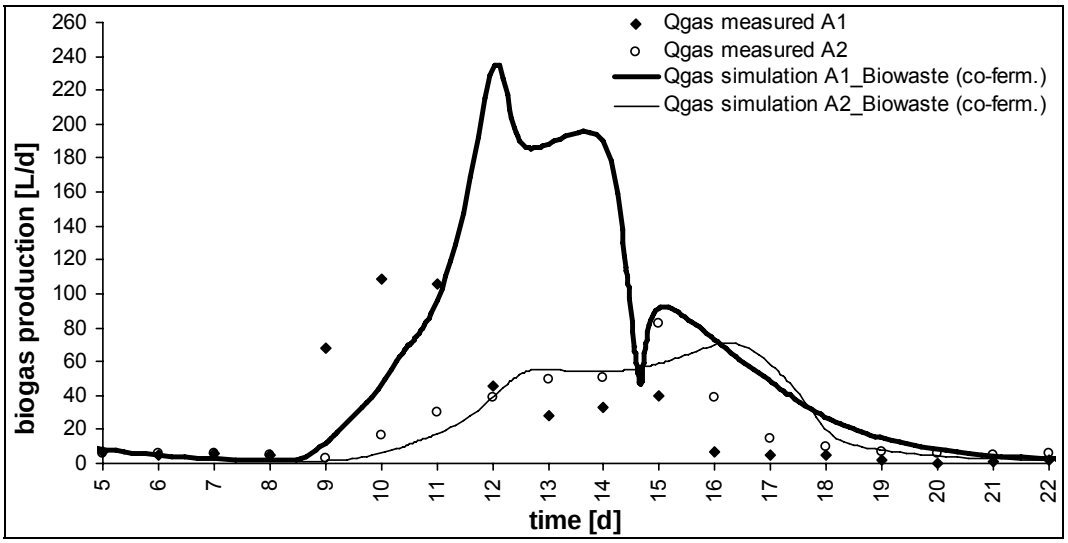

Figure C-2 Simulation results vs. measured values of biogas production from biowaste

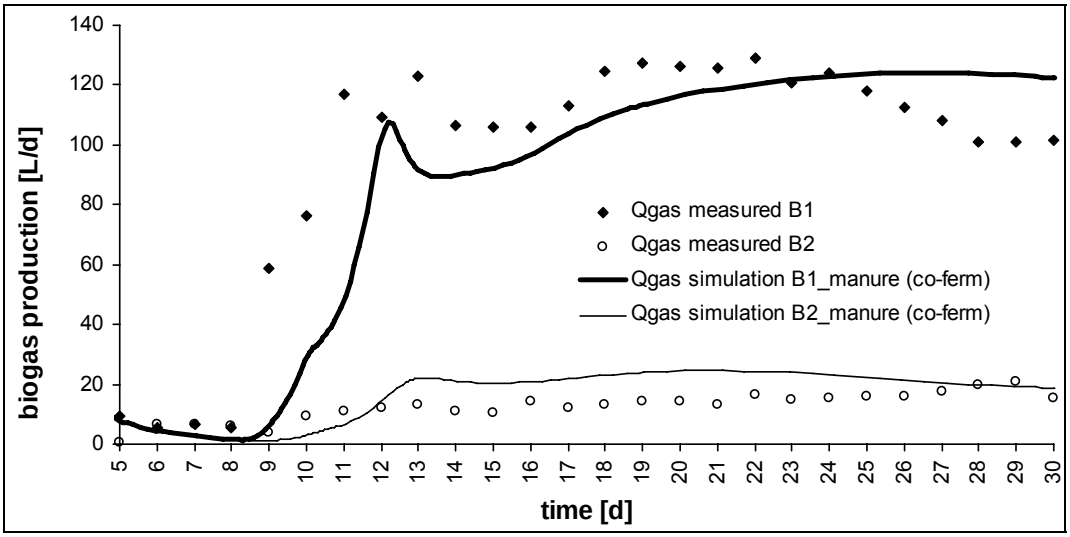

Figure C-3 Simulation results vs. measured values of biogas production from manure

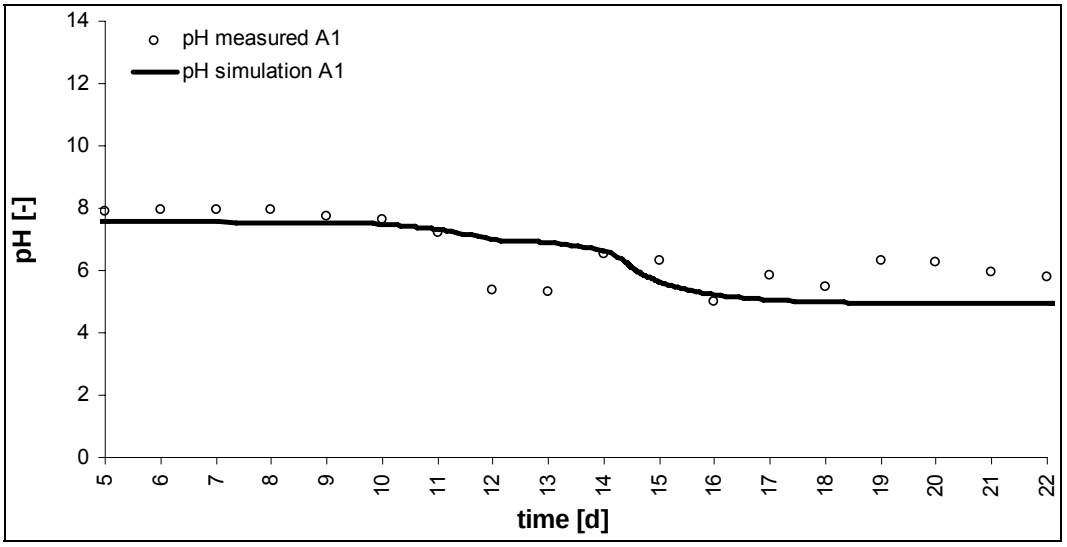

Figure C-4 Simulation results vs. measured values of pH for biowaste

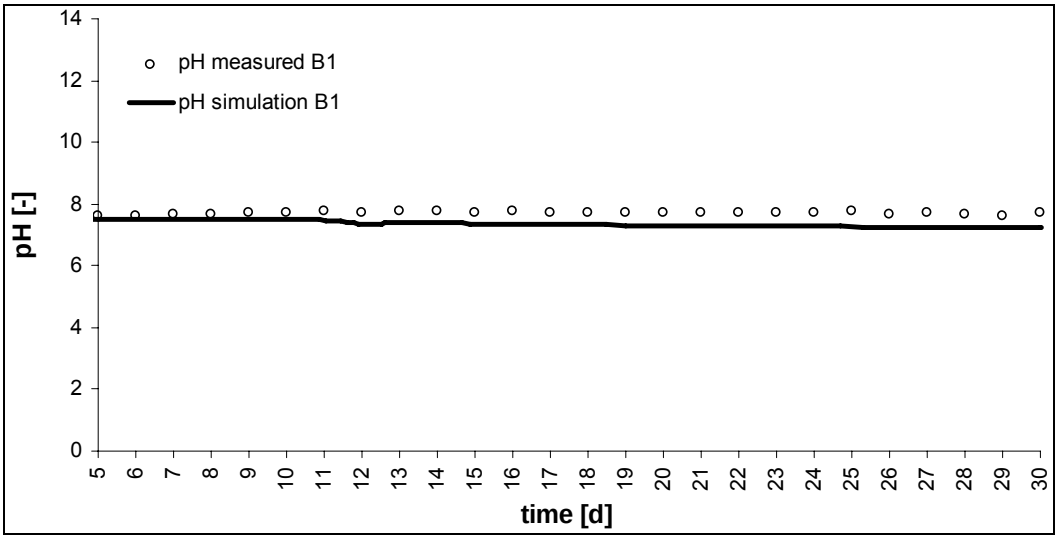

Figure C-5 Simulation results vs. measured values of pH for manure

D APPENDIX FOR PAPER (D)

COMPARISON OF BIOGAS PLANT START-UP PROCEDURES

In the following, supplementary information and data for paper (D) is given. These values were primarily used for the setup and calibration of the numerical models as described in the paper.

D.1 MEASURED RESULTS

Table D-1 Feeding characteristics of inoculum and manure

	Sampling Date	COD_{tot}	COD_x	COD_{sol}	N_{tot}	NH_4-N	C_{tot}	TS	pH
		[mg/L]	[mg/L]	[mg/L]	[mg/L]	[mg/L]	[mg/L]	[%]	[-]
Inoculum	24. Oct.	49589	37800	11789	1431	2232	17844	4.9	8.7
Manure	24. Oct.	31425	17745	13680	883	871	11861	3.2	8.3
Manure	12. Nov.	28616	20221	8395	1128	1123	13133	3.6	8.4
Manure	20. Nov.	42529	28742	13787	1647	1037	18850	4.8	8.3
Manure	22. Nov.	44119	30367	13752	1603	1111	18000	5.0	8.5

Table D-2 Characteristics of digested substrates

A1										
15 L inoculum + 60 L water || low-load feeding with manure || constant temperature 37°C										
Day	TS	VS	COD_{tot}	COD_{sol}	COD_x	NH_4-N	N_{tot}	C_{tot}	Alkalinity	org. Acids
	[%]	[% TS]	[mg/L]	[mg/L]	[mg/L]	[mg/L]	[mg/L]	[mg/L]	[mmol H^+-equ./L]	[mg/L]
0	1.0	66.7	6474	2188	4286	414	267	3307	46	866
4	1.1	67.6	7287	2219	5068	450	291	3267	53	337
7	1.0	63.6	10082	2194	7888	461	309	3347	55	315
11	1.2	64.0	10874	2416	8459	531	264	3387	62	424
14	1.2	62.2	9563	2751	6812	680	348	3833	68	435
18	1.3	57.4	11998	3183	8815	680	600	4953	83	474
21	1.6	59.6	12914	3609	9305	709	568	5750	94	663
25	2.0	63.5	23645	4860	18785	824	910	7905	111	809
28	2.5	65.8	20523	5631	14892	941	1010	10100	113	756
32	3.4	66.5	26574	6950	19625	1195	1169	12400	159	1238
35	3.5	64.3	32155	6584	25571	1325	1190	13650	162	975
39	3.6	65.8	27312	7409	19904	1226	1148	13300	172	1025

Table D-2 (continued)

A2

75 L manure || no feeding || fast temperature increase

Day	TS	VS	COD_{tot}	COD_{sol}	COD_x	NH_4-N	N_{tot}	C_{tot}	Alkalinity	org. Acids
	[%]	[% TS]	[mg/L]	[mg/L]	[mg/L]	[mg/L]	[mg/L]	[mg/L]	[mmol H^+-equ./L]	[mg/L]
0	2.7	67.2	17220	6826	10394	788	761	9860	114	1895
4	2.9	69.5	19418	6598	12821	983	688	9557	115	1960
7	3.7	75.7	19979	5746	14234	815	674	9350	117	1257
11	2.6	64.4	17289	5210	12079	891	606	8267	120	908
14	2.6	62.5	17270	5169	12101	866	621	8090	126	875
18	3.1	65.3	18529	4977	13552	920	957	11933	129	778
21	3.1	63.9		6501	-6501	891	959	11500	129	908
25	3.0	65.0	30412	8858	21555	1019	1100	11050	144	2052
28	3.5	66.4	31280	11685	19595	1093	1296	13100	153	3695
32	5.1	71.6	35586	12273	23313	1249	1510	18900	169	4206
35	4.7	70.7	36590	10665	25925	1283	1421	19100	171	3137
39	4.8	69.9	30835	7889	22947	1222	1399	20350	186	2186

Table D-2 (continued)

B1

15 L inoculum + 60 L water || high-load feeding with manure || constant temperature 37°C

Day	TS	VS	COD_{tot}	COD_{sol}	COD_x	NH_4-N	N_{tot}	C_{tot}	Alkalinity	org. Acids
	[%]	[% TS]	[mg/L]	[mg/L]	[mg/L]	[mg/L]	[mg/L]	[mg/L]	[mmol H^+-equ./L]	[mg/L]
0	1.4	64.8	8762	2447	6315	508	398	4404	53	346
4	1.4	63.5	9020	2311	6709	587	443	4947	59	346
7	1.5	62.6	10665	2240	8425	592	418	4850	62	381
11	1.6	61.4	11111	2534	8578	637	475	5023	72	478
14	1.8	62.0	11783	2780	9003	680	470	5660	81	477
18	2.0	59.9	19888	3447	16441	770	712	6870	99	612
21	2.4	64.0	15621	4566	11055	814	769	8427	113	890
25	3.3	65.9	32810	7497	25313	1004	1147	12400	143	1986
28	4.2	66.6	33045	10970	22075	1107	1451	16200	159	3080
32	4.6	69.8	36160	11426	24735	1238	1458	17550	177	2847
35	4.4	67.3	37165	8751	28414	1280	1373	15900	183	1768
39	4.2	66.2	31168	7316	23852	1186	1316	15850	194	1465

Table D-2 (continued)

B2										
75 L manure || no feeding || slow temperature increase										
Day	TS	VS	COD_{tot}	COD_{sol}	COD_x	NH_4-N	N_{tot}	C_{tot}	Alkalinity	org. Acids
	[%]	[% TS]	[mg/L]	[mg/L]	[mg/L]	[mg/L]	[mg/L]	[mg/L]	[mmol H^+-equ./L]	[mg/L]
0	3.7	63.1	26295	6852	19443	947	1032	11900	126	1678
4	3.6	62.6	25212	6534	18678	943	1002	12133	127	1821
7	3.4	61.8	24812	5574	19238	1006	959	12167	129	1440
11	3.4	60.4	25153	5382	19771	1094	974	11267	134	1192
14	3.5	62.0	22015	5390	16626	1069	951	11767	137	975
18	3.3	60.3	30566	5188	25378	1105	1098	11533	141	889
21	3.3	59.5	31024	5952	25072	1192	1095	11300	141	995
25	3.4	62.8	24122	6137	17985	1096	1168	11400	146	1219
28	3.6	64.0	26287	6813	19474	1130	1190	12600	153	1455
32	3.8	65.4	27907	7020	20887	1197	1197	13200	163	1514
35	3.5	61.9	26318	6912	19406	1253	1220	14550	168	1083
39	3.5	62.5	25566	6530	19036	1195	1135	13150	170	1081

Table D-3 Biogas production, pH and gas quality of digested substrates in lab experiments

A1									
15 L inoculum + 60 L water || low-load feeding with manure || constant temperature 37°C									
day	gas production [L/d]	pH [-]	CH_4 [%]	CO_2 [%]	day	gas production [L/d]	pH [-]	CH_4 [%]	CO_2 [%]
0	0.00	8.1			21	7.12	7.5	61.8	37.2
1	0.28	7.9			22	8.96	7.5	61.0	37.9
2	0.88	7.8			23	9.94	7.6	61.1	37.7
3	0.56	7.7			24	14.18	7.6	62.6	36.3
4	1.38	7.6			25	17.80	7.8	63.1	35.8
5	1.61	7.6			26	22.09	7.6	63.3	35.7
6	2.01	7.5			27	23.57	7.6	63.2	35.8
7	2.08	7.5			28	22.83	7.6	63.0	35.9
8	3.89	7.5	70.4	28.3	29	21.51	7.7	63.6	35.4
9	3.41	7.4			30	25.54	7.6	63.0	36.0
10	3.62	7.4			31	28.37	7.7	62.5	36.5
11	3.25	7.4	67.2	31.7	32	35.28	7.7	64.5	34.4
12	3.84	7.4			33	36.48	7.8	65.5	33.5
13	3.14	7.4	65.4	33.5	34	28.18	7.7	65.6	33.4
14	3.70	7.4	64.1	34.8	35	24.24	7.8	65.6	33.4
15	4.88	7.4	62.4	36.5	36	21.01	7.8	65.6	33.4
16	5.00	7.5	62.9	36.0	37	17.11	7.7		
17	5.91	7.4	62.5	36.5	38	18.05	7.8	65.9	33.1
18	6.71	7.5	61.7	37.2	39	15.38	7.8	65.3	33.7
19	6.00	7.5	62.0	36.9	40	13.35	7.9	65.2	33.7
20	6.59	7.5	61.8	37.2	41	0.98	7.8	64.1	34.5

Table D-3 (continued)

A2

75 L manure || no feeding || fast temperature increase

day	gas production [L/d]	pH [-]	CH_4 [%]	CO_2 [%]	day	gas production [L/d]	pH [-]	CH_4 [%]	CO_2 [%]
0	0.00	7.8			21	7.62	7.5	59.4	39.6
1	0.00	7.8			22	13.08	7.6	57.9	41.1
2	0.00	7.7			23	16.85	7.6	58.2	40.7
3	0.00	7.6			24	21.42	7.6	60.4	38.5
4	0.00	7.6			25	23.01	7.6	60.5	38.4
5	0.00	7.6			26	25.96	7.5	58.2	40.7
6	0.58	7.5			27	29.36	7.5	55.1	43.8
7	4.77	7.7			28	31.92	7.4	52.2	46.7
8	6.70	7.7	71.9	27.0	29	33.23	7.5	52.6	46.4
9	11.21	7.7			30	37.78	7.5	52.3	46.7
10	11.65	7.7			31	37.41	7.5	51.3	47.8
11	9.95	7.6	70.2	28.8	32	36.20	7.5	53.9	45.0
12	9.12	7.6			33	43.62	7.7	53.7	45.4
13	11.09	7.7	64.7	34.3	34	49.42	7.8	57.2	41.8
14	12.77	7.6	61.5	37.6	35	51.92	7.7	61.6	37.4
15	11.77	7.7	60.1	39.0	36	49.09	7.8	62.1	36.9
16	8.24	7.9	60.2	38.8	37	34.68	7.8		
17	7.09	7.8	60.4	38.6	38	39.48	7.8	61.6	37.4
18	6.48	7.6	60.2	38.8	39	35.91	7.8	59.6	39.4
19	7.19	7.7	60.0	39.0	40	31.26	7.8	59.1	39.9
20	6.69	7.7	59.8	39.2	41	26.52	7.8	59.0	40.0

Table D-3 (continued)

B1

15 L inoculum + 60 L water || high-load feeding with manure || constant temperature 37°C

day	gas production [L/d]	pH [-]	CH_4 [%]	CO_2 [%]	day	gas production [L/d]	pH [-]	CH_4 [%]	CO_2 [%]
0	0.00	7.9			21	15.19	7.6	60.9	38.0
1	0.00	7.8			22	16.35	7.6	62.4	36.5
2	0.00	7.7			23	16.23	7.7	64.5	34.4
3	0.00	7.6			24	19.79	7.6	64.9	34.0
4	0.00	7.6			25	21.97	7.6	64.2	34.7
5	0.00	7.5			26	25.13	7.6	62.4	36.5
6	3.11	7.6			27	34.04	7.5	60.9	38.1
7	2.34	7.4			28	31.53	7.6	60.8	38.1
8	2.50	7.4	66.6	32.2	29	32.81	7.6	63.3	35.7
9	3.29	7.4			30	34.46	7.7	64.4	34.6
10	4.62	7.4			31	39.29	7.7	63.3	35.7
11	6.39	7.4	63.3	35.6	32	32.52	7.8	64.8	34.2
12	7.49	7.4			33	35.40	7.9	65.6	33.4
13	7.33	7.4	63.1	35.8	34	27.73	7.8	64.0	35.0
14	7.74	7.4	61.8	37.2	35	24.14	7.7	61.2	37.7
15	7.95	7.4	60.1	38.8	36	24.44	7.8	60.3	38.7
16	9.29	7.5	60.7	38.2	37	16.41	7.8		
17	10.12	7.5	60.1	38.8	38	16.96	7.8	59.9	39.1
18	10.87	7.5	60.1	38.8	39	18.42	7.8	61.0	38.0
19	12.02	7.5	60.4	38.5	40	16.19	7.9	62.7	36.3
20	13.68	7.5	61.4	37.5	41	0.83	7.8	62.6	36.4

Table D-3 (continued)

B2

75 L manure || no feeding || slow temperature increase

day	gas production [L/d]	pH [-]	CH_4 [%]	CO_2 [%]	day	gas production [L/d]	pH [-]	CH_4 [%]	CO_2 [%]
0	0.00	7.8			21	6.27	7.5	60.9	38.1
1	3.14	7.8			22	9.62	7.6	59.5	39.4
2	4.05	7.7			23	12.41	7.6	58.5	40.3
3	4.80	7.6			24	16.76	7.6	59.8	39.0
4	5.89	7.6			25	20.68	7.7	60.8	38.0
5	5.33	7.5			26	24.31	7.7	61.1	37.7
6	7.13	7.6			27	27.09	7.7	61.5	37.4
7	7.37	7.6			28	28.85	7.7	62.0	36.9
8	7.09	7.6	71.1	27.8	29	28.05	7.7	62.5	36.4
9	8.99	7.8			30	26.94	7.7	63.6	35.4
10	9.24	7.7			31	27.18	7.7	61.0	37.9
11	8.44	7.6	72.1	26.9	32	28.29	7.8	61.9	37.1
12	6.17	7.6			33	25.15	7.8	62.2	36.8
13	7.19	7.7	70.4	28.6	34	21.76	7.8	62.6	36.4
14	7.50	7.6	68.6	30.4	35	18.26	7.8	62.7	36.3
15	7.61	7.6	66.3	32.7	36	18.14	7.8	59.7	39.3
16	7.70	7.7	65.9	33.1	37	12.84	7.7		
17	6.92	7.8	64.7	34.3	38	13.32	7.7	58.9	40.1
18	5.71	7.5	63.4	35.6	39	12.66	7.7	57.9	41.1
19	6.28	7.6	61.7	37.3	40	8.90	7.8	57.4	41.6
20	6.47	7.6	61.3	37.7	41	9.40		56.7	42.3

D.2 MODEL CALIBRATION

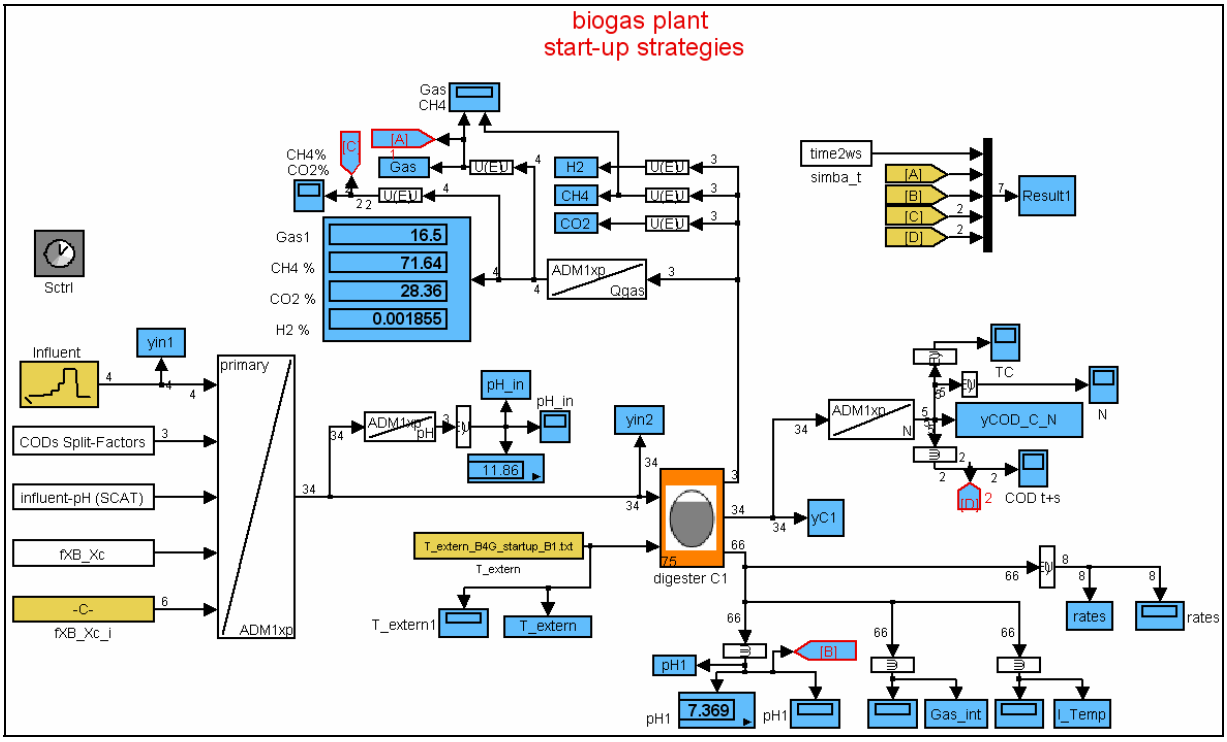

Figure D-1 Simulation model of a lab-scale digestion reactor edited in the SIMBA environment

Table D-4 Fraction balance

A1

15 L inoculum + 60 L water || low-load feeding with manure || constant temperature 37°C

Feed							**After disintegration**					
fraction	COD	TKN		TC	TKN	TC	f_dis	fXB_XC_i	fi_XB	COD	TKN	TC
	kg COD/m³	k mole N/ kg COD	%	k mole C/kg COD	g/m³	g/m³			= fXB_XC*fXB_XC_i	kg COD/m³	g/m³	g/m³
SSU	6.729			0.0313		2527.3				6.729		2527.3
SAA	3.461	0.0072	10%	0.0300	346.4	1245.8				3.461	346.4	1245.8
SFA	1.346			0.0217		350.4				1.346		350.4
SVA				0.0240						0.000		
SBU				0.0250						0.000		
SPRO				0.0268						0.000		
SAC				0.0313						0.000		
SH2												
SCH4				0.0156								
SIC				1.0000								
SIN		1.0000	100%		1035.0						1035.0	
Si	0.868	0.0014	2%	0.0300	17.0	312.6	0.05			2.082	40.8	749.4
Xc	24.269	0.0022	3%	0.0299	740.1	8710.0						
Xch				0.0313			0.35			8.494		3190.4
Xpr		0.0071	10%	0.0300			0.18			4.368	436.7	1572.6
Xli				0.0220			0.07			1.699		448.5
XSU		0.0057	8%	0.0313		fXB_Xc:	0.01	0.102	0.00102	0.025	2.0	9.3
XAA		0.0057	8%	0.0313				0.124	0.00124	0.030	2.4	11.3
XFA		0.0057	8%	0.0313				0.143	0.00143	0.035	2.8	13.0
XC4		0.0057	8%	0.0313				0.136	0.00136	0.033	2.6	12.4
XPRO		0.0057	8%	0.0313				0.090	0.00090	0.022	1.7	8.2
XAC		0.0057	8%	0.0313				0.335	0.00335	0.081	6.5	30.5
XH2		0.0057	8%	0.0313				0.071	0.00071	0.017	1.4	6.5
XI		0.0014	2%	0.0300			0.24			5.825	114.2	2096.8
XP		0.0043	6%	0.0300			0.10			2.427	146.1	873.7
sum	36.672				2138.5	13146.2	1	1		36.672	2138.5	13146.2
measured	36.672				1315.4	15461.0				36.672	1315.4	15461.0

Table D-4 (continued)

A2

75 L manure || no feeding || fast temperature increase

Feed							**After disintegration**					
fraction	COD	TKN		TC	TKN	TC	f_dis	fXB_XC_i	fi_XB	COD	TKN	TC
	kg COD/m³	k mole N/ kg COD	%	k mole C/kg COD	g/m³	g/m³			= fXB_XC*fXB_XC_i	kg COD/m³	g/m³	g/m³
SSU	3.710			0.0313		1393.5				3.710		1393.5
SAA	1.908	0.0072	10%	0.0300	191.0	686.9				1.908	191.0	686.9
SFA	0.742			0.0217		193.2				0.742		193.2
SVA	0.000			0.0240						0.000		
SBU	0.000			0.0250						0.000		
SPRO	0.000			0.0268						0.000		
SAC	0.000			0.0313						0.000		
SH2												
SCH4				0.0156								
SIC				1.0000								
SIN		1.0000	100%		871.2						871.2	
Si	0.479	0.0014	2%	0.0300	9.4	172.3	0.05			1.225	24.0	440.9
Xc	14.919	0.0022	3%	0.0299	454.9	5354.2						
Xch				0.0313			0.35			5.222		1961.2
Xpr		0.0071	10%	0.0300			0.18			2.685	268.4	966.7
Xli				0.0220			0.07			1.044		275.7
XSU		0.0057	8%	0.0313		fXB_Xc:	0.01	0.102	0.00102	0.015	1.2	5.7
XAA		0.0057	8%	0.0313				0.124	0.00124	0.018	1.5	6.9
XFA		0.0057	8%	0.0313				0.143	0.00143	0.021	1.7	8.0
XC4		0.0057	8%	0.0313				0.136	0.00136	0.020	1.6	7.6
XPRO		0.0057	8%	0.0313				0.090	0.00090	0.013	1.1	5.0
XAC		0.0057	8%	0.0313				0.335	0.00335	0.050	4.0	18.8
XH2		0.0057	8%	0.0313				0.071	0.00071	0.011	0.8	4.0
XI		0.0014	2%	0.0300			0.24			3.580	70.2	1289.0
XP		0.0043	6%	0.0300			0.10			1.492	89.8	537.1
sum	21.757				1526.5	7800.2	1.00	1.000		21.757	1526.5	7800.2
measured	31.425				883.4	11860.6				31.425	883.4	11860.6

Table D-4 (continued)

B1

15 L inoculum + 60 L water || high-load feeding with manure || constant temperature 37°C

Feed							**After disintegration**					
fraction	COD	TKN		TC	TKN	TC	f_dis	fXB_XC_i	fi_XB	COD	TKN	TC
	kg COD/m³	k mole N/ kg COD	%	k mole C/kg COD	g/m³	g/m³			= fXB_XC*fXB_XC_i	kg COD/m³	g/m³	g/m³
SSU	6.729			0.0313		2527.3				6.729		2527.3
SAA	3.461	0.0072	10%	0.0300	346.4	1245.8				3.461	346.4	1245.8
SFA	1.346			0.0217		350.4				1.346		350.4
SVA				0.0240		0.0				0.000		
SBU				0.0250		0.0				0.000		
SPRO				0.0268		0.0				0.000		
SAC				0.0313		0.0				0.000		
SH2												
SCH4				0.0156		0.0						
SIC				1.0000		0.0						
SIN		1.0000	100%		1035.0						1035.0	
Si	0.868	0.0014	2%	0.0300	17.0	312.6	0.05			2.082	40.8	749.4
Xc	24.269	0.0022	3%	0.0299	740.1	8710.0						
Xch				0.0313			0.35			8.494		3190.4
Xpr		0.0071	10%	0.0300			0.18			4.368	436.7	1572.6
Xli				0.0220			0.07			1.699		448.5
XSU		0.0057	8%	0.0313		fXB_Xc:	0.01	0.102	0.00102	0.025	2.0	9.3
XAA		0.0057	8%	0.0313				0.124	0.00124	0.030	2.4	11.3
XFA		0.0057	8%	0.0313				0.143	0.00143	0.035	2.8	13.0
XC4		0.0057	8%	0.0313				0.136	0.00136	0.033	2.6	12.4
XPRO		0.0057	8%	0.0313				0.090	0.00090	0.022	1.7	8.2
XAC		0.0057	8%	0.0313				0.335	0.00335	0.081	6.5	30.5
XH2		0.0057	8%	0.0313				0.071	0.00071	0.017	1.4	6.5
XI		0.0014	2%	0.0300			0.24			5.825	114.2	2096.8
XP		0.0043	6%	0.0300			0.10			2.427	146.1	873.7
sum	36.672				2138.5	13146.2	1.00	1.000		36.672	2138.5	13146.2
measured	36.672				1315.4	15461.0				36.672	1315.4	15461.0

Table D-4 (continued)

B2

75 L manure || no feeding || slow temperature increase

Feed							**After disintegration**					
fraction	COD	TKN		TC	TKN	TC	f_dis	fXB_XC_i	fi_XB	COD	TKN	TC
	kg COD/m³	k mole N/ kg COD	%	k mole C/kg COD	g/m³	g/m³			= fXB_XC*fXB_XC_i	kg COD/m³	g/m³	g/m³
SSU	3.710			0.0313		1393.5				3.710		1393.5
SAA	1.908	0.0072	10%	0.0300	191.0	686.9				1.908	191.0	686.9
SFA	0.742			0.0217		193.2				0.742		193.2
SVA				0.0240		0.0				0.000		
SBU				0.0250		0.0				0.000		
SPRO				0.0268		0.0				0.000		
SAC				0.0313		0.0				0.000		
SH2												
SCH4				0.0156		0.0						
SIC				1.0000		0.0						
SIN		1.0000	100%		871.2						871.2	
Si	0.479	0.0014	2%	0.0300	9.4	172.3	0.05			1.225	24.0	440.9
Xc	14.919	0.0022	3%	0.0299	454.9	5354.2						
Xch				0.0313			0.35			5.222		1961.2
Xpr		0.0071	10%	0.0300			0.18			2.685	268.4	966.7
Xli				0.0220			0.07			1.044		275.7
XSU		0.0057	8%	0.0313		fXB_Xc:	0.01	0.102	0.00102	0.015	1.2	5.7
XAA		0.0057	8%	0.0313				0.124	0.00124	0.018	1.5	6.9
XFA		0.0057	8%	0.0313				0.143	0.00143	0.021	1.7	8.0
XC4		0.0057	8%	0.0313				0.136	0.00136	0.020	1.6	7.6
XPRO		0.0057	8%	0.0313				0.090	0.00090	0.013	1.1	5.0
XAC		0.0057	8%	0.0313				0.335	0.00335	0.050	4.0	18.8
XH2		0.0057	8%	0.0313				0.071	0.00071	0.011	0.8	4.0
XI		0.0014	2%	0.0300			0.24			3.580	70.2	1289.0
XP		0.0043	6%	0.0300			0.10			1.492	89.8	537.1
sum	21.757				1526.5	7800.2	1.00	1.000		21.757	1526.5	7800.2
measured	31.425				883.4	11860.6				31.425	883.4	11860.6

Table D-5 Calibrated uniform parameter set for A1, A2, B1 and B2

Name	Value	Name	Value	Name	Value
fSI_XC	0.05	Yaa	0.15	pHUL_ac	7
dummy_fXI_XC	0.23	fH2_FA	0.3	pHLL_ac	6
fCH_XC	0.35	Yfa	0.0454	km_h2	33.3
fPR_XC	0.18	fH2_VA	0.15	KS_h2	1.00E-06
fLI_XC	0.07	fPRO_VA	0.54	pHUL_h2	8
fXP_XC	0.1	fH2_BU	0.2	pHLL_h2	4.5
N_Xc	0.0022	Yc4	0.06	kdec_Xsu	0.7
N_I	0.0014	fH2_PRO	0.43	kdec_Xaa	0.8
N_aa	0.0072	Ypro	0.04	kdec_Xfa	0.06
C_Xc	0.0299	C_Sch4	0.0156	kdec_Xc4	0.06
C_SI	0.03	Yac	0.025	kdec_Xpro	0.02
C_Xch	0.0313	Yh2	0.06	kdec_Xac	0.02
C_Xpr	0.03	kdis	0.1	kdec_Xh2	0.3
C_Xli	0.022	khyd_ch	0.31	Kw	2.08E-14
C_XI	0.03	khyd_pr	0.31	Kava	1.35E-05
dummy_C_su	0.0313	khyd_li	0.31	Kabu	1.51E-05
dummy_C_aa	0.03	KS_IN	1.00E-04	Kapro	1.32E-05
fFA_Xli	0.95	km_su	8	Kaac	1.74E-05
C_Sfa	0.0217	KS_su	0.5	Kaco2	5.10E-07
fH2_SU	0.19	pHUL_a	5.5	Kain	1.50E-09
fBU_SU	0.0772	pHLL_a	4.5	kA_Bva	1.00E+08
fPRO_SU	0.1522	km_aa	26.66	kA_Bbu	1.00E+08
dummy_fAC_SU	0.5806	KS_aa	0.05	kA_Bpro	1.00E+08
N_XB	0.08/14	km_fa	13.2	kA_Bac	1.00E+08
C_Sbu	0.025	KS_fa	1	kA_Bco2	1.00E+08
C_Spro	0.0268	KI_H2_fa	3.00E-06	kA_Bin	1.00E+08
C_Sac	0.0313	km_c4	10	klaH2	200
C_XB	0.0313	KS_c4	0.5	klaCH4	200
Ysu	0.1	KI_H2_c4	1.00E-05	klaCO2	200
fH2_AA	0.06	km_pro	13	KH_CO2	1/(0.0271*0.08314*(T+273.15))
fVA_AA	0.1531	KS_pro	0.5	KH_CH4	1/(0.00116*0.08314*(T+273.15))
fBU_AA	0.173	KI_H2_pro	3.50E-06	KH_H2	1/(7.38e-4*0.08314*(T+273.15))
fPRO_AA	0.0333	km_ac	30	C_Xp	0.03
dummy_fAC_AA	0.5806	KS_ac	0.75	N_Xp	0.06/14
C_Sva	0.024	KI_NH3	0.0013	fP	0.4
				Parameter k1 for rel. methanogenic activity function	0.75
				Parameter a1 for rel. methanogenic activity function	0.15
				Parameter k2 for rel. methanogenic activity function	0.14
				Parameter a2 for rel. methanogenic activity function	0.3
				Parameter T_0 for rel. methanogenic activity function	30

Table D-6 Influent files for start-up simulations

A1									
15 L inoculum + 60 L water || low-load feeding with manure || constant temperature 37°C									
Day	**COD_x**	**COD_s**	**NH_4-N**	**Q**	**Day**	**COD_x**	**COD_s**	**NH_4-N**	**Q**
	g/m³	g/m³	g/m³	m³/d		g/m³	g/m³	g/m³	m³/d
0	17745	13680	871	1	21	20221	8395	1123	6
1	17745	13680	871	1	22	20221	8395	1123	6
2	17745	13680	871	1	23	28742	13787	1037	6
3	17745	13680	871	1	24	28742	13787	1037	6
4	17745	13680	871	1	25	28742	13787	1037	6
5	17745	13680	871	1	26	28742	13787	1037	6
6	17745	13680	871	1	27	28742	13787	1037	6
7	17745	13680	871	2	28	30367	13752	1111	6
8	17745	13680	871	2	29	30367	13752	1111	6
9	17745	13680	871	2	30	30367	13752	1111	6
10	17745	13680	871	2	31	30367	13752	1111	6
11	17745	13680	871	2	32	30367	13752	1111	6
12	17745	13680	871	2	33	30367	13752	1111	6
13	17745	13680	871	2	34	30367	13752	1111	6
14	17745	13680	871	3	35	30367	13752	1111	6
15	17745	13680	871	3	36	30367	13752	1111	6
16	17745	13680	871	3	37	30367	13752	1111	6
17	17745	13680	871	3	38	30367	13752	1111	6
18	20221	8395	1123	3	39	30367	13752	1111	6
19	20221	8395	1123	3	40	30367	13752	1111	0
20	20221	8395	1123	3	41	30367	13752	1111	0

Table D-6 (continued)

A2									
75 L manure || no feeding || fast temperature increase									
Day	**COD_x**	**COD_s**	**NH_4-N**	**Q**	**Day**	**COD_x**	**COD_s**	**NH_4-N**	**Q**
	g/m³	g/m³	g/m³	m³/d		g/m³	g/m³	g/m³	m³/d
0	14919	6839	871	0	21	14919	6839	871	0
1	14919	6839	871	0	22	14919	6839	871	0
2	14919	6839	871	0	23	14919	6839	871	0
3	14919	6839	871	0	24	14919	6839	871	0
4	14919	6839	871	0	25	14919	6839	871	0
5	14919	6839	871	0	26	14919	6839	871	0
6	14919	6839	871	0	27	14919	6839	871	0
7	14919	6839	871	0	28	30367	13752	871	24
8	14919	6839	871	0	29	30367	13752	871	24
9	14919	6839	871	0	30	30367	13752	871	24
10	14919	6839	871	0	31	30367	13752	871	24
11	14919	6839	871	0	32	30367	13752	871	0
12	14919	6839	871	0	33	30367	13752	871	0
13	14919	6839	871	0	34	30367	13752	871	0
14	14919	6839	871	0	35	30367	13752	871	0
15	14919	6839	871	0	36	30367	13752	871	0
16	14919	6839	871	0	37	30367	13752	871	0
17	14919	6839	871	0	38	30367	13752	871	0
18	14919	6839	871	0	39	30367	13752	871	0
19	14919	6839	871	0	40	30367	13752	871	0
20	14919	6839	871	0	41	30367	13752	871	0

Table D-6 (continued)

B1

15 L inoculum + 60 L water || high-load feeding with manure || constant temperature 37°C

Day	COD_x	COD_s	NH_4-N	Q	Day	COD_x	COD_s	NH_4-N	Q
	g/m³	g/m³	g/m³	m³/d		g/m³	g/m³	g/m³	m³/d
0	17745	13680	871.2	0.75	21	20221	8395	1123.2	12
1	17745	13680	871.2	0.75	22	20221	8395	1123.2	12
2	17745	13680	871.2	0.75	23	28742	13787	1036.8	12
3	17745	13680	871.2	0.75	24	28742	13787	1036.8	24
4	17745	13680	871.2	0.75	25	28742	13787	1036.8	24
5	17745	13680	871.2	1.5	26	28742	13787	1036.8	24
6	17745	13680	871.2	1.5	27	28742	13787	1036.8	24
7	17745	13680	871.2	1.5	28	30367	13752	1110.6	24
8	17745	13680	871.2	1.5	29	30367	13752	1110.6	24
9	17745	13680	871.2	1.5	30	30367	13752	1110.6	24
10	17745	13680	871.2	3	31	30367	13752	1110.6	24
11	17745	13680	871.2	3	32	30367	13752	1110.6	0
12	17745	13680	871.2	3	33	30367	13752	1110.6	0
13	17745	13680	871.2	3	34	30367	13752	1110.6	0
14	17745	13680	871.2	3	35	30367	13752	1110.6	0
15	17745	13680	871.2	6	36	30367	13752	1110.6	0
16	17745	13680	871.2	6	37	30367	13752	1110.6	0
17	17745	13680	871.2	6	38	30367	13752	1110.6	0
18	20221	8395	1123.2	6	39	30367	13752	1110.6	0
19	20221	8395	1123.2	6	40	30367	13752	1110.6	0
20	20221	8395	1123.2	12	41	30367	13752	1110.6	0

Table D-6 (continued)

B2

75 L manure || no feeding || slow temperature increase

Day	COD_x	COD_s	NH_4-N	Q	Day	COD_x	COD_s	NH_4-N	Q
	g/m³	g/m³	g/m³	m³/d		g/m³	g/m³	g/m³	m³/d
0	14919	6839	871	0	21	14919	6839	871	0
1	14919	6839	871	0	22	14919	6839	871	0
2	14919	6839	871	0	23	14919	6839	871	0
3	14919	6839	871	0	24	14919	6839	871	0
4	14919	6839	871	0	25	14919	6839	871	0
5	14919	6839	871	0	26	14919	6839	871	0
6	14919	6839	871	0	27	14919	6839	871	0
7	14919	6839	871	0	28	30367	13752	871	6
8	14919	6839	871	0	29	30367	13752	871	6
9	14919	6839	871	0	30	30367	13752	871	6
10	14919	6839	871	0	31	30367	13752	871	6
11	14919	6839	871	0	32	30367	13752	871	0
12	14919	6839	871	0	33	30367	13752	871	0
13	14919	6839	871	0	34	30367	13752	871	0
14	14919	6839	871	0	35	30367	13752	871	0
15	14919	6839	871	0	36	30367	13752	871	0
16	14919	6839	871	0	37	30367	13752	871	0
17	14919	6839	871	0	38	30367	13752	871	0
18	14919	6839	871	0	39	30367	13752	871	0
19	14919	6839	871	0	40	30367	13752	871	0
20	14919	6839	871	0	41	30367	13752	871	0

D.3 SIMULATION RESULTS

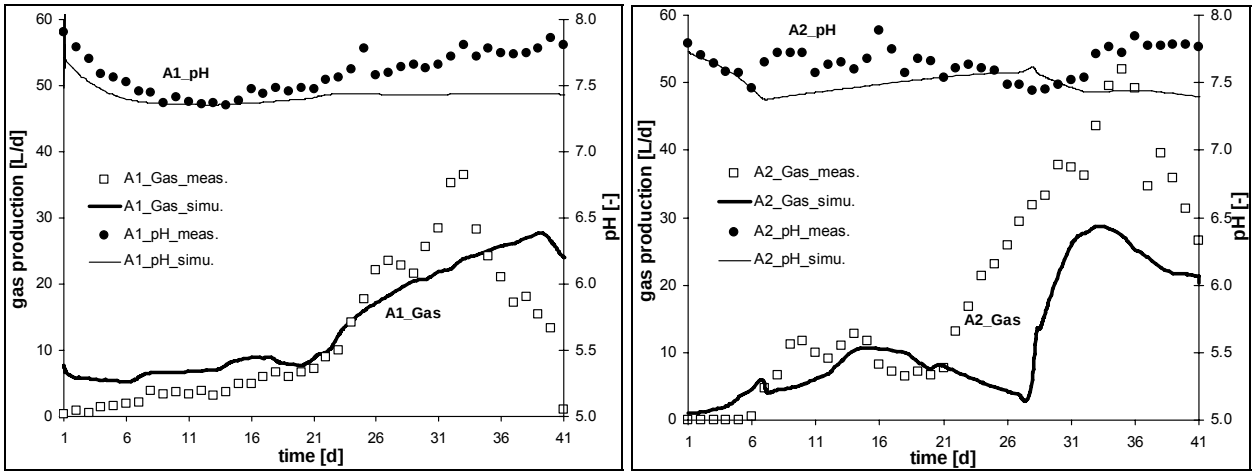

Figure D-2 A1 and A2 simulation results vs. measured values for biogas production and pH

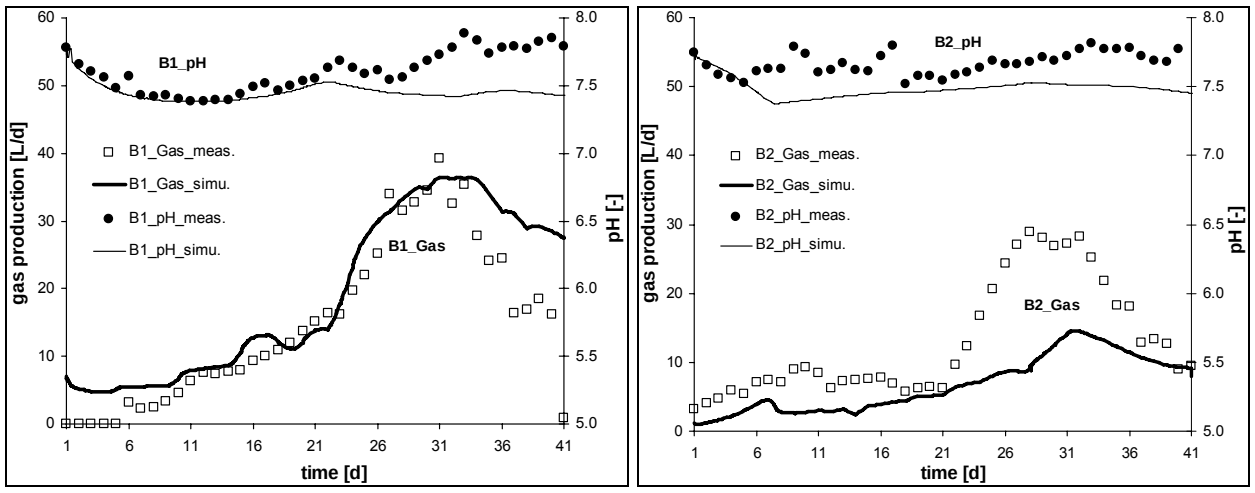

Figure D-3 B1 and B2 simulation results vs. measured values for biogas production and pH

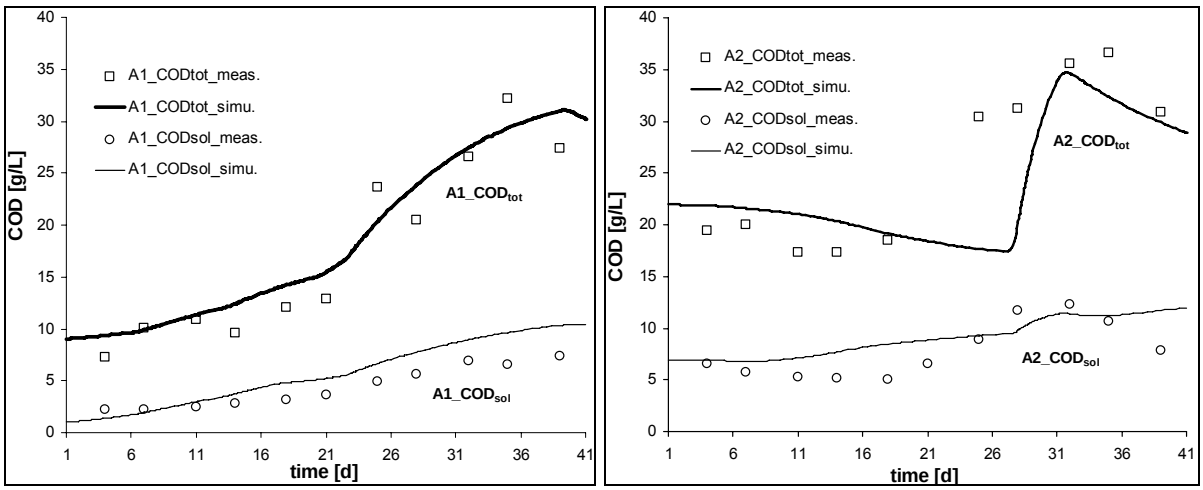

Figure D-4 A1 and A2 simulation results vs. measured values for total and soluble COD

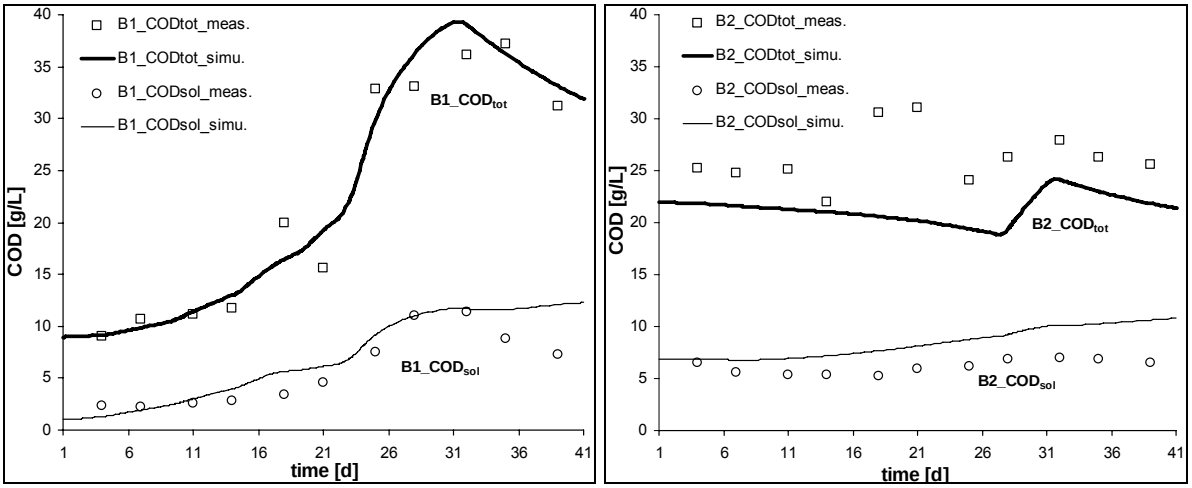

Figure D-5 B1 and B2 simulation results vs. measured values for total and soluble COD

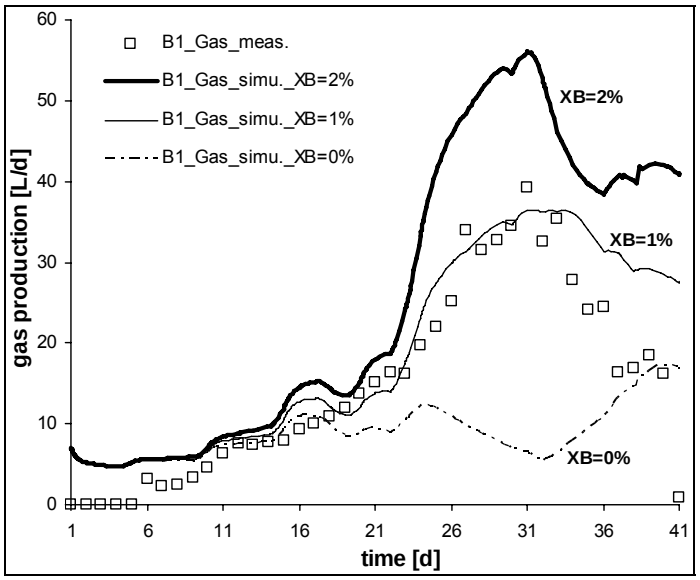

Figure D-6 B1 simulation results vs. measured values for biogas production at different fluxes of additional active biomass to account for incoming cattle-borne biomass (in % of particulate COD; see also *fXB_Xc* in fraction balances in Table D-4)

E APPENDIX FOR PAPER (E)

POPULATION DYNAMICS AT DIGESTER OVERLOAD CONDITIONS

In the following, supplementary information and data for paper (E) is given. These values were primarily used for the setup and calibration of the numerical models as described in the paper.

E.1 MEASURED RESULTS

Table E-1 TS, biogas production, gas quality and pH at WWTP Salzburg

day	TS[1]	gas prod.[2]	CH_4[2]	pH[3]	day	TS[1]	gas prod.[2]	CH_4[2]	pH[3]
	[g/L]	[m³/d]	[%]	[-]		[g/L]	[m³/d]	[%]	[-]
0	41	11100	60		28	42	6100	60	
1	36	10100	61		29	43	16000	60	
2	48	11600	60		30	36	5400	60	
3	43	10400	60		31	41	13000	60	
4	42	11100	60	7.4	32	44	10500	60	7.2
5	43	10900	61		33	43	9100	60	
6	43	9100	60		34		6800	58	
7	43	10100	59		35	44	1700	48	
8	51	11100	60		36	50	2900	43	
9	49	12400	60		37	43	4400	41	
10	43	10600	59		38	44	4200	40	
11	44	11700	59	7.3	39	46	3100	39	
12	41	11700	60		40	39	4400	38	6.9
13	44	11400	60		41	37	2600	36	
14	42	17000	59		42	37	1800	33	
15	47	5300	60		43	41	3300	33	
16	40	13600	60		44	40	3300	34	
17	38	12200	60		45	38	2500	35	
18	42	12600	60	7.4	46	38	300	38	6.4
19	42	19400	60		47	50	200	48	6.3
20	45	7400	60		48	43	5500	58	6.6
21	48		60		49	50	7200	57	6.8
22	41	10500	60		50	46	200	55	
23	45	5600	60		51	47	2900	51	
24	42	6100	60		52	52	6500	50	6.8
25	45	6500	60	7.4	53	47	9300	55	6.9
26	44	9100	60		54	52	8000	60	7.1
27	52	11500	60						

[1]TS calculated from effluents of high-rate and low-rate stage to thickener
[2]until day 34: average values of digester FT1 + FT2; from day 34 only FT2
[3]pH of digester FT2

E.2 MODEL CALIBRATION

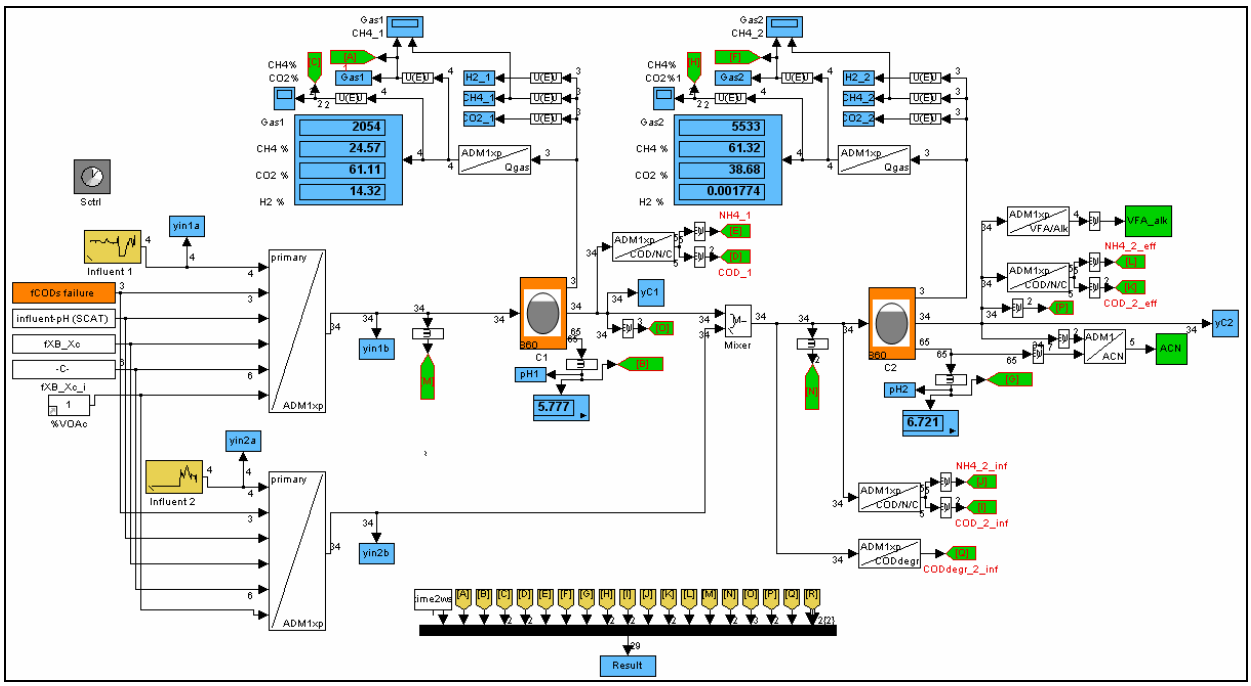

Figure E-1 Simulation model of WWTP Salzburg digesters edited in the SIMBA environment

Table E-2 Calibrated uniform parameter set for WWTP Salzburg

Name	Value	Name	Value	Name	Value
fSI_XC	0.016	Yaa	0.15	pHUL_ac	7
dummy_fXI_XC	0.101	fH2_FA	0.3	pHLL_ac	6
fCH_XC	0.165	Yfa	0.0454	km_h2	33.3
fPR_XC	0.144	fH2_VA	0.15	KS_h2	1.00E-06
fLI_XC	0.277	fPRO_VA	0.54	pHUL_h2	8
fXP_XC	0.297	fH2_BU	0.2	pHLL_h2	4.5
N_Xc	0.00247	Yc4	0.06	kdec_Xsu	0.7
N_I	0.02/14	fH2_PRO	0.43	kdec_Xaa	0.8
N_aa	0.1/14	Ypro	0.04	kdec_Xfa	0.06
C_Xc	0.028	C_Sch4	0.0156	kdec_Xc4	0.06
C_SI	0.03	Yac	0.025	kdec_Xpro	0.02
C_Xch	0.0313	Yh2	0.06	kdec_Xac	0.1305
C_Xpr	0.03	kdis	1	kdec_Xh2	0.3
C_Xli	0.022	khyd_ch	0.31	Kw	2.08E-14
C_XI	0.03	khyd_pr	0.31	Kava	1.35E-05
dummy_C_su	0.0313	khyd_li	0.31	Kabu	1.51E-05
dummy_C_aa	0.03	KS_IN	1.00E-04	Kapro	1.32E-05
fFA_Xli	0.95	km_su	30	Kaac	1.74E-05
C_Sfa	0.0217	KS_su	0.5	Kaco2	5.10E-07
fH2_SU	0.19	pHUL_a	5.5	Kain	1.50E-09
fBU_SU	0.0772	pHLL_a	4.5	kA_Bva	1.00E+08
fPRO_SU	0.1522	km_aa	26.66	kA_Bbu	1.00E+08
dummy_fAC_SU	0.5806	KS_aa	0.05	kA_Bpro	1.00E+08
N_XB	0.08/14	km_fa	13.2	kA_Bac	1.00E+08
C_Sbu	0.025	KS_fa	1	kA_Bco2	1.00E+08
C_Spro	0.0268	KI_H2_fa	3.00E-06	kA_Bin	1.00E+08
C_Sac	0.0313	km_c4	10	klaH2	200
C_XB	0.0313	KS_c4	0.5	klaCH4	200
Ysu	0.1	KI_H2_c4	1.00E-05	klaCO2	200
fH2_AA	0.06	km_pro	13	KH_CO2	1/(0.035*0.08314*(T+273.15))
fVA_AA	0.1531	KS_pro	0.5	KH_CH4	1/(0.0014*0.08314*(T+273.15))
fBU_AA	0.173	KI_H2_pro	3.50E-06	KH_H2	1/(7.8e-4*0.08314*(T+273.15))
fPRO_AA	0.0333	km_ac	20	C_Xp	0.03
dummy_fAC_AA	0.5806	KS_ac	0.75	N_Xp	0.06/14
C_Sva	0.024	KI_NH3	0.0013	fP	0.4

Table E-3 Influent file for WWTP Salzburg simulations

digester FT1									
Day	COD_x	COD_s	TKN	Q	Day	COD_x	COD_s	NH_4-N	Q
	g/m³	g/m³	g/m³	m³/d		g/m³	g/m³	g/m³	m³/d
0	54944	3000	2039.8	593	28	50321	3000	1879.9	517
1	45920	3000	1727.8	617	29	46823	3000	1759.0	517
2	51768	3000	1930.0	618	30	40972	3000	1556.7	517
3	50502	3000	1886.2	618	31	46232	3000	1738.5	520
4	51277	3000	1913.0	618	32	47966	3000	1798.5	517
5	49000	3000	1834.3	618	33	43271	3000	1636.2	623
6	50082	3000	1871.7	618	34	25103	3000	1007.9	778
7	52698	3000	1962.1	541	35	39084	3000	1491.4	0
8	59249	3000	2188.7	602	36	45699	3000	1720.1	0
9	57710	3000	2135.5	618	37	41663	3000	1580.6	0
10	53986	3000	2006.7	618	38	45780	3000	1722.9	0
11	53315	3000	1983.5	618	39	50659	3000	1891.6	0
12	52006	3000	1938.2	618	40	39761	3000	1514.8	5
13	60899	3000	2245.7	589	41	36709	3000	1409.2	6
14	61427	3000	2264.0	517	42	39137	3000	1493.2	96
15	57805	3000	2138.7	517	43	38527	3000	1472.1	212
16	53610	3000	1993.7	518	44	36753	3000	1410.7	275
17	51821	3000	1931.8	517	45	50114	3000	1872.8	526
18	56366	3000	2089.0	516	46	41817	3000	1585.9	459
19	49202	3000	1841.3	643	47	70819	3000	2588.8	719
20	49794	3000	1861.7	720	48	49621	3000	1855.7	702
21	52755	3000	1964.1	628	49	45886	3000	1726.6	702
22	53242	3000	1980.9	570	50	44595	3000	1681.9	702
23	56457	3000	2092.1	572	51	44857	3000	1691.0	355
24	56303	3000	2086.8	554	52	50906	3000	1900.2	502
25	55564	3000	2061.2	518	53	77515	3000	2820.3	823
26	56868	3000	2106.3	524	54	50974	3000	1902.5	471
27	62212	3000	2291.1	496					

Table E-3 (continued)

diegster FT2									
Day	COD_x	COD_s	TKN	Q	Day	COD_x	COD_s	NH_4-N	Q
	g/m³	g/m³	g/m³	m³/d		g/m³	g/m³	g/m³	m³/d
0	0	0	0	0	28	0	0	0	0
1	0	0	0	0	29	0	0	0	0
2	0	0	0	0	30	0	0	0	0
3	0	0	0	0	31	0	0	0	0
4	0	0	0	0	32	0	0	0	0
5	0	0	0	0	33	0	0	0	0
6	0	0	0	0	34	0	0	0	0
7	0	0	0	0	35	39084	3000	1491.4	660
8	0	0	0	0	36	45699	3000	1720.1	430
9	0	0	0	0	37	41663	3000	1580.6	474
10	0	0	0	0	38	45780	3000	1722.9	467
11	0	0	0	0	39	50659	3000	1891.6	330
12	0	0	0	0	40	39761	3000	1514.8	516
13	0	0	0	0	41	36709	3000	1409.2	689
14	0	0	0	0	42	39137	3000	1493.2	818
15	0	0	0	0	43	38527	3000	1472.1	816
16	0	0	0	0	44	36753	3000	1410.7	692
17	0	0	0	0	45	50114	3000	1872.8	478
18	0	0	0	0	46	41817	3000	1585.9	429
19	0	0	0	0	47	70819	3000	2588.8	274
20	0	0	0	0	48	49621	3000	1855.7	494
21	0	0	0	0	49	45886	3000	1726.6	464
22	0	0	0	0	50	44595	3000	1681.9	411
23	0	0	0	0	51	44857	3000	1691.0	406
24	0	0	0	0	52	50906	3000	1900.2	421
25	0	0	0	0	53	77515	3000	2820.3	175
26	0	0	0	0	54	50974	3000	1902.5	457
27	0	0	0	0					

E.3 SIMULATION RESULTS

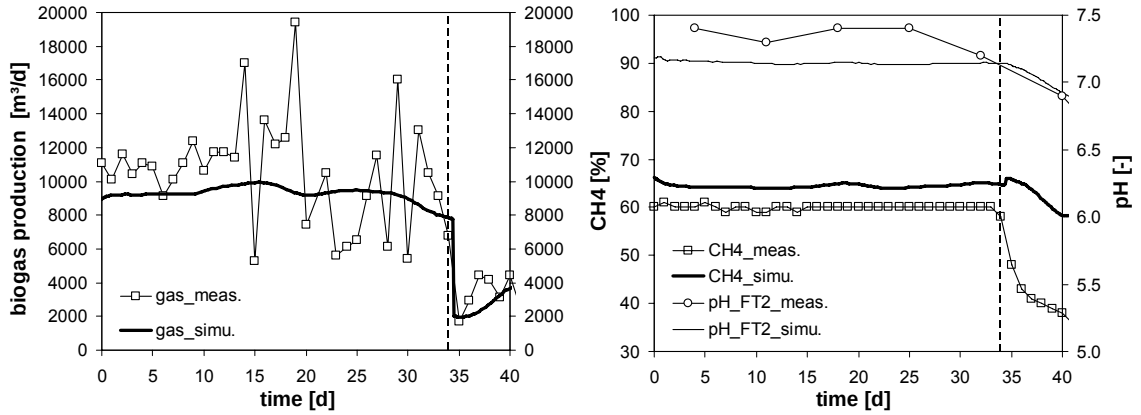

Figure E-2 WWTP Salzburg simulation results and measured values for gas production, pH and methane content. Note that on day 34 digester FT1 was shut down and sludge was by-passed to FT2.

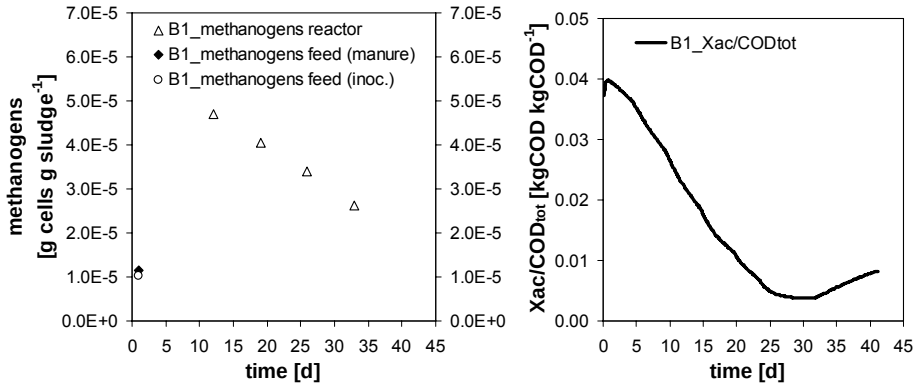

Figure E-3 Measured relative portion of methanogens in reactor B1 and in the feed (per g sludge; left) and simulation values for acetate degarders (Xac) (per kg COD; right) in reactor B1

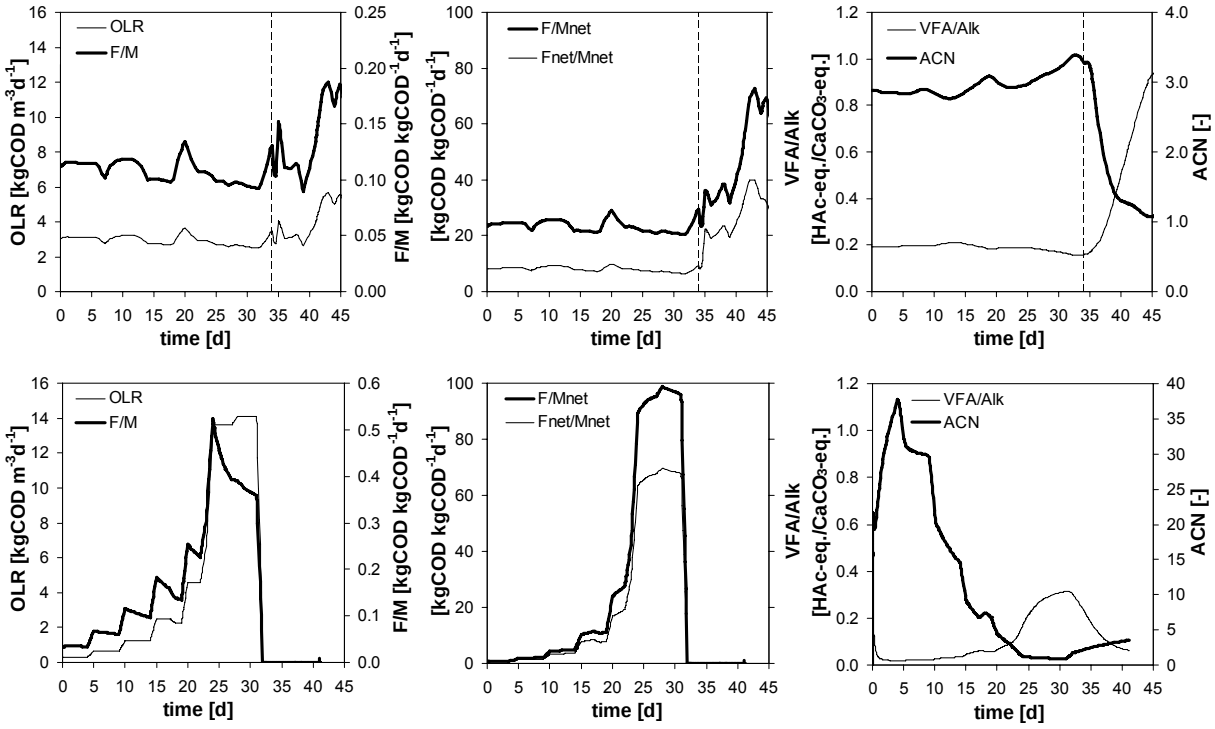

Figure E-4 Simulation results of key indicators for Salzburg WWTP (upper charts) and start-up experiment (lower charts). Note that different y-axis scaling was used for F/M and ACN.